Theses and Dissertations | 1. Thesis and Dissertation Collection, all items

1985

A determination of particle density distributions above fluidized beds.

Piper, Glenn Alvah III.

http://hdl.handle.net/10945/21265

DEPARTMENT OF OCEAN ENGINEERING

MASSACHUSETTS INSTITUTE OF TECHNOLOGY
CAMBRIDGE, MASSACHUSETTS 02139

A DETERMINATION OF PARTICLE DENSITY

DISTRIBUTIONS ABOVE FLUIDIZED BEDS

GLENN A. PIPER

XIII A

MAY 85

A DETERMINATION OF PARTICLE DENSITY DISTRIBUTIONS

ABOVE FLUIDIZED BEDS

by

GLENN ALVAH PIPER III

B.S.M.E., University of Washington
(1980)

Submitted to the Department of Ocean Engineering in Partial
Fulfillment of the Requirements for the Degrees of

MASTER OF SCIENCE IN NAVAL ARCHITECTURE AND MARINE ENGINEERING

and

MASTER OF SCIENCE IN MECHANICAL ENGINEERING

at the

MASSACHUSETTS INSTITUTE OF TECHNOLOGY

MAY 1985

A DETERMINATION OF PARTICLE DENSITY DISTRIBUTIONS
ABOVE FLUIDIZED BEDS

by

Glenn Alvah Piper III

Submitted to the Department of Ocean Engineering on May 16, 1985 in partial fulfillment of the requirements for the Degrees of Master of Science in Mechanical Engineering and Master of Science in Naval Architecture and Marine Engineering. The author hereby grants to the U.S. Government permission to reproduce and to distribute copies of this thesis document in whole or in part.

ABSTRACT

An experimental apparatus to measure the particle density distribution in the freeboard of an atmospheric fluidized bed was designed and constructed. The density versus height measured by the sampling apparatus gives a similar exponential decrease as previous investigations have found.

A particle trajectory model is developed which calculates the height and particle density distributions above the bed surface of an atmospheric fluidized bed. The parameters input to the model are the superficial velocity, initial partical velocity, gas jet velocity and duration, and the particle size distribution of the bed mass. The model was evaluated using the experimental data for jet velocity, duration, and particle size. The predicted slope of the particle density versus height in the freeboard agrees with the experimentally measured slope within 20%.

A sensitvity analysis using the trajectory model, resulted in a determination of the particle distributions in the freeboard of a fluidized bed as affected by varying the input parameters to the trajectory model. The most significant effects were achieved when the jet velocity or duration was altered.

Thesis Supervisor: Dr. Leon Glicksman
           Title: Senior Research Scientist

ACKNOWLEDGEMENTS

A DETERMINATION OF PARTICLE DENSITY DISTRIBUTIONS ABOVE FLUIDIZED BEDS

TABLE OF CONTENTS

LIST OF FIGURES

LIST OF TABLES

CHAPTER I

INTRODUCTION

Fluidized beds have been used in industry for many years. They have been used to mix and dry particulate materials and are the principle process in catalytic cracking plants. In the past decade or so, the use of fluidized bed combustors for power generation has become a source of major interest. Prototype coal burning beds have already been built which are comparable to existing coal plants. Fluidized bed combustors have the added benifit of low NOx, SO_2 and hydrocarbon emissions and the flexibility of being able to burn a wide range of fuels ranging from refuse and high sulfur content coal to high grade fuels.

A fluidized bed [Fig 1] is composed of a distributor through which an air flow is introduced through thousands of small orfices. This air then passes through the dense zone of the bed which is comprised of a mass of particles. The air velocity through the dense zone is maintained above the minimum fluidization velocity (Umf) during normal operations. At velocities equal to or greater than Umf, the frictional force (Drag) of the air flowing past a particle is equal to the weight of the particle. Under these conditions, the particle mass behaves very much like a fluid. It will maintain a horizontal surface if the container is tilted, flow out of holes in the

14
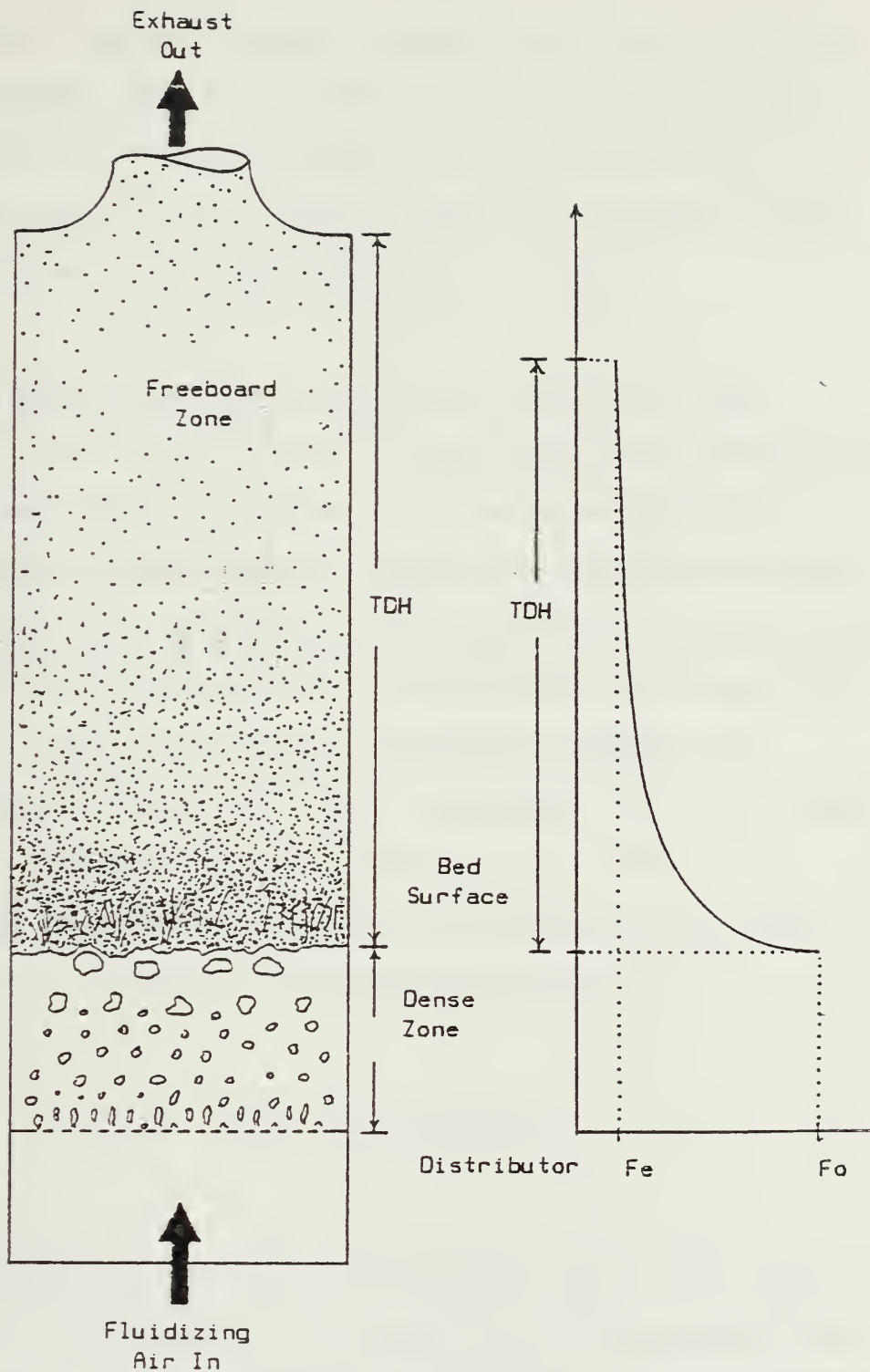
Fig. 1   Model of a fluidized bed. Particle
          entrainment decreases exponentially
          with increasing freeboard height.

15

container, and has a pressure drop across any section of the bed

apprxamately equal to the weight of air and particles in the

section [1]. At velocities above Umf, the excess air will

coalesce and form small voids or bubbles as it procedes towards

the surface of the fluidized bed.

As bubbles break at the surface of the bed, the solid

particles are thrown up above the bed surface and are entrained by

the upward flowing gas stream. This zone above the bed surface is

the freeboard zone. In the freeboard, some particles are carried

by the gas flow far above the bed surface and are removed from the

fluidized bed (elutriated) , while the remainder fall back to the

bed. In general the amount of bed solids suspended in the

freeboard (entrainment) decreases exponentially along the freeboard

height. This distribution is similar to that of the

Maxwell-Boltzmann distribution for the case of discrete energy

states as it applies to the Law of Atmospheres [2].

$$N(z) = No \exp\{-mgz/kT\} \qquad\qquad (1)$$

Research in the area of entrainment by Lewis et al. [3], Zenz

and Weil [4] and others has resulted in the following correlation

for entrainment as a function of gas velocity and freeboard height

for small-particle beds [1].

$$\frac{F}{At\ Uo} = B\ \exp\{-[(b/Uo)^{Z} + a\ H]\} \tag{Z}$$

where:

    F = Entrainment
    At = Area of bed
    Uo = Superficial velocity through bed
    B = Particle dependent constant
    b = Particle dependent constant
    a = Particle dependent constant
    H = Height of freeboard

At some point above the bed surface, the quantity of entrained particles becomes constant. At this point, the free fall velocity of the remaining particles is equal to or less than the uniform superficial operating velocity. The height at which the entrainment becomes constant is called the transport disengagement height (TDH) [1].

The particles that are thrown above the bed are affected in the freeboard region by hydrodynamic parameters such as: bubble size, bubble frequency, fluidizing velocity, height above the bed, particle size, particle density, column diameter [5], and baffles [6]. The intermittent high velocity bursts of gas which occurs when a bubble bursts, imposes a flucuating and highly irregular time dependent velocity profile over the cross section of the bed surface. At successively higher levels above the bed surface, this velocity profile becomes more and more uniform until at the TDH, the flow is at the uniform superficial operating velocity (Uo) [4].

17

Until recently, little attention was paid to the understanding of the freeboard reactions for large particle beds. However, due to recent work in fluidized bed combustors, the extent of particle and fines loading in the freeboard has been shown to significantly affect the SO_2 absorbtion, NOx reduction, CO emission. In general, the last 5 to 10% of the combustibles will burn in the freeboard. It was shown that the fine sorbent particles entrained into the freeboard will enhance sulphur capture and that entrained char particles will react with NOx and reduce its emission [7]. Fines reinjection has been shown to significantly increases the fine particle concentration in the bed and in the freeboard with the consequence of further enhancing char oxidation. However, this can result in overheating in the freeboard region and excess SO_2 and NOx emission [7]. The end result is that the potential for fluidized bed combustion power plants is enhanced by their ability to burn high sulphur content fuels and maintain low SO_2 emissions. Further research in the area directly above the bed surface is required to properly model the reactions occuring within the freeboard.

Extensive studies on entrainment rate and elutriation have been made with numerous correlations, some of which are proposed in [1, 3, 4, 5, 6, 7, 8]. However, most of the reported work on entrainment from fluidized beds has been carried out with either a closely sized fraction of particles or a mixture of two such fractions. Virtually all of this work has been conducted on bench scale or catalytic cracking fluidized beds. The results of these

18

studies have been shown to produce much lower entrainment rates than full sized beds or tend to operate in the slugging condition. Therefore, the entrainment rates and transport disengagement heights (TDH) for fluidized beds are generally estimated from empirical or semiempirical correlations obtained from this data and most of them show extreme discrepancies between different experimental results. Extrapolation of these empirical correlations usually leads to strange results [5] with discrepancies which can vary by two orders of magnitude.

The lack of good correlations stems mainly from the difficulty in obtaining accurate entrainment rate data. Most of the data is based on pressure measurements at incremental heights in fluidized cracking plant type beds [11]. The effect of wall loading by particles and the actual relation between pressure and particle concentration is considered to be major sources of error when using this method with large particles. As a result, none of the correlations are widely accepted as giving accurate predictions [8].

A complete model of the entrainment process from fluidized beds must take into account all the mechanisims involved within the process. The arrival of bubbles at the bed surface, ejection of particles from the dense-phased bed into the freeboard region as the bubbles erupt, particle-particle interactions, and the trajectories of ejected particles are all important [8]. Much work has been done concerning bubble growth, velocity, volume,

etc. and their behavior is fairly well understood.

The mechanism of solids ejection at the bubbling bed surface
is still not well understood. The origin of ejected particles is
reported to be primarily due to two sources. The particles which
have been lifted by the bubble wake and thrown upwards following
the bubble burst at the surface is the first source. This theory
is supported by work done by George and Grace [8] who performed
experiments which concluded that the vast majority of the ejected
particles did not originate from the surface layers but from
bubble wake pick up. Work done by Page and Harrison [6] also
appears to agree with this. The second theory suggests that the
ejected particles originate at the nose of the bursting bubbles
and are thrown outward when the bubble breaks. Research by Rowe
and Partridge [8] and Glicksman et al [12] have shown this second
mechanisim as being the dominate particle ejection source and thus
supporting this second theory. Their work has also shown that
under the conditions in which 2 bubbles coalesce just below the
surface of the bed, the jet of gas produced can result in a
significant amount of particles being ejected from the wake of
the first bubble.

The effect of multiparticle interactions have been for the
most part ignored except by Peters and Prybylowski [13]. The
motion of any individual particle is influenced by the presence
of other particles, i.e., through direct particle-particle
interactions and deviations in the fluid drag force. The major

drawback of their work is that the paper compares their theory
with only a single set of experimental results [3].

Studies to model the trajectories of particles in the
freeboard have been conducted several times. The work of Walsh
et al.[7], George and Grace [8], and Peters and Prybylowski [13]
name just a few of the latest efforts. All of these studies
relied upon experimental data to develope their theories.
However, to check the accuracy of their theories, more
experimental data is required.

As of yet, none of the entrainment models available can be
incorporated into fluidized bed combustion models with sufficient
accuracy to warrent their use. This is due to a lack of
experimental information on entrainment rate as a function of the
complete fluidization parameters of the bed to test the models
with. As a result, the purpose of this study has been to obtain
particle density distributions above a cold atmospheric fluidized
bed containing a continuous particle size distribution [Appendix
E].

CHAPTER II

PARTICLE SAMPLING APPARATUS

Design Alternatives

There are many methods available for determining particle distributions in fluid flows. The more commonly used methods are:

1) Catching mechanisms

2) Trapping mechanisms

3) Radiation attenuation measurements

4) Optical measurements

5) Capacitance and Inductance measurements

Catching mechanisms are passive devices. That is, particles are captured merely by the presence of the catching mechanism in the fluid flow containg the particles to be sampled. The data obtained using this method is position dependent and produces average values for the particle flux loadings. These catching mechanisims are also limited in that they can only catch particles with particle fluxes traveling in a single direction. The device used by Walsh et al [10] only captured falling particles while the device used by George and Grace [8] required the upward moving particles to deflect off of a baffle surface and fall into a collecting trough.

22

Trapping mechanisims, unlike catching mechanisms, are active particle samplers. Their operation involves the trapping and isolation of a finite volume of the fluid flow at a specific period in time. This sampling technique produces time dependent as well as position dependent data. This will allow correlations between bubble eruption and particle density to be made using multiple bubble conditions rather than single bubble capture. As the number of random samples taken by this method increases, the average value of this data will approach that of the catching mechanism. Trapping mechanisims also capture particle fluxes traveling in multiple directions. This ability reduces the error inherent in measuring only the downward or only the upward particle flux. The apparatus used in this paper is a trapping mechanism.

Attenuation of nuclear particles from a radioactve source can be used to give average particle density distributions across a suspension. However, this method is not adaptable to density determinations at a point. An average time dependent density determination can be achieved with this method. Another draw-back of this method is the radiation hazards involved with the use of nuclear particles.

Optical density determinations consists of two seperate methods. The first method uses a very small light beam which is eclipsed by the transition of a particle through it. A related

23

method uses the absorbtion and scattering of a somewhat larger light beam to correlate the change in light intensity with particle density. This method has been used frequently in the study of aerosols but requires complicated and intricate equipment [14]. The second method involves high speed photographs of a small volume of space. This method cannot be used when the particle density is so large that multiple particles eclipse each other frequently enough to produce unacceptable error. This is the case when the probe height above the bed is less than 7-15 cm (3-6 in).

Measurements at a point can also be made by inserting either a toroidial inductor or a parallel plate capacitor in the flow. The presence of the particles changes the permeability and thus the inductance of the inductor, or the dielectric strength and thus the capacitance of the capacitor. The draw-backs of these methods involves the unknown effects of particle velocity and external particles on the inductor and charge transfer to particles from the capacitor [14].

Apparatus Requirements

The goal of this study was to determine the density distribution of particles above an atmospheric fluidized bed with particle velocities of up to 10 meters per second. The particle size distribution of material ejected from bubbles is required for particle trajectory calculations. A correlation between the

24

average density and the density present immediately after a bubble
bursts from the bed surface was also of interest. These
requirements dictated that the method used for measuring densities
have the following capabilities:

    1) Measure densities with good spatial resolution.

    2) Measure densities at specific moments in time.

    3) Obtain particle size information.

    4) Operate under extremely dirty conditions.

    5) Easy sample removal from bed.

    6) Remote operation of sampler.

    The radiation attenuation and inductance/capacitance methods
can not determine particle sizes. Therefore, these methods were
no longer considered as possible measurement alternatives.
Because the optical methods are either not reliable at small
heights above the bed or their use is too complex, they were not
used. Catching devices, although simple to use, do not have the
ability to measure data at specific points in time and determine
particle density loading in space. As a result, the determination
to use a trapping mechanism as the method of measuring particle
densities was made.

Apparatus Design

General Design Criteria

The following criteria was used in determining the design of the trapping device.

1) The closure time of the trap was chosen to be equal to the time for a particle with a velocity of 10 m/s to transit 1/10 the length of the sample container. This velocity is considered to be the upper limit of the particle velocity distribution present in the test bed, based on the work of George and Grace [8].

2) The apparatus must be capable of frequent sampling without requiring access to the sampling device itself.

3) The samples trapped, must be easily accessable from outside the fluidized bed without interupting the bed conditions.

4) The apparatus must be able to operate in the high particle flux environment of the fluidized bed.

5) The actuation of the trapping device must be able

to be accurately determined to allow correlation

with other time resolved measurements.

General Design

The apparatus is shown in Figs. 2 and 3. A description and
list of all components is given in Appendix H. The sample
container is mounted on an extension arm to minimize the
disturbance to the air flow around the sample trap caused by the
rest of the mechanism. The sample container is closed using two
(2) paddle arms, one above and the other below. These paddle arms
are attached to aluminum interfaces which are used to connect them
to a rotary solenoid. The solenoid is used to swing the paddles
over the sample trap and shut it. Not shown in these figures are
the power supply for the solenoid, the vacuum system used to
remove the particles from the sample trap and the water-proof
nylon shell used to keep the particles from interfering with the
operation of the solenoid. All of these systems are described in
greater detail in the following sections.

Sample Container

To ensure that the sampling device had minimal effect on the
fluid flow, the cross sectional area presented to the flow had to
be minimized. This constraint required that the sample container
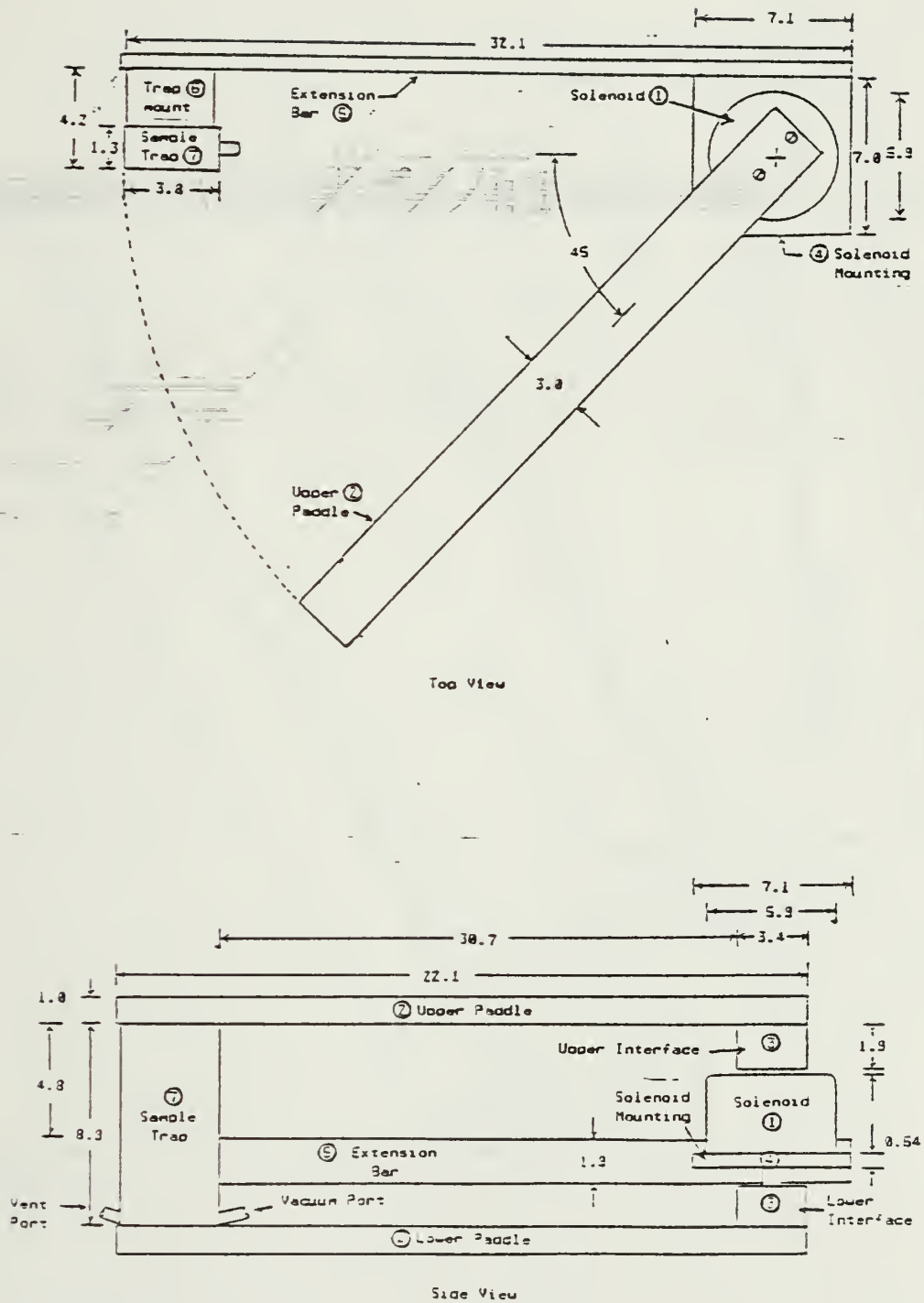
Fig. 2   Side and top views of sampling apparatus.
All dimensions are in cm.   ○ Reference
number for component listed in Appendix H.

28
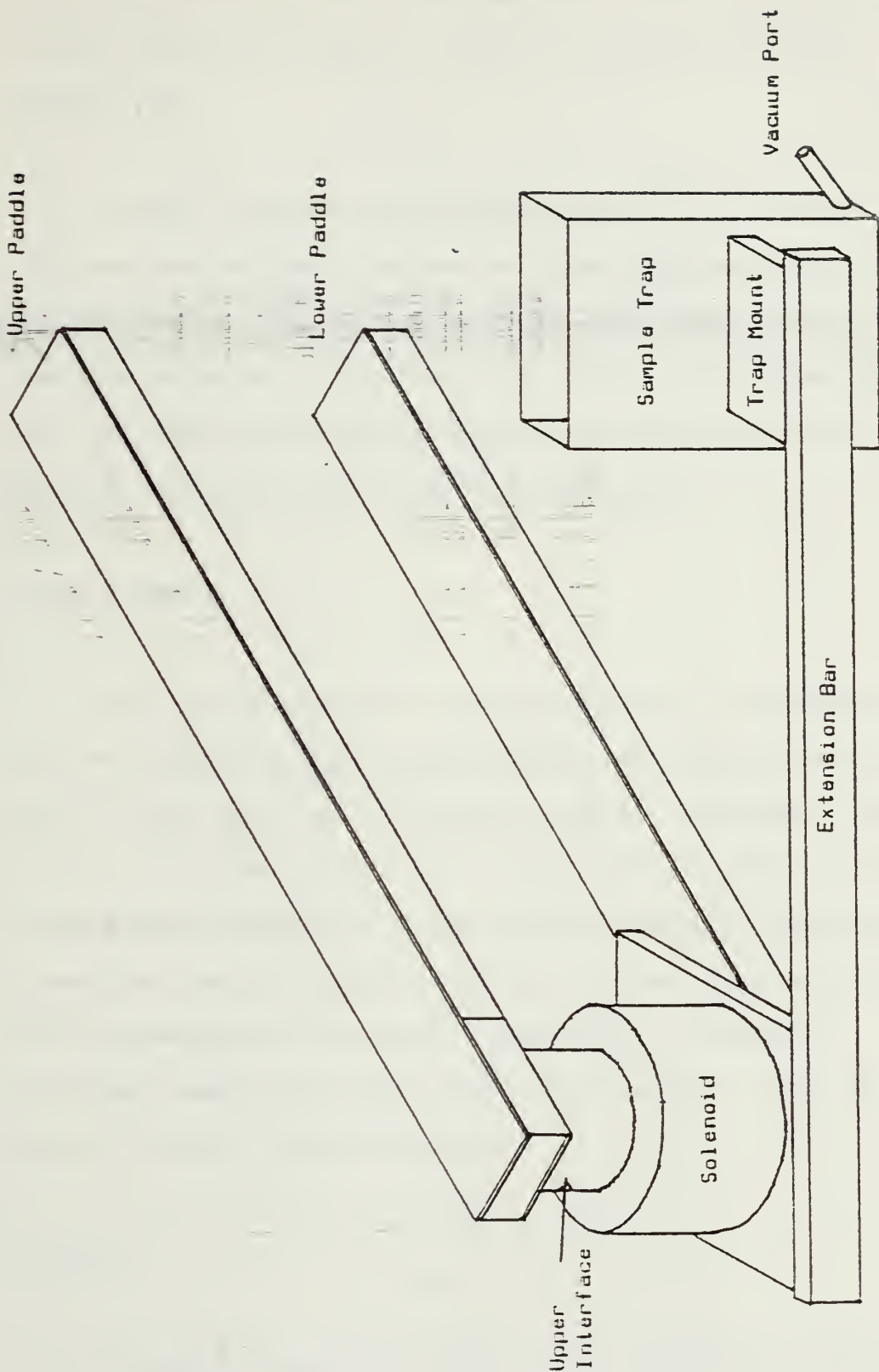
Fig. 3   Perspective view of sampling apparatus

29

be seperated from the rest of the apparatus. This was benificial in the final design because it helped to reduce the apparatus closure time.

To ensure a good seal was achieved when the trap was shut, felt was used as a gasket between the sample container and the closure paddles. Fig. 4 shows the final design used for the sampling mechanism. It is constructed of 1/16 inch aluminum with 1/4 inch square stock used for the frame and mounting structure. Epoxy is used to seal the sides of the container.

Closure Paddles

After several iterations on paddle designs, it was determined that the paddle construction which offered the greatest stiffness for the least weight was a composite laminate. The paddle, shown in Fig. 5, is made using a 0.4 in thick foam core with 1/32 inch thick Basswood laminations on the exterior. Hardwood (Maple) end pieces were used to provide a noncompressive connection between the foam paddles and the aluminum interfaces. The aluminum interfaces couple the solenoid shaft to the paddles. Epoxy was used to join the laminate materials.

Actuator

A rotating mechanism utilizing a rotary solenoid was chosen to shut the sample trap. A rotary solenoid was selected because
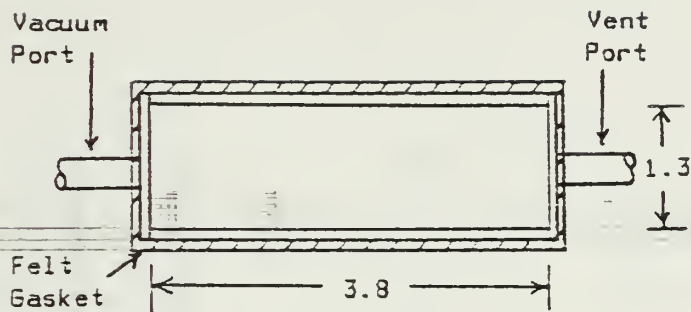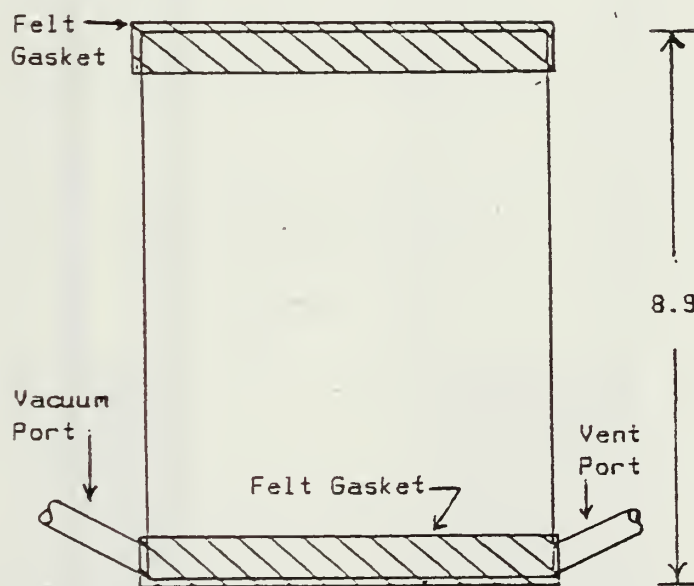
Fig. 4   Top and side view of sample trap.
           Dimensions in cm.

31
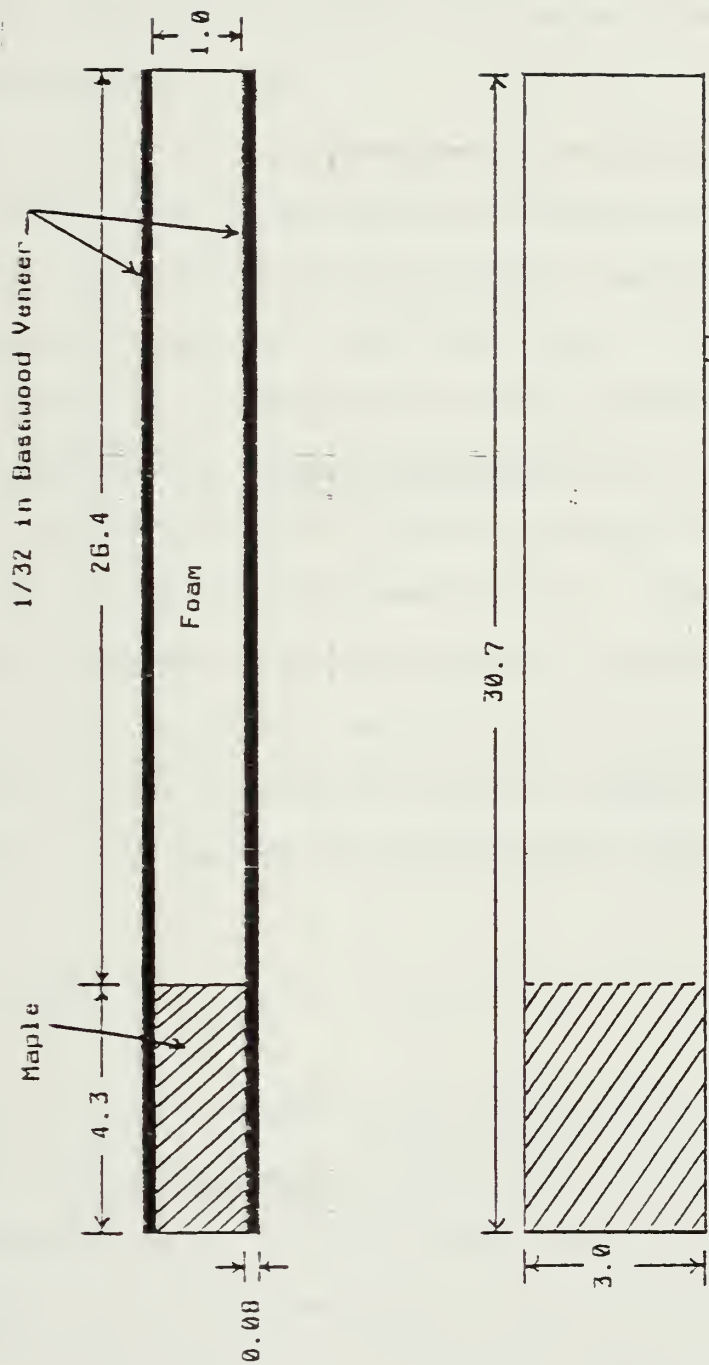
Fig. 5   Design of Closure Paddles.   Dimensions in cm.

of the problems of maintaining low friction surfaces for sliding

mechanisms in the presence of the particulate matter being

sampled. This precluded the use of any sliding mechanism to shut

the sample trap. The calculations found in Appendix A and

Appendix C determined the size of the solenoid required to achieve

the desired closure time.

The 45 degree stroke solenoid was chosen to place the paddle

arms far enough away from the sample trap, such that when

de-energized it prevents interference with the particle flow.

This stroke also minimized the area which must be clear of

obstructions to the travel of the paddles. The solenoid operates

at a 1/10 duty cycle power rating when initially actuated,

providing the torque output shown in Fig. 6. After the solenoid

has shut the sample trap, the solenoid is operated at a lower

power rating, providing a holding torque of 5.5 in-lbs. This

decreased rating is necessary to prevent overheating of the

solenoid. This assembly is encased within a nylon shell.

Power Supply

Fig. 7 is a schematic of the electrical system used to power

the solenoid. Appendix H contains a list of all components used

in the power supply. The power supply plugs directly into a

standard 115 volt AC line source. Switch S1 is used to apply

power to the solenoid M1. The full wave bridge rectifier assembly

converts the AC line voltage to DC. The rectifier assembly is

33
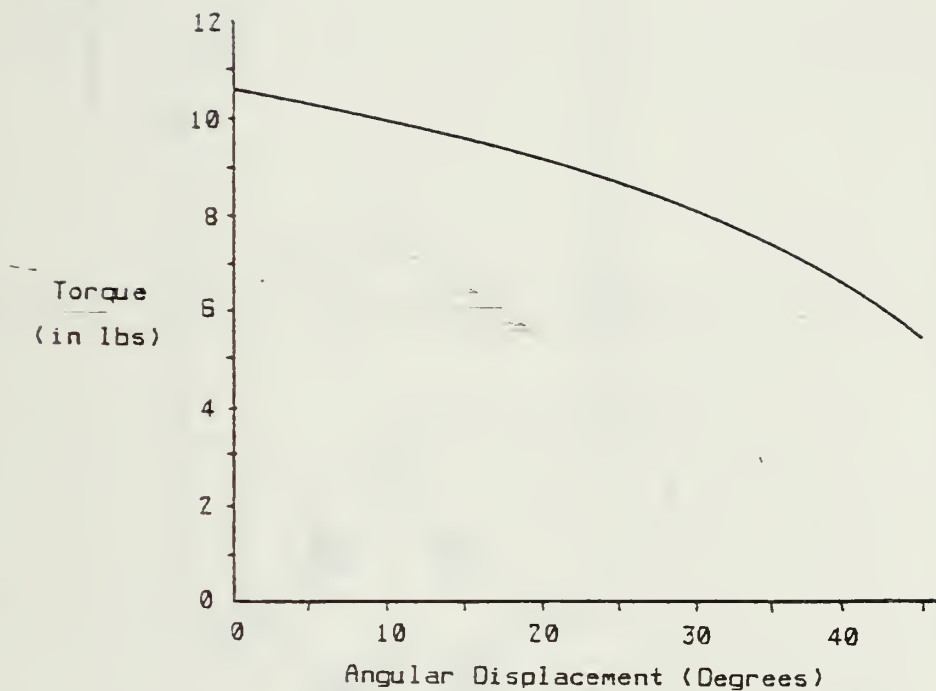
Fig. 6   Torque Output Curve for
          Rotary Solenoid.
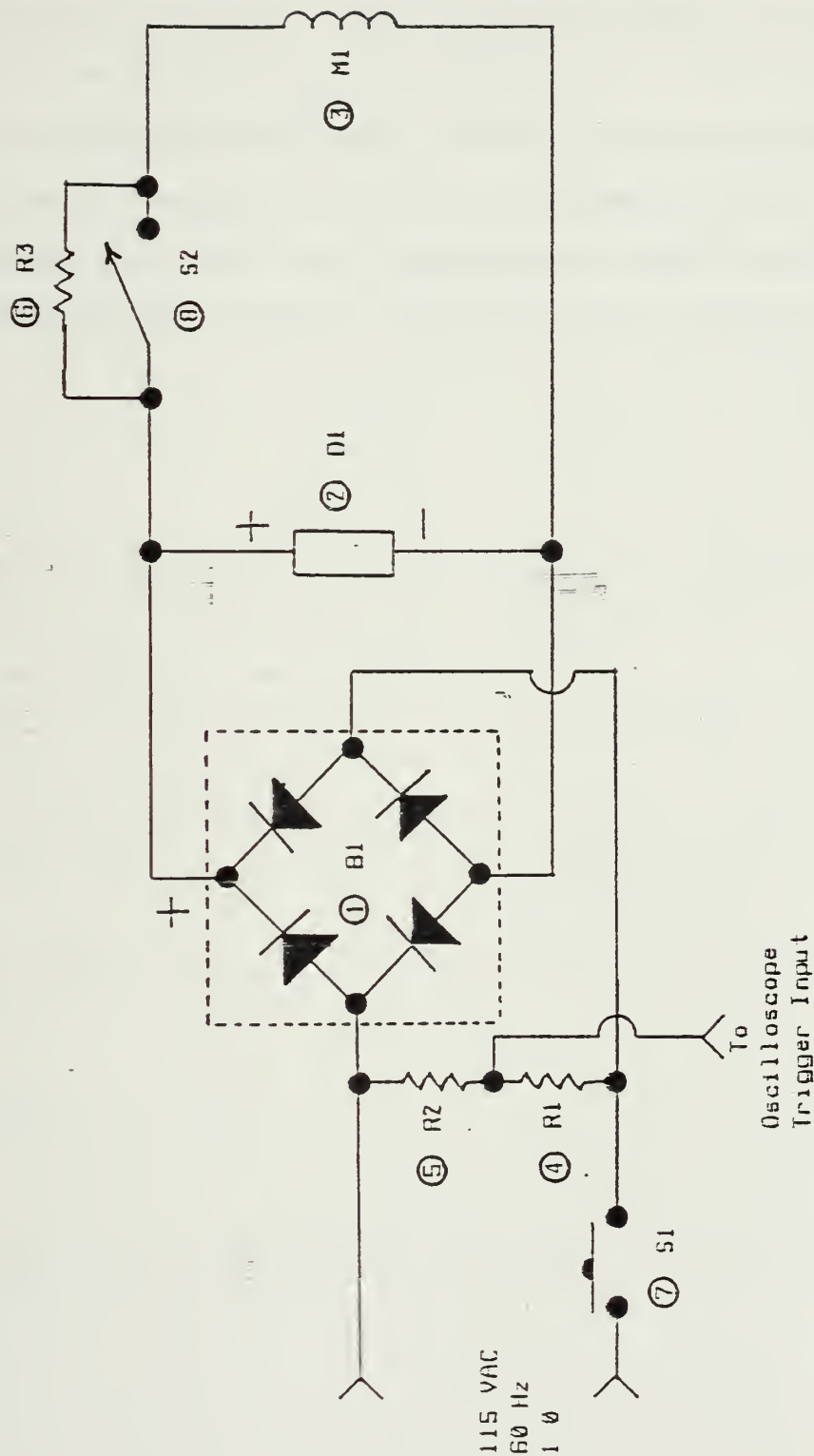
Fig. 7   Schematic of Solenoid Power Supply.
⃝ Reference number for component
list in Appendix H.

35

protected by the arc suppresser D1 from the large voltage spike

induced in the solenoid coil when the solenoid is actuated.

Resistor R3 is used to reduce the current through the solenoid

after the solenoid has been closed to prevent it from overheating.

To initially shut the sample trap, full current is applied to the

solenoid by shutting switch S2, which bypasses resistor R3.

Resistors R1 and R2 form a voltage divider network to provide a

low voltage (5.5 volts AC) trigger source for an oscilloscope.

Vacuum System

To remove the particles in the sample trap, a vacuum system was developed. This system is shown in Fig. 8 with a list of the components given in Appendix H. A vacuum is produced by allowing air from a 100 psi air source to flow through valve V1 into the venturi eductor P1. The vacuum places a suction on the sample container C2 via a fine mesh screen. The purpose of this screen is to prevent particles from escaping the sample container. The suction is applied to the sample trap C1 through 1/4 inch polyflow tubing. It is through this tube that the particles are removed from the sample trap and collected in the sample container. An equalization and agitaion line is connected to the opposite side of the sample trap. This line serves two purposes. First, it ensures that the vacuum system does not pull in particles from outside of the sample trap. Second, it allows a flow of air to be introduced which stirs up the particles trapped inside. This helps push them into the suction line and reduce the remaining particles to a minimum.

Apparatus Testing

Two tests were run to determine the effectiveness of the system. The first test determined the closing time of the sample trap. The second evaluated the error from the loss of particles which were left in the sample trap by the vacuum system.
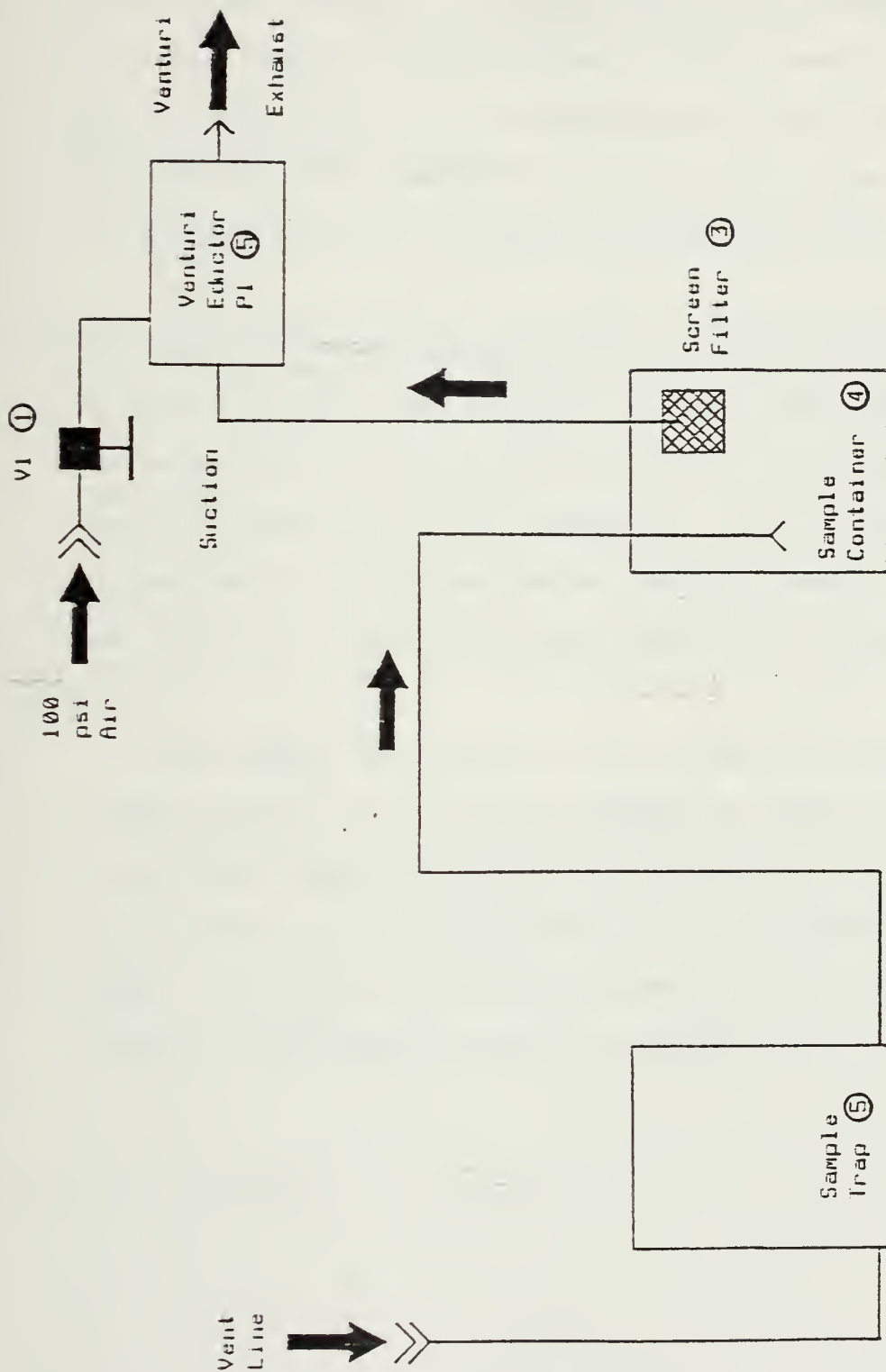
Fig. 8   Schematic Diagram For Vacuum System.
⃝ Reference number for component
          list in Appendix H.

The procedure and method used to determine closure time for the sample trap is given in Appendix C. From the results of these tests given in Appendix C, the closure time was determined to have an average value of 1.44 milliseconds. This is equal to a 10 m/s particle traveling 1.44 cm or approximately 16 % of the sample trap length. The average particle velocity will be less than 2 m/s and will therefore introduce an average error of less than 3 %.

Using the sample trap closure time, a dynamic analysis determined that the total time from initially applying power to the solenoid until it shut the sample trap is 42.6 milliseconds. These calculations are given in Appendix D. This actuation time is important for determining whether a specific bubble's debris was within the vicinity of the trap at the time of closure.

The procedure and results for the testing of the sample removal vacuum system are given in Appendix B. The average amount of particles lost by the vacuum system was determined to be 0.52 % of the initial sample placed in the trap. The maximum error was 0.93 %. The error from the vacuum system is therefore considered to have an insignificant effect on the data obtained.

CHAPTER III

EXPERIMENTAL PROCEDURE

Fluidized Bed Configuration

The M.I.T. atmospheric fluidized bed, in which the sampling
device was used, is a model of the 20 MW atmospheric fluidized bed
combustor prototype, jointly sponsored by the Tennessee Valley
Authority and the Electric Power Research Institute. The
fluidized bed model is described in Lord et al [15] and Jones et
al [16]. While using the sampling apparatus, a different heat
exchanger tube bundle configuration was used than is described in
Jones et al [16]. The heat exchanger configuration used is shown
in Figs. 9 and 10.

The heat exchanger used during this work is made of 1.26 cm
(0.5 in) O.D. tubing arranged in 4 rows of 22 pipes each. The
tubes are aligned as shown in Fig. 10. Each pipe is spaced with
a vertical center to center distance of 5.08 cm (2 in) and a
horizontal center to center distance of 3.91 cm (1.5 in). The
distance from the distributor to the center of the upper most tube
is 27.62 cm (10.875 in). A 5.08 cm (2 in) spacing separates the
front and back walls of the fluidized bed from the end tubes of
the bundel. The cross sectional area of the bed is 1.079 sq m
(11.61 Sq Ft). The particulate material used in the bed is a
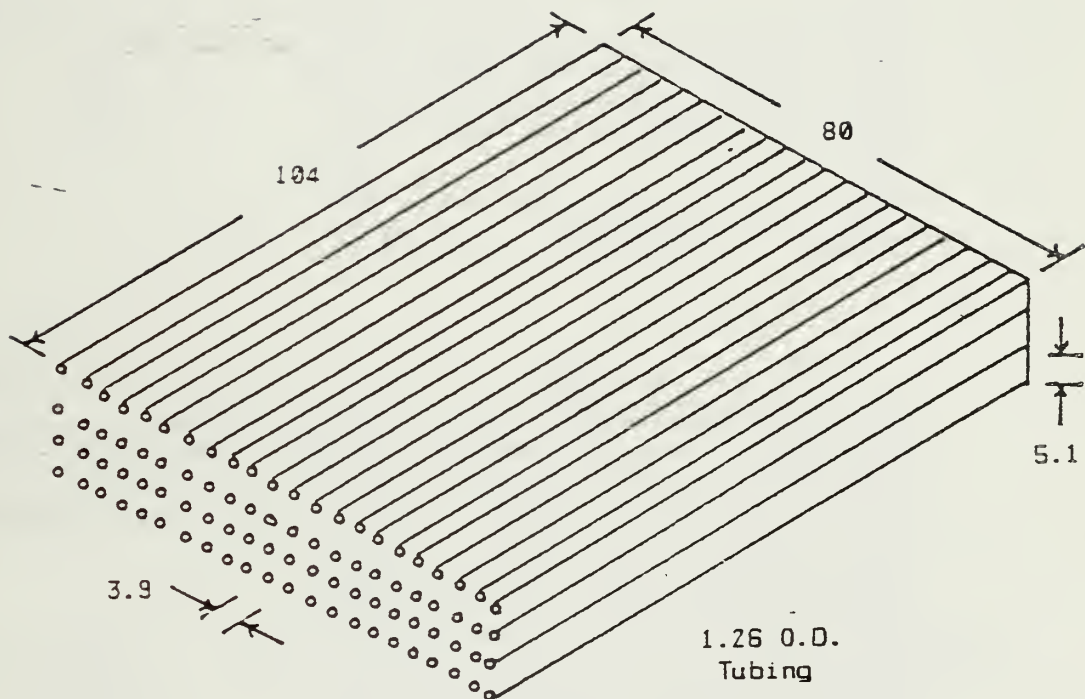
Fig. 9   Heat Exchanger Tube Design Showing The
          Four (4) Rows of 22 Tubes.
          All Dimensions in cm.

41
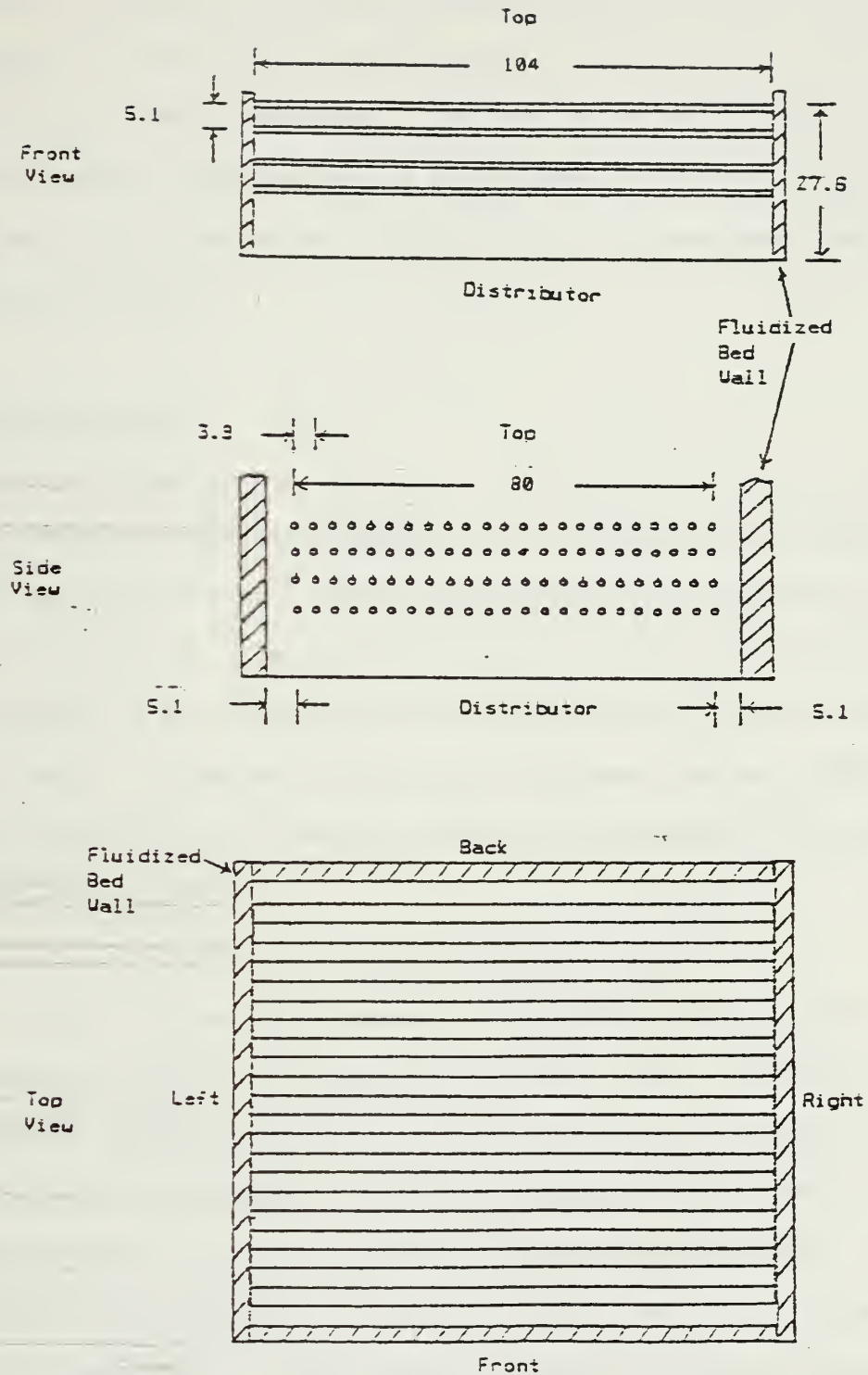
Fig. 10   Heat Exchanger Tube Design.
All Dimensions in cm.

42

mixture of steel grit abrasive having a specific gravity of 8.1.

Appendix E lists the size distribution of the steel grit used

during the sampling operation. The bed was operated without

recycling the fines captured in the cyclones. The static bed

height of the material was 22.54 cm (8.875 in) throughout the data

collection period.

Equipment Set-up

Fig. 11 shows the placement of the sampling device inside

the fluidized bed. The sample trap was positioned such that it

was directly over a spacing between tubes [22.86 cm (9 in) from

the center of the front-most tube] and 41.91 cm (16.5 in) from the

left wall. The height of the sample trap above the distributor

was varied during the sampling process as discussed in the section

on sampling procedure.

Fig. 12 shows the placement of the bubble probe and the

anemometer probe with respect to the sample trap. The bubble

probe was placed directly below the sample trap and 26.67 cm (10.5

in) above the distributor. The probe extension was placed at an

angle so as not to interfere with the sample trap operation. To

protect the anemometer wire from particles impacting it, a special

shield consisting of # 320 mesh screen and an aluminum frame was

placed around it. The anemometer probe was attached to the bubble

probe extension with the entrance to the anemometer probe 29.21 cm

(11.5 in) above the distributor. This placed the entrance to the

43

|←—— 24.8 ——→|

Sample Trap→□

Back   Front
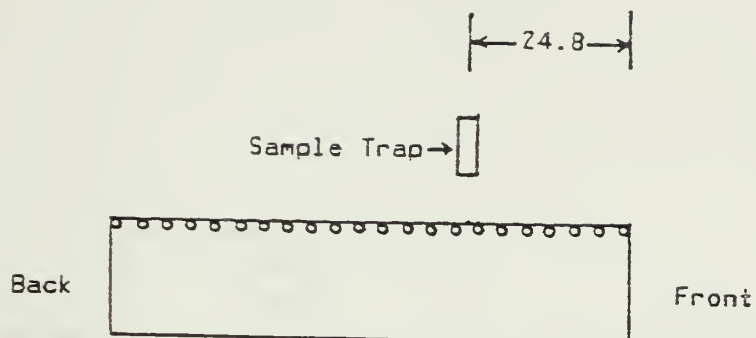
(a) Right Side of Heat Exchanger Tubes

|←———— 41.9 ————→| Bubble Probe
                        Extension

Sample Trap—⌐

                        Bubble and
                        Anemometer Probes

Left   Right
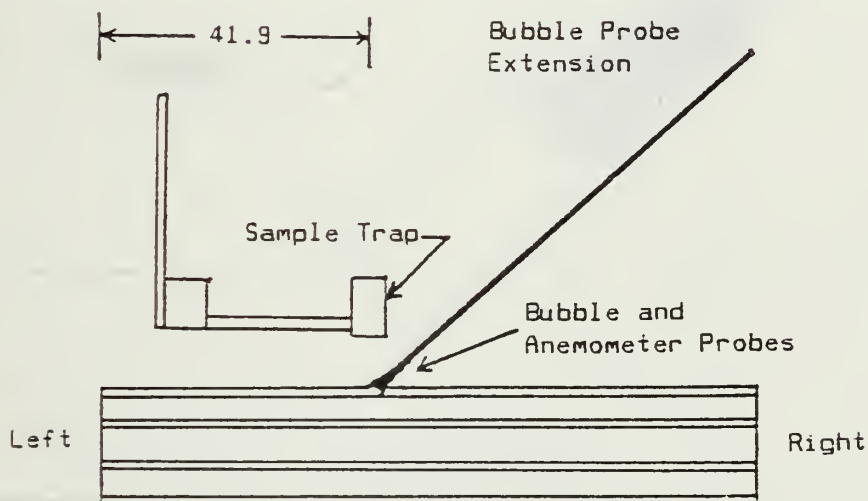
(b) Front of Heat Exchanger Tubes

Fig. 11   Position of Sample Trap, Bubble Probe,
           and Anemometer Probe Above Heat Exchanger
           Tubes. All Dimensions in cm.

44
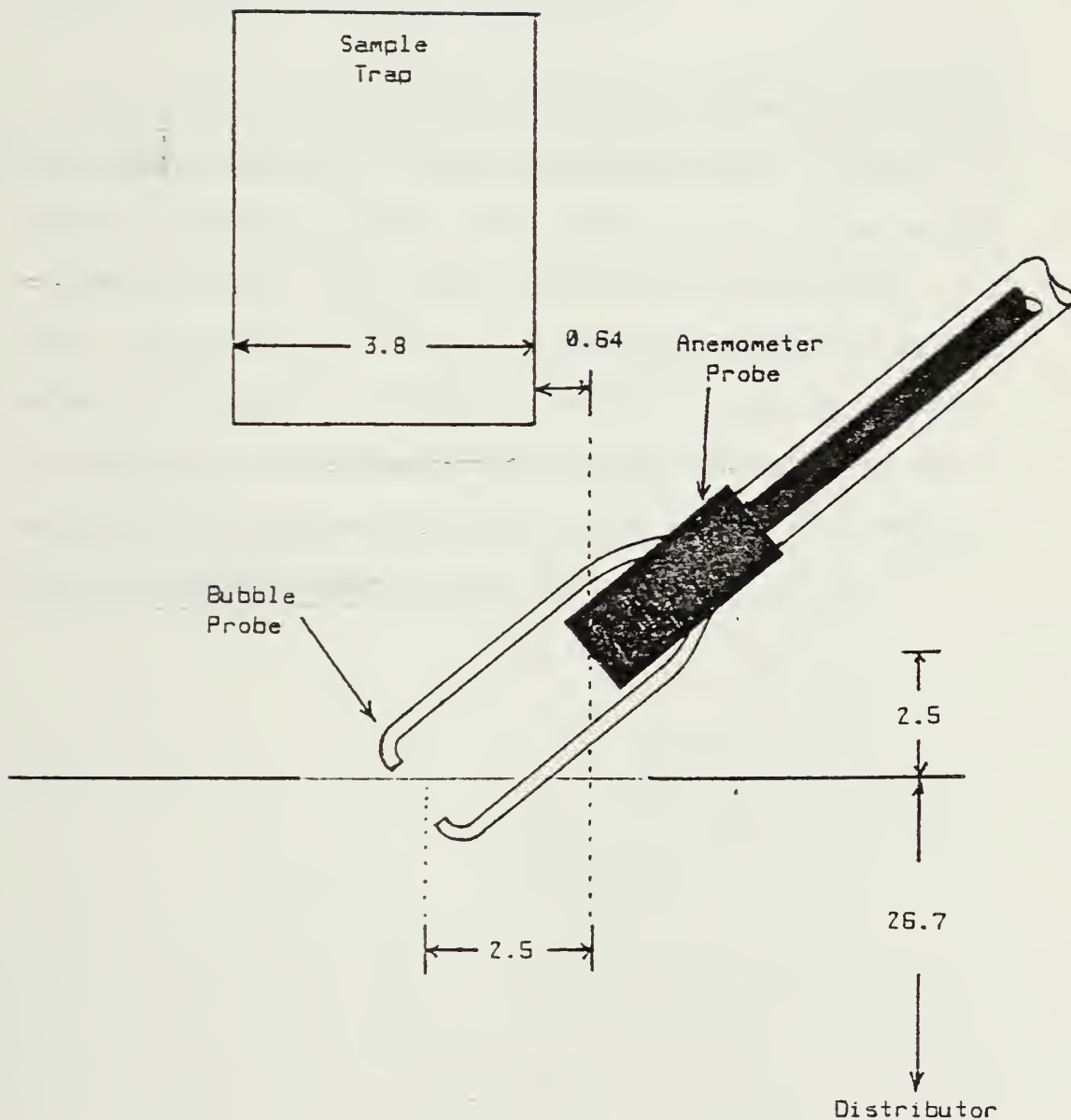
Fig. 12   Position of Bubble and Anemometer
           Probe with Respect to the Sample
           Trap and Distributor. All Dimensions
           are in cm.

45

anemometer probe 2.54 cm (1.0 in) away from the center of the sample trap and 0.64 cm (0.25 in) outside the area directly below the sample trap. As a result, the probe has a minimum effect on the air flow from the bed to the sample trap, but will only measure the gas velocity at the edge of the sample trap perimeter. The positioning of the two probes above the distributor remained constant throughout the sampling evolution.

Fig. 13 is a block diagram showing the equipment used during the sampling operations and their interconnections . Table 1 is a listing of the equipment used. The oscilloscope time base was set for MANUAL TRIGGER, SINGLE SWEEP mode and a sweep time of 50 ms/div. The channels of the dual trace amplifier were set at 5 volts per division for the bubble probe and 2 volts per division for the sample trap inputs. On the differential amplifier, one channel was not used and the second channel was set at 1 volt per division for the anemometer probe input.
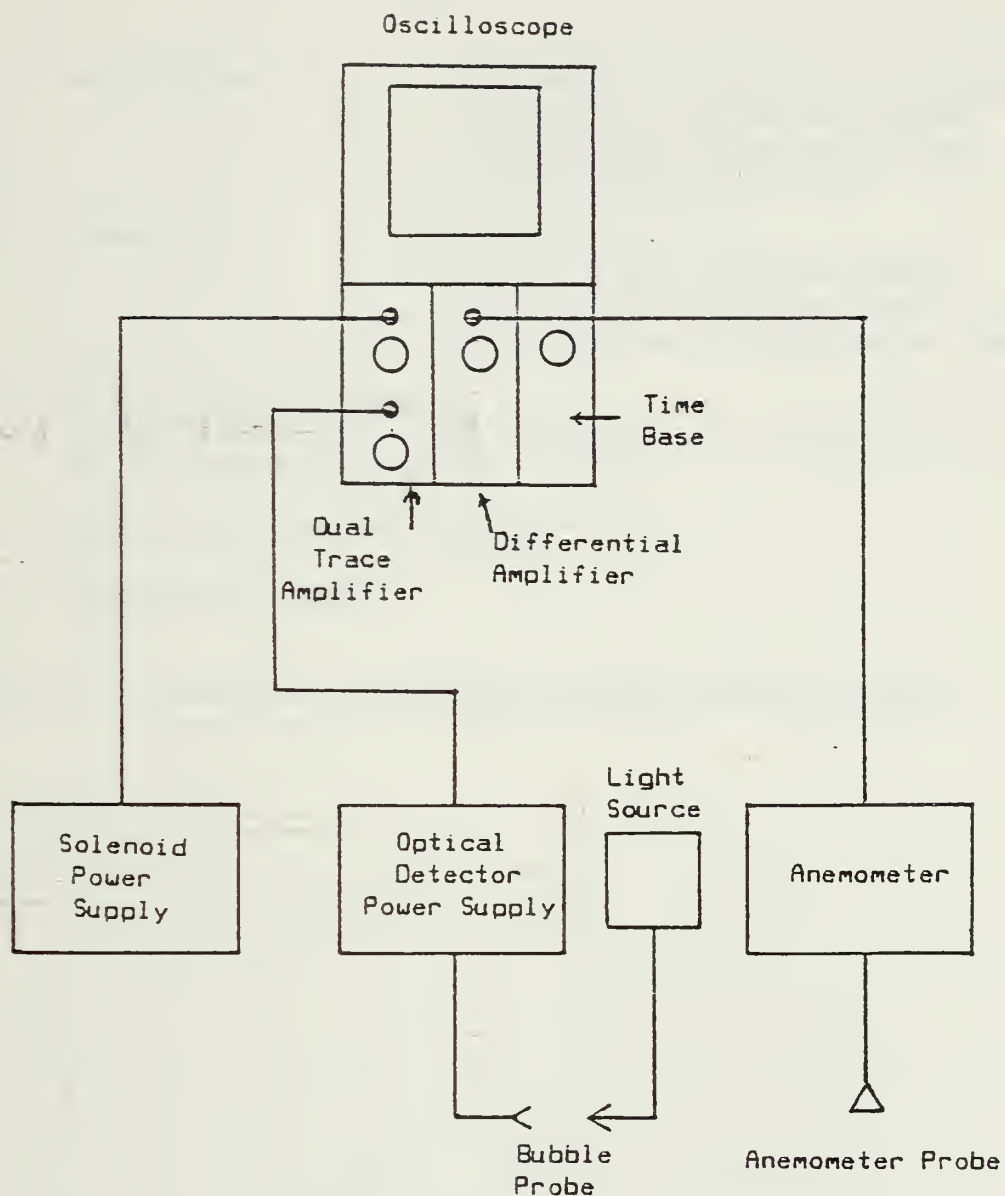
Fig. 13   Block Diagram of the Equipment Used
During the Sampling Operations.

47

TABLE 1

Oscilloscope   TEKTRONIX 5111 Storage Oscilloscope
                                TEKTRONIX 5A18N Dual Trace Ampl
                                TEKTRONIX 5A21N Differential Ampl
                                TEKTRONIX 5B10N Time Base

Anemometer   Thermal Systems Inc.
                                1051-2 Monitor and Power Supply
                                1054-A Linearized Anemometer
                                Anemometer wire w/ #320 screen guard

Optical Signal Detector

Optical Signal Detector Power Supply

Optical Source and Power Supply

Oscilloscope Camera

        Listing of equipment used during particle sampling
        operations.

To determine the fluidization conditions within the bed, a set of manometers were used. These manometers measured pressures within the bed, at heights from 4.13 cm (1.62 in) to 37.15 cm (14.62 in) above the distributor, in 2.54 cm (1 in) increments. The pressure data corresponding to each trap position and bed velocity is listed in Appendix I.

To determine the gas flow conditions within the bed, an orfice flow meter with 1D - 1/2D taps was located upstream of the distributor. The computer program listed in Appendix G was used to convert the pressure tap data to mean air velocities within the bed.

Sampling Procedure

Data was collected for four (4) mean bed velocities at six (6) different sample heights. The sample trap was placed at a given sampling height (measured from the distributor to the bottom of the trap), and ten (10) samples were collected at each desired velocity. The trap position was then changed to a new height.

During certain sampling conditions, those which involved low sampling heights with the higher air velocities, the paddle arms would occasionally impact the sides of the sample trap and not close the sample trap completely. It is assumed that this occured

49

when a large bubble erupted directly under the paddle arm and deflected the paddle arm into the side of the trap. Whenever this occured, the trap was de-energized and the closure cycle repeated.

Each time the height or velocity was changed, a complete sampling cycle was conducted and this sample discarded. This was to prevent any accumulation of particles (in the entrance to the vacuum or purge lines on the sample trap) from being added to the first sample at the new height or velocity.

For each set of data at a given height and velocity the following information was recorded:

1) Fluidized bed height above the distributor determined visually and by pressure measurements.

2) Pressure upstream of orfice plate (P1)

3) Pressure difference across orfice plate (delta P)

4) Air temperature in bed

5) Pressure distribution in bed

6) Height of sample trap above distributor

The following procedure was used during sampling:

For each sample to be taken within a data set.

A. Initial conditions

1) Vacuum air supply   OFF

2) Sweep trigger on oscilloscope   RESET

3) O-scope memory   ON-CLEAR

4) Solenoid power supply switch S1   OFF

5) Solenoid trigger switch S2   ON

B. Sampling Procedure

1) Trigger oscilloscope sweep and wait until sweep
   is at the center of the CRT.

2) Close the Solenoid power supply switch S1. When
   S1 is shut, the oscilloscope will show an
   additional trace. This third trace is used to
   determine the closure time relative to the
   presence of gas jets and bubble eruptions. An
   example of a typical oscilloscope trace is shown
   in Fig. 14.

3) Open the solenoid trigger switch S2. This
   reduces the current to the solenoid to prevent
   overheating. The maximum allowed time to let S2
   remain closed is five (5) seconds.

4) Turn on the air supply to the vacuum system and
   leave on one (1) minute. The exhaust air from
   the venturi on the vacuum system must be directed
   into the purge line in an oscillatory manner.
   This will agitate the particles within the trap

51
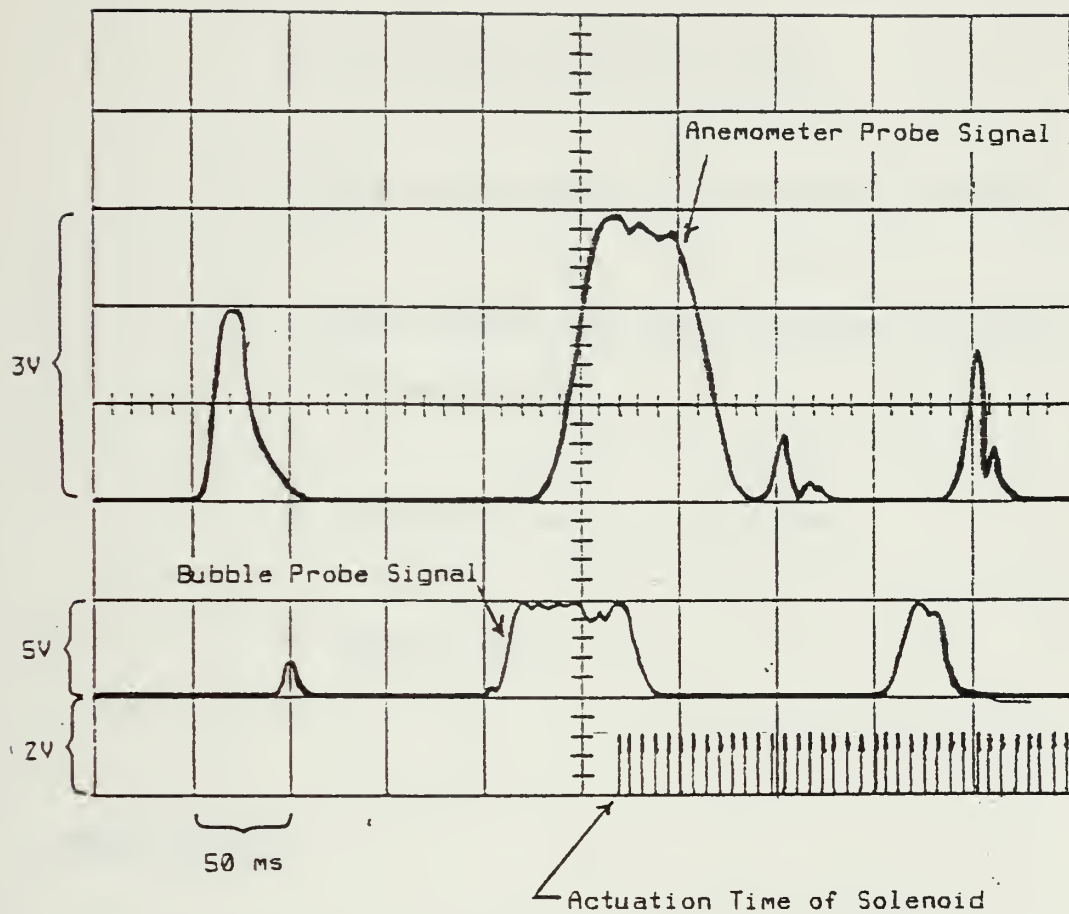
Fig. 14   Typical Oscilloscope Trace Obtained
           During Sampling Operation.

52

so as to move them into the vacuum line.

5) Turn off the vacuum air supply.

6) Turn off the solenoid power supply switch S1.

7) Remove sample from sample container and place in specimen bottle.

8) Photograph trace on oscilloscope.

9) Repeat from A.

Sample Analysis

Sample Weight Determination

Each sample obtained was weighed, using a Torsion Balance Co. TORBAL scale, to an accuracy of 0.01 grams. The average value and standard deviation was then determined for each set (specific height and velocity) of samples. The weight of particles in a completely filled sample trap was also determined for void determination. These results are listed in Appendix I.

Determination of Particle Size Distribution

To determine the particle size distribution which occurs at various heights for a specified gas velocity, three (3) samples from each set of data at a specified height and velocity, and from the bulk bed material were analyzed using a Zeiss Videoplan 2 Image analyzer. The software used was the "Image Analysis System MOP-Videoplan" distributed by KONTRON Electronics Group.

For each sample selected, a microscope slide was prepared using double sided adhesive tape on which a portion of the selected sample was placed. To ensure a sharp contrast was achieved, each slide was backed with white paper. The sample was then placed under a Zeiss microscope to which the image analyzer was connected via a vidiocon tube. The magnification used was 50X which provided an average view of about 8 particles at a time. The analyzer was then used to analyze the partices present on each slide of interest. The mode in which the image analyzer was used was the equivalent diameter mode. This mode determined the cross sectional area of each particle sampled and calculated the diameter of a circle with the same area. When a data set was completed, the data was analyzed for particle size distribution. The resulting output (Appendix J) consists of a particle count vs particle size histogram, a cumulative frequency plot and a classification data list. A gaussian distribution fit for the data is also plotted on the histogram and cumulative frequency

plots. The X axis of the plots are normalized with a range of zero (0) to four (4). To determine the actual diameter of the particle in microns for a given normalized value, the normalized value must be multiplied by the conversion factor 248.887.

CHAPTER IV

COMPUTER MODEL

Introduction

This chapter descibes the theory, logic flow and testing of a particle trajectory computer model to predict the particle loading in the freeboard due to erupting buubles. The program, listed in Appendix L, is written in HP BASIC 2.0 and was run on a Hewlett Packard 9816 microcomputer. The output from the model is discussed in chapter VI and compared with experimental results. An in depth analysis of the program logic and structure is given in Appendix L.

Model Theory

The model developed here, is based on calculating the trajectory of a single particle as it is ejected from the bed surface and is acted upon by gravitational and drag forces. The drag force is due to the difference in absolute particle and air velocities. The air velocity is a combination of the initial jet velocity produced when a bubble bursts, and the superficial bed velocity. To ensure that the particle drag is calculated accurately, the following drag coefficient correlation given by White [17] was used.

$$Cd = \frac{24}{Re} + \frac{6}{1 + \sqrt{Re}} + 0.4 \tag{3}$$

where:

Cd = Drag coefficient for sphere

Re = Reynolds number

Eqn 3 is valid over the range $0 < Re < 10^5$. To calculate the particles position and velocity, the computer uses a forward difference method. Using Newton's Law ($\Sigma F = ma$) the acceleration of the particle due to gravity and drag is determined. Inserting this acceleration into Eqn 4, the particles new velocity is determined.

$$V = Vo + a \, t \tag{4}$$

where:

V = Particles new velocity

Vo = Particles present velocity

a = Acceleration of particle

t = Time increment of calculation

To determine the particles new position, the velocity calculated in Eqn 4 is inserted into Eqn 5.

$$H = H_0 + \frac{(V_0 + V)\, t}{2} \qquad (5)$$

where:
H = Particles new height
H_0 = Particles present height
V_0 = Particles present velocity
V = Particles new velocity
t = Time increment of calculation

Using Eqns 3,4,and 5, the trajectory of the particle is calculated from the time it initially leaves the bed until the time that it returns to the bed.

These calculations are repeated over a range of particle diameters from 80 to 570 microns. By determining the residence time of each particle within a specified height increment (ΔH) above the surface of the bed, a particle density distribution above the bed is determined. The height increment (ΔH) used in the program is 2 cm. At the end of each time step when the height calculation (Eqn 5) is completed, the counter representing the particular 2 cm height increment which the particle is in, is incremented by one. Each particle size has its own set of counters to allow individual particle analysis.

The calculated density distribution is then weighted with the particle size distribution of the bulk bed material since the

58

probability of a given size particle being present at a specified

height is dependent upon the number of particles within the

system. This is accomplished by multiplying each height counter

of a given particle size with the number of particles for that

given size present in the input bed distribution. By summing the

density values for each set of particle diameters at a given

height over the entire freeboard of the bed, the overall particle

density above the bed surface is determined.

The model assumes that all the particles are ejected

perpendicular to the surface of the bed and are initially at a

uniform velocity. Because the model uses single particles for the

analysis, the effects of multiparticle interactions are not

included in the model.

Testing of Program

To evaluate the validity of the program, two tests were

conducted. The first test compared the height solution produced

by the computer with a closed form solution. The second test

involved running the program with different particle diameter and

particle distribution height intervals to ensure that a valid

sample size was being used.

Closed Form Solution

To determine a closed form solution for particle height as a

function of initial particle velocity and superficial velocity Uo,
a force balance was used. The forces acting on a particle are
gravitational and drag. The gravitational force, F1, is simply
the volume of the particle multiplied by the particles density and
the gravitational acceleration, and can be written as:

$$F1 = - \frac{Pp \, \pi \, D^3}{6} \, g \tag{6}$$

where:

F1 = Force due to gravity
Pp = Density of particle
 D = Diameter of particle
 g = gravitational acceleration

In order to get a closed form solution that did not involve
non-linear differential equations, Stokes flow was used for the
closed form solution only. The computer model used the Stokes
equation only to compare results with the closed form solution,
afterward, Eqn 3 was used. Using the Stokes drag coefficient
relation, the drag force on a particle can be determined as:

$$F2 = 3 \, (Uo - Up) \, \mu \, D \tag{7}$$

where:

F2 = Force due to drag
Uo = Superficial bed velocity
Up = Velocity of particle
 μ = Absolute viscosity of air
 D = Diameter of particle

By inserting Eqns 6 and 7 into Newton's Law ($\sum F = ma$) and simplifying, the following differential equation is obtained:

$$\ddot{X} + C_1 \, \dot{X} = C_2 \tag{8}$$

where:

$\ddot{X}$ = Acceleration of particle

$\dot{X}$ = Velocity of particle

$C_1 = \dfrac{18 \, \mu}{P_p \, D^2}$

$C_2 = C_1 \, U_o - g$

boundary conditions:

1) $t=0$ $\dot{X}=U_o$
2) $t=0$ $X=0$

This second order linear differential equation can be solved using the given boundary conditions with the resulting closed form solution given as:

$$X = C3 + \frac{C2}{C1} \, t - C3 \exp(-C1 \, t)$$

(9)

where:

X = Height of particle

$$C3 = \left[Uo - \frac{C2}{C1} \right] \frac{1}{C1}$$

Using the initial conditions listed in table 2, the solution

obtained using the computer model (maximum height= 15.270 cm, time

to maximum height= 0.275 sec) was identical to three decimal

places with the solution obtained using Eqn 9.

TABLE 2

Superficial Velocity (Uo):   60.96 cm/s (2 ft/s)
Initial particle velocity (Upo): 304.8 cm/s (10 ft/s)
Particle diameter: 200   microns
Particle density: 5000   kg/m^3
Time increment (computer):   0.001 sec
Jet velocity: 0.0   cm/s

List of parameters used to check computer
calculations against closed form solution.

Sample Size Sensitivity Test

To ensure that appropriate sample sizes were used to minimize errors due to coarse sampling intervals, two sensitivity tests were run. One test involved changing the particle diameter interval from 10 microns to 5 microns. The second test changed the height sampling interval (ΔH) from 2 cm to 5cm and then 1 cm. For each of the tests, the same initial conditions were input into the program. Table 3 shows the resulting output from the program listing the initial conditions and the resulting diameter versus maximum height data calculated. Fig. 15 shows a plot of the calculated maximum height vs particle diameter data listed in table 2. Fig. 16 shows the bed particle distribution used for each of the tests.

Fig. 17a shows the entrainment calculation using a diameter interval of 10 microns and a ΔH of 2 cm. Fig. 17b shows the same calculation using a diameter interval of 10 microns and a ΔH of 5 cm. The curve is not as smooth but still retains the same general shape. The peak of the curve shown in Fig. 17b occurs at a height of about 20 cm whereas the peak in Fig. 17a occurs at about 16 cm. A semi-log plot of these curves would show that the slope of the line to the right of the peak would be larger for the data represented by Fig. 17b. The effect of maintaining ΔH at 5 cm but decreasing the diameter interval to 5 microns is shown in Fig. 17c. There is no readily detectable difference between Fig.

63

	cm/s
Mean Bed Velocity=	57.912
Initial Particle Velocity=	97.2312
Peak Jet Velocity=	609.6
Gas Jet Duration=	.02 s

Diameter um	Maximum Height cm	Max Ht Time seconds	Diameter um	Maximum Height cm	Max Ht Time seconds
80	56.1	.292	90	57.0	.290
100	57.2	.297	110	56.8	.302
120	55.8	.305	130	54.4	.307
140	52.7	.307	150	50.8	.305
160	48.8	.303	170	46.8	.299
180	44.7	.295	190	42.7	.290
200	40.7	.285	210	38.8	.280
220	37.0	.275	230	35.3	.270
240	33.7	.264	250	32.2	.259
260	30.8	.254	270	29.5	.249
280	28.2	.245	290	27.1	.240
300	26.1	.236	310	25.1	.232
320	24.2	.228	330	23.3	.224
340	22.5	.220	350	21.8	.217
360	21.1	.213	370	20.4	.210
380	19.8	.207	390	19.2	.204
400	18.7	.201	410	18.2	.199
420	17.7	.196	430	17.3	.194
440	16.9	.191	450	16.5	.189
460	16.1	.187	470	15.7	.185
480	15.4	.183	490	15.1	.181
500	14.8	.179	510	14.5	.178
520	14.2	.176	530	14.0	.174
540	13.7	.173	550	13.5	.171
560	13.2	.170	570	13.0	.168

Table 3   Listing of Input and Resulting Maximum
          Particle Heights with Time to Maximum
          Height. Thes Values Were Used During
          the Increment Sensitivity Tests.

64
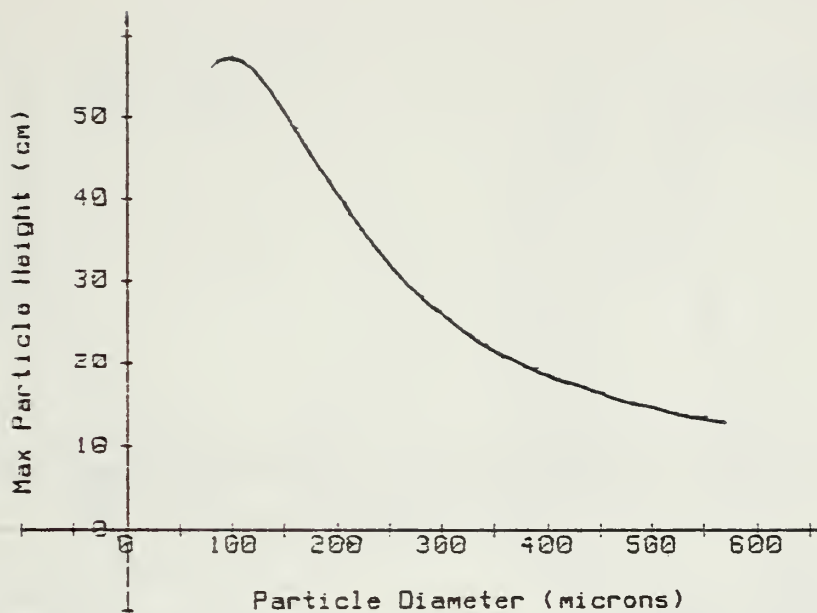
Fig. 15   Maximum Particle Height vs Particle Diameter
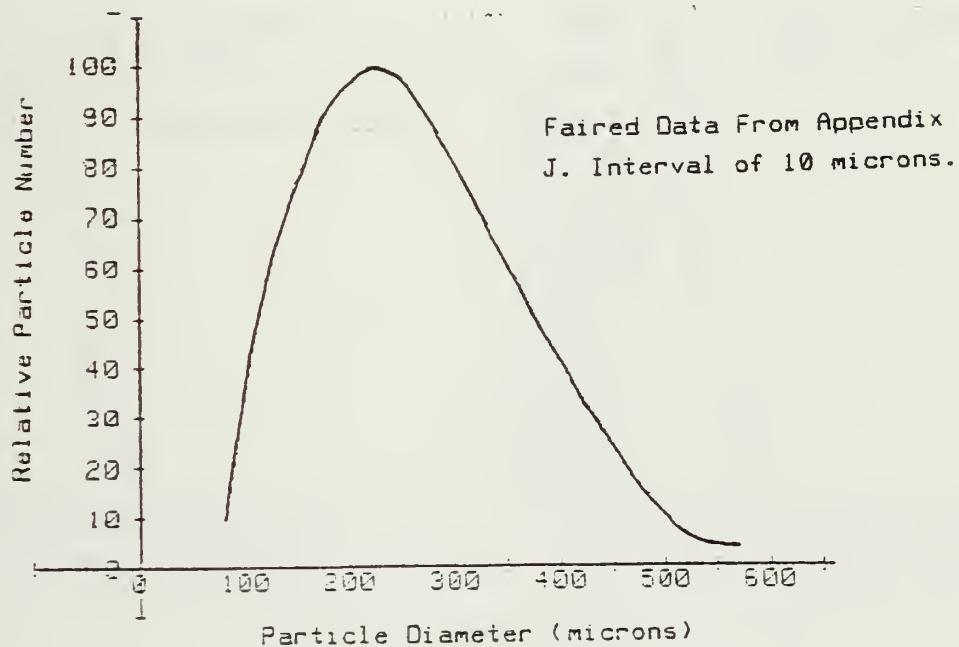
Fig. 16   Particle Size Distribution of Bed Mass Used
           in Increment Sensitivity Analysis.
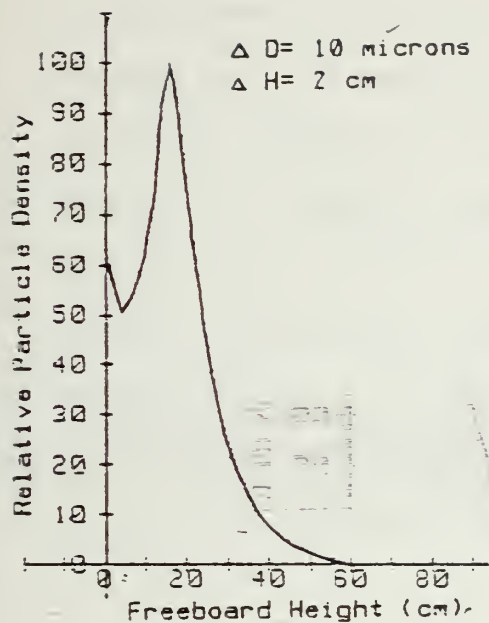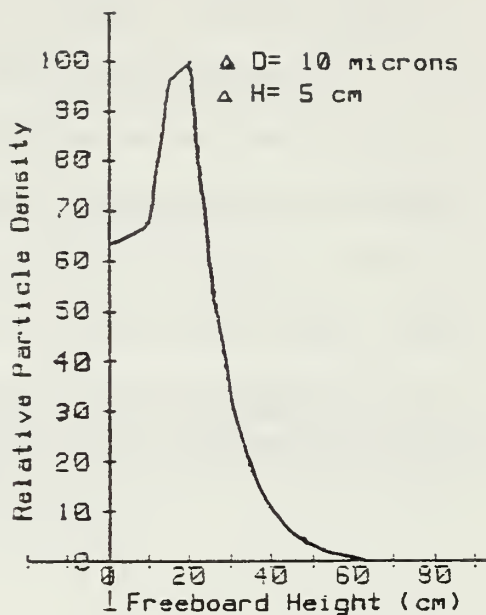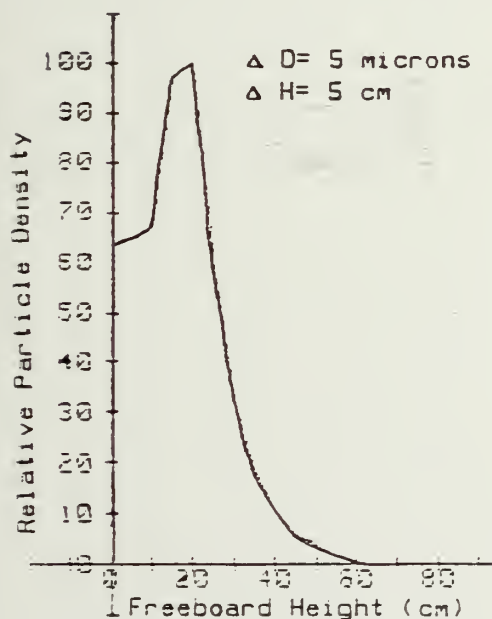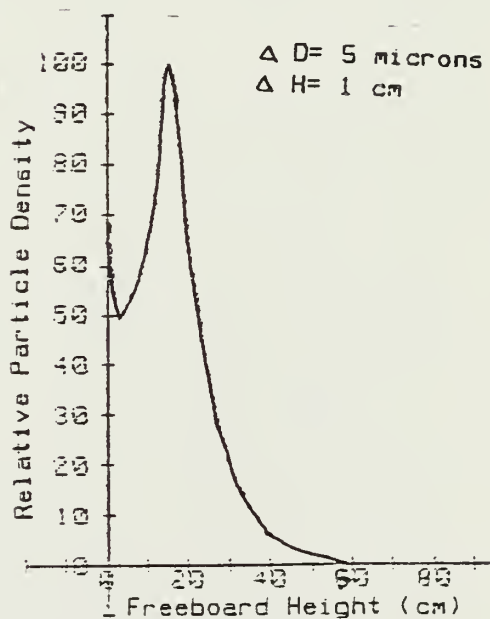
Fig. 17   Plots of Relative Particle Density vs Freeboard
            Height showing the effects of varying Diameter
            Interval and Height Interval.

17c and Fig. 17b. In Fig. 17d, the effect of changing ΔH to 1

cm and diameter spacing to 5 microns is shown. The difference

between Fig. 17a and Fig. 17d is barely noticable and no

detectable change in the slope to the right of the peaks is

present. As a result of this analysis, the program was operated

with a ΔH of 2 cm and a diameter interval of 10 microns. This

reduced the calculation time to half of that required when using a

diameter spacing of 5 microns when the same total diameter span

was used and, as was seen in Figs. 17a and 17d, the difference in

output does not require the finer increment.

CHAPTER V

EXPERIMENTAL RESULTS AND DISCUSSION

Minimum Fluidization Velocity

Fig. 18 is a plot of mean bed velocity (Uo) vs pressure drop through the bed (Pb). The velocity values were determined using the program in Appendix G and the pressure data listed in Appendix I. From this plot, the minimum fluidization velocity (Umf) for the bed conditions used during this study is determined to be 0.15 m/s (0.5 Ft/sec).

Entrainment Analysis

Table 4 lists the averaged sample weights and their standard deviations for the samples (Appendix I) collected by the sampling apparatus. Looking at the standard deviation of the sample groups, the standard deviation is fairly large compared to the average values. However, visual observations of the fluidized bed in operation would suggest that a larger standard deviation would be expected. The short sample cycle (2 ms) and the bubble burst activity in the bed are the main reasons for this conclusion. The average standard deviation is 29 % of the average sample weight
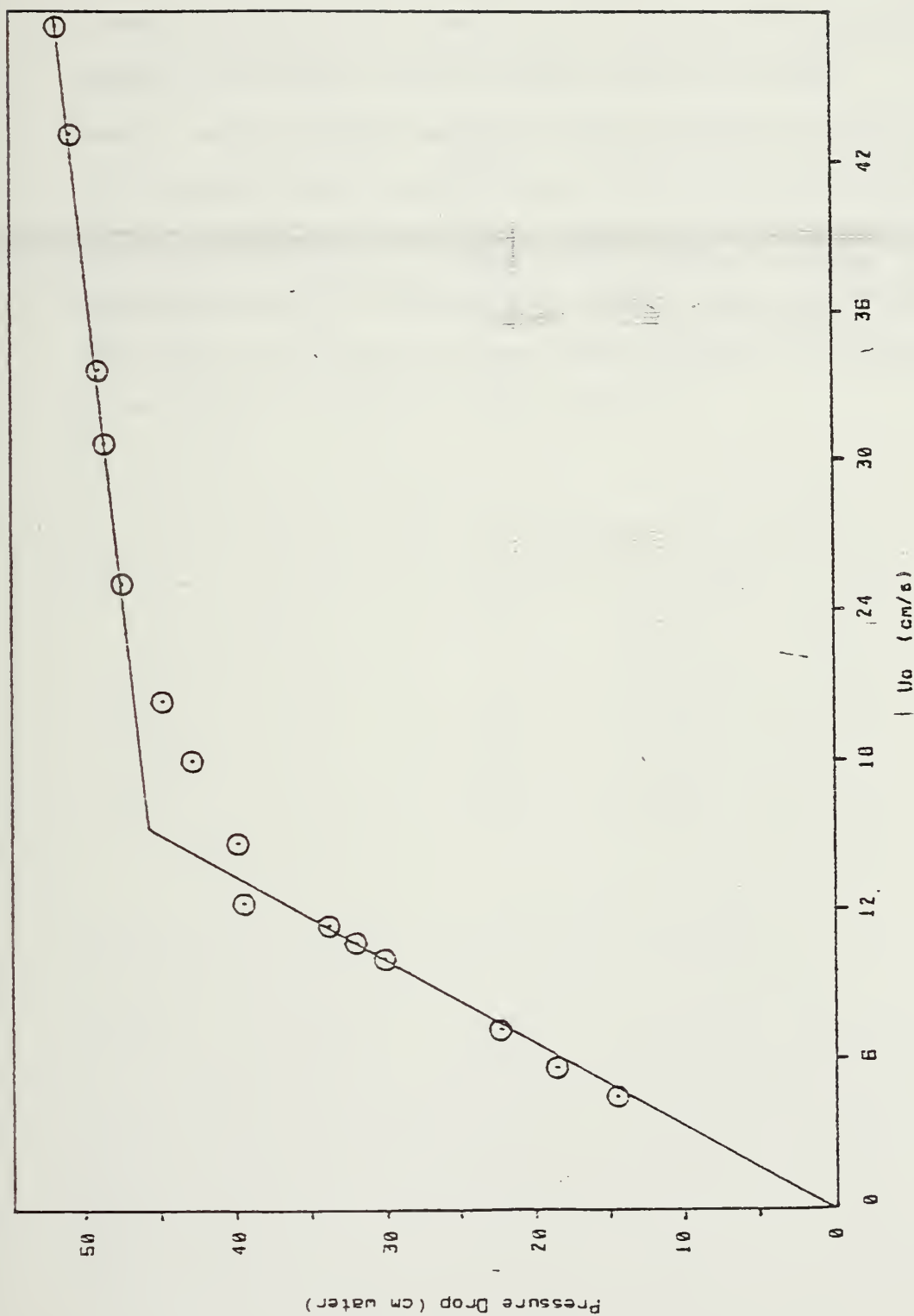
Fig. 18 Plot of Pressure Drop Across Bed vs Uo. The Estimate of Umf from this Plot is 15.2 cm/s (0.5 ft/s).

69

and the range extends from 68 % of the average for the sample set
numbers 106 thru 115 to only 7 % of the average for the samples
285 thru 295. This variation is believed to be due to the nature
of the bubble activity within the bed. It would appear that when
a bubble erupts at a time just prior to closure of the trap, a
sample weight greater than the average would be obtained.
However, when no bubble has been present, the material caught by
the trap should comsist mainly of particles returning to the bed
and therefore be below the average weight caught. Table 4 also
shows the density of each sample collected. These values were
determined by dividing the averaged sample weights by the volume
of the sample trap which is 43.02 cubic cm.

TABLE 4

Superficial Bed Velocity (Uo):   58.1 cm/s (1.905 ft/s)
Non-dimensionalised velocity (Uo/Umf): 3.81

Sample Numbers	Height Above Bed (cm)	Average Weight (grams)	Standard Deviation (grams)	Average Density (grams/cm)
286-295	3.8	7.22	0.51	1.68 (-01)
246-255	7.6	4.48	0.72	1.04 (-01)
116-125	12.4	2.41	0.76	5.60 (-02)
166-175	17.8	1.08	0.16	2.51 (-02)
76-85	22.2	1.32	0.23	3.07 (-02)
176-185	31.1	0.31	0.10	7.21 (-03)

Superficial Bed Velocity (Uo):   48.3 cm/s (1.585 ft/s)
Non-dimensionalised velocity (Uo/Umf): 3.17

Sample Numbers	Height Above Bed (cm)	Average Weight (grams)	Standard Deviation (grams)	Average Density (grams/cm)
276-285	5.1	4.35	1.05	1.01 (-01)
236-245	8.9	1.88	0.22	4.37 (-02)
96-105	13.6	1.36	0.32	3.16 (-02)
156-165	19.1	0.60	0.12	1.39 (-02)
56-65	24.1	0.92	0.36	2.14 (-02)
186-195	31.8	0.18	0.04	4.18 (-03)

Superficial Bed Velocity (Uo):   39.5 cm/s (1.297 ft/s)
Non-dimensionalised velocity (Uo/Umf): 2.59

Sample Numbers	Height Above Bed (cm)	Average Weight (grams)	Standard Deviation (grams)	Average Density (grams/cm)
266-275	5.7	1.31	0.37	3.05 (-02)
226-235	9.5	0.62	0.17	1.44 (-02)
126-135	14.3	0.28	0.08	6.51 (-03)
136-145	19.7	0.08	0.04	1.86 (-03)
86-95	24.8	0.09	0.05	2.09 (-03)
196-205	32.4	0.06	0.02	1.39 (-03)

TABLE 4 (cont)

Superficial Bed Velocity (Uo):   35.4 cm/s (1.161 ft/s)
Non-dimensionalised velocity (Uo/Umf):   2.32

Sample Numbers	Height Above Bed (cm)	Average Weight (grams)	Standard Deviation (grams)	Average Density (grams/cm)
256-265	6.4	0.63	0.13	1.46 (-02)
216-225	10.2	0.32	0.04	7.44 (-03)
106-115	14.9	0.22	0.15	5.11 (-03)
146-155	20.3	0.02	0.01	4.65 (-04)
66-75	26.0	0.12	0.04	2.79 (-03)
206-215	33.0	0.01	0.004	2.32 (-04)

List of experimental data showing sample averages, standard
deviations, heights, and velocity conditions measured.
Density values are calculated by dividing the average sample
weight by the sample trap volume.

Fig. 19 shows the relationship between the average particle
density caught in the sample trap and the sample trap height above
the bed surface as a function of Uo/Umf.

For the relatively low fluidization velocities used during
the data measurements, (maximum Uo/Umf = 3.81) the freeboard
height can be assumed infinite. Using this assumption implies
that all of the particles return to the bed and none are
elutriated, ie complete reflux. Under these conditions, the
following equation has been suggested by Lewis et al [3] and Kunii
and Levenspiel [1] to model the particle loading within the
freeboard.
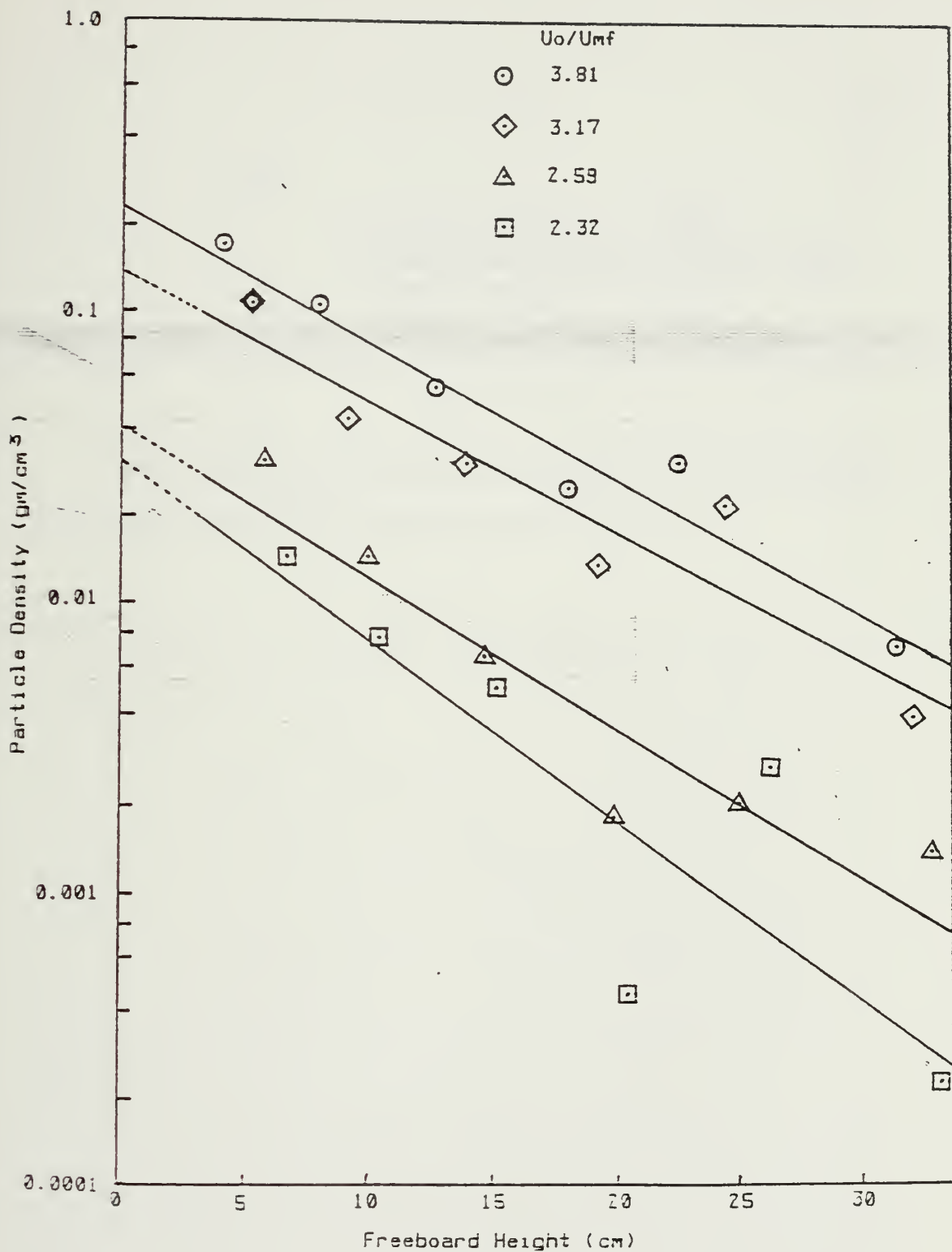
Fig. 19   Plot of Particle Density vs Freeboard Height
as a Function of Uo/Umf. This data was
Obtained Using the Particle Sampler.

73

$$Pr = Po \exp\{-a\ 1\} \qquad\qquad (10)$$

where:

     Pr = Particle density at height 1
     Po = Particle density at (+)bed surface
      a = Characteristic particle decay length
      1 = Height above bed surface

Table 5 shows the values for the parameters Po and a obtained by linear regression for the curves shown in Fig. 19.

TABLE 5

Uo/Umf	Po	a	Correlation Coefficient
3.81	0.238	0.1097	0.979
3.17	0.137	0.1029	0.944
2.59	0.040	0.1181	0.937
2.32	0.031	0.1399	0.857

$$Pr = Po \exp\{-a\ l\}$$

Results of linear regression analysis for particle loading density (grams/cm) vs height above the bed surface (cm).

The parameter Po physically represents the particle loading density which would be obtained if the sample were taken at the surface of the bed. This is not necessarily the case as is indicated by the computer model which is discussed in chapter VI, but is only a parameter descibing the particle loading distribution in the region of the data obtained. The dashed lines below freeboard heights of 4 cm indicate the region in question. The parameter a is a characteristic length of decay for the particle flux.

A correlation between the values for Po in table 5 and Uc/Umf is shown in Fig. 20. This plot shows that Po is closely related with Uo/Umf. Po varies with (Uo/Umf - 1) approximately to the 2.9

75
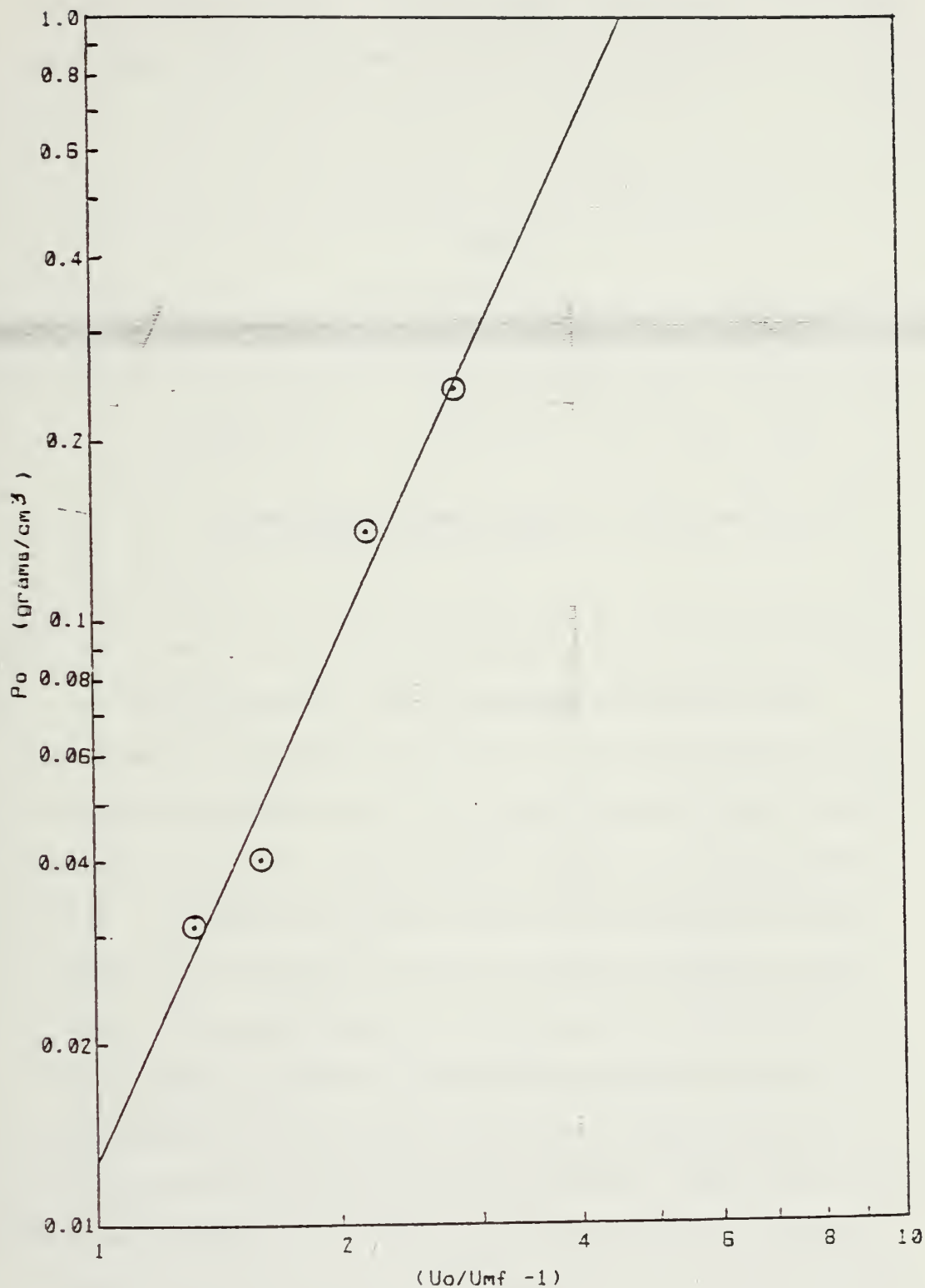
Fig. 20   Plot of Po vs (Uo/Umf -1) Showing Strong
Dependence of Po on Uo.

power, where as Walsh et al [10] determined the coefficient to be
about 2.1. Wen and Chen [5] reported a correlation for particle flux
which is proportional to bubble diameter and (Uo/Umf - 1) to the
5/2 power. These correlations are listed in table 6.

TABLE 6

Present work $B = 0.13 (Uo/Umf - 1)$ kg/ m   sec
       Wen and Chen $B = 1.34 (04) (Uo-Umf)$ kg/ m   sec
       Walsh et al $B = 18 (Uo - Umf)$ kg/ m   sec

       Comparison of least square fit relations for Po
       as functions of Uo and Umf.

The differences in these correlations are due to the
different bed configurations in which the data was taken and the
measurement technique used. The present work utilized a bed with
a relatively closely spaced tube configuration and steel grit
(S.G. 8.1, median size 230 microns) for the bed mass. Both
ascending and descending particle fluxes were captured in the
sample. The work of Walsh et al [10], used a bed with two (2)
widely spaced horizontal serpentine tubes and Ottawa sand (S.G.
2.6, median size 755 microns). Also, only descending particle
flux was used in determining their relations. The correlations of
Wen and Chen [5] are a result of studies conducted on previous
research using cylindrical column beds and low mass bed materials

77

(S.G. 0.8 - 2.6). The data for these analysis is based mainly on pressure measurements.

It has been observed by Lewis et al [3] and Wen and Chen [5] that a is not a strong function of Uo. Both of these studies recommend that the characteristic particle decay length, 1/a, could be approximated by an expression of the form:

$$1/a = C \; Uo \qquad\qquad\qquad (11)$$

Table 7 is a list of correlations obtained by other studies and in the present work. The study by Lewis et al [3] was conducted with 75 micron glass spheres in a cylindrical bed. Fig. 21 shows the relationship between 1/a and Uo in the present work.

TABLE 7

Present work	1/a = (0.19 ± 0.03 s)Uo	m
Lewis et al	1/a = (1.42 ± 0.14 s)Uo	m
Wen and Chen	1/a = (0.25 ± 0.09 s)Uo	m
Walsh et al	1/a = (0.32 ± 0.05 s)Uo	m

Comparison of least square fit relations for
1/a as functions of Uo (m/s).
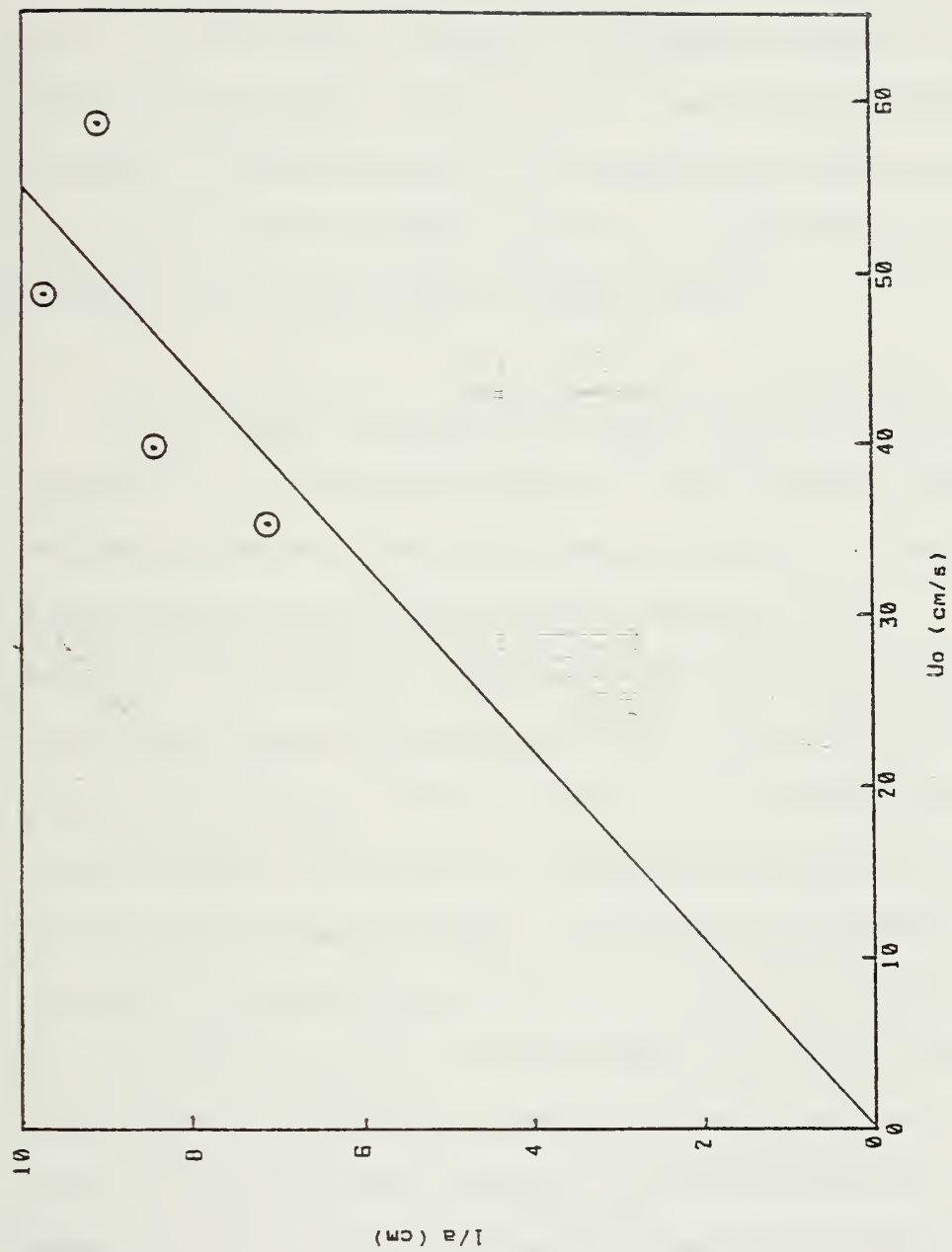
Fig. 21   Plot of 1/a vs Uo Showing Linear
           Dependence of 1/a on Uo.

Particle Size Distribution

Two methods for determining particle size distribution were
used. The sieve method, described in Appendix E, was used for bed
material analysis only, due to the small sample sizes obtained from
the trap. To analyze the small trap samples, an image analyzer
was utilized. The procedure used with the image analyzer is
described in the experimental procedure chapter.

The sieve data representing bed mass as a function of
particle size, is listed in Appendix E. Fig. 22a shows the bed
mass data converted to particle number as a function of particle
diameter where the interval of particle diameter between
successive measurements is 10 microns. These plots are faired
from the data listed in Appendicies E and J. Fig. 22b shows the
bed mass distribution. The conversion from a mass distribution to
a particle number distribution was calculated assuming that each
particle was spherical in shape. The volume corresponding to a
given particle diameter was multiplied by the particle density to
get a unit particle mass. The mass fraction of the sieve analysis
corresponding to the specified particle diameter was then divided
by the unit particle mass to obtain the representitive particle
number. The overall resulting particle number distribution curve
was then normalized with respect to a maximum value of 100.

The particle size distribution data obtained from the image
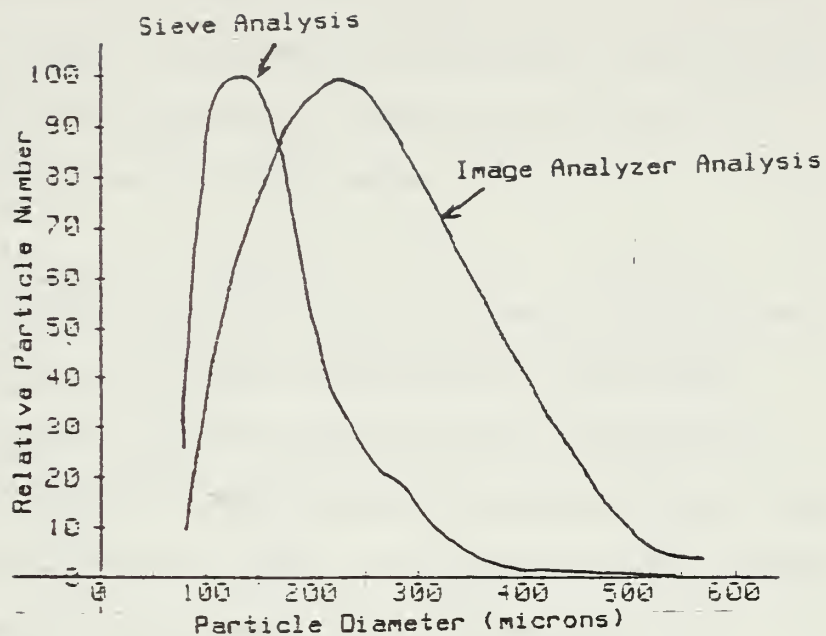
a) Particle Distributions
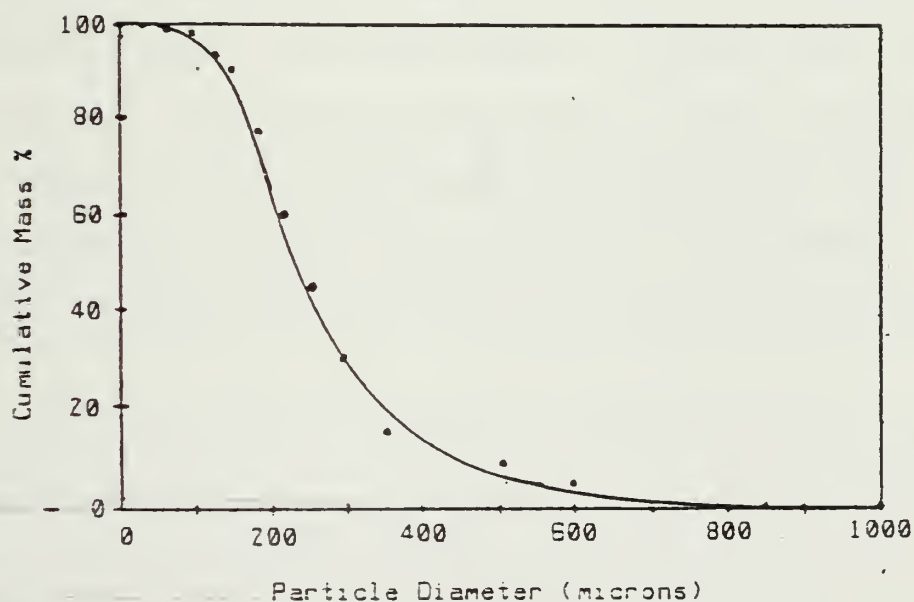
b) Mass Distribution

Fig. 22   Particle Size vs Mass distribution
and Particle Number of Bed Material.

analyzer is listed in Appendix J. The image analyzer was used to analyze the bed mass and sample data from the Uo/Umf = 3.81 data set. The bar graphs and the cumulative percentage plots show the number of particles viewed by the image analyzer plotted as a function of normalized particle diameter.

Fig. 22a shows a plot of the particle number distribution as a function of particle diameter as determined by the image analyzer. The data is normalized with respect to 100 and is compared with the data as determined by the sieve analysis. The descrepancy between the two plots can be explained by the methods used to determine the respective data. The analyzer first determines the cross sectional area of the viewed particle. A circle, having the same cross sectional area, is then calculated. This results in averaging the smaller minimum diameter with the larger maximum diameter of all particles with long cylindrical or ellipsoidal shapes. In the sieve however, a large portion of the particles will pass through the sieve screen by means of the small cross sectional area presented by their longitudinal direction. To be consistant in the following sections, the image analyzer data will be used to correlate all particle density distributions.

The particle size distribution as a function of height above the bed surface was evaluated using the data collected at Uo/Umf = 3.81. The image analyser was used to determine the distribution by viewing three (3) random samples from each of the six (6) height positions. Table 8 lists the various statistical values

for the particle size distribution data obtained (Appendix J).

TABLE 8

Freeboard Height	Average Diameter	Median Diameter	Mode Diameter	Diameter at 50% of Cumulative Number Distribution
(cm)	(microns)	(microns)	(microns)	(microns)
3.8	199	192	142	159
7.6	219	214	187	203
12.3	204	189	162	167
17.8	179	164	154	179
22.2	197	179	152	177
31.1	212	197	194	190

Staistical values for particle number distribution
as a function of freeboard height. A complete
listing of the data is given in Appendix J.

Fig. 23 shows these values plotted against the bed height at
which they were taken. The excursion of points at the 7.6 cm
height is assumed to be due to analysis error. The linear
regression lines for the average and median values show that they
are weak functions of collection height. For the particle
diameter values representing the mode and the 50% point on the
cumulative percentage plot, the linear regression lines show a
stronger dependence on collection height.
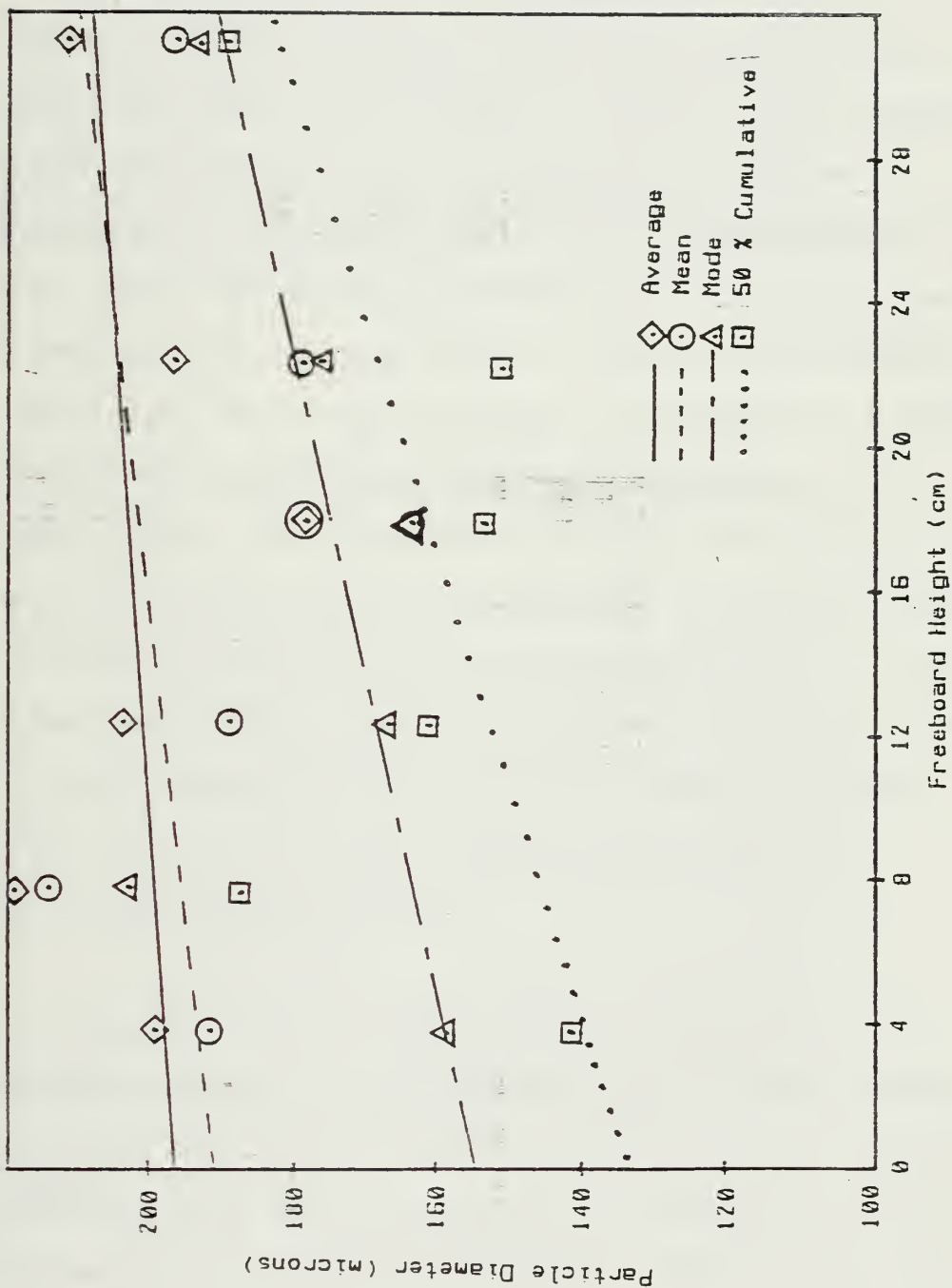
Fig. 23   Analysis of Variation of Particle
Size vs Freeboard Height.

84

Oscilloscope Trace Analysis

Figs. 24 thru 27 show examples of the oscilloscope traces
given in Appendix K. Figs. 24 and 25 represent the traces
obtained during low Uo coditions. Under these conditions, the
normal bubble probe output is high (+ 5 volts dc). When a bubble
errupts, particles are thrown from the surface of the bed and
eclipse the light path at the tip of the probe (trace goes to
zero). Figs. 26 and 27 represent the traces obtained at higher
Uo conditions when the bubble probe is normally eclipsed (bubble
probe output is low, zero) by particles. The presence of a bubble
is detected by a high output from the bubble probe due to the
bubble creating a void through which the light beam can pass. The
anemometer output just above the bubble probe is used to determine
the velocity of the gas jet leaving the erupting bubble. As seen
in the figures, there is not always a bubble associated with a gas
jet and vice versa. This is due to the anemometer probe being
slightly offset from the bubble probe as described in the
experimental procedure section.

The gas jet in Fig. 24 is delayed 5 ms and the gas jet in
Fig. 25 is delayed 35 ms from the point where the bubble traces
begin their excursion to the zero (eclipsed) condition. Since the
seperation between the bubble probe and the anemometer is 1 cm,
this results in an estimated jet velocity of 200 cm/s (Fig. 24)
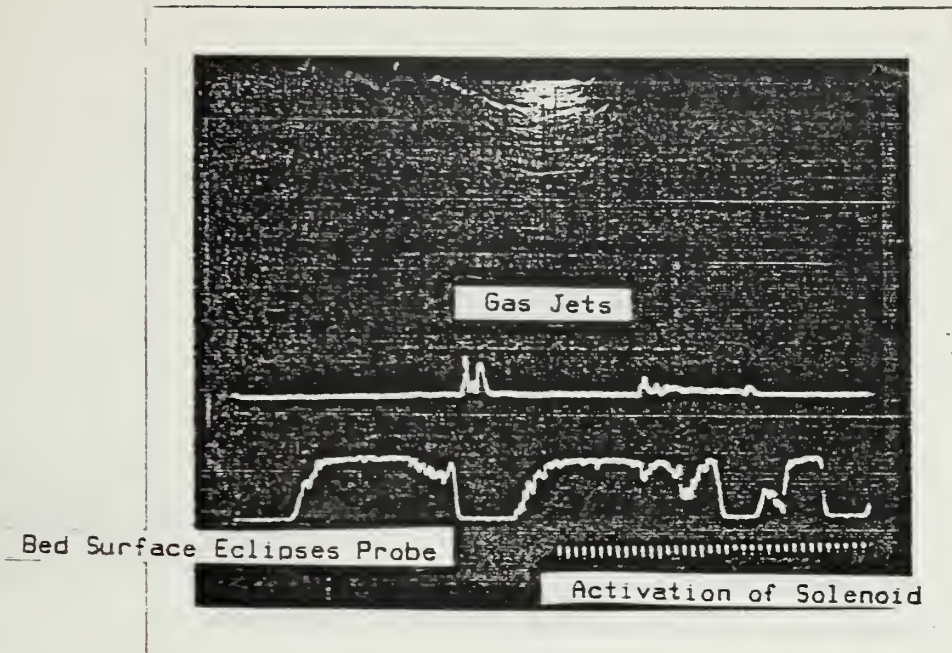
Fig. 24   Oscilloscope Trace of Bubble Probe,
            Anemometer Probe, and Solenoid
            Actuation at Low Uo.
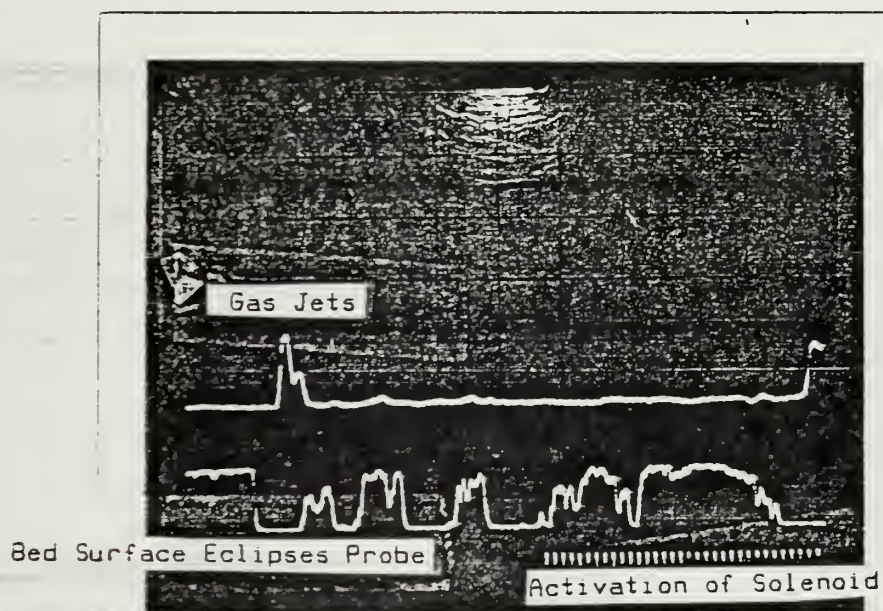
Fig. 25   Oscilloscope Trace of Bubble Probe,
            Anemometer Probe, and Solenoid
            Actuation at Low Uo.
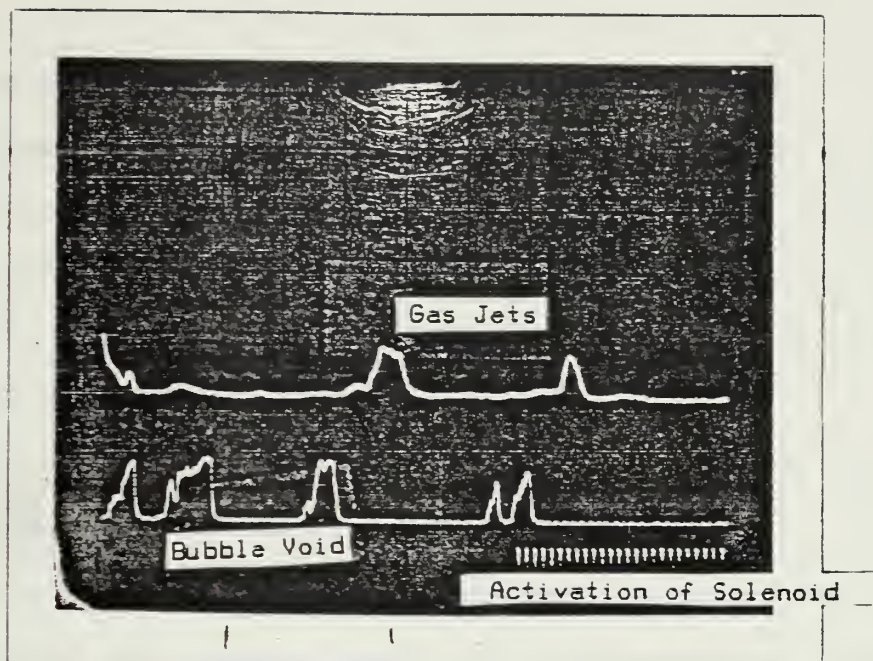
Fig. 26   Oscilloscope Trace of Bubble Probe,
           Anemometer Probe, and Solenoid
           Actuation at Higher Uo.
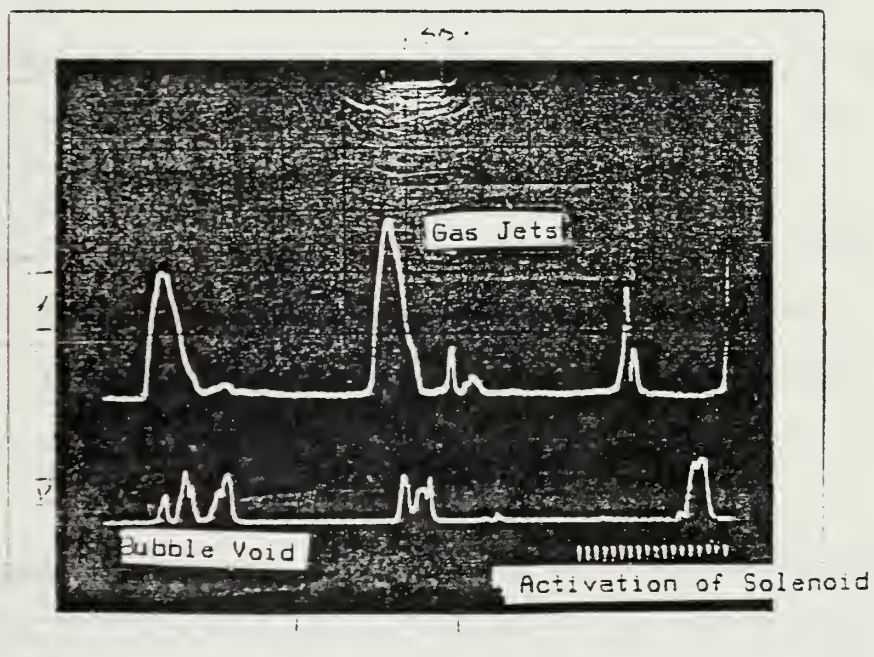
Fig. 27   Oscilloscope Trace of Bubble Probe,
           Anemometer Probe, and Solenoid
           Actuation at Higher Uo.

and 28 cm/s (Fig. 25). Using the calibration curve in Appendix M, the velocities are determined to be 518 cm/s for the jet in Fig. 24 and 792 cm/s for the jet in Fig. 25. The large difference in these values could be due to a bulge in the bed surface from the bubble underneath eclipsing the bubble probe. If this is the case, there would be a delay between the time at which the bubble probe was eclipsed and the eruption of the bubble from the bed surface.

An analysis of Figs. 26 and 27 results in the same discrepancies between velocities calculated from delay times and measured by the anemometer probe. Fig. 27 shows another phenomena which occurs quite frequently. The gas jet appears before the bubble is detected. There are several possibilities which can explain these occurances. First, the bubble occurs off center from the bubble probe. Under this condition, the bubble may erupt and initiate a jet which is registered by the anemometer. The bubble then continues to rise and the side of the bubble is registered by the bubble probe. This explanation can be altered to include bubbles coalescing below the surface. Under this condition, a bubble may be pulled into the vortex of an already erupting bubble and it eclipses the bubble probe.

An analysis of the jet velocities and durations for all the oscilloscope traces in Appendix K, resulted in the data listed in table 9. In later calculations, the values to be used for the jet velocity and duration will be 609.6 cm/s (20 ft/s) and 20 ms

88

respectively.

TABLE 9

	Average		Stnd Dev	
Jet Velocity	689	cm/s	533	cm/s
	22.5	ft/s	18.	ft/s
Jet duration	21.25	ms	13.22	ms

Average and standard deviation of jet velocity
determined from oscilloscope traces in
Appendix K.

Sample Weight Versus Bed Activity Correlation

The main purpose of inserting the bubble and anemometer probe
beneath the sampling apparatus was to determine whether a
correlation exists between the sample weight collected and the
presence of bubble eruptions and gas jets. To evaluate the
photographs taken of the oscilloscope traces (Appendix K), the
following information was required:

A. The average velocity of the particles as they
travel from the bed surface to the trap.

B. The distance the particle must travel to reach
the trap.

C. The closure time of the trap relative to the
bubble eruptions and gas jets.

The average particle velocity was calculated by determining the average particle size and using the height output from the computer trajectory model. The average particle size as determined by the image analyzer was 180 micons. To determine the average velocity using the model, the following initial conditions were input to the program:

Superficial velocity (U_o) = 57.9 cm/s (1.9 ft/s)

> This was the actual velocity measured during sampling.

Jet velocity (U_j) = 609.6 cm/s (20 ft/s)

> This value was determined from the anemometer data.

Jet duration (t jet) = 20 ms

> This value was determined from the oscilloscope traces.

The height attained by a 180 micron particle, as determined by the model with the above conditions is 44.7 cm in 0.295 seconds. This results in an average velocity of 44.7/0.295 = 151.5 cm/s (4.97 ft/s).

The distance a particle must travel to reach the center of the trap from the bed surface is obtained from the data listed in Appendix I. Since trap height is measured from the bed surface to the bottom of the trap, 4 cm (0.13 ft) must be added to the trap

heights to obtain the distance to the center of the trap. The
total time required for the particles to leave the bed surface and
arrive at the center of the trap can now be determined. Table 10
shows the transit time for each set of data for which the
oscilloscope traces were photographed (Appendix K).

TABLE 10

Data set Number	Trap Height Bottom (cm)	Trap Height Center (cm)	Total Transit Time (ms)	Time Before Actuation (ms)
56-65	24.13	27.13	179	136
66-75	26.03	30.03	198	155
76-85	22.23	26.23	173	130
86-95	24.76	28.76	190	147
96-105	13.65	17.65	116	73

List of transit times for particles traveling from
the bed surface to the center of the trap. The time
prior to actuation of the sample trap is also shown
(Total time - 42.6 ms).

The total closure time of the sampling apparatus (closure of
solenoid power supply switch S1 until trap is shut) is determined
in Appendix D to be 42.6 ms. This value is subtracted from the
particle transit time to obtain the time before actuation in which
particles leaving the bed surface will be caught in the trap.

To determine whether or not a correlation exists between the

91

weight of a sample and the amount of bed activity present in the bed, a weighted analysis was used. Each sample was evaluated three ways. First, if the sample weight was less than the average sample weight, a weight factor (W) of -1 was assigned to it. If the sample weight was greater than the average, a weight factor of +1 was assigned. Second, the oscilloscope trace was analyzed at the point corresponding to the "time before actuation" listed in Table 10. This position is the time before the solenoid power supply trace is present (Fig. 28). If the trace showed signs of a bubble eruption or a gas jet at this point, the position factor (p) was assigned a value of +1. If no activity was present, the position factor was assigned a value of -1. Third, each trace was analyzed again at the "before actuation time" but bed activity within a +/- 25 ms region was counted. If there was bed activity within this region, the region factor (r) was assigned the value of +1. If no activity was present, the region factor was assigned the value of -1. The following equation was used to assign a correlation factor to each sample:

$$Q = W\,p + W\,r \qquad\qquad (10)$$

where:

Q = Correlation factor

W = +1 if sample is > average of data set
    -1 if sample is < average of data set

p = -1 if no activity is present in bed
    +1 if bubble or gas jet activity present
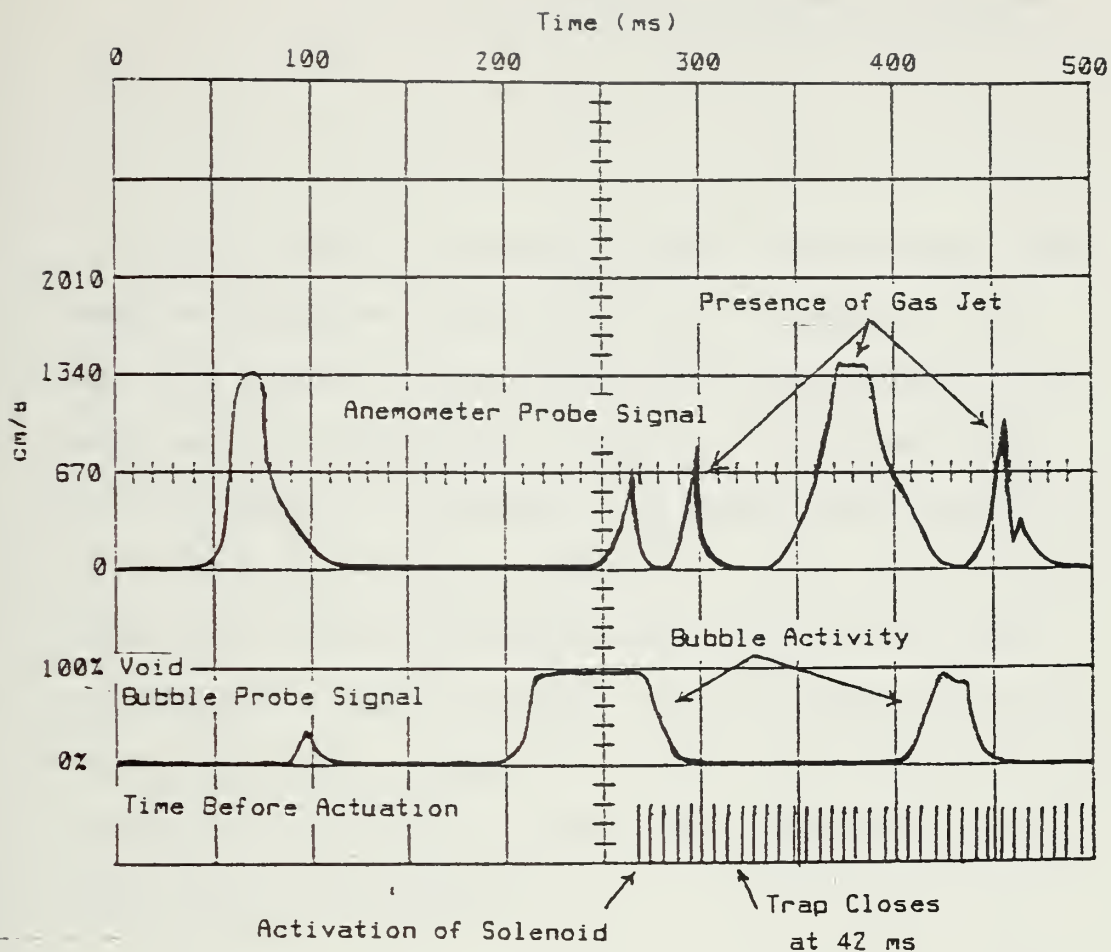
Fig. 28   Typical Oscilloscope Trace During
            Sampling Procedure.

$$r = -1 \text{ if no activity is present } +/- \text{ 25 ms}$$
$$+1 \text{ if activity is present } +/- \text{ 25 ms}$$

Table 11 shows the correlation factor for each sample. The resulting average correlation factor for all samples is 0.32. This value suggests that no correlation can be made between the sample weight and bed activity. There are several explanations for this. Bubbles not detected by the bubble probe or debris from previous bubbles returning to the bed surface can influence the sample weight by increasing the amount of particles collected. Also, bubbles of smaller size have a smaller velocity and would therefore produce a particle stream which is either slower or just delayed in leaving the bed surface. This would result in lower sample weights than expected.

TABLE 11

Sample Number	W	p	r	Q
56	1	1	1	2
57	-1	1	1	-2
58	1	1	1	2
59	-1	-1	-1	2
60	1	-1	-1	-2
62	-1	1	1	-2
63	1	1	1	2
64	-1	-1	-1	2
66	-1	-1	1	0
67	1	1	1	2
69	-1	1	1	-2
70	-1	1	1	-2
77	1	1	1	2
79	-1	1	1	-2
83	1	1	1	2
84	1	1	1	2
86	-1	-1	1	0
88	1	1	1	2
89	-1	1	1	-2
90	-1	-1	1	0
92	-1	-1	1	0
93	1	1	1	2
94	-1	-1	1	0
95	1	1	1	2
96	-1	-1	1	0
97	-1	-1	-1	2
98	1	-1	1	0
99	1	-1	-1	-2
100	1	-1	-1	-2
101	1	1	1	2
102	-1	-1	1	0

Average = 0.32

List of samples and their correlation parameters. The
resulting average value for Q indicates that no
correlation can be made from the data obtained to
indicate by sample weight whether or not any bed
activity occured below the sample trap.

CHAPTER VI

TRAJECTORY MODEL RESULTS AND DISCUSSION

Selection of Baseline Parameters

The input to the model consists of the following five (5) parameters:

1) Superficial bed velocity (U_o)

2) Initial particle velocity (U_{po})

3) Peak gas jet velocity (U_j)

4) Gas jet duration (t_j)

5) Particle distribution of the bed mass

The baseline values for each of these inputs was determined to be as close to the actual experimental bed conditions as possible.

Superficial Bed Velocity

The superficial bed velocity was determined directly from the experimental data. For the bed conditions discussed in this section, the superficial velocity used is the same as the highest velocity condition under which the particle sampler was used. The superficial velocity within the bed for these samples was

calculated to be 57.9 cm/s (1.9 ft/s).

Initial Particle Velocity

To determine the initial velocity of the particle, it was
assumed that the particle was located at the nose of a bubble and
would therefore have the bubbles velocity. To determine the
bubble velocity, Kunii and Levenspiel [1] give the following
equation:

$$Ub = 0.711 [g \; Db]^{1/2} + Uo - Umf \qquad (11)$$

where:

Ub = Bubble velocity
Uo = Superficial bed velocity
Umf = Minimum fluidization velocity
Db = Bubble diameter
g = graviatational acceleration

Observations of the bed material during the sampling
operation suggests that the average bubble diameter present in the
bed is approximately 6 cm (2.4 in). For Uo = 57.9 cm/s, Umf =
15.2 cm/s and Db = 6cm, the bubble velocity is calculated to be
97.2 cm/s (3.19 ft/s). This value was used as the initial
particle velocity for the base line data.

Peak Gas Jet Velocity

To determine an average peak jet velocity, the anemometer
output on the oscilloscope traces (Appendix K) were analyzed. To
determine the relationship between the voltage output from the
anemometer (which is displayed on the oscilloscope) and the actual
gas jet velocity, the anemometer was calibrated in a wind tunnel.
The resulting calibration curve for the anemometer output, as
displayed on the oscilloscope trace, is given in Appendix M. The
average peak velocity of the anemometer traces analyzed in chapter
V was determined to be approximately 609.6 cm/s (20 ft/s).

Gas Jet Duration

To determine an average gas jet duration time to use as a
baseline, the anemometer traces in Appendix K were used. The time
duration of each gas jet analyzed is determined directly from the
oscilloscope trace. The average duration of a gas jet was
determined to be approximately 20 ms in chapter V.

Particle Distribution of the Bed Mass

Two particle distributions for the bed mass were available
for use as the baseline data. Both particle distributions were
determined using the same sample but analyzed using different
analysis techniques. The two methods used are the sieve method
and the image analyzer method, both of which are described earlier

98

in chapter V. The two distributions are shown in Fig. 29.
The bed distribution determined by the image analyzer was used to
be consistent with the particle distributions measured at various
freeboard heights.

Typical Output Using Baseline Parameters

Fig. 30 shows the resulting maximum particle height obtained
as a function of particle diameter for the baseline conditions.
The general shape of the curve is determined by the dominating
force acting on the particle. For large particles, the dominating
force at these air velocities is gravity. Therefore, momentum
(initial particle velocity) is the controlling factor determining
the maximum height attained by the particle. As the particle size
decreases, the proportion of drag force to gravitational force
becomes larger. For the smaller particles, the drag force becomes
the dominate force. The result is that the maximum height
attained by a particle continues to increase as particle size
decreases. This continues until the value of Uo approaches the
terminal velocity of the smaller particles. At this point, the
particle is totally dominated by the air flow in the bed. This is
seen in the small decrease in height attained by particles less
than 110 microns as a result of the particles rapid deacceleration
to Uo after the gas jet has stopped while the larger particles
continue a little higher due to momentum. The particle height
continues to decrease for a short time until Uo becomes equal to

Faired Data From Appendix E and J. Interval of 10 microns.
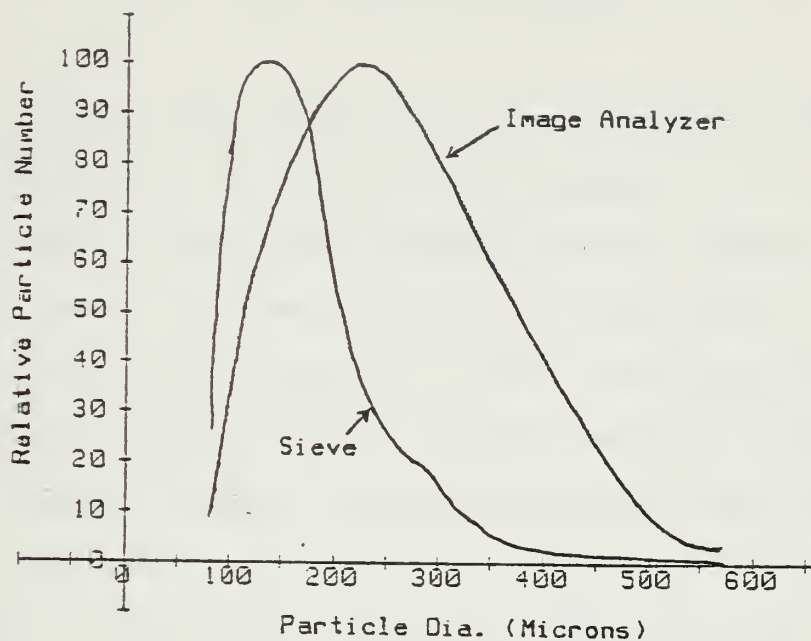
Fig. 29   Relative Particle Number Distributions
            of Bed Material by Sieve and Image
            Analyzer Analysis.
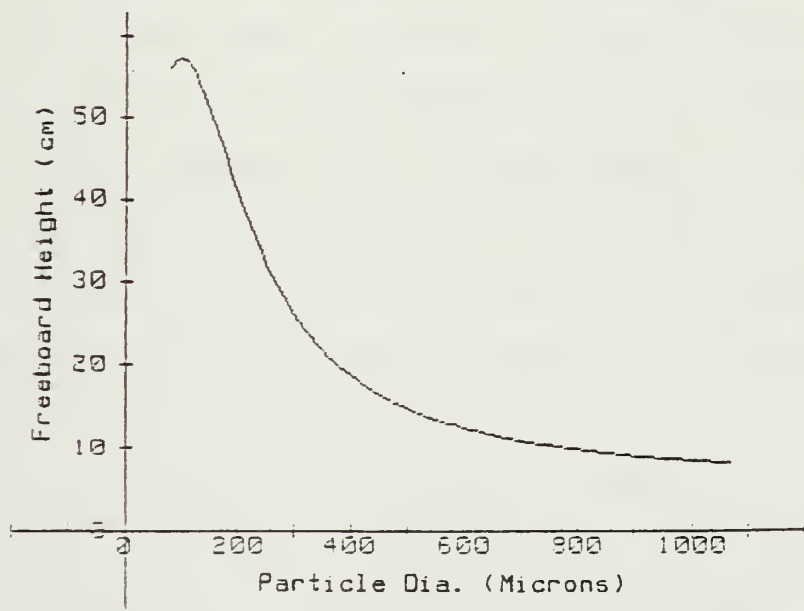
Fig. 30   Maximum Particle Height vs Particle
            Diameter for Baseline Conditions.

100

or greater than the terminal velocity for the remaining particles.
These particles would be elutriated from the system.

Figs. 31 thru 36 show the individual particle densities at
different heights above the bed. All of the heights show an
increase in particle density for the smaller diameter particles.
This is the result of the smaller particles falling at their
respective terminal velocities which is slower than for the larger
particles. The result is that the smaller the particle velocity,
the longer the particle exists within a given height region and
thus, the larger the particle density. It is also due to the
larger number of smaller particles present within the system.

Fig. 37 shows the particle density distribution above the
bed. The two curves represent the effect of varying the range of
particle diameters used in the model. The two ranges are 80 - 570
microns and 80 - 1070 microns. The peak of the 80 - 570 micron
distribution is at about 18 cm of bed height whereas the other
distribution peaks at about 11 cm. The region shown on the graph
below these heights is the area known as the splash zone. The
shape of this part of the curve is due to the initial acceleration
of the particles leaving the surface of the bed by the gas jet.
The particles then begin to slow down due to drag and gravity
resulting in an increase in particle density. The peak on this
curve coincides with the maximum height attained by the largest
particles, and therefore, it can be assumed that the change in
slope is due to the loss of particles as they return to the bed.

Fig. 31   Relative Particle Number vs Particle
           Diameter for Baseline Conditions.
           Freeboard Height of 4 cm.
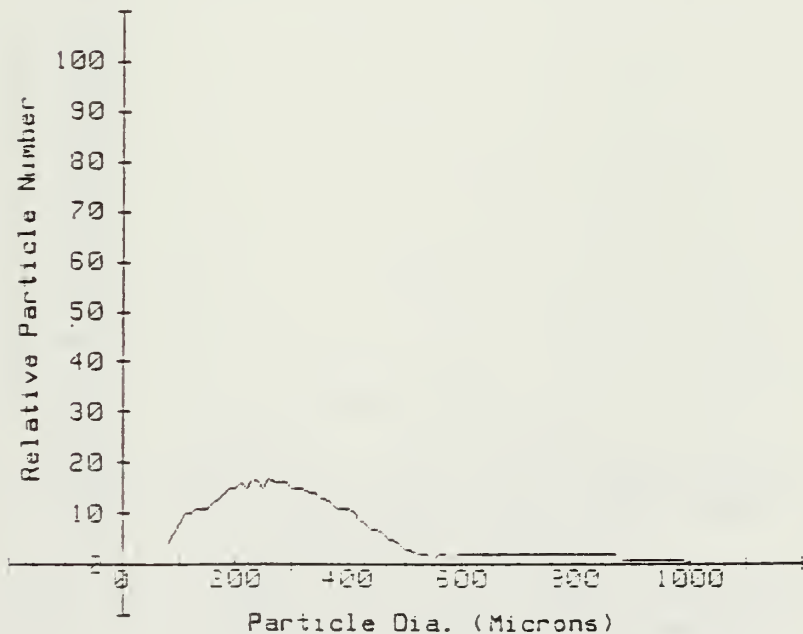
Fig. 32   Relative Particle Number vs Particle
           Diameter for Baseline Conditions.
           Freeboard Height of 8 cm.

102
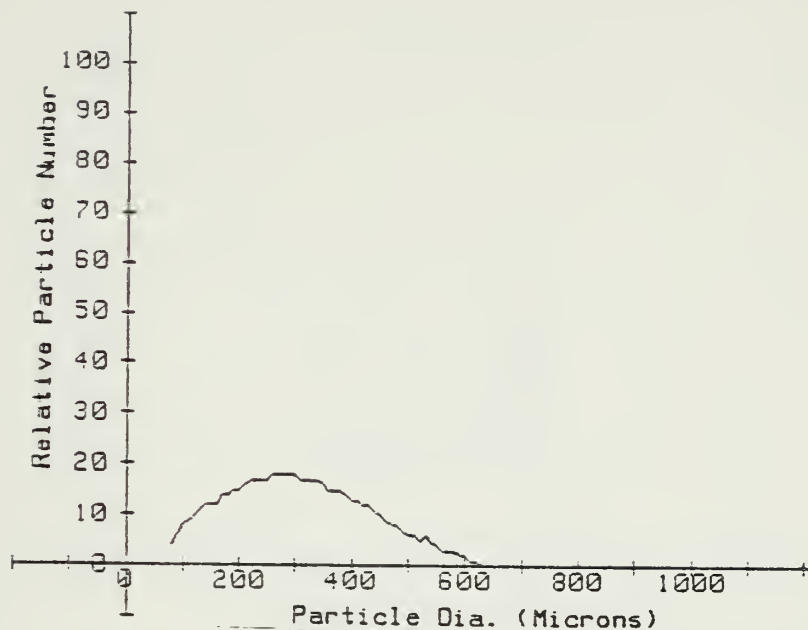
Fig. 33   Relative Particle Number vs Particle
Diameter for Baseline Conditions.
Freeboard Height of 12 cm.
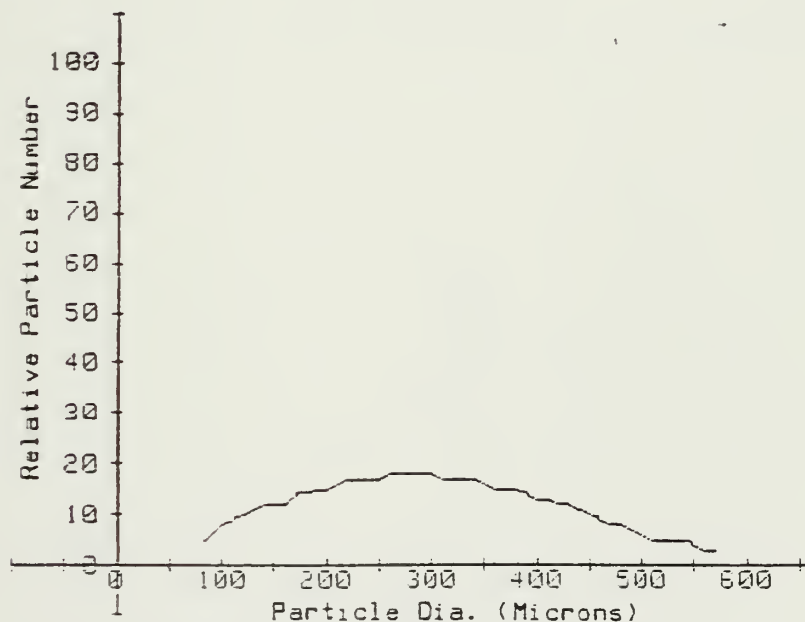
Fig. 34   Relative Particle Number vs Particle
Diameter for Baseline Conditions.
Freeboard Height of 18 cm.

103
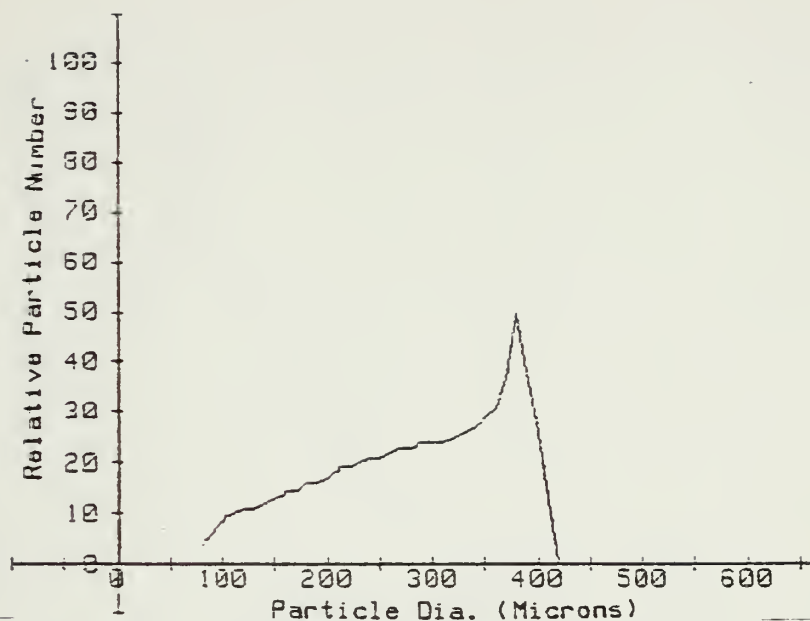
Fig. 35   Relative Particle Number vs Particle
Diameter for Baseline Conditions.
Freeboard Height of 22 cm.
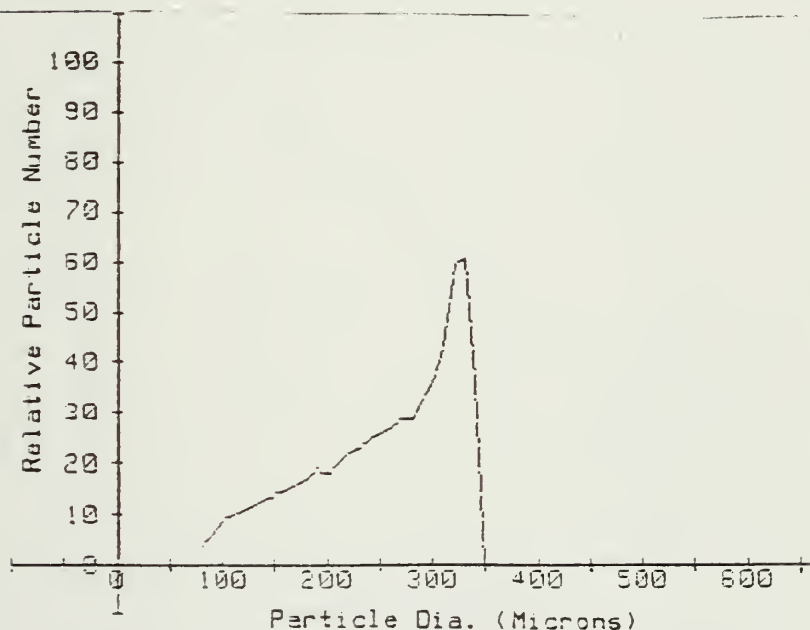
Fig. 36   Relative Particle Number vs Particle
Diameter for Baseline Conditions.
Freeboard Height of 31 cm.

104

Fig. 37   Particle Density/Unit Volume vs
            Freeboard height for Baseline
            Conditions.
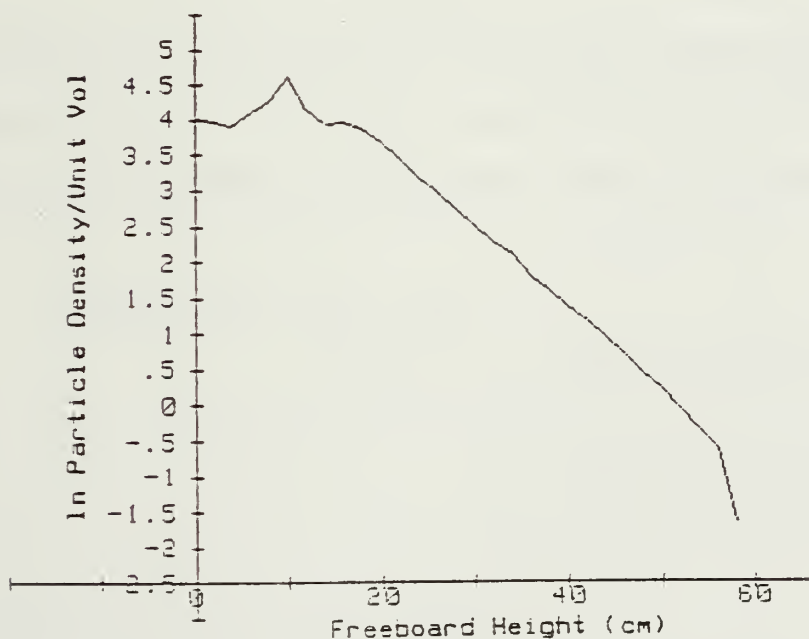
Fig. 38   In Particle Density/Unit Volume
            vs Freeboard height for Baseline
            Conditions.

Fig. 38 is a semi-ln plot of the same data as plotted in Fig. 37. The sharp drop at the right end of the plot is due to analyzing particles with a minimum diameter of 80 microns. Had smaller particles been included, the slope would have approached zero instead of infinity which would model the elutriation of particles. The slope of the line to the right of the peaks shown in Fig. 38, which are located at 11 and 18 cm of height above the bed surface are the same and are approximately -0.117 grams/cm . To decrease computation time, the 80 - 570 micron particle distribution was used in the following sensitivity analysis as the decay slopes are equal.

Model Sensitivity Analysis

An analysis of the change in bed characteristics due to a change in one of the five model input parameters was conducted. The parameters changed and the values used are as follows:

Superficial velocity (Uo):

       Baseline Uo: 57.9 cm/s (1.9 ft/s)

       1.   30.5 cm/s (1 ft/s)

       2.   91.4 cm/s (3 ft/s)

Initial particle velocity (Upo):

       Baseline Upo: 119.2 cm/s (3.19 ft/s)

       1.   61.0 cm/s (2 ft/s)

       2.   152.4 cm/s (5 ft/s)

3.   305.0 cm/s (10 ft/s)

Gas Jet velocity (Uj):

　　　　Baseline Uj:　　609.6 cm/s (20 ft/s)

　　　　　　　　1.   305.0 cm/s (10 ft/s)

　　　　　　　　2.   457.2 cm/s (15 ft/s)

Gas jet duration (tj):

　　　　Baseline tj:　　20 ms

　　　　　　　　1.   10 ms

　　　　　　　　2.   30 ms

Particle distribution of bed mass:

　　　　　　Baseline distribution: Image Analyzer

　　　　　　　　　　　　　　1.   Sieve analysis data

The bed characteristics which are evaluated against the baseline characteristics are:

1.   The maximum height attained by each particle from 80 to 570 microns.

2.   The density of each particle size (80 - 570 microns) at freeboard heights of:

　　　　　　　　a.   4 cm (1.5 in)

　　　　　　　　b.   8 cm (3.1 in)

c. 12 cm (4.7 in)

d. 18 cm (7.1 in)

e. 22 cm (8.7 in)

f. 31 cm (12.2 in)

3. The particle density distribution in the freeboard.

Variation of Superficial Velocity (Uo)

Fig. 39 shows the influence of Uo on the maximum height attained by the particles. As was described in the previous section, the larger particles are dominated by momentum and not drag. This is shown in Fig. 39 by the small change in maximum height attained by the large particles due to a change in Uo. As the particle size decreases, the drag force becomes the dominate force and the effect of Uo on particle height increases. As seen in Fig. 39, a change in Uo produces a moderate change in the maximum height attained by the small particles.

Figs. 40 thru 45 show the effect of Uo on individual particle densities at different heights above the bed. All of the heights show an increase in particle density for the smaller diameter particles as Uo is increased. This is the result of the smaller particles falling at their respective relative terminal velocities which is slower for smaller particles. A decrease in the maximum particle diameter present at a given freeboard height as Uo is decreased can be observed in Figs. 40 thru 45. This
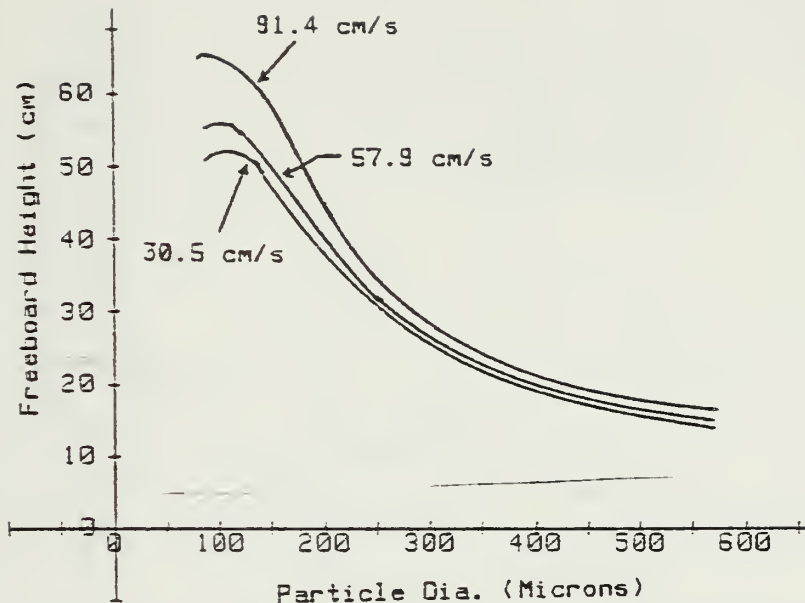
Fig. 39   Maximum Particle Height vs Particle Diameter as a Function of Uo.

Fig. 40   Relative Particle Number vs Particle Diameter as a Function of Uo. Freeboard Height of 4 cm.

109

Fig. 41   Relative Particle Number vs Particle
Diameter as a Function of Uo.
Freeboard Height of 8 cm.

Fig. 42   Relative Particle Number vs Particle
Diameter as a Function of Uo.
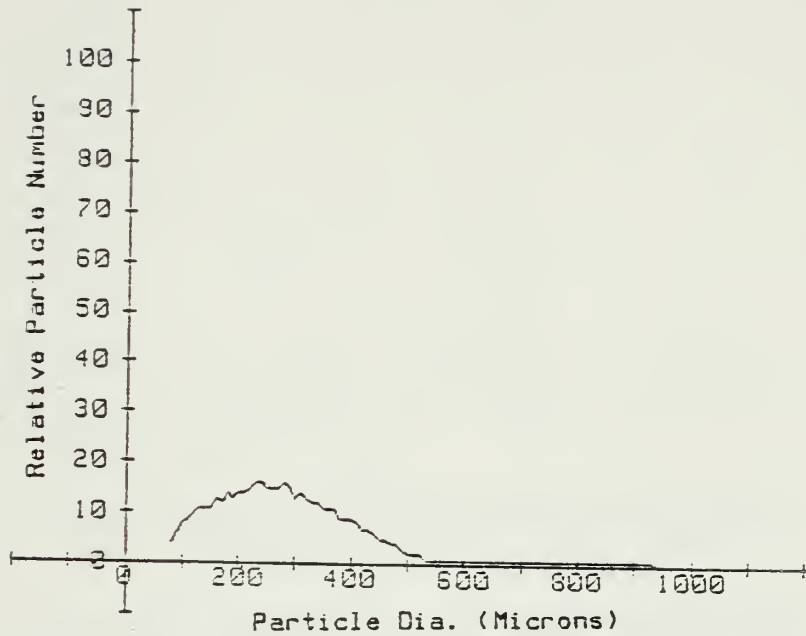Freeboard Height of 12 cm.

110

Fig. 43   Relative Particle Number vs Particle
           Diameter as a Function of Uo.
           Freeboard Height of 18 cm.

Fig. 44   Relative Particle Number vs Particle
           Diameter as a Function of Uo.
           Freeboard Height of 22 cm.

111

Fig. 45   Relative Particle Number vs Particle
Diameter as a Function of Uo.
Freeboard Height of 31 cm.

decrease is due to the decrease in lift given to the ascending particle as Uo is decreased. As a result, all particles achieve a lower maximum height when Uo is decreased.

Fig. 46 shows the effect of Uo on the particle density distribution above the bed. There is a slight increase in overall particle density with an increase in Uo. As expected, there is also an increase in the maximum height attained by the particles with an increase in Uo. Fig. 47 is a semi-ln plot of the same data plotted in Fig. 46. Table 12 lists the slopes of the lines to the right of the peak shown in Fig. 47 which is located at about 18 cm of height above the bed surface. This table shows an increase in the particle distribution slope as Uo is decreased.

TABLE 12

Uo cm/s	Slope gms/cm	Intercept gms/cm
30.5	-0.136	7.036
57.9	-0.117	6.758
91.4	-0.098	6.473

Effect of Uo on the slope of the particle density distribution as a function of height for the distributions shown in Fig. 47.
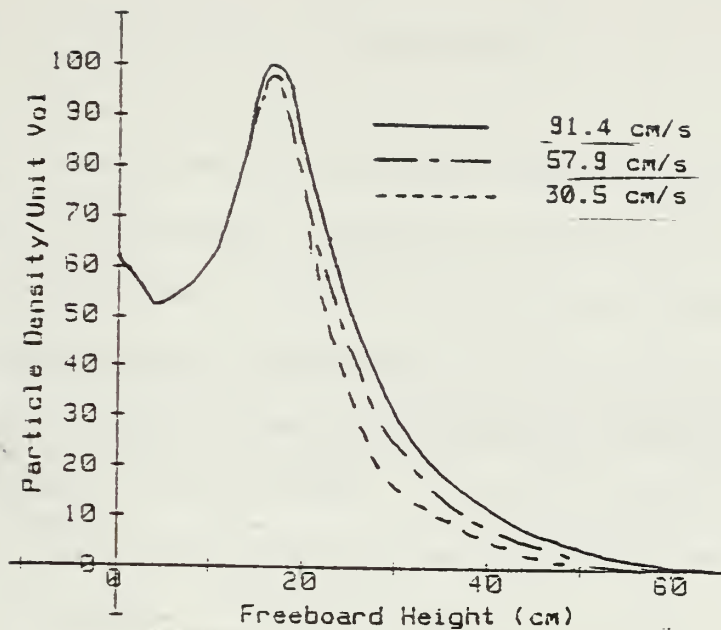
Fig. 46　Particle Density/Unit Volume vs Freeboard height as a Function of Uo.
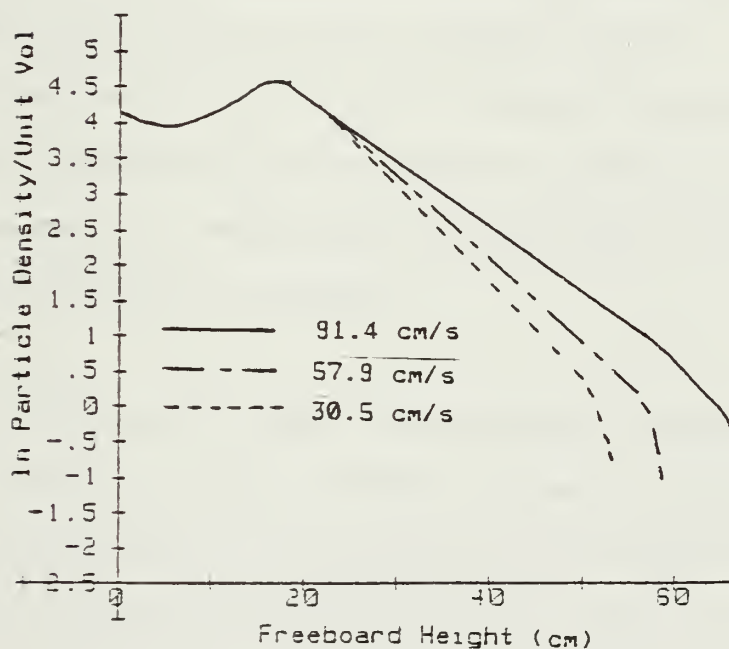
Fig. 47　ln Particle Density/Unit Volume vs Freeboard height as a Function of Uo.

114

Variation of Initial Particle Velocity (Upo)

Fig. 48 shows the relation between initial particle velocity
(Upo) and the maximum height attained by particles of different
size. This figure also shows that the larger particles are mainly
momentum dependent while the smaller particles are drag dependent.
If Upo were increased further, the larger particles would continue
to increase their maximum height. The smaller particles would
approach a height limit which is dependent upon the superficial
velocity in the bed.

Figs. 49 thru 54 show the effects of increasing Upo on the
individual particle densities for increasing heights. In general,
the individual particle distributions undergo the same relative
changes from the bed surface to the maximum height position. The
difference being the height above the bed surface at which the
particular distribution is present.

Fig. 55 shows the effect of varying Upo on the particle
density distribution in the freeboard. As was noted previously,
the peak density occurs at the point where the largest particles
attain their maximum height above the bed. As Upo is increased,
the curve to the right of the peak becomes shorter and steeper.
This trend will continue until the the effect of the smaller
particles returning to the bed cause the slope to decrease. Fig.
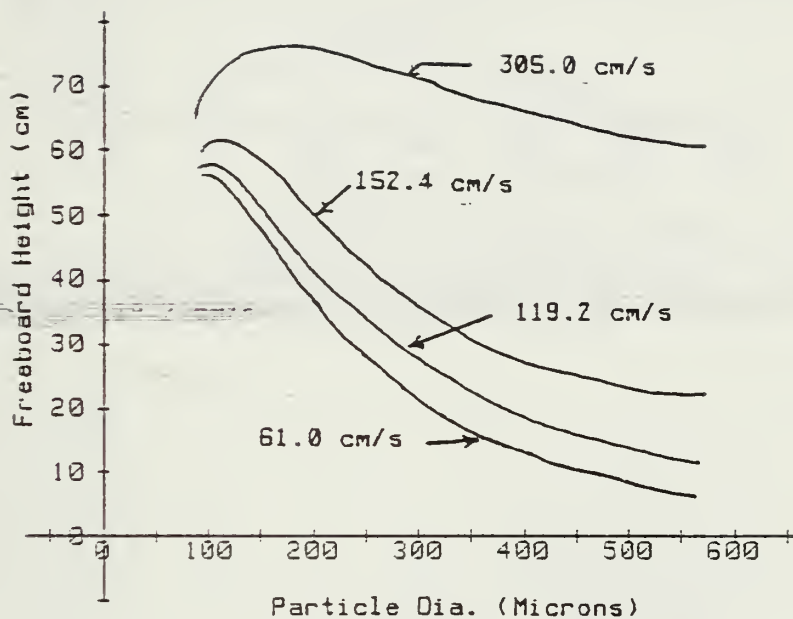
Fig. 48   Maximum Particle Height vs Particle
   Diameter as a Function of Upo.

Fig. 49   Relative Particle Number vs Particle
           Diameter as a Function of Upo.
           Freeboard Height of 4 cm.

Fig. 50   Relative Particle Number vs Particle
           Diameter as a Function of Upo.
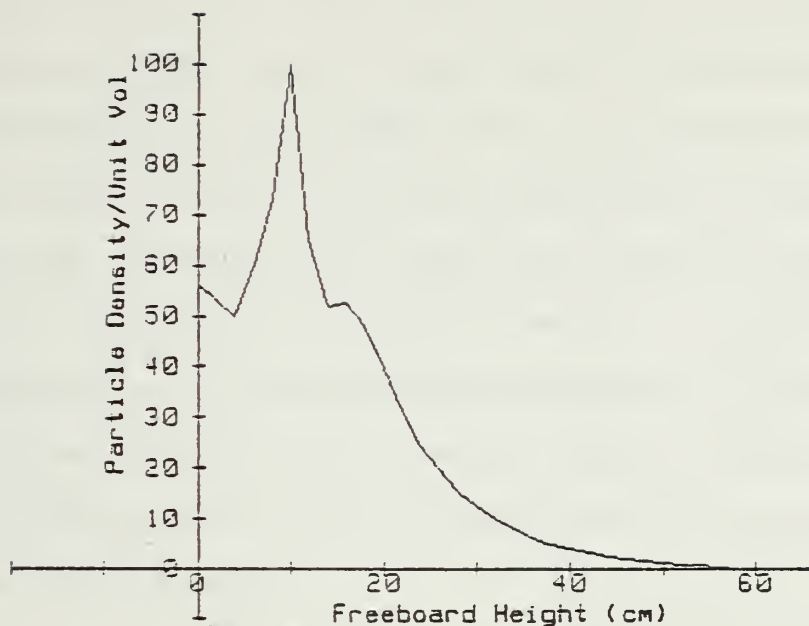   Freeboard Height of 8 cm.

117

Fig. 51   Relative Particle Number vs Particle
Diameter as a Function of Upo.
Freeboard Height of 12 cm.

Fig. 52   Relative Particle Number vs Particle
Diameter as a Function of Upo.
Freeboard Height of 18 cm.

118

Fig. 53   Relative Particle Number vs Particle
           Diameter as a Function of Upo.
           Freeboard Height of 22 cm.

Fig. 54   Relative Particle Number vs Particle
           Diameter as a Function of Upo.
           Freeboard Height of 31 cm.

119

Fig. 55   Particle Density/Unit Volume vs
           Freeboard height as a Function
           of Upo.

Fig. 56   ln Particle Density/Unit Volume
           vs Freeboard height as a Function
           of Upo.

120

56 is a semi-ln plot of the data in Fig. 55. Table 13 confirms

that the slope is becoming steeper as Upo is increased although

the influence of initial particle velocity on the slope of the

density vs height curve is moderate.

TABLE 13

Upo cm/s	Slope gms/cm	Intercept gms/cm
61.0	-0.118	6.058
97.2	-0.117	6.758
152.4	-0.125	8.500
304.8	-0.200	18.20

Effect of Upo on the slope of the
particle density distribution as a
function of height for the
distributions shown in Fig. 56.

Variation of Jet Velocity (Uj)

Fig. 57 shows the effect on maximum particle height when Uj

is varied. As in the two previous analysis', the influence of

momentum and drag on the different particle sizes is apparent. A

decrease in jet velocity from the baseline value results in a

large drop in small particle height and a small change in large

particle height. This suggests that jet velocity has a strong

effect on the dispersion, or seperation of particles of different

sizes at increasing freeboard heights. Increasing Uj results in a

stretching effect of the particle size distributions above the

121
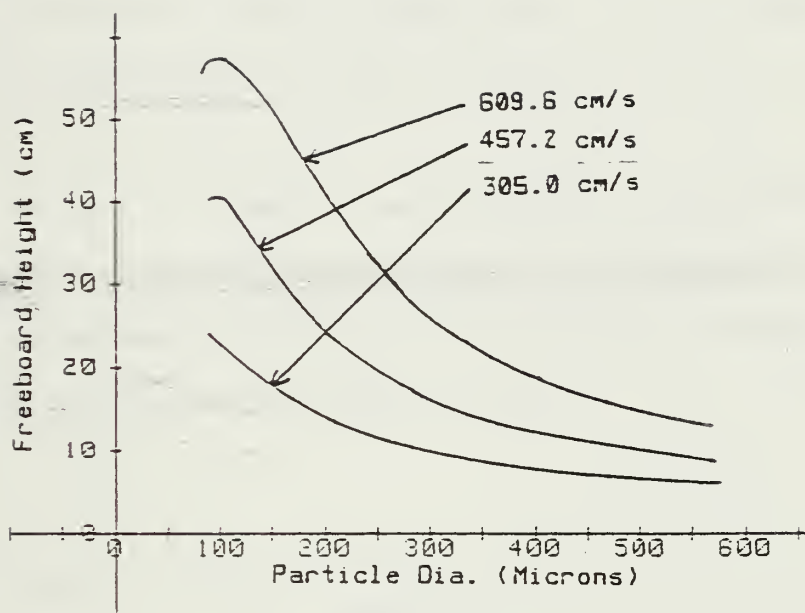
Fig. 57   Maximum Particle Height vs Particle
          Diameter as a Function of Uj.

122

bed.   One interesting point to note is the loss of the rounded

edge at the heights corresponding to the smaller particles.   This

shows the extremely large effect that drag plays when the air

velocity is very close to the terminal velocity of the particle.

Figs. 58 thru 63 show the effect of varying Uj on the

individual partical densities at varying heights above the bed.

Again, as in the previous parameter analysis, the same

distribution shapes can be seen for each value of Uj, the only

difference being the height at which it occurs.

Fig. 64 shows the change in particle density distribution as

Uj is varied. Fig. 65 is a semi-ln plot of this data showing

that as Uj is decreased, the slope of the distribution changes

substantially.   Table 14 also shows this effect.

TABLE 14

Uj cm/s	Slope gms/cm	Intercept gms/cm
609.6	-0.117	6.758
457.2	-0.207	7.380
304.8	-0.400	7.900

Effect of Uj on the slope of the
particle density distribution as a
function of height for the
distributions shown in Fig. 65.
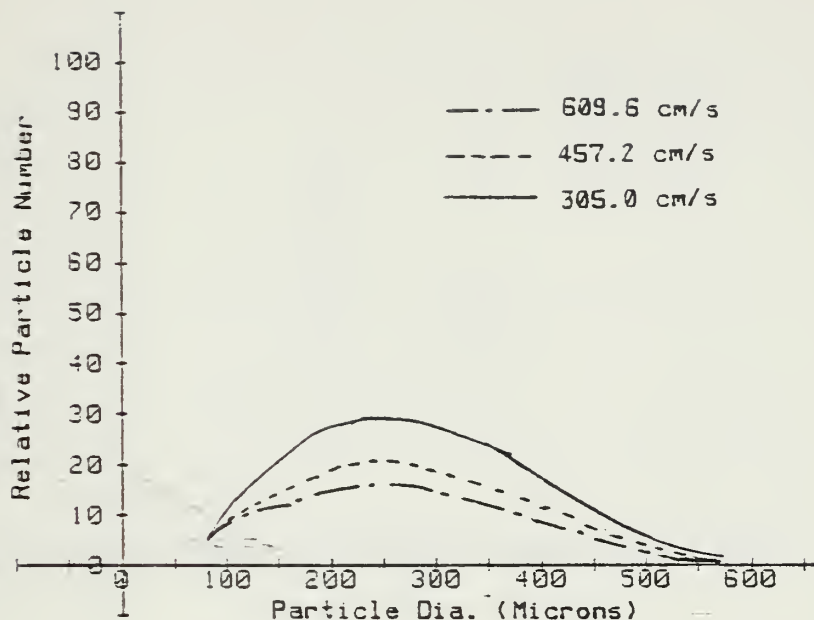
Fig. 58   Relative Particle Number vs Particle
           Diameter as a Function of Uj.
           Freeboard Height of 4 cm.
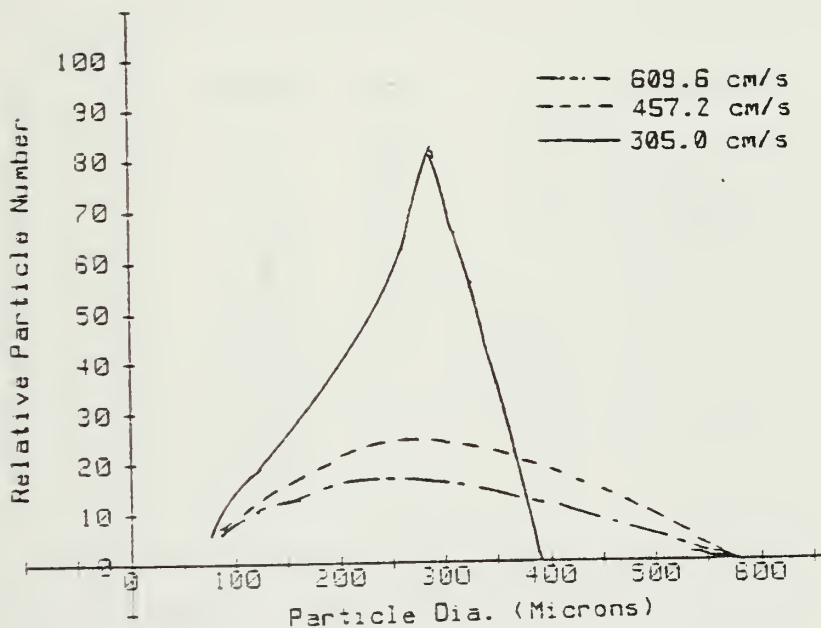
Fig. 59   Relative Particle Number vs Particle
           Diameter as a Function of Uj.
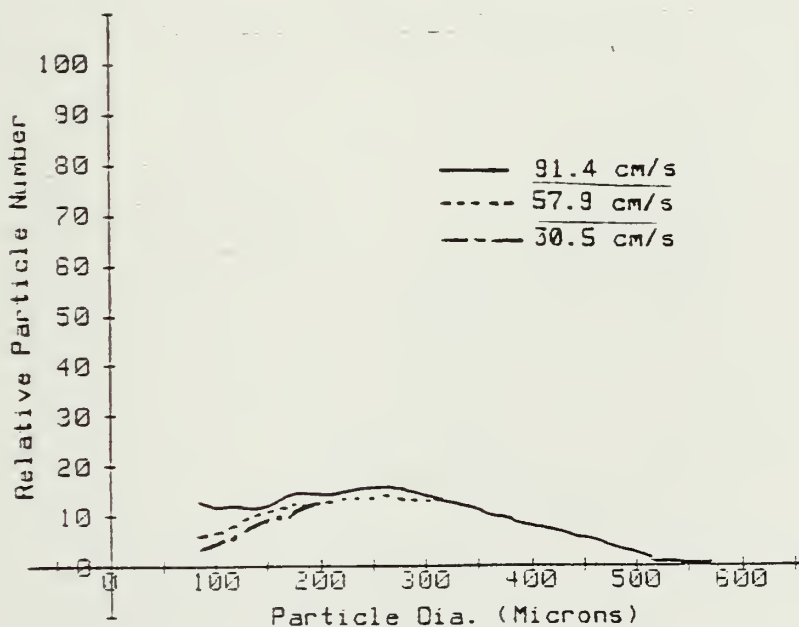   Freeboard Height of 8 cm.
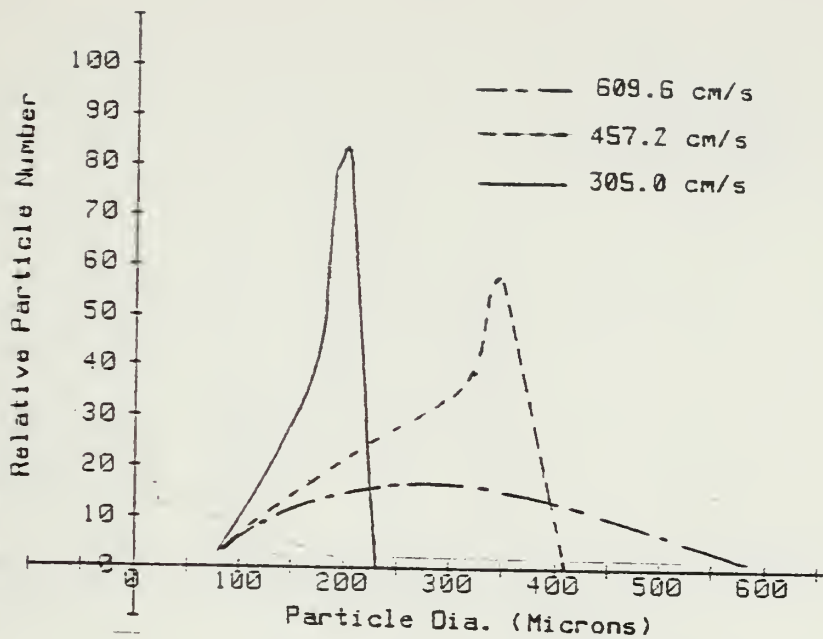
Fig. 60   Relative Particle Number vs Particle
           Diameter as a Function of Uj.
           Freeboard Height of 12 cm.
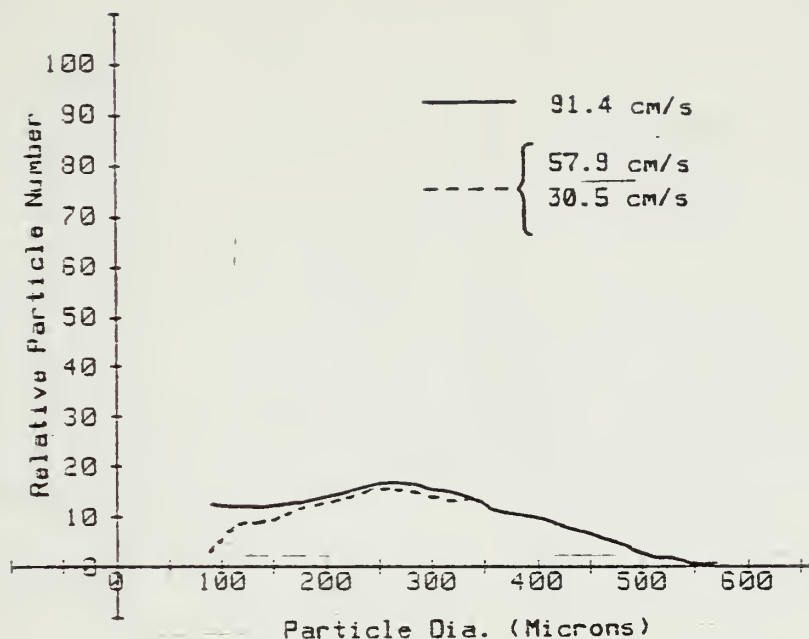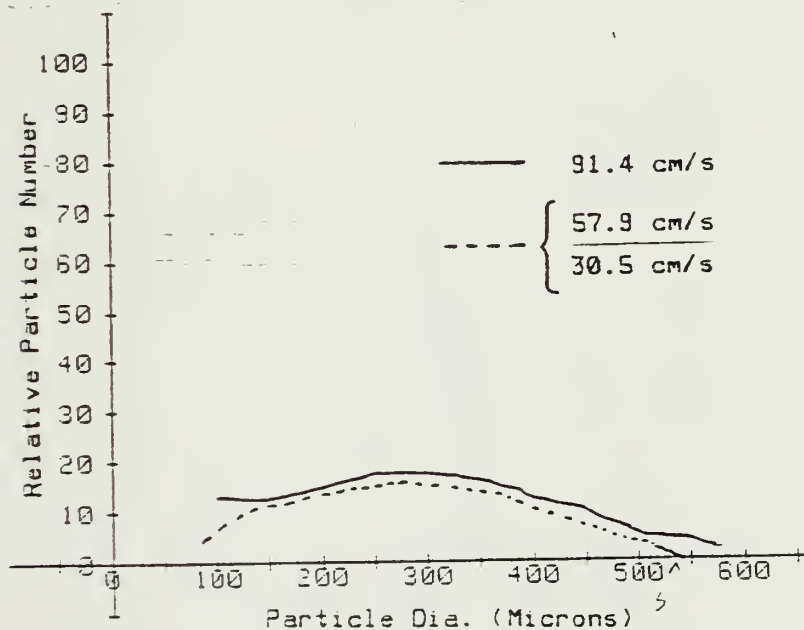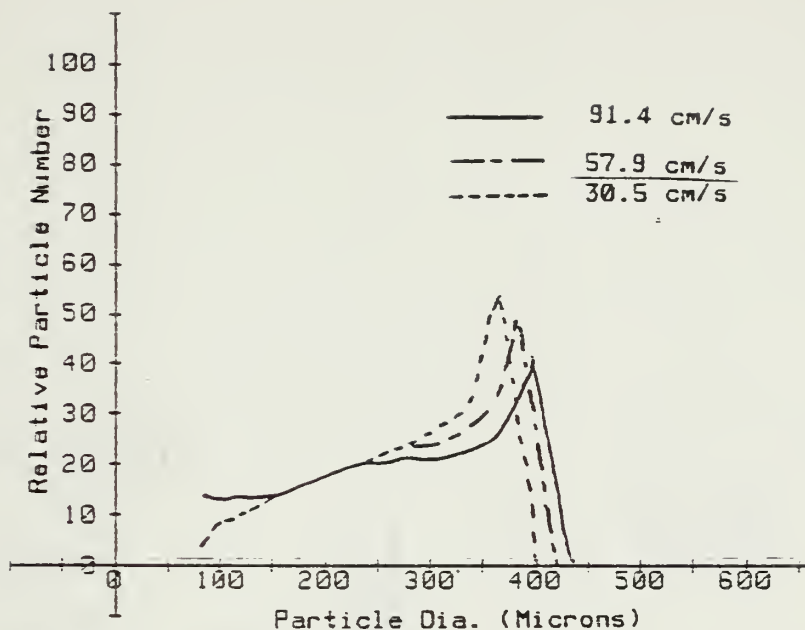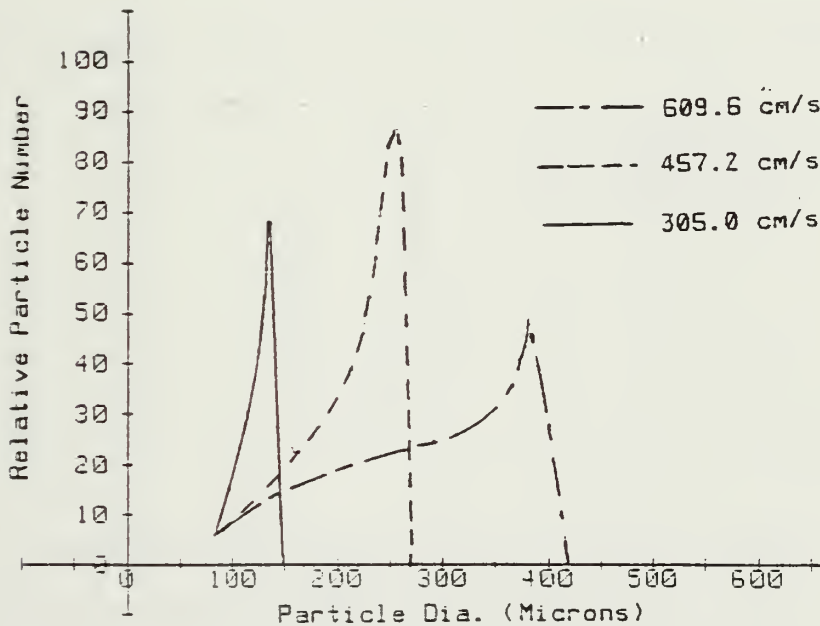

Fig. 61   Relative Particle Number vs Particle
           Diameter as a Function of Uj.
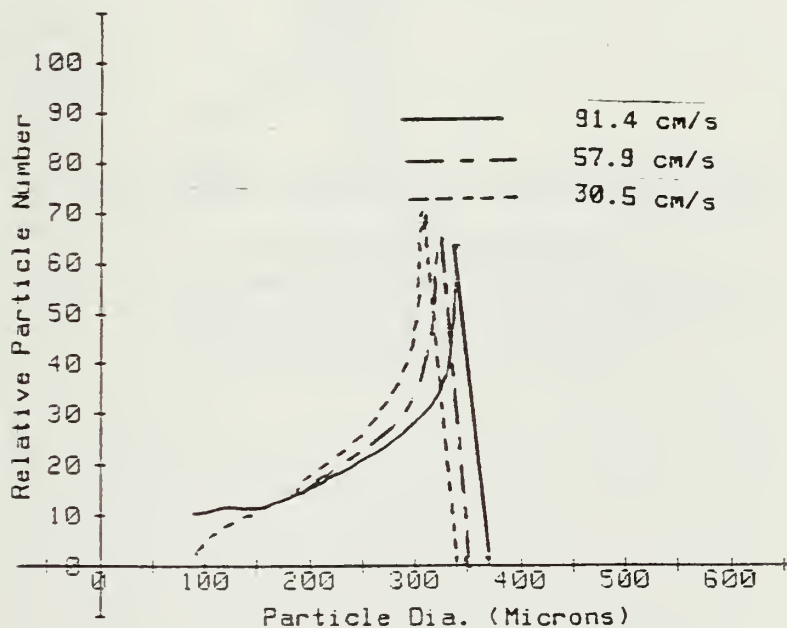   Freeboard Height of 18 cm.

125
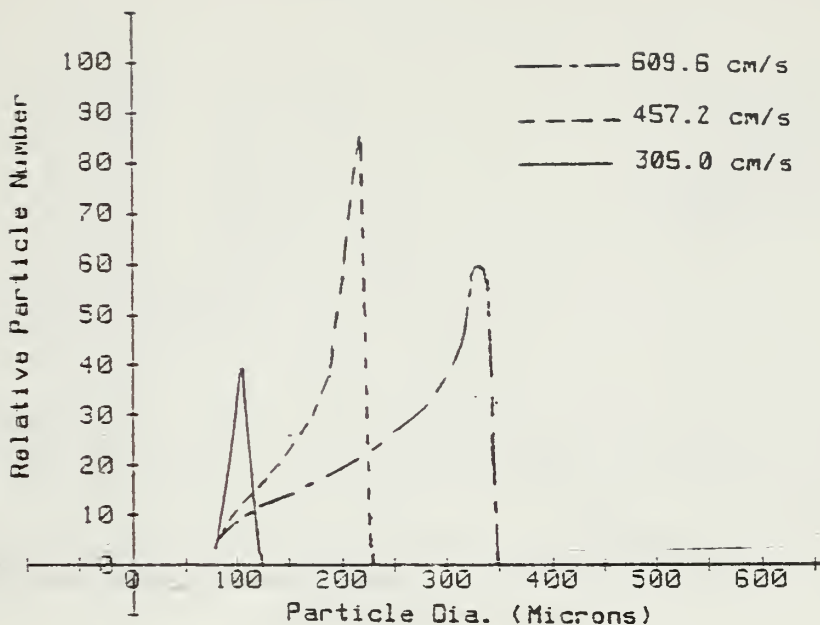
Fig. 62   Relative Particle Number vs Particle
            Diameter as a Function of Uj.
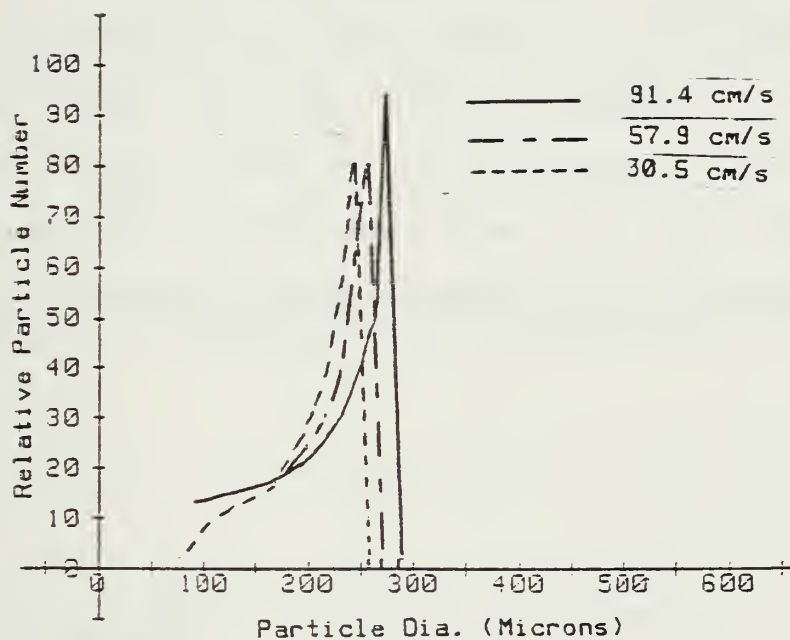   Freeboard Height of 22 cm.
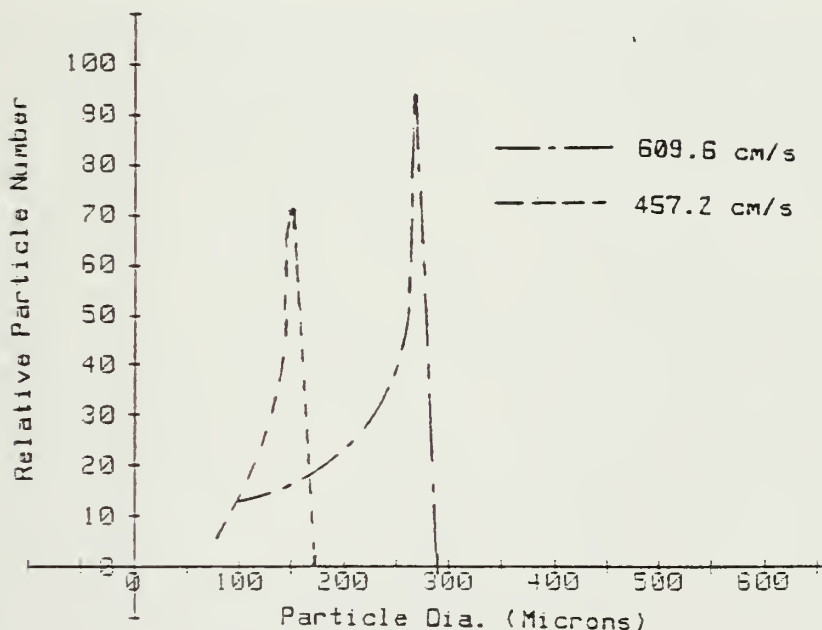
Fig. 63   Relative Particle Number vs Particle
            Diameter as a Function of Uj.
            Freeboard Height of 31 cm.

126
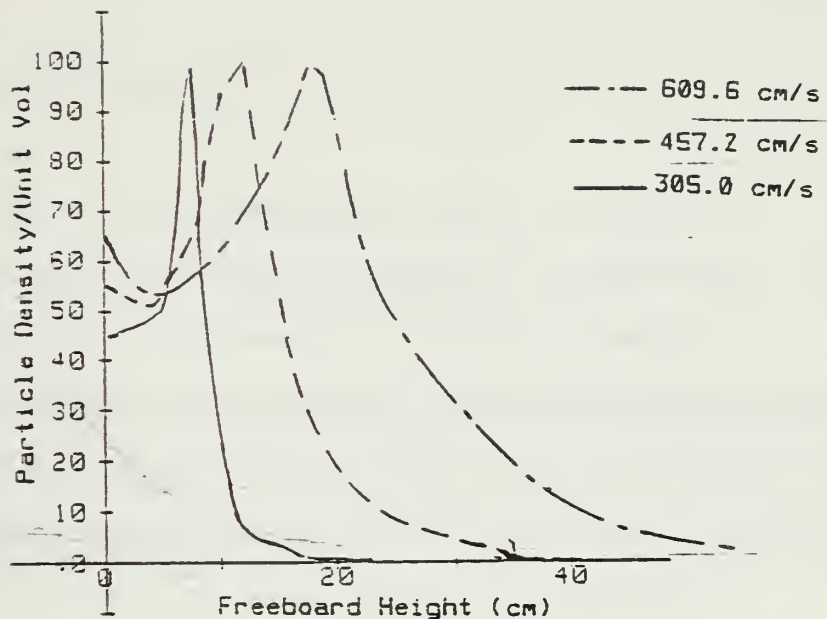
Fig. 64   Particle Density/Unit Volume vs
           Freeboard height as a Function
           of Uj.
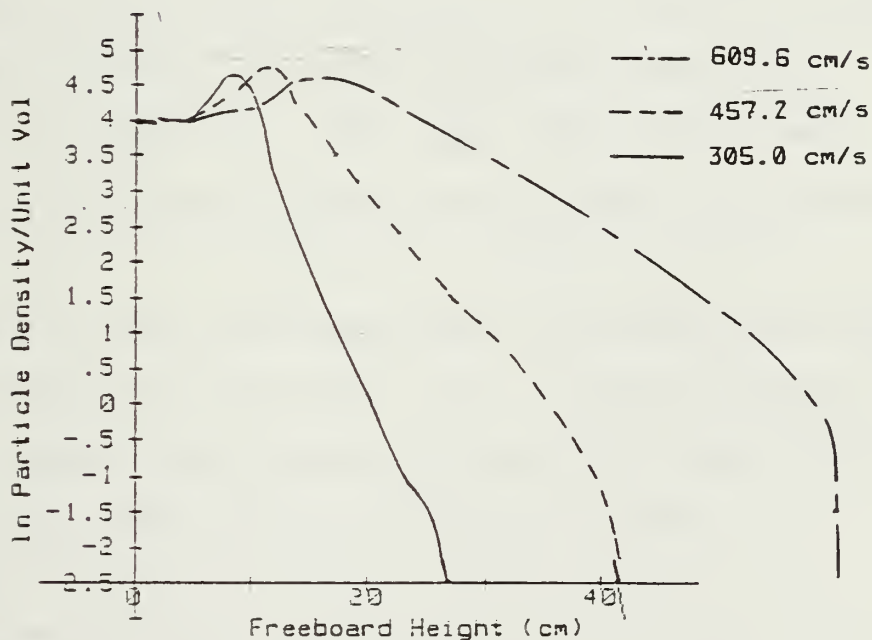
Fig. 65   In Particle Density/Unit Volume
           vs Freeboard height as a Function
           of Uj.

127

Variation of Jet Duration (tj)

Fig. 66 is a graph showing the effect of varying jet
duration on the maximum heights attained by the particles. It is
easily seen that a small change in jet duration results in a
substantial change in particle height. This effect indicates that
the distribution present in an actual fluidized bed is probably a
statistical average of a rapidly fluctuating particle distribution
which is controled by the durations of the jets from the
neighboring bubble eruptions as well as local eruptions.

Figs. 67 thru 72 show the effects on the individual particle
density distributions, at different freeboard heights, as a
function of jet duration. These figures also show the drastic
change in density distributions caused by changes in jet duration.

Fig. 73 shows the particle density distributions above the
bed as affected by jet duration. Fig. 74, which is a semi-ln
plot of the data, shows the drastic changes in the decay slopes.
Table 15 also shows this drastic variation in slope.
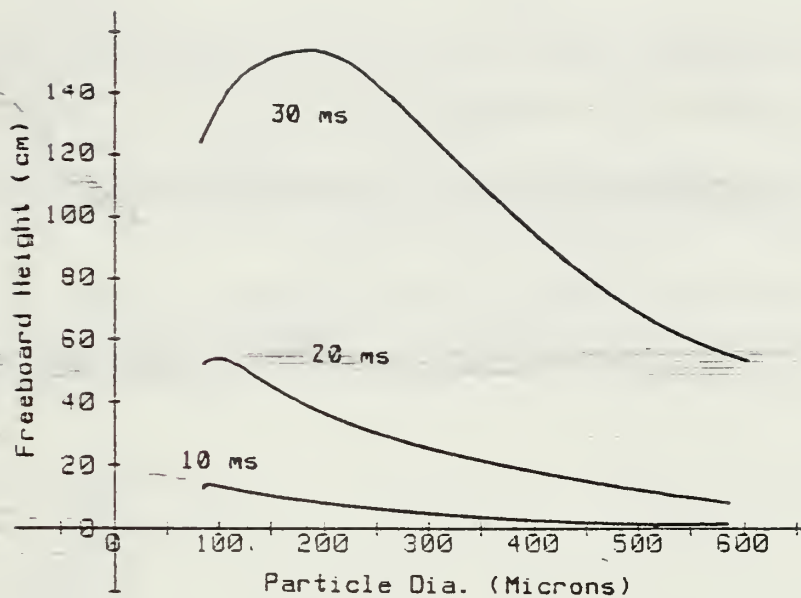
Fig. 66   Maximum Particle Height vs Particle
Diameter as a Function of tj.
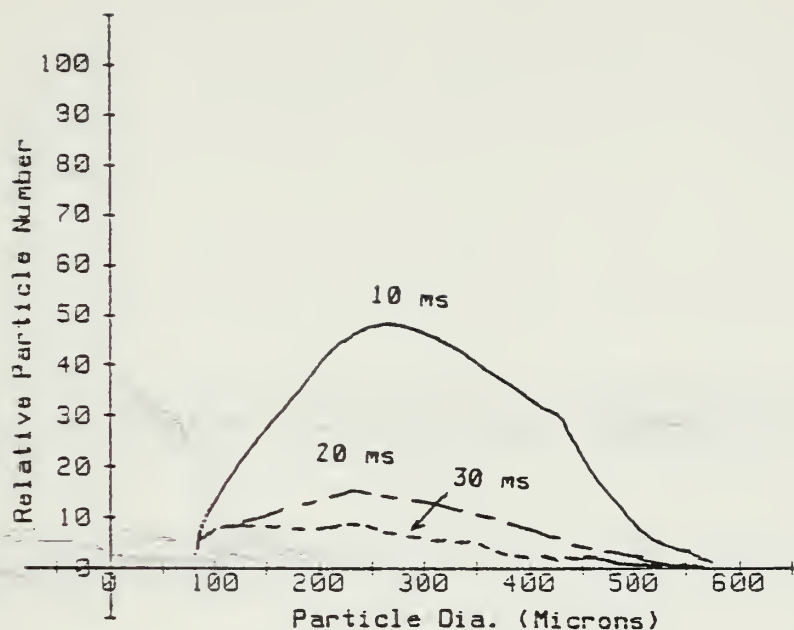
Fig. 67   Relative Particle Number vs Particle
Diameter as a Function of tj.
Freeboard Height of 4 cm.
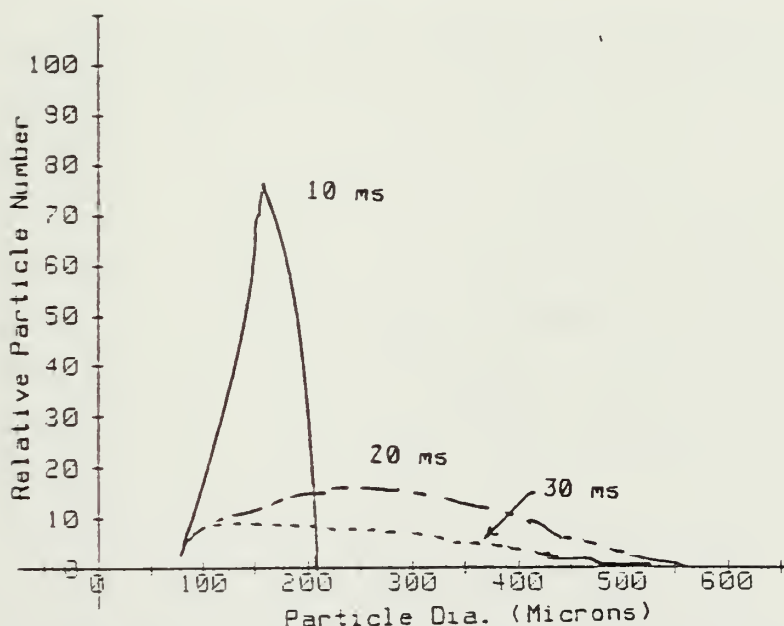
Fig. 68   Relative Particle Number vs Particle
Diameter as a Function of tj.
Freeboard Height of 8 cm.

130
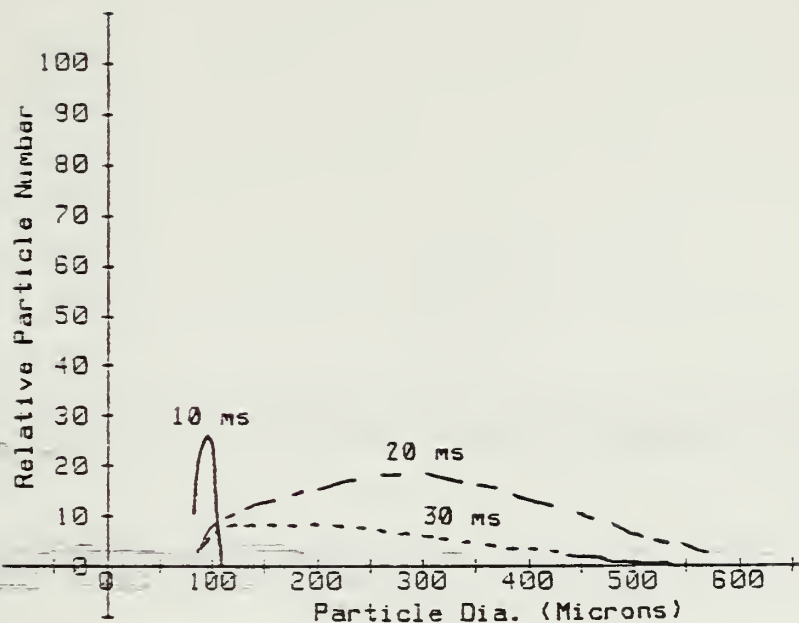
Fig. 69   Relative Particle Number vs Particle
           Diameter as a Function of tj.
           Freeboard Height of 12 cm.
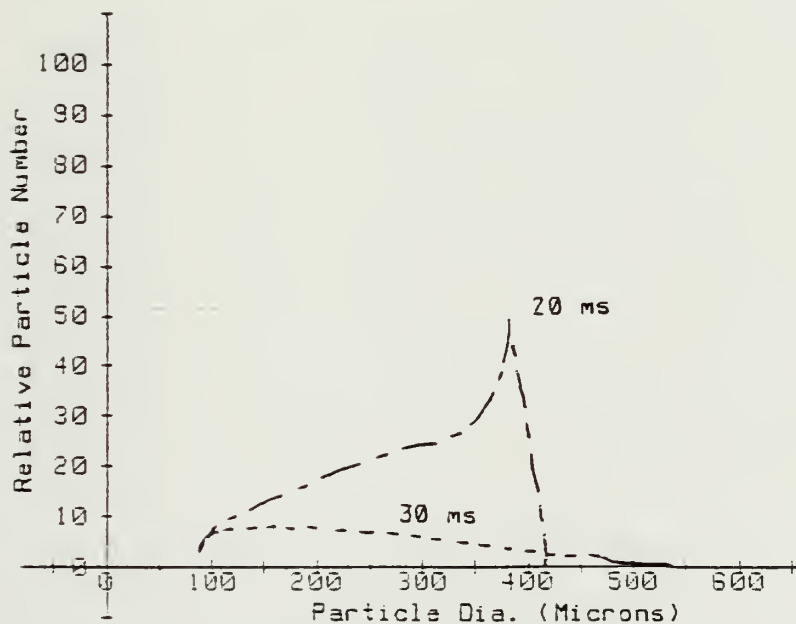
Fig. 70   Relative Particle Number vs Particle
           Diameter as a Function of tj.
           Freeboard Height of 18 cm.

131
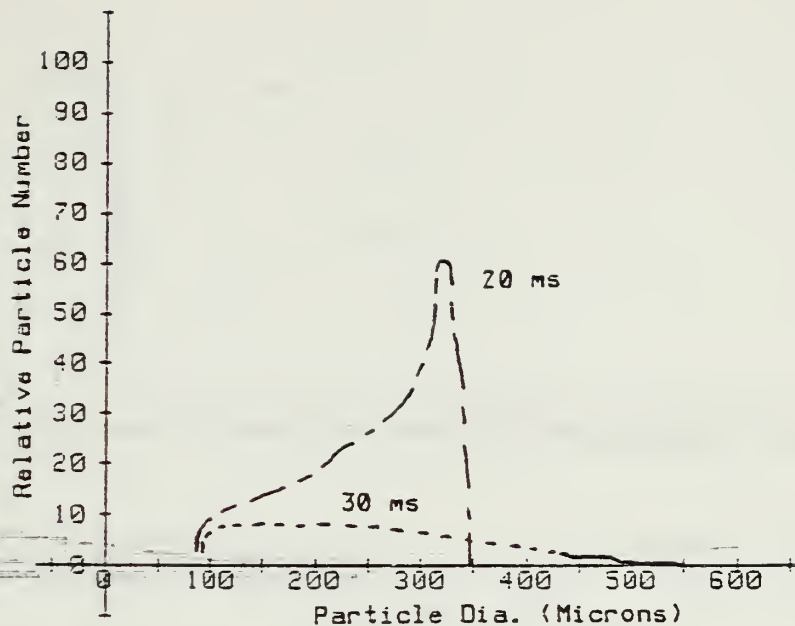
Fig. 71   Relative Particle Number vs Particle
           Diameter as a Function of tj.
           Freeboard Height of 22 cm.
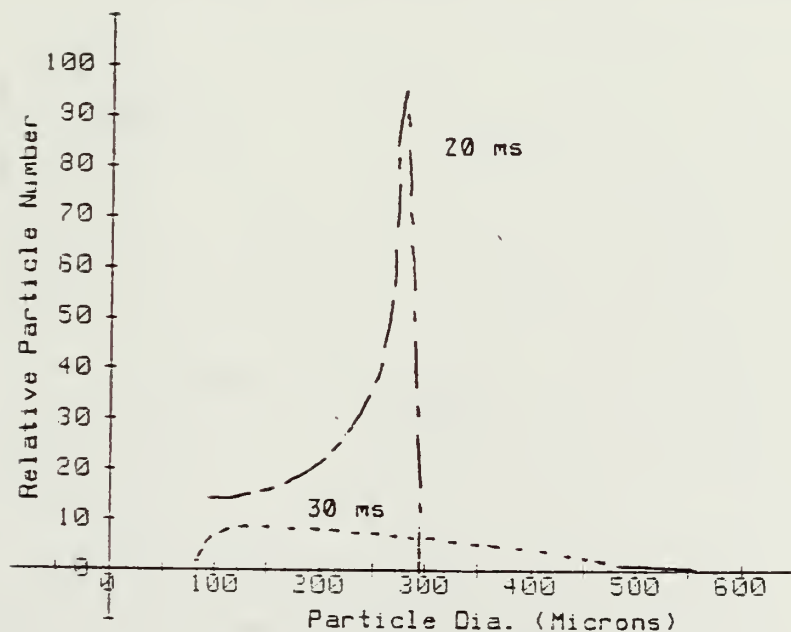
Fig. 72   Relative Particle Number vs Particle
           Diameter as a Function of tj.
           Freeboard Height of 31 cm.

132
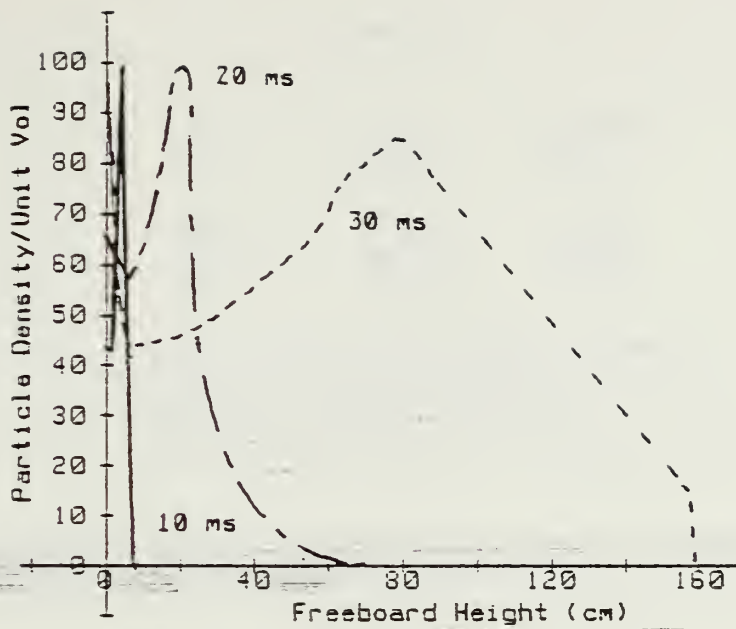
Fig. 73   Particle Density/Unit Volume vs
           Freeboard height as a Function
           of tj.
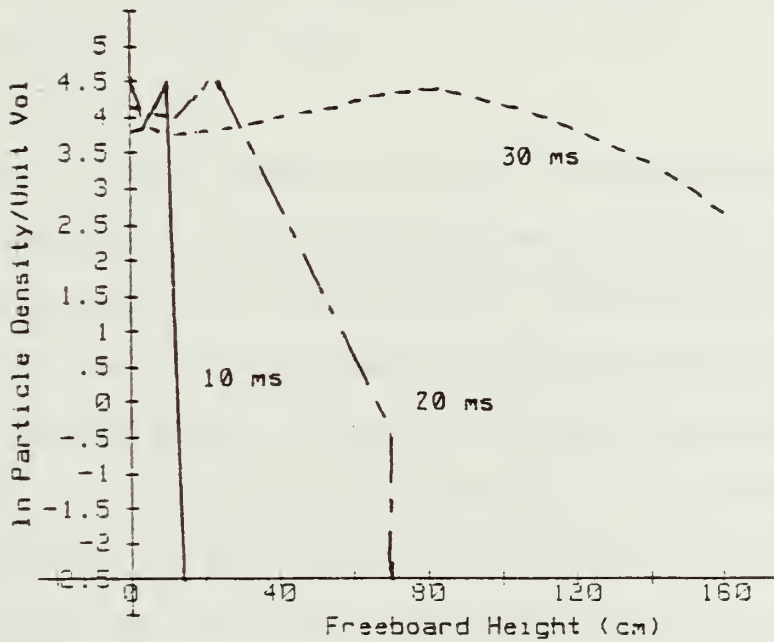
Fig. 74   ln Particle Density/Unit Volume
           vs Freeboard height as a Function
           of tj.

133

TABLE 15

tj	Slope	Intercept
cm/s	gms/cm	gms/cm
10.0	-1.071	12.50
20.0	-0.117	6.758
30.0	-0.020	6.234

Effect of tj on the slope of the
particle density distribution as a
function of height for the
distributions shown in Fig. 74.

Variation of Particle Distribution in Bed Mass

Fig. 75 shows the two bed particle distributions used in
this analysis. The determination of these distributions is
descibed earlier in this work.

Figs. 76 thru 81 show the effects of varying the bed
particle distribution on the individual particle distributions at
different heights above the bed surface. Using the sieve particle
distribution instead of the image analysis distribution produces a
shift in the mean particle distribution towards the smaller
particles. The distributions resulting from the sieve data do not
shift as much as the image analyzer data when the freeboard height
is increased. The small shift in mean diameter exhibited by these
plots is consistant with the distributions listed in Appendix J.

Fig. 82 shows the particle density distributions in the

Faired Data From Appendix E and J. Interval of 10 microns.
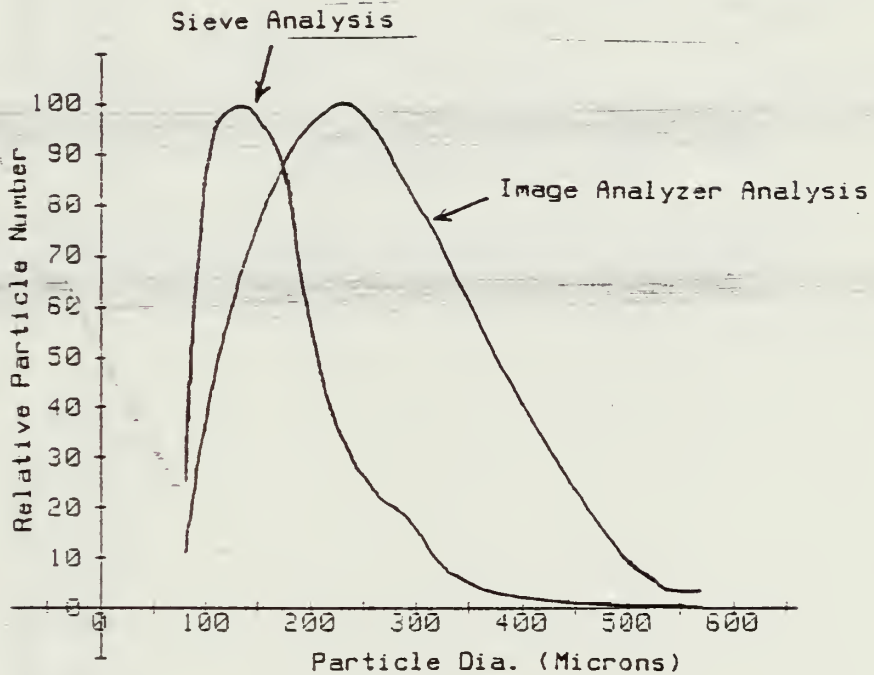
Fig. 75   Relative Particle Number vs Particle
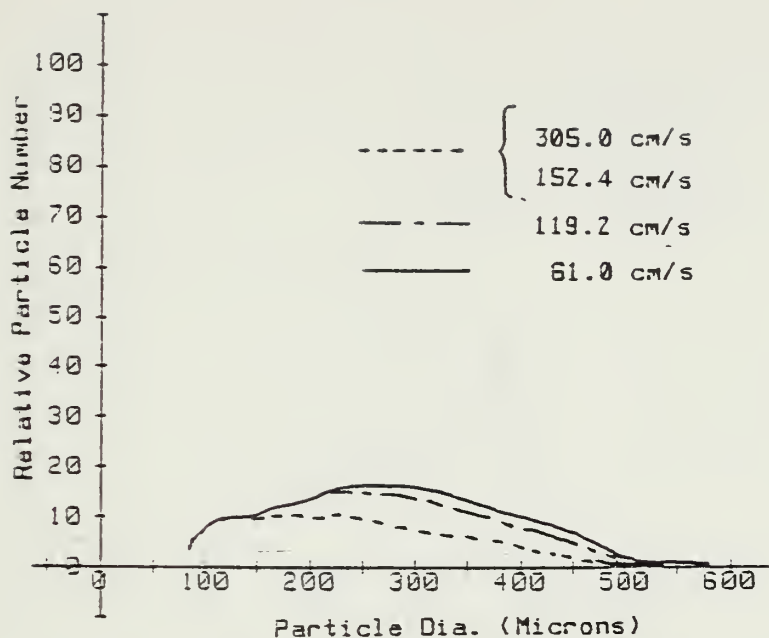   Diameter for Bed Mass Material.
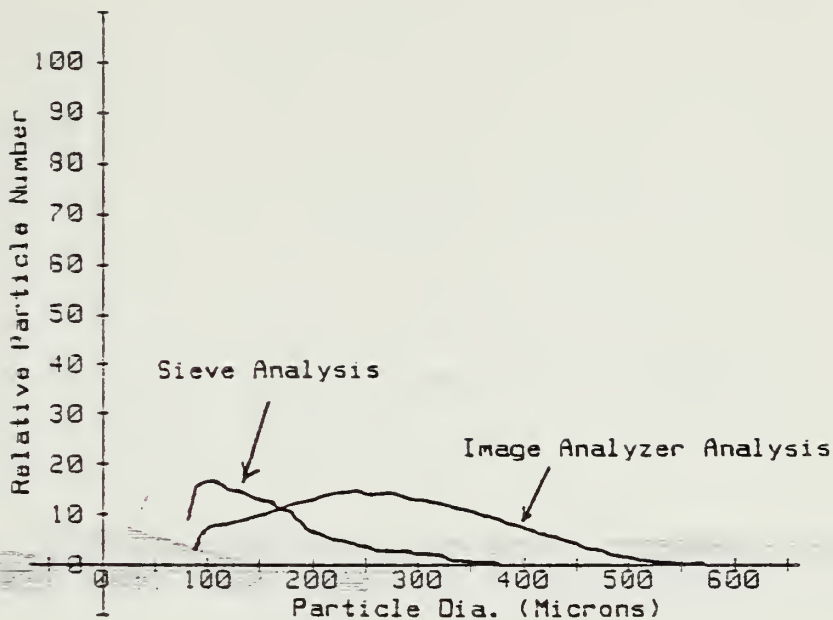
Fig. 76   Relative Particle Number vs Particle
Diameter as a Function of Bed Mass.
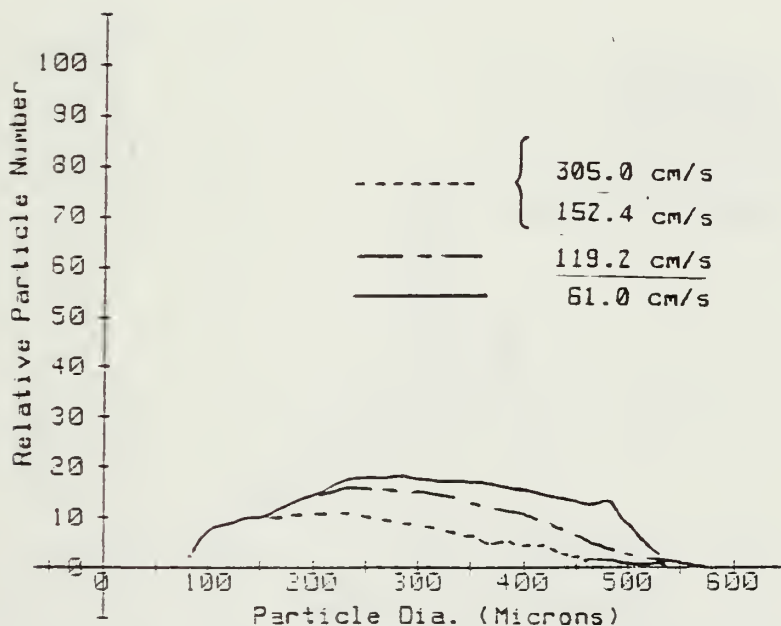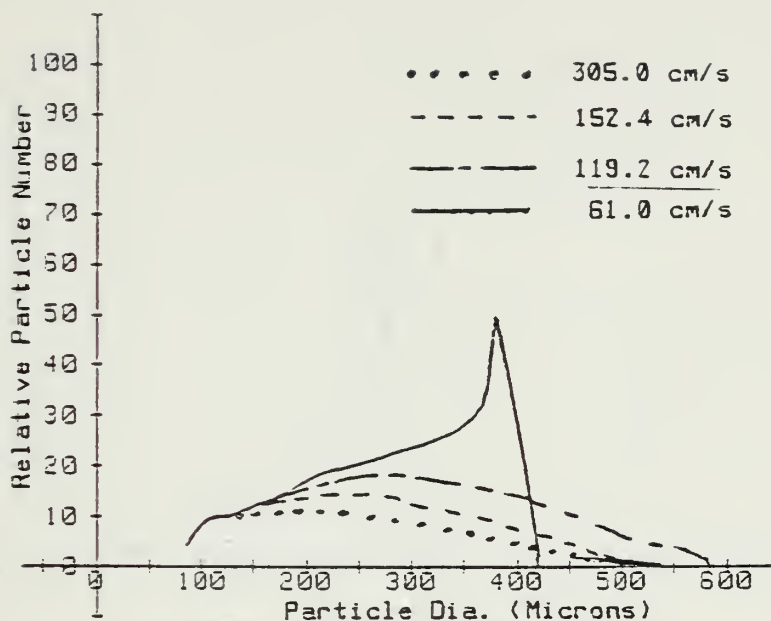Freeboard Height of 4 cm.
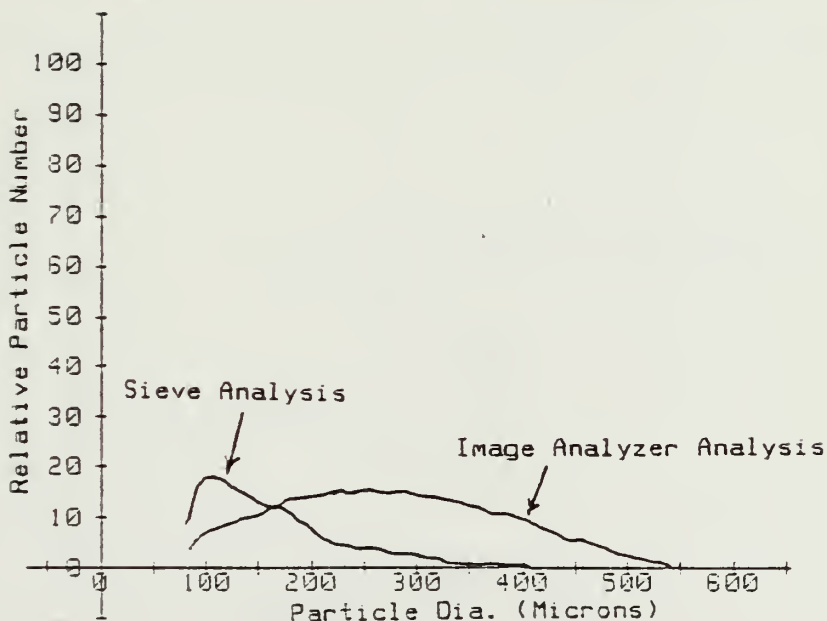
Fig. 77   Relative Particle Number vs Particle
Diameter as a Function of Bed Mass.
Freeboard Height of 8 cm.
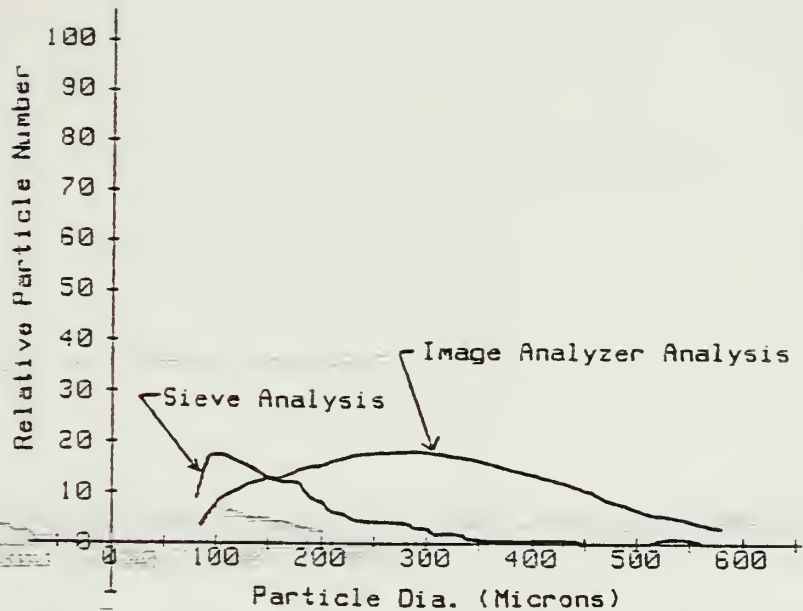
Fig. 78   Relative Particle Number vs Particle
Diameter as a Function of Bed Mass.
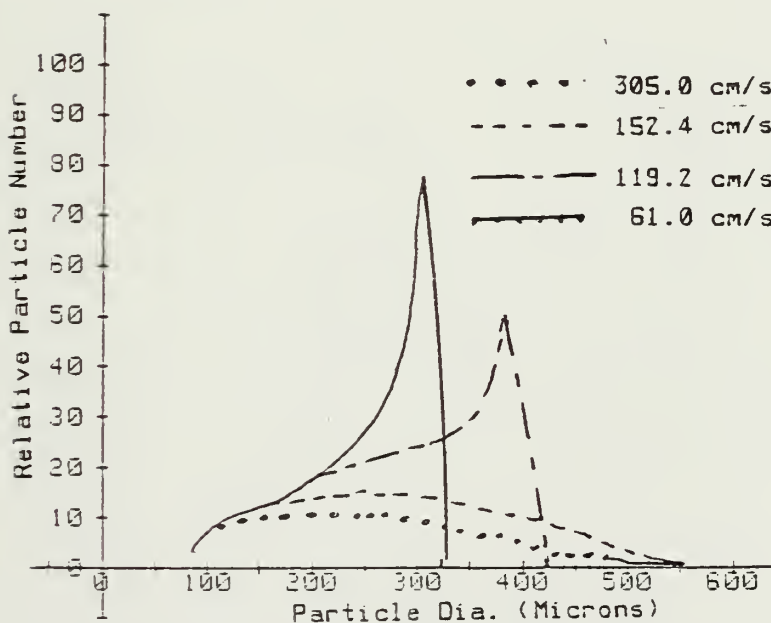Freeboard Height of 12 cm.
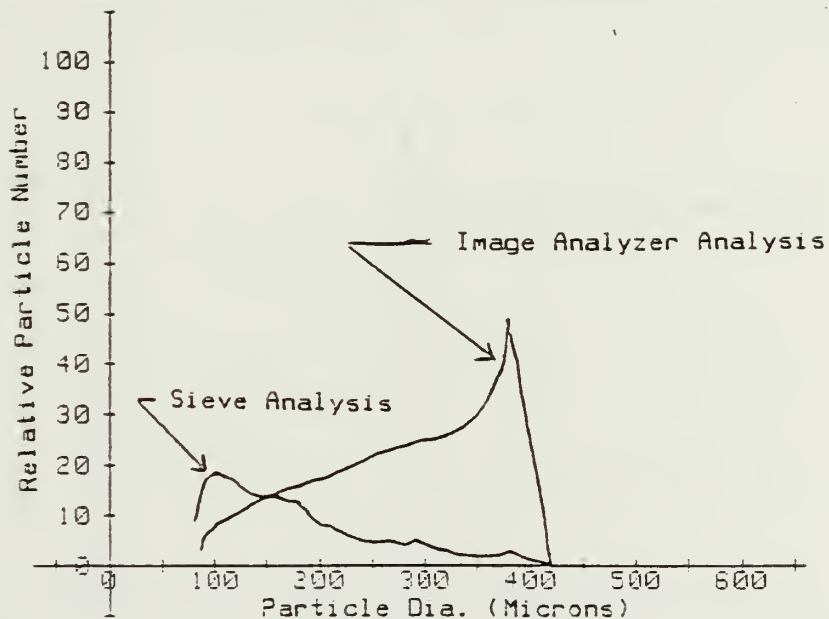
Fig. 79   Relative Particle Number vs Particle
Diameter as a Function of Bed Mass.
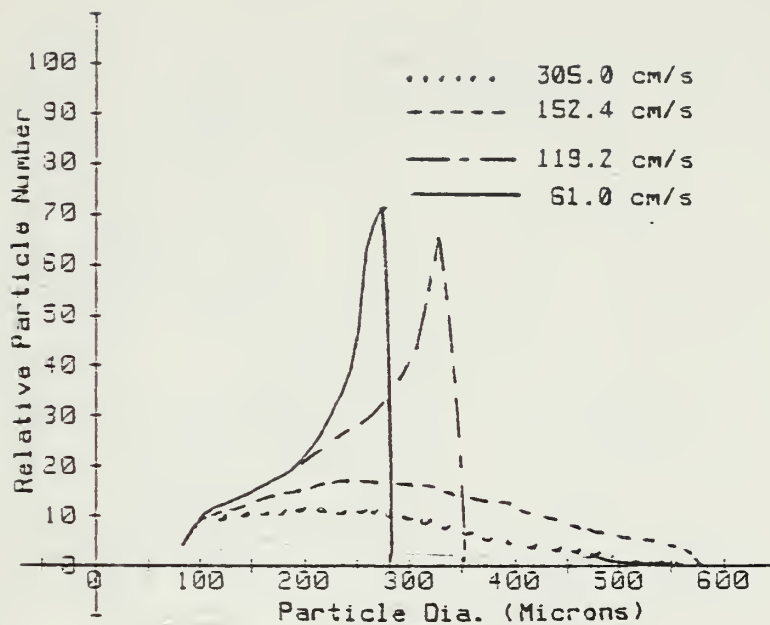Freeboard Height of 18 cm.
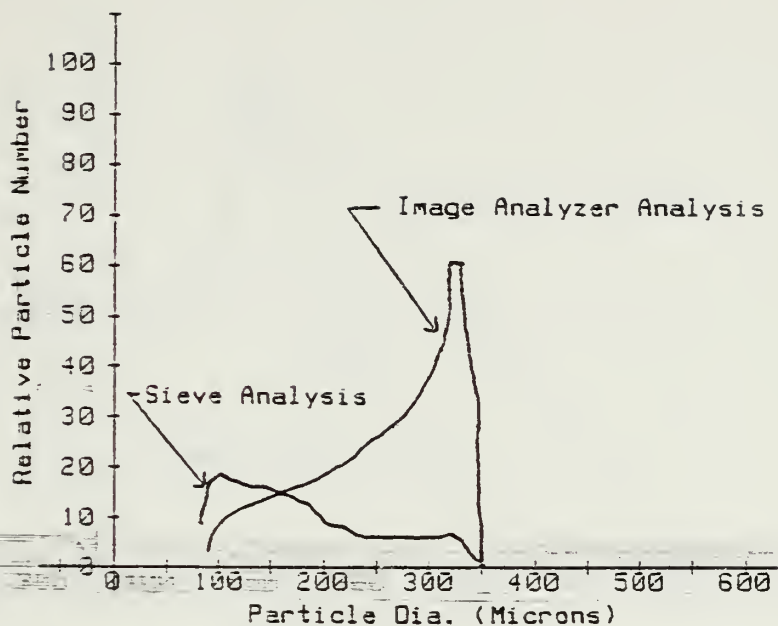
Fig. 80   Relative Particle Number vs Particle
Diameter as a Function of Bed Mass.
Freeboard Height of 22 cm.
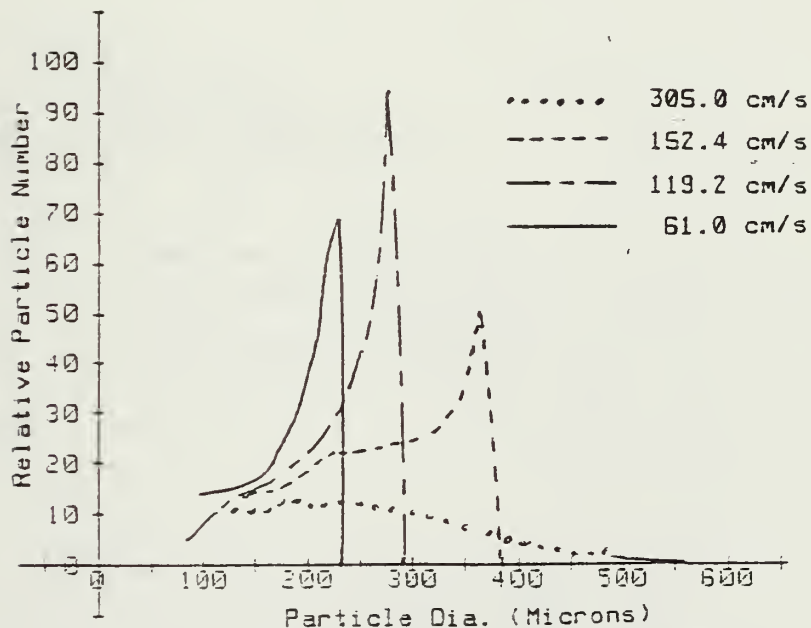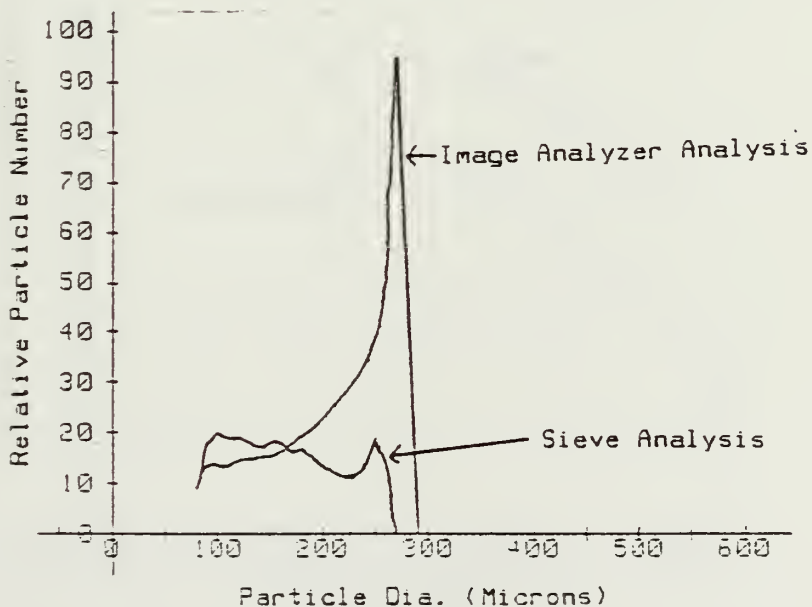

Fig. 81   Relative Particle Number vs Particle
Diameter as a Function of Bed Mass.
Freeboard Height of 31 cm.

138
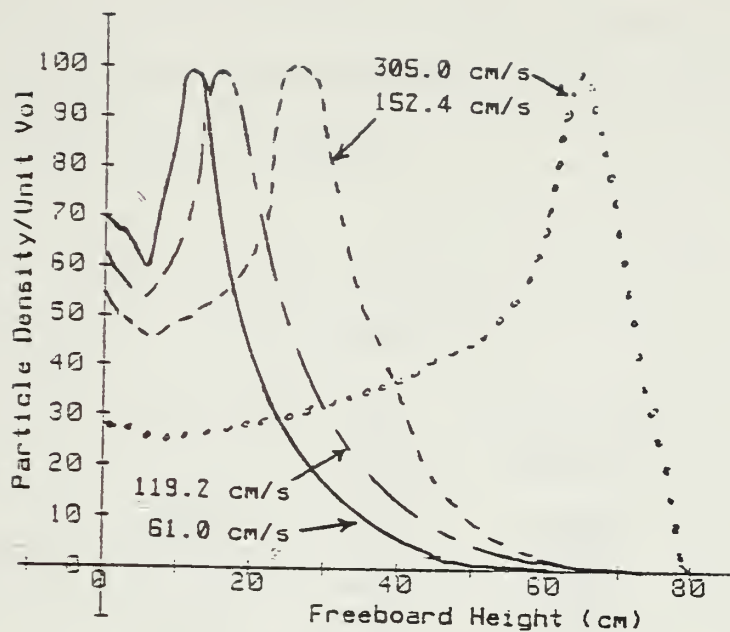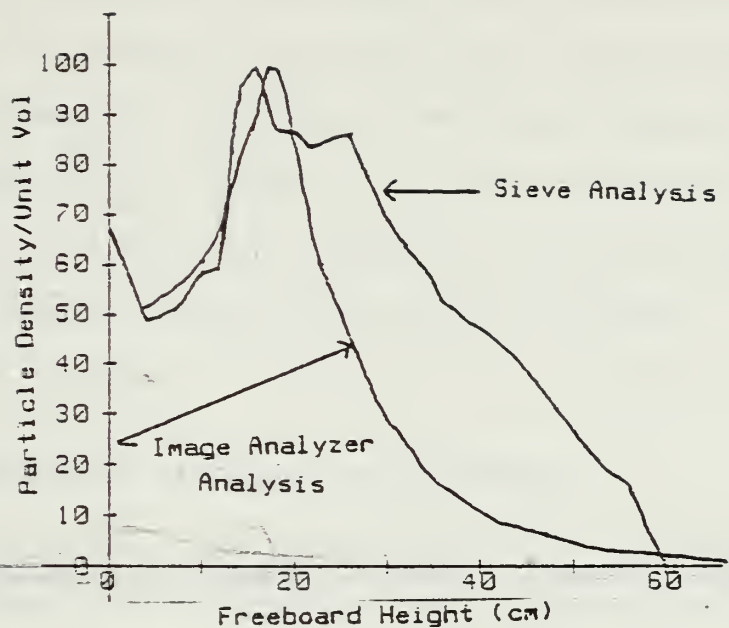
Fig. 82 a   Particle Density/Unit Volume vs
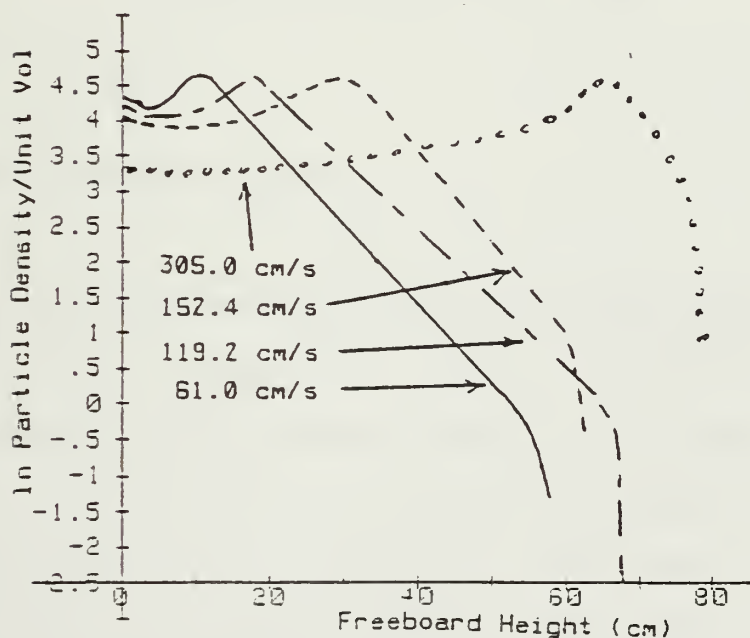   Freeboard height as a Function
            Bed Mass.

Fig. 82b

139
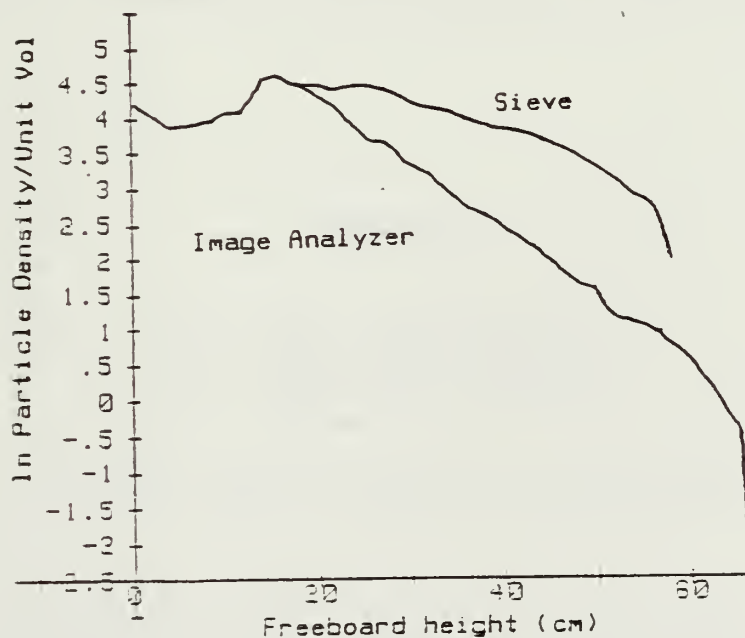
freeboard for the two bed mass conditions. The effect of the
sieve distribution (which has a much lower average particle
diameter) is to decrease the initial rate at which particle mass
returns to the bed. This is due to the smaller particles having a
much smaller terminal velocity. This will not only raise the bulk
of the particles to a higher height, but will also increase the
time required for the particles to return to the bed.

Comparison of Model with Experimental Results

As discussed in the previous section, the baseline parameters
were selected as the experimental conditions present in the bed
when sampling at the highest Uo setting. Table 16 lists these
baseline parameters again for review.

TABLE 16

U_o = 57.9 cm/s (1.9 ft/s)
U_{po} = 97.2 cm/s (3.19 ft/s)
U_j = 609.6 cm/s (20 ft/s)
t_j = 20 ms

Baseline parameters used in computer model.

Fig. 83 shows the particle density distribution predicted by
the model using the baseline conditions. Fig. 84 is a semi-log
plot of this same data. A comparison of the slope of the
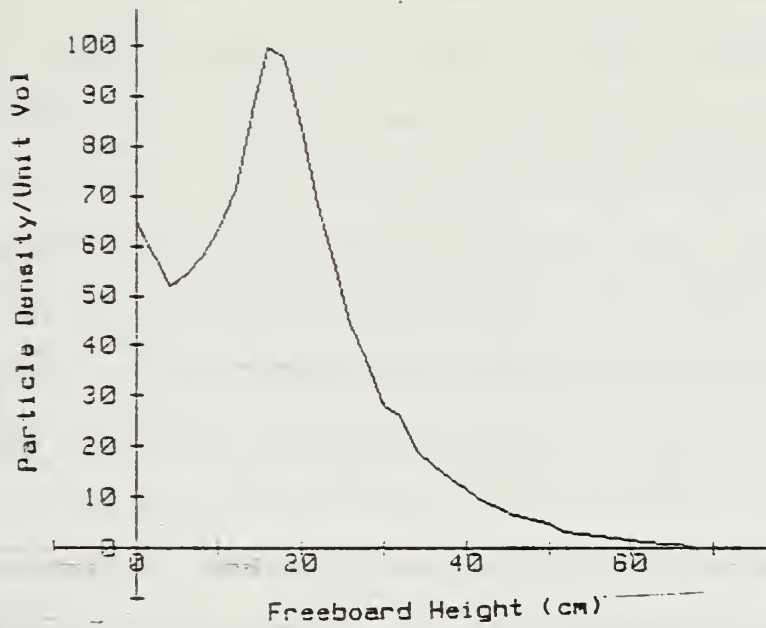
Fig. 83   Particle Density/Unit Volume vs
           Freeboard height for Baseline
           Conditions.
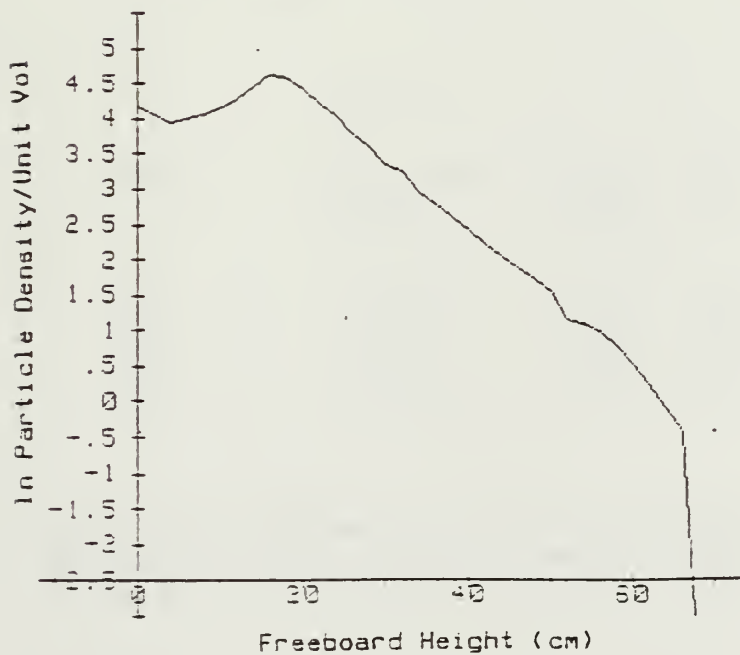
Fig. 84   ln Particle Density/Unit Volume
           vs Freeboard height for Baseline
           Conditions.

141

distribution line after the peak value in Fig. 84 with the slope

obtained from the experimental data shows very good agreement

between the two. This data is also given in Table 17 along with

the data obtained for the other experimental data sets and is

shown plotted in Fig. 85. The slopes for the model data show a

steady increase in slope as Uo/Umf is decreased. This trend is

also followed by the experimental data but is not as smooth. The

slope of the experimental data is also changing faster than the

slope of the model data. One reason for this is that all the model

calculations were performed using the same value for jet velocity

and duration of 609.6 cm/s and 20 ms respectively. The magnitudes

of these values should decrease with decreaseing Uo/Umf, but the

values to be used for these different conditions could not be

determined.

TABLE 17

Uo/Umf	Experimental Slope gms/cm	Model Slope gms/cm	Diff %
3.81	-0.1097	-0.117	6.6
3.17	-0.1029	-0.123	19.5
2.59	-0.1181	-0.129	9.2
2.32	-0.1399	-0.132	5.6

Comparison of slopes for the particle density
distributions above the bed as derived from
the experimental data and the computer model.
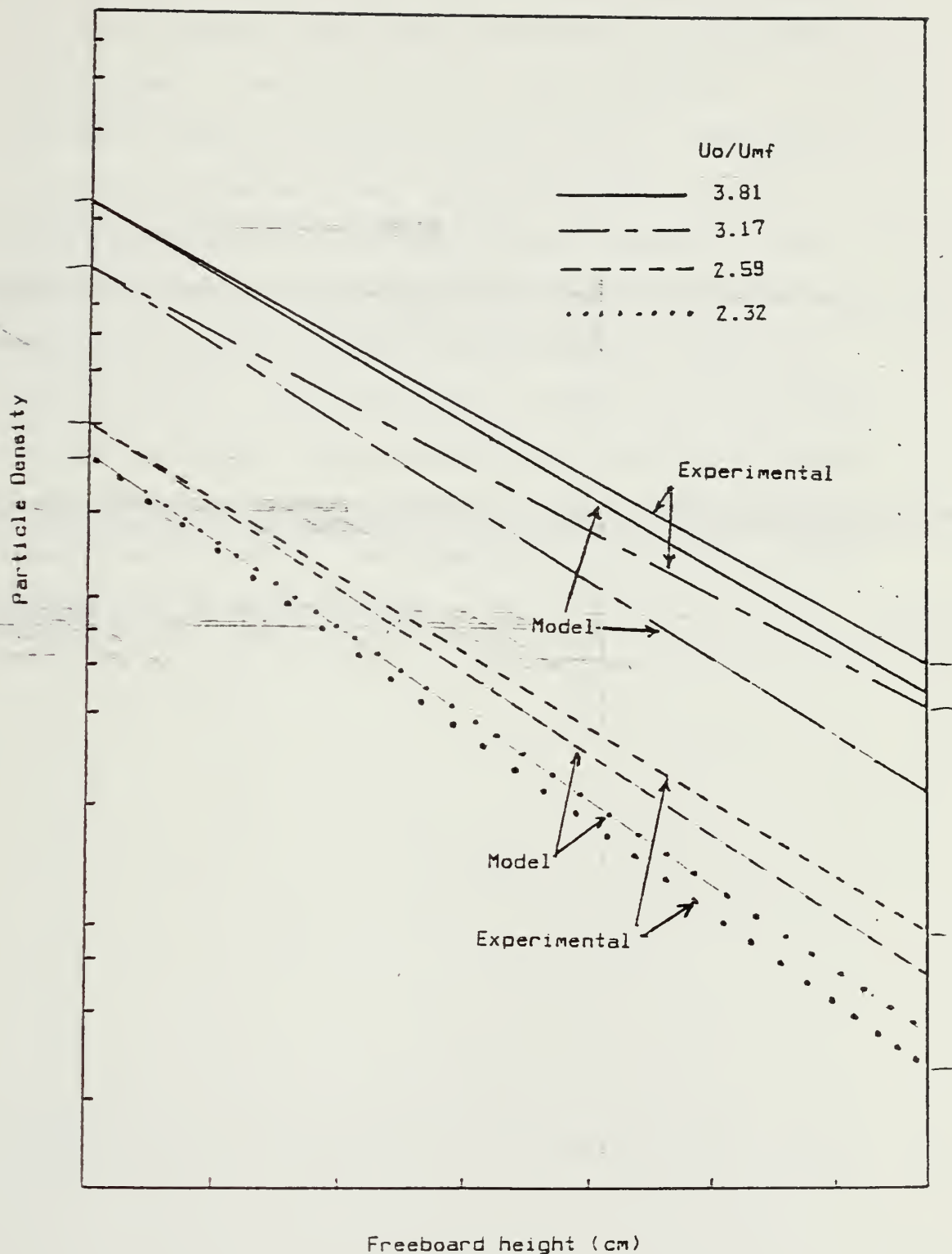
Fig. 85   Comparison of slopes for the particle
density distribution above the bed
as derived for experimental data and
computer model output.

143

The slope shown in Fig. 84 for heights between approximately 4 and 18 cm is totally different from the slopes listed in table 17. This is also the lower range in which the experimental data was collected. As was shown earlier, when the particle distribution analyzed included particles from 80 - 1070 microns, the peak was located at 11 cm. This is the height where the largest particles attain their maximum height and begin to fall back to the bed. It does not seem likely that including the few particles present above 1070 microns would totally account for this discrepancy. Other factors which the model has not accounted for which may explain these discrepancies is the effect of varying jet velocities and durations which were shown in chapter V to vary greatly, and the effect of particles whose velocity vector is not perpindicular to the bed surface.

CHAPTER VII

CONCLUSIONS AND RECOMMENDATIONS

Conclusions

Several important conclusions can be made concerning the particle trajectory computer model and the experimental data.

1. A particle trajectory model, even as simple as the one discussed in this work, produces results which closely predict several aspects of particle activity within a fluidized bed. The more important predictions include the particle density distribution in the freeboard and the height distribution of particles. The results obtained with the current model indicate that further work on improving the particle trajectory model to include particle-particle interactions and paticle velocities not perpendicular to the bed surface is very desirable.

2. The sensitivity analysis indicates that the jet duration and jet velocity are critical parameters in determining particle loading conditions in the freeboard. Since these are constantly changing from one bubble eruption to the next, a statistical distribution will be required to accuarately model freeboard particle activity. The developement of a basic model to predict

145

the jet duration and velocity as a function of bubble size, Uo, Umf, etc is therefore needed.

3. Particle distribution analysis of experimental samples at increasing heights above the bed, show the presence of large particles. Many of these are above the maximum calculated trajectory heights for these particle sizes. This indicates that either the jet velocity or jet duration carried these particles to these heights, or, particle-particle collisions are present in numbers great enough to be important in the analysis.

4. The sampling apparatus designed and built for this study appears to operate satisfactory. The data obtained correlates with work done by other researchers and with the computer model. However, additional work is needed to correlate sample size and particle size distribution with freeboard height.

Recommendations

1. Further experimental data is needed at higher velocities and higher heights above the bed using the sampling apparatus designed in this work. This will provide additional data to evaluate the operation of the sampling apparatus and the computer model. Also, a scale capable of measuring quantities of samples less than 0.01 grams and a particle removal system which removes the particles with less error from the sample trap is necessary for accurate work.

2.   A sampling device which has a shorter trap height should

be designed.   The present sample trap is very direction oriented

and samples particles traveling only in a narrow range from the

vertical.   This would allow more accurate work to be done in the

splash zone where particles are more likely to be traveling in

directions other than vertical.

3.   The computer model needs to have encorporated in it, a

statistical distribution model for jet velocity and jet duration.

This will allow the determination of the effects of varying jet

velocity and duration on particle distributions in the freeboard.

4.   A correlation for jet velocity and duration as functions

of bubble diameter, Uo, and Umf should be determined and included

in the model.

REFERENCES

[1]   D. Kunii and O. Levenspiel, <u>Fluidization Engineering</u>,
        Robert E. Krieger Pub Co., Huntington, NY, 1977.

[2]   P.A. Tipler, <u>Modern Physics</u>, Worth Publishers Inc,
        New York, NY, 1978, p74.

[3]   W.K. Lewis, E.R. Gilliland and Peter M. Lang, "Entrainment
        From Fluidized Beds", Fluidization, AIChE Symposium Series, No.
        38, Vol. 58, 1962, p65.

[4]   F.A. Zenz and N.A. Weil, "The Theoretical-Empirical Approach
        to the Mechanism of Particle Entrainment from Fluidized Beds",
        AIChE Journal, No. 4, Vol. 4, 1958, p472.

[5]   C.Y. Wen and L.H. Chen, "Fluidized Bed Freeboard Phenomena:
        Entrainment and Elutriation", Chemical Engineering Research and
        Developement, AIChE Journal, Vol. 28, No. 1, January 1982,
        p117.

[6]   R.E. Page and D. Harrison, "Particle Entrainment from a
        Three-Phase Fluidized Bed", Fluidization and its Applications,
        Proceedings of the International Symposium, 1974, p393.

[7]   P.M. Walsh, T.Z. Chaung, A. Dutta, J.M. Beer, and A.F.
        Sarofim, "Particle Entrainment and Nitric Oxide Reduction in
        the Freeboard of a Fluidized Coal Combustor", American Chemical
        Society Division of Fuel Chemistry, No. 1, Vol. 27, 1982,
        p243.

[8]   S.E. George and J.R. Grace, "Entrainment of Particles from
        Aggregative Fluidized Beds", Fluidization: Application to Coal
        Conversion Processes, AIChE Symposium Series, No. 176, Vol.
        74, 1978, p67.

[9]   T.P. Chen and S.C. Saxena, "A Theory of Solids Projection
        from a Fluidized Bed Surface as a First Step in the Analysis of
        Entrainment Processes", Fluidization, Procedings, Cambridge
        University Press, 1978, p151.

[10]   P.M. Walsh, J.E. Mayo, and J.M. Beer, "Refluxing Particles
        in the Freeboard of a Fluidized Bed", Fluidization and
        Fluid-particle Systems: Theories and Applications, AIChE
        Symposium Series, No. 234, Vol. 80, 1984, p119.

[11]   A. Nazemi, M.A. Bergougnou, and C.G.J. Baker, "Dilute Phase
        Hold-up in a Large Gas Fluidized Bed", Fluidization and
        Fluid-particle Systems: Theories and Applications, AIChE
        Symposium Series, No. 141, Vol. 70, 1974, p98.

148

[12]   L. R. Glicksman, W. K. Lord, G. McAndrews, M. Sakagami,
        "Measurement of Bubble Properties in Fluidized Beds",
        Procedings of the Seventh International Conference on Fluidized
        Beds, 1982.

[13]   M.H. Peters and D.L. Prybylowski, "Particle Motion Above the
        Surface of a Fluidized Bed: Multiparticle Effects",
        Fluidization and Fluid-particle Systems: Theories and
        Applications, AIChE Symposium Series, No. 222, Vol. 79, 1983,
        p83.

[14]   R.G. Boothroyd, Flowing Gas-Solids Suspensions,
        Chapman and Hall LTD, London, 1971.

[15]   W.K Lord, "Bubbly Flow in Fluidized Beds of Large Particles",
        Sc.D. Thesis, M.I.T., Department of Mechanical Engineering,
        1983.

[16]   H.S. Bean, "Fluid Meters Their Theory and Application", Report
        of ASME research committee on fluid meters, sixth edition,
        The American Society of Mechanical Engineers, New York, NY,
        1971.

[17]   Frank M. White, Viscous Fluid Flow, McGraw-Hill, 1974,
        p209.

APPENDIX A

Moment of Inertia Calculations for Paddles

The calculation of the total Moment of inertia (I) of the
paddles can be broken up into three seperate calculations. First,
the moment of inertia (I1) of the two aluminum cylinders used to
mount the paddle arms to the solenoid shaft is calculated. The
second calculation (I2), accounts for the moment of inertia of the
paddles themselves, which are constructed of a foam, basswood and
epoxy laminate (Fig. A-1). Finally, the moment of inertia (I3) of
the hardwood mounting ends on the paddles is calculated.

The following equations were used to calculate the mass
moments of inertia:

$$I1 = \frac{P \; H \; r^4}{2} \tag{A1}$$

$$I2 = \frac{L \; W \; (L^2 + W^2) \; (P1 \; t1 + P2 \; t2)}{12} \tag{A2}$$

$$I3 = \frac{2 \; L \; W + P \; (L^2 + W^2)}{12} \tag{A3}$$

Table A.1 is a listing of parameters required for the moment
calculations.
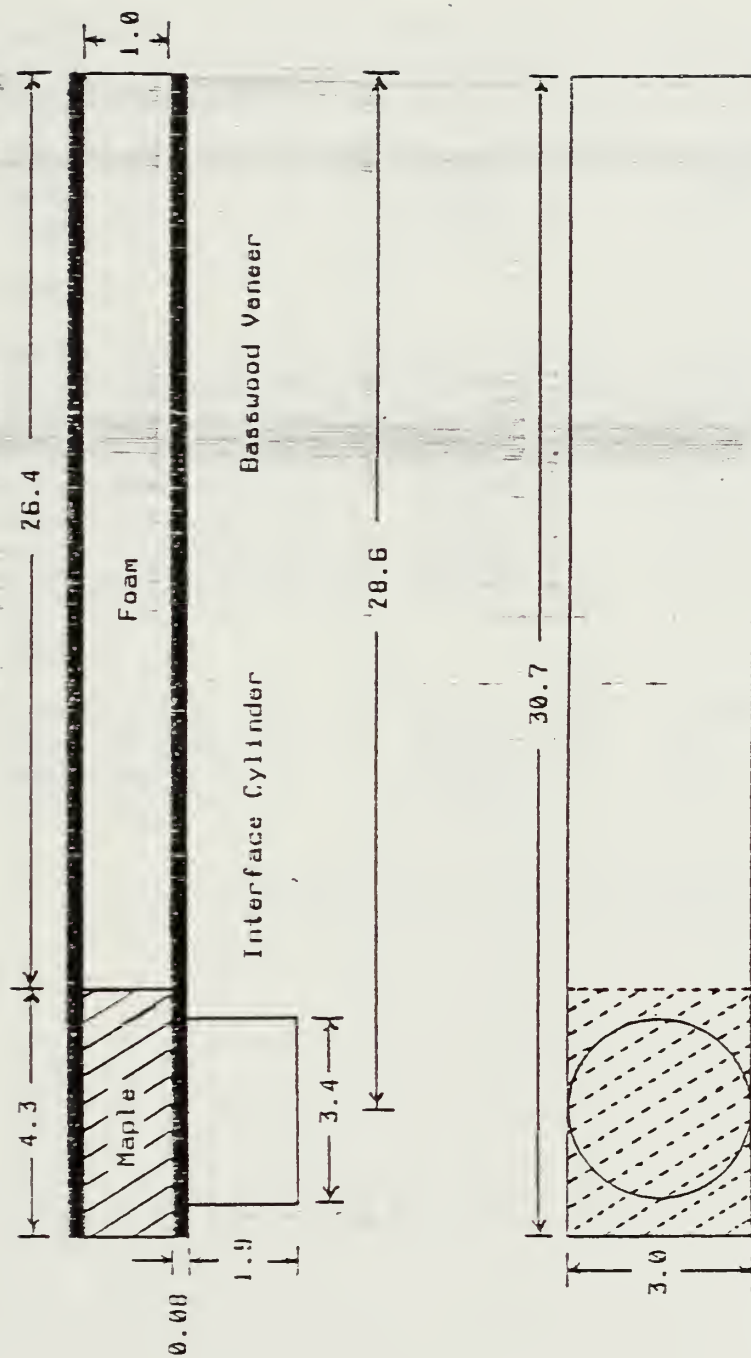
Fig. A-1 Construction of Paddles with Aluminum
Interface Cylinder Shown. All
Dimensions in cm.

TABLE A.1

Component	MKS units		English units	
Aluminum Cylinder				
Density Al [P]	2780	kg/m^3	0.1004	lbf/in^3
Radius [r]	0.0171	m	0.675	in
Height [H]	0.0381	m	1.5	in
Paddles				
Density Foam [P1]	50	kg/m^3	0.00181	lbf/in^3
Density Basswood [P2]	400	kg/m^5	0.0144	lbf/in^3
Thickness Foam [t1]	0.0102	m	0.4	in
Thickness Basswood [t2]	0.00159	m	0.0625	in
Length Foam [L1]	0.5842	m	23.0	in
Length Basswood [L2]	0.5842	m	23.0	in
Width Foam [W1]	0.0305	m	1.2	in
Width Basswood [W2]	0.0305	m	1.2	in
Hardwood				
Density Maple [P]	650	kg/m^3	0.0235	lbf/in^3
Thickness Maple [t]	0.0102	m	0.4	in
Length Maple [L]	0.0432	m	1.7	in
Width Maple [W]	0.0348	m	1.2	in

Listing of paddle components and parameters.

Equation (A.1) is used to calculate the mass moment of

inertia for a right circular cylinder rotating about its Z axis

(Fig. A-2). The height H, accounts for both the upper and the

lower solenoid shaft cylinders. Equations (A.2) and (A.3)

determine the mass moment of inertia for a rectangular prism

rotating about its X-Y centroidal axis (Fig. A-3). The length L

in equation A2 accounts for both the upper and lower paddle

lengths. The factor of 2 in equation (A.3) is because both the

upper and lower hardwood sections are identical and can be

combined. By inserting the respective values from Table A.1 into

equations (A.1), (A.2), and (A.3), the value for each inertia

component can be calculated. Adding these components, the total

mass moment of inertia applied to the solenoid by the paddles is

determined. These results are listed in Table A.2.
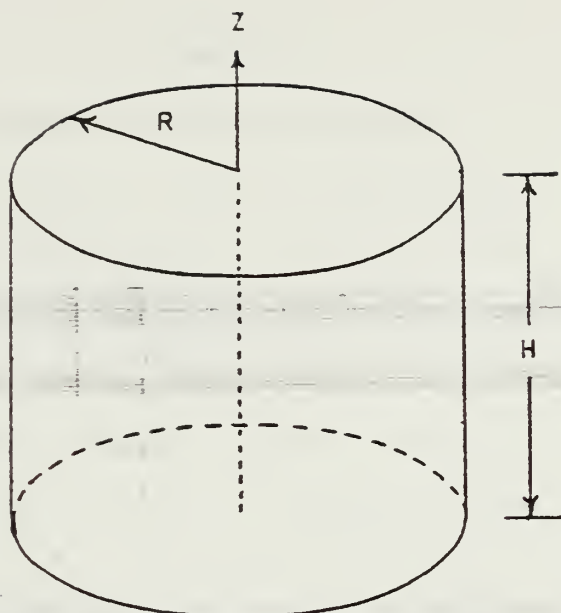
Fig. A-2   Diagram for Moment of Inertia Calculation
            Used for Cylinder About Z Axis.
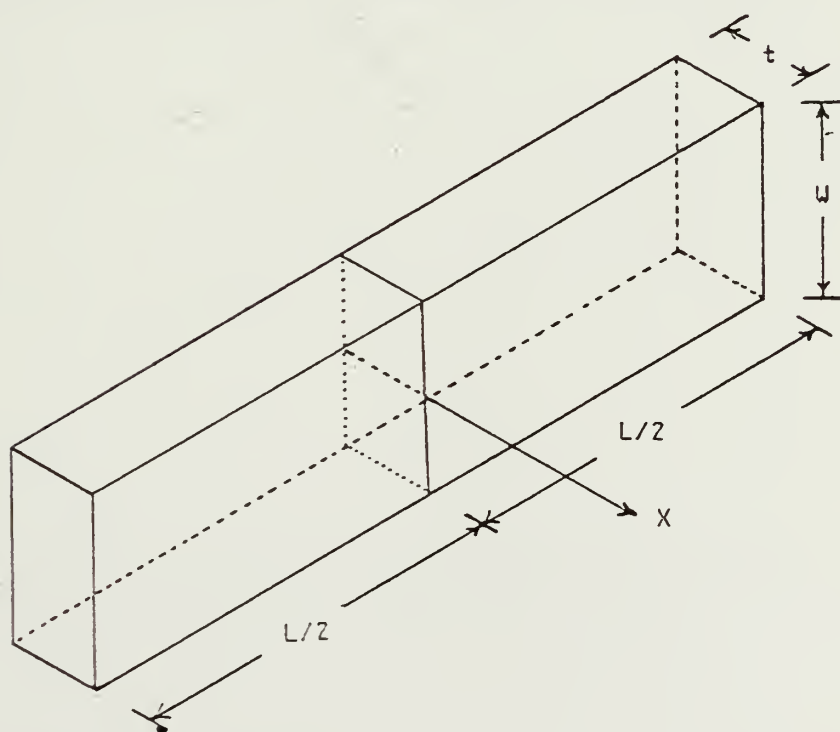
Fig. A-3   Diagram for Moment of Inertia Calculation
            Used for Rectangular Prisim About X Axis.

TABLE A.2

Moment of inertia components:

MKS units	English units
$I1 = 1.422\ (-05)\ kg\ m^2$	$4.911\ (-02)\ lbf\ in^2$
$I2 = 5.823\ (-04)\ kg\ m^2$	$1.982\ (00)\ lbf\ in^2$
$I3 = 2.556\ (-06)\ kg\ m^2$	$6.919\ (-03)\ lbf\ in^2$

Total moment: $I = I1 + I2 + I3$

$I = 5.991\ (-04)\ kg\ m^2$ $2.037\ (00)\ lbf\ in^2$

Calculated values for mass moment of inertia of
paddles and paddle components. I1 is inertia
value for the aluminum cylinders. I2 is the
inertia value for the paddles themselves and I3
is for the hardwood end pieces.

APPENDIX B

Error Determination of Vacuum Collection System

Tests of the vacuum sample removal system indicated that some particles remained in the sample trap. These particles were located in the corners of the trap where the equalizing air stream could not agitate them enough to move them into the vacuum stream. As a result, it became necessary to determine to what extent these remaining particles affected the accuracy of the sample attained.

The procedure used involved placing samples of known weight and particle size distribution (equivalent to the bed material) inside the sample trap. Sample sizes of 10, 15, 20, and 25 grams were used. The sample particles were then vacuumed out and their weight determined. The difference in weights of the samples were then calculated along with the percentage differences. These results are listed in Table B.1.

An analysis of the results listed in Table B.1 indicates that the average difference between the two sample weights is only 0.52 % while the maximum difference observed was 0.93 %. It can therefore be concluded that the particles remaining in the sample trap do not significantly affect the accuracy of the sample attained.

TABLE 8.1

SAMPLE No.	Initial Weight grams	Sample Weight grams	Weight Difference grams	Weight Difference Percent
1	10	9.95	0.05	0.50
2	10	9.92	0.08	0.80
3	10	9.95	0.05	0.50
4	10	9.98	0.02	0.20
5	15	15.03	-0.03	-0.20
6	15	15.02	-0.02	-0.13
7	15	14.86	0.14	0.93
8	15	14.87	0.13	0.87
9	15	14.97	0.03	0.20
10	20	19.93	0.07	0.35
11	20	19.86	0.14	0.70
12	20	19.90	0.10	0.50
13	20	19.93	0.07	0.35
14	20	19.94	0.06	0.30
15	25	24.83	0.17	0.68
16	25	24.80	0.20	0.80
17	25	24.78	0.22	0.88
18	25	24.83	0.17	0.68
19	25	24.77	0.23	0.93
		AVG=	0.10	0.52
		STNDV=	0.08	0.34

Results of vacumn sample removal test.

APPENDIX C

Sample Trap Closure Time Test

Due to the high velocity of the particles with respect to the size of the sample trap, it was important to ensure that the sample trap was closed in a very short period of time. To measure the closure time, the set-up shown in Fig. C-1 was used.

An electric eye, consisting of a light emitting diode and a photo transistor, was used. The diode was powered by a 6 volt battery and the photo transistor was wired directly to an oscilloscope. The electric eye circuit was then placed at a distance of 0.267 m (10.5 in) from the pivot point of the paddles. At this position, the closing time calculation involves only a simple proportion relationship between the paddle and the sample trap widths. The eye was also positioned as close to the trailing edge of the fully closed paddle as possible to minimize error.

The oscilloscope sweep was set to trigger off of the initial change of state from the photo transistor when the paddle first eclipsed the light beam. The resultant traces were then analysed to determine closure time. Time t=0 was set equal to the initiation of the trace on the oscilloscope. Time t=t1 was defined as the point at which the trace begins its excursion back

158
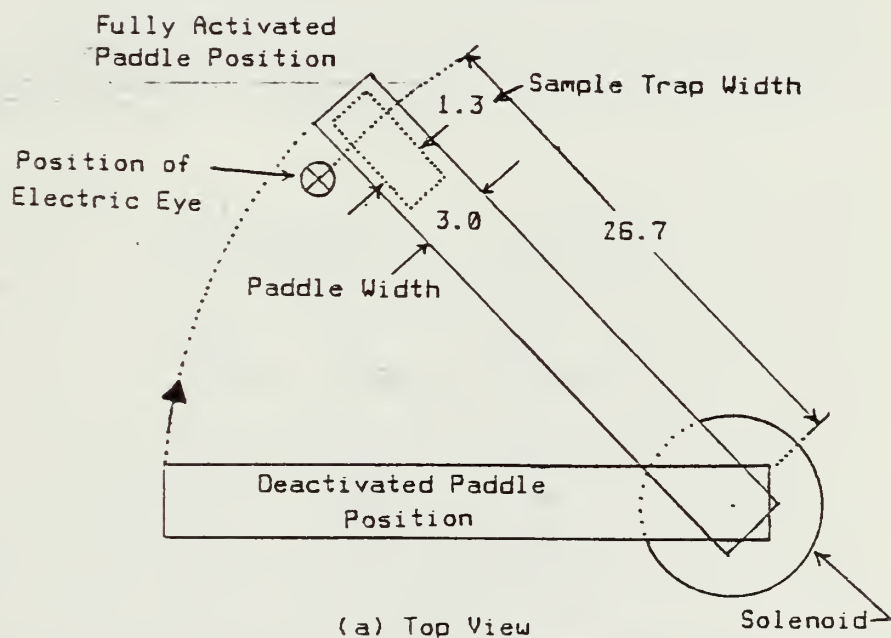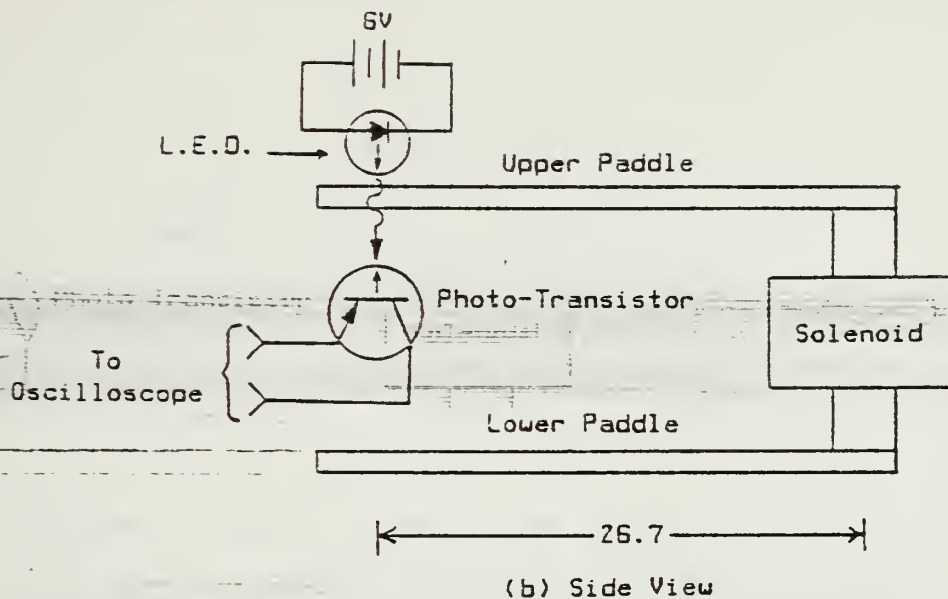
Fig. C-1   Diagram of Closure Time Determination Set Up.
            All Dimensions in cm.

159

to the base voltage as shown in Fig. C-2. By using the ratios:

$$\frac{W1}{t1} = \frac{W2}{t2}$$

<div align="right">(C.1)</div>

Where:

W1 = width of the paddle
W2 = width of sample trap
t1 = time delay measured on oscilloscope
t2 = closure time of sample trap

the closure time of the sample trap can be determined. Several

trials were run with the resulting data listed in Table C-1. All

of the trials were very consistant. The resultant determination

for the average closure time was 1.44 ms.

TABLE C-1

W1 = 0.0305 m   (1.2 in)
W2 = 0.0127 m   (0.5 in)

Trial No.	t1 ms	t2 ms
1	3.4	1.42
2	3.4	1.42
3	3.55	1.48
4	3.5	1.46
5	3.5	1.46
Avg	3.47	1.44

Sample trap closure data: W1 is the width of
the paddle, W2 is the width of the sample trap
and time t1 is eclipse time of paddle through
light beam. Time t2 is closure time of Sample
trap as calculated using equation (C.1).
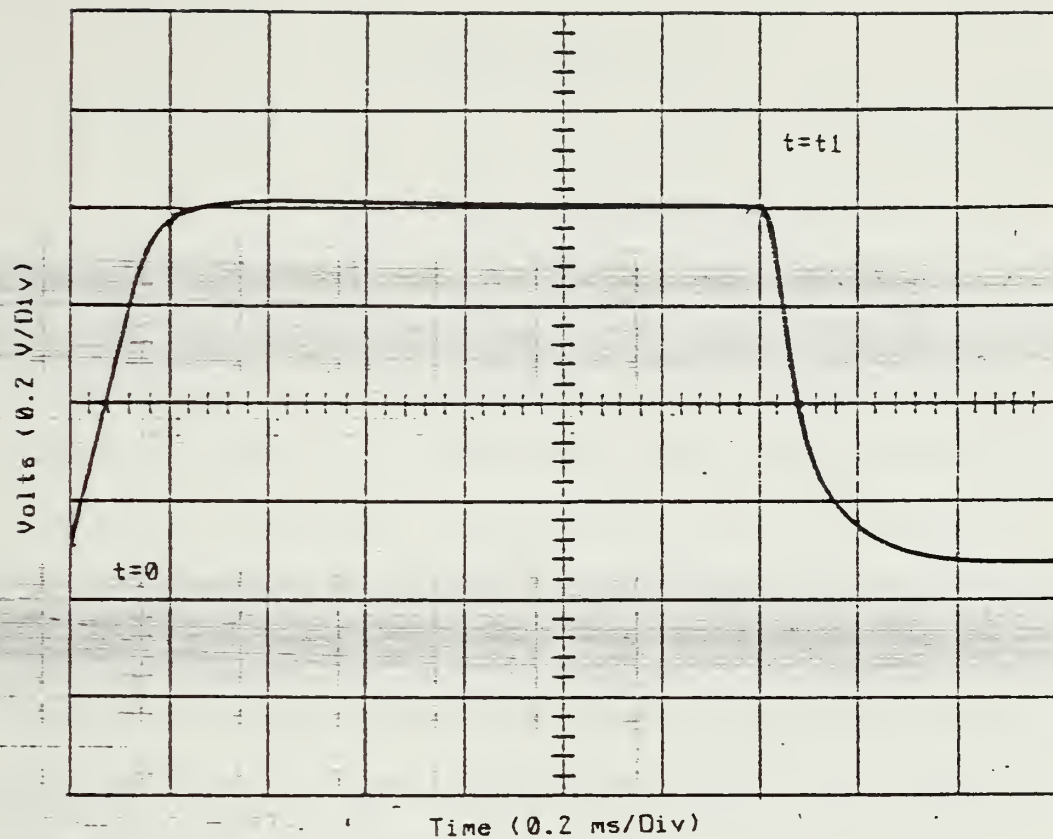
Fig. C-2   Oscilloscope Trace of Paddle
Eclipsing Electric Eye.

161

APPENDIX D

Solenoid Torque and Dynamic Analysis

The goal of this design was to shut the sample trap in about 1 millisecond (ms). At this speed, a particle traveling at 10 meters per second (m/s) would travel 1 cm or approximately 11 % of the sample trap length. A velocity of 10 m/s is at the upper limit of the particle velocity distribution and would account for only a small percentage of the particles ejected by the bed. The majority of the particles, for the fluidization conditions used in the bed, have an average ejection velocity of 1-2 m/s, based on data from George and Grace [8].

TORQUE ANALYSIS

To determine the minimum required torque output of the solenoid, two analysis were performed. The first analysis calculates an average torque required to produce the desired velocity. The second analysis uses the torque data from the selected solenoid and calculates the expected closure time and swing time for the paddle arms.

First Analysis

To close the sample trap in 1 ms, the angular velocity of the
paddles at closure can be calculated as:

$$w = \frac{W2}{R \ t2} \qquad (D.1)$$

where: w = Angular velocity of paddles
$W2$ = Width of sample trap
R = Paddle pivot to sample trap distance
$t2$ = Closure time of sample trap

Using the values of $W2$= 0.00197 m, R= 0.0413 m, and $t2$= 1 ms,
equation (D.1) results in an angular velocity of 47.70 rad/sec.
The radial acceleration required to attain this velocity through a
deflection of $\pi/4$ radians (45 Deg), is calculated by:

$$a = \frac{w^2}{2 \ \theta} \qquad (D.2)$$

where: a = Angular acceleration of paddles
w = Angular velocity of paddles
θ = Angular deflection of paddles

Using the result of equation D1 and θ=$\pi/4$ radians, equation D2
gives the required angular acceleration of the paddles as 1448.5

163

rad/s/s. Combining this result with the result for the total mass
moment of inertia from Appendix A, the required average torque
output of the solenoid can be calculated as:

$$T = I \, a \qquad\qquad (D3)$$

where: a = Angular acceleration of paddles
        I = Mass moment of inertia
        T = Required solenoid torque

The resultant value for the torque (T) is 0.87 N m (7.7 Lbf in).
A geometric average of the selected solenoid's torque output, as
shown in Fig. D-1a, indicates an average of 1.0 N m (8.8 Lbf in).
Therefore, the selected solenoid has sufficient torque output to
achieve the desired paddle velocity.

SECOND ANALYSIS

For the second analysis, it will be assumed that the torque
output of the selected solenoid can be modeled as a linear spring.
Fig. D-1b shows the torque output of the solenoid as a function
of angular displacement. From Fig. D-1b, a spring constant of k=
0.72 N m/rad (0.11 Lbf in/deg) can be used to approximate the
torque curve. The spring constant is derived from the slope of
the torque-angular displacement curve.
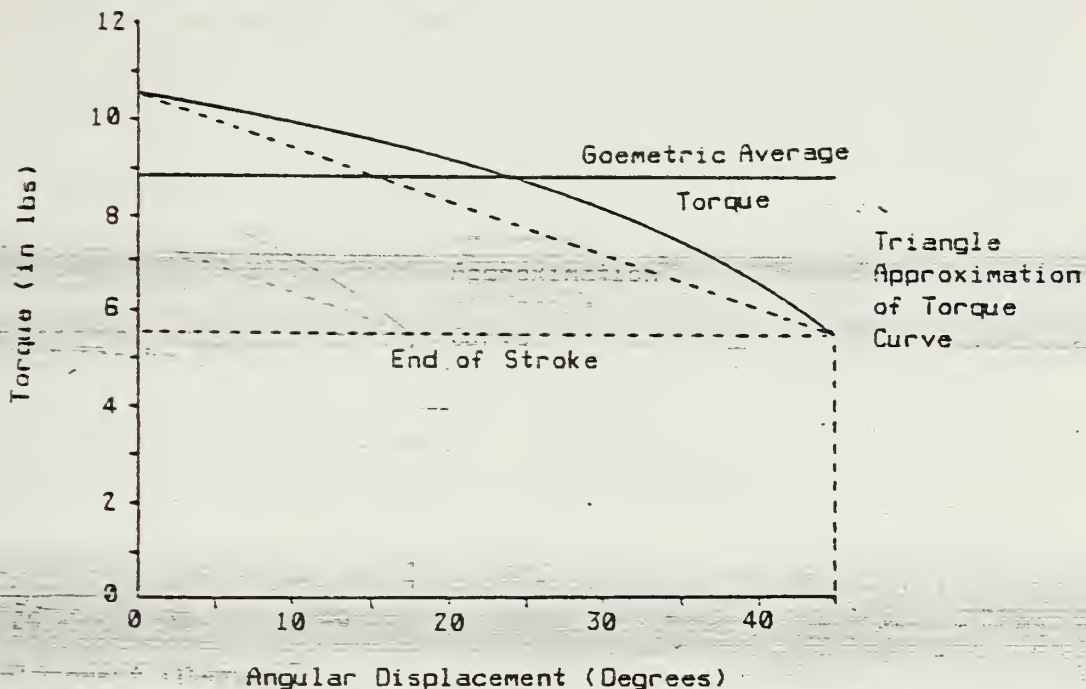
Fig. D-1a Torque Output of Rotary Solenoid
Showing Triangle Approximation.
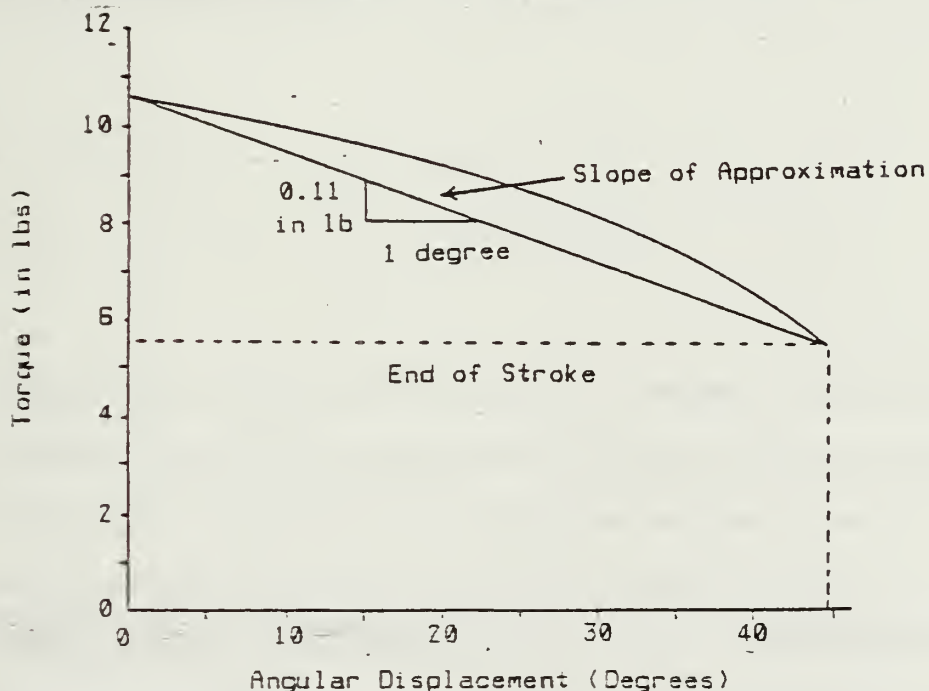
Fig. D-1b Torque Output of Rotary Solenoid
Showing Slope of Approximation
Curve Used to Determine Spring
Constant.

165

The system can then be modeled as a simple rotational mass -
spring system. The differential equation of motion, general
solution, and boundary conditions are:

Diff Eqn:$\qquad I \ddot{\theta} + k \theta = 0 \qquad\qquad$ (D.4a)

Gen Soln:$\qquad \theta = C1 \sin(m\ t) + C2 \cos(m\ t) \qquad$ (D.4b)

$\qquad$ where:$\quad m^2 = \dfrac{k}{I}$

b.c.:$\qquad$ 1)$\quad t = 0:\qquad \dot{\theta} = 0$
$\qquad\qquad$ 2)$\quad t = 0:\qquad \theta = 1.65$ rad

Solving equation (D.4b) using the given boundary equations, gives
the following expressions for any angular displacement (θ) and
angular velocity ($\dot{\theta}$):

$$\theta = 1.65 \cos(m\ t) \qquad\qquad \text{(D.5a)}$$

$$\dot{\theta} = -1.65\ m\ \sin(m\ t) \qquad\qquad \text{(D.5b)}$$

Knowing that the solenoid stroke is $\pi/4$ radians, the total solenoid
actuation time can be obtained from equation (D.5a) by setting 0 =
(1.65 - $\pi/4$). The total actuation time was determined to be 29.2
ms. Inserting this value for time into equation (D.5b), a
rotational velocity of 48.6 rad/s was found. This velocity is
very close to the desired velocity obtained from equation (D.1).

DYNAMIC ANALYSIS

The desire to determine whether the debris of a specific
bubble has been trapped by the sampling device requires the
determination of the total actuation time for the apparatus.
Knowing this value, the delay between the detection of a bubble
and the closure of the sample trap can be determined, and hence,
whether the particles from the detected bubble were within the
vicinity of the trap.

Appendix C determined that the actual closure time for the
sample trap was 1.44 ms. Using this value in equation (D.1), a
rotational velocity at the end of the stroke of only 33.12 rad/sec
is calculated. Because the mass moment of inertia for the
solenoid was unknown in the beginning, the analysis ignored it.
With the determintion of the actual closure time in Appendix C,
the total moment of inertia, including the solenoid can be
approximated. By iterating equations (D.5a) and (D.5b) with $\dot{\theta}$ =
33.12 radians/sec, a new inertia value of 1.27 (-03) kg m is
determined. Using this inertia value in equation (D.5b), the
total actuation time is 42.6 ms. This increase in actuation time
of 13.5 ms is relativily close to the manufactures quoted
actuation time for the solenoid of 12 ms and suggests that the
values are within reason.

Table D.1 provides a summary of the results obtained from the
dynamic analysis.

TABLE D.1

Mass moment of inertia:

Paddles (I)	$5.991\ (-04)\ kg\ m^2$
	$2.037\ (00)\ lb\ in^2$
Paddles + Solenoid (It)	$1.27\ (-03)\ kg\ m^2$
	$4.32\ (00)\ lb\ in^2$

Closure time:

Sample trap (t2)	1.44 ms
Total swing (t3)	42.6 ms

Summary of dynamic analysis results.

APPENDIX E

Bed Particle Size Distribution Analysis

A sample of particles was obtained from the fluidized bed
after the bed had been operating for several hours. Sample sizes,
ranging from 1.2 to 2.8 kg, were then taken from the central area
of the bed. Each sample was then sieved through a series of 14 US
standard wire mesh sieves using a Tyler Industrial Products Model
RX-24 portable sieve shaker for 30 minuites. The contents of each
sieve was then weighed, using a Torsion Balance Co TORBAL scale,
to an accuracy of 0.01 gram. The resulting average particle size
distribution is listed in Table E.1 and shown in fig. E-1.

169

TABLE E.1

US Standard Seive No.	Seive Size um	Weight In Seive grams	Percent of Total Sample	Cumulative Percent
18	1000	8.49	0.31	0.31
20	850	24.60	0.90	1.21
30	600	101.96	3.73	4.95
35	500	110.85	4.06	9.01
45	355	176.35	6.46	15.46
50	297	430.77	15.78	31.24
60	250	385.59	14.12	45.36
70	212	395.32	14.48	59.84
80	180	469.20	17.19	77.03
100	149	339.93	12.45	89.48
120	125	125.01	4.58	94.06
140	106	109.45	4.01	98.06
170	90	46.67	1.71	99.77
200	75	5.91	0.22	99.99
	<75	0.30	0.01	100.00

Particle Specific Gravity = 8.1

Average particle size distribution of bed material in grams
and percentage of total weight using sieve analysis.

APPENDIX F

Mean Bed Flow Velocity Determination

To determine the mean velocity of air flowing through the bed, the ASME report on fluid meters [17] was used. Based on this paper, equation (F.1) was used for determining the mass flow rate of air through the bed.

$$W = 0.099702 \ (K \ Y \ F \ d^2) \ (\rho \ dP)^{\frac{1}{2}} \qquad (F.1)$$

where:

W = Mass flow rate (lbm/sec)
d = Orfice diameter (inches)
K = Flow coefficient
F = Thermal expansion factor (1 for air)
Y = Expansion factor
dP = Differential pressure (inches water)
ρ = Density of air (ahead of orfice)

The flow coefficient (K) is a function of Reynold's number, the orfice diameter (d), and the pipe diameter (D). For the pressure tap configuration used in the MIT atmospheric fluidized bed (1-D / 1/2-D) the flow coefficient is calculated using equation (F.2).

$$K = Ko + \frac{1000\ b}{\sqrt{B\ Re}}$$ (F.2)

where:

Re = Reynolds No.

B = d/D = (orfice dia / pipe dia)

$$Ko = (0.6014 - 0.01352\ D^{-1/4})$$

$$+ (0.3760 + 0.07257\ D^{-1/4})$$

$$\left(\frac{0.00025}{D^2\ B^2 + 0.00025\ D} + B^4 + 1.5\ B^{16} \right)$$

$$b = \left(0.0002 + \frac{0.0011}{D}\right)$$

$$\div \left(0.0038 + \frac{0.0004}{D}\right)$$

$$(B^2 + (16.5 + 5\ D)\ B^{16})$$

The expansion factor (Y) is determined from equation (F.3) and is a function of the diameter ratio (B), the ratio of specific heats (s), and the ratio of the differential pressure to inlet pressure.

$$Y = 1 - (0.410 + 0.350\ B^4)\ \frac{dP}{P1\ s}$$ (F.3)

where:

P1 = Inlet pressure

s = Ratio of specific heats (1.4 for air)

Mass flow rate is a function of velocity, and therefore, by definition a function of Reynold's number. Equation (F.4) is used to determine mass flow rate as a function of viscosity and Reynold's number.

$$W = \frac{u \ DZ}{C \ Re}$$ (F.4)

where :

u = Absolute viscosity (lbm/ft sec)
C = Constant (15.28)

This requires that the solutions of equation (F.1) and equation (F.4) be iterated until the Reynold's numbers converge. The determination of mean air velocity is obtained from the mass flow rate (W) using equation (F.5).

$$V = \frac{W}{e \ A}$$ (F.5)

where:

e = Density of air (lbm/ft^3)
A = Area of bed (ft^2)

To perform these calculations, a computer program was used. The program (APPENDIX G) is written in HP BASIC 2.0 for running on an HP 9816 series 200 micro-computer. Convergence usually required four to seven iterations and should be correct to within 0.5%.

APPENDIX G

This Appendix lists the BASIC computer program used to calculate mean bed velocity as discussed in Appendix F. It is written in HP BASIC 2.0.

```
10      !........MAIN Program.......
20      ! Metering of gases by means of the ASME square-edged orfice with
30      ! 1-D 1/2-D taps.  Reference Fluid Meters Their Theory and
40      ! Application.  ASME Report 6th edition, ASME New York, NY. 1971
50      ! Program must be altered for Orfice diameter other than 7.071 in
60      ! and pipe diameter other than 10.02 in. (see line 130)
70      !
80      !
90      !
100     INTEGER Answer
110     REAL D1,D2,W,K,Y1,P1,P1a,T1,S,P_del,Beta,Area_bed,Vmu,Reynolds_no,Rho,Rho1
,Patm,Velocity
120     DIM Home$[2],Clear$[2]
130     DATA 7.071,10.02,1.4,11.611,50000.,76.
140     READ D2,D1,S,Area_bed,Reynolds_no,Patm
150     Clear$=CHR$(255)&CHR$(75)                        ! CLEAR screen
160     Home$=CHR$(255)&CHR$(84)                         ! HOME screen
170     !
180     ! Input variables
190     !
200     INPUT "Enter static pressure P1 (cm Hg): ",P1
210     INPUT "Enter pressure drop dP (inches water): ",P_del
220     INPUT "Enter air temperature (Degrees F): ",T1
230     !
240     ! Compute data
250     !
260     OUTPUT 2;Home$;                                  ! Home display
270     OUTPUT 2;Clear$;                                 ! Clear display
280     Beta=D2/D1                                       ! Calculate beta
290     P1a=P1+Patm                                      ! Absolute pressure
300     P1=(P1a)/2.54                                    ! Change to inches
310     T2=T1+459.67                                     ! Convert to R
320     Rho=FNDensity(Patm,T2)                           ! Air density bed
330     Rho1=FNDensity(P1a,T2)                           ! Air density upstream
340     Vmu=FNViscosity(T2)                              ! Air viscosity
350     Y1=FNExpan(Beta,P1,S,P_del)                      ! Expansion factor Y
360     K=FNFlow_coeff(Reynolds_no,Beta,D1)              ! Flow coefficient K
370     W=FNMass_flow(D2,K,Y1,Rho1,P_del)                ! Mass flow rate
380     Rd=FNReyn(W,Vmu,D2)                              ! Reynolds # calculated
390     IF ABS(Rd-Reynolds_no)>1. THEN                   ! Check accuracy
400        Reynolds_no=Rd
410        GOTO 360
420     END IF
430     Velocity=W/(Rho*Area_bed)                        ! Velocity calculation
440     PRINT "Velocity= ";Velocity;" ft/s"             ! Output results
450     INPUT "Enter (1) to continue, (0) to stop",Answer
460     IF Answer=0 THEN STOP
470     IF Answer<>1 THEN
480        PRINT "Value must be either 1 or 0; try again"
490        GOTO 450
500     END IF
510     GOTO 150
520     END
530     !
540     ! End MAIN.......Begin FUNCTIONS
550     !
560     DEF FNExpan(Beta,P1,S,P_del)                     ! Expansion factor Y
570        Hold=P_del/(P1*S+13.6666)
580        Y=1-(.41+.35*Beta^4)*Hold
590        RETURN Y
```

176

```
600    FNEND
610    !
620    !
630    DEF FNFlow_coeff(Reynolds_no,Beta,D1)            ! Flow coefficient K
640      Ko=.6014-.01352*D1^(-.25)+(.376+.07257*D1^(-.25))*(.0002S/(D1*D1*Beta*Be
ta+.0002S*D1)+Beta^4+1.5*Beta^16)
650      B=.0002+.0011/D1+(.0038+.0004/D1)*(Beta*Beta+(16.5+5*D1)*Beta^16)
660      K=Ko+1000*B/SQR(Beta*Reynolds_no)
670      RETURN K
680    FNEND
690    !
700    !
710    DEF FNMass_flow(D2,K,Y1,Rho1,P_del)              ! Mass flow rate W
720      W=.099702*D2*D2*K*Y1*SQR(Rho1*P_del)
730      RETURN W
740    FNEND
750    !   .
760    !
770    DEF FNReyn(W,Vmu,D2)                             ! Reynolds # calculated
780      Rd=15.26*W/(Vmu*D2)
790      RETURN Rd
800    FNEND
810    !
820    !
830    DEF FNDensity(Patm,T2)                           ! Calculate air density
840      Rho=.522406*Patm/T2
850      RETURN Rho
860    FNEND
870    !
880    !
890    DEF FNViscosity(T2)                              ! Calculate air viscosity
900      Vmu=7.303E-7*T2^1.5/(T2+198.6)
910      RETURN Vmu
920    FNEND
```

177

APPENDIX H

This Appendix contains the parts list for the sampling system in three tables. Table H.1 is a list of components for the sampling apparatus. Table H.2 is a list of components for the electrical circuit while Table H.3 is for the vacuum system.

Table H.1

Item No.	Component	Description
1	Solenoid	LEDEX Size 6S 45 Degree Right Hand Stroke Rotary Solenoid Part No. S-8204-029 LEDEX Inc. 801 Scholz Dr, P.O. Box 427 Vandalia, Oh 45377 (513) 898-3621
2	Paddle	Foam, Basswood epoxy laminate with Maple mounting blocks 0.5 X 1.2 X 11.5 inches
3	Interface	Aluminum Cylinders with set screw fastener. R= 0.675 in H= 1.5 in
4	Solenoid Mounting	Aluminum mounting plate 1/4 X 2.8 X 2.8 inches
5	Extension Bar	Aluminum bar 1/4 X 3/4 X 12.6 inches
6	Trap Mount	Aluminum Plate 1/4 X 1.1 X 1.5 inches
7	Sample Trap	1/16 inch Aluminum plate Inside Dimensions: 0.5 X 1.5 X 3.5 inches
8	Vertical Mounting Slide	Aluminum bar 1/4 X 3/4 X 24 inches Adjustment holes drilled every 0.5 inch
9	Base Structure	Tripod Aluminum Structure

List of components for sampling apparatus.

TABLE H.2

Item No.	Component	Description
1	B1	Bridge rectifier assembly, Silicon, LEDEX Part No. 121011-001, includes arc suppressor in unit.
2	D1	Arc Suppressor, not needed if above rectifier assembly used. LEDEX Part No. 122655-001
3	M1	Solenoid (see Table H.1)
4	R1	Resistor, 2 Mohm, 1%, 2 Watt
5	R2	Resistor, 100 kohm, 1%, 1 Watt
6	R3	Resistor, 250 ohm, 10%, 50 Watt
7	S1	Switch, SPST, Push Button, 10 A, 250 V
8	S2	Switch, SPST, Toggle, 10 A, 250 V

List of components for solenoid power supply.

TABLE H.3

Item No.	Component	Description
1	V1	3/8 inch Ball Valve
2	P1	Eductor
3	F1	Screen Filter, 320 um mesh
4	C1	Sample Container, Small Plastic Bottle, 1 Pt
5	C2	Sample Trap (see Table H.1)
6	L1	1/4 inch Polyflow Tubing

List of components for vacuum system.

APPENDIX I

This Appendix contains a complete listing of all data
obtained during this study.   The data is arranged
acording to the distance of the trap height above the
distributor.

DATA for Umf DETERMINATION

Hb (inches)	P1 (cm Hg)	Pb (cm H2O)	dP (n H2O)	T (F)
10.75	7.2	51.9	1.805	62.0
10.75	6.8	50.9	1.517	62.0
10.25	6.2	49.1	0.932	62.0
9.75	6.0	48.8	0.772	62.0
9.50	5.6	47.5	0.515	62.0
9.25	5.1	44.9	0.335	62.5
8.75	4.8	42.9	0.265	63.0
8.50	4.5	39.9	0.177	63.0
8.50	4.0	39.5	0.125	63.5
8.50	3.7	33.9	0.107	64.0
8.50	3.5	32.0	0.094	64.0
8.50	3.3	30.1	0.084	64.0
8.50	2.4	22.3	0.043	64.5
8.50	2.0	18.5	0.027	65.0
8.50	1.6	14.6	0.017	65.0

```
Trap  Height above Distributor: cm (in)   = 30.96   (12.19)
Bed   Height above Distributor: cm (in)   = 25.4    (10)
Trap Height above bed surface: cm (in)    = 5.56    (2.19)
P1: cm Hg  (in Hg)                        = 5.8     (2.28)
dP: cm water  (in water)                  = 1.234   (0.486)
Temp:  C (F)                              = 19.5    (67.0)


            SAMP #      Weight of Sample
                          (grams)


              1             3.16
              2             2.06
              3             1.88
              4             2.43
              5             2.48
              6             2.10
              7             1.84
              8             2.67
              9             2.57
             10             2.15
             11             2.16
             12             1.03
             13             2.46
             14             1.13      AVG    = 2.09   grams
             15             1.21      STN DV = 0.60   grams



Trap  Height above Distributor: cm (in)   = 30.96   (12.19)
Bed   Height above Distributor: cm (in)   = 26.67   (10.5)
Trap Height above bed surface: cm (in)    = 4.29    (1.69)
P1: cm Hg  (in Hg)                        = 6.8     (2.68)
dP: cm water  (in water)                  = 1.887   (0.743)
Temp:  C (F)                              = 18      (64.5)


            SAMP #      Weight of Sample
                          (grams)


             16             7.72
             17             9.12
             18             3.83
             19             4.04
             20             5.66
             21             3.09
             22             8.86
             23             4.50
             24             6.55      AVG    = 5.96   grams
             25             5.84      STN DV = 2.12   grams
```

```
Trap  Height above Distributor: cm (in)   = 37.31  (14.69)
Bed   Height above Distributor: cm (in)   = 25.4   (10)
Trap Height above bed surface: cm (in)    = 11.91  (4.69)
P1: cm Hg  (in Hg)                        = 5.8    (2.28)
dP: cm water  (in water)                  = 1.201  (0.473)
Temp:  C (F)                              = 20.5   (69.0)


              SAMP #      Weight of Sample
                            (grams)

                26          0.62
                27          0.55
                28          0.54
                29          0.64
                30          0.76
                31          0.58
                32          0.61
                33          0.47
                34          0.85      AVG    = 0.62 grams
                35          0.61      STN DV = 0.11 grams



Trap  Height above Distributor: cm (in)   = 37.31  (14.69)
Bed   Height above Distributor: cm (in)   = 26.67  (10.5)
Trap Height above bed surface: cm (in)    = 10.64  (4.19)
P1: cm Hg  (in Hg)                        = 6.3    (2.28)
dP: cm water  (in water)                  = 1.897  (0.747)
Temp:  C (F)                              = 19     (66.0)


              SAMP #      Weight of Sample
                            (grams)

                36          2.87
                37          1.42
                38          1.89
                39          1.34
                40          1.18
                41          1.52
                42          1.57
                43          1.68
                44          1.56      AVG    = 1.66  grams
                45          1.57      STN DV = 0.46  grams
```

```
Trap  Height above Distributor: cm (in)   = 37.31   (14.69)
Bed  Height above Distributor: cm (in)   = 27.94   (11.0)
Trap Height above bed surface: cm (in)   = 9.37    (3.69)
P1: cm Hg  (in Hg)                       = 6.8     (2.68)
dP: cm water  (in water)                 = 1.887   (0.743)
Temp:  C (F)                             = 19      (66.0)


            SAMP #      Weight of Sample
                           (grams)

               46           4.32
               47           2.48
               48           3.12
               49           2.83
               50           4.46
               51           2.37
               52           4.46
               53           4.95
               54           4.15    AVG    = 3.61  grams
               55           2.96    STN DV = 0.95  grams
```

TRAP HEIGHT = 20.25 in

Height of Pressure Tap above Distributor (inches)	Pressure for Samples 66-75 (cm H2O)	Pressure for Samples 86-95 (cm H2O)	Pressure for Samples 56-65 (cm H2O)	Pressure for Samples 76-85 (cm H2O)
1.6	52.9	54.0	56.1	58.5
2.6	48.8	49.8	51.7	52.8
3.6	40.6	41.3	43.8	44.7
4.6	34.9	35.8	38.9	40.0
5.6	27.8	29.7	32.6	33.6
6.6	21.2	22.3	25.5	27.6
7.6	14.6	16.1	19.1	20.7
8.6	8.3	9.7	12.5	14.8
9.6	2.2	3.5	6.4	8.5
10.6	0.0	0.1	1.5	2.4
11.6	0.0	0.0	0.0	0.3
12.6	0.0	0.0	0.0	0.0
13.6	0.0	0.0	0.0	0.0
14.6	0.0	0.0	0.0	0.0

TRAP HEIGHT = 23.25 in

Height of Pressure Tap above Distributor (inches)	Pressure for Samples 206-215 (cm H2O)	Pressure for Samples 196-205 (cm H2O)	Pressure for Samples 186-195 (cm H2O)	Pressure for Samples 176-185 (cm H2O)
1.6	52.0	53.4	56.3	57.7
2.6	48.9	49.6	51.8	52.2
3.6	40.7	41.5	43.6	44.7
4.6	34.7	35.8	38.8	40.0
5.6	28.3	29.3	32.0	33.3
6.6	21.5	22.9	25.6	26.6
7.6	14.9	16.6	18.8	20.3
8.6	8.4	9.8	12.9	13.8
9.6	2.2	3.3	5.2	7.5
10.6	0.0	0.1	1.3	2.9
11.6	0.0	0.0	0.0	0.3
12.6	0.0	0.0	0.0	0.0
13.6	0.0	0.0	0.0	0.0
14.6	0.0	0.0	0.0	0.0

187

```
Trap  Height above Distributor: cm (in)   = 51.44  (20.25)
Bed  Height above Distributor: cm (in)    = 29.21  (11.5)
Trap Height above bed surface: cm (in)    = 22.23  (8.75)
Static Bed Height: cm (in)                = 22.56  (8.88)
P1: cm Hg  (in Hg)                        = 8.3    (3.21)
dP: cm water  (in water)                  = 6.985  (2.75)
Temp:  C (F)                              = 16.5   (62.0)


            SAMP #       Weight of Sample
                           (grams)


               76              1.47
               77              1.35
               78              1.24
               79              1.29
               80              0.74
               81              1.38
               82              1.38
               83              1.47
               84              1.58    AVG    = 1.32  grams
               85              1.33    STN DV = 0.23  grams



Trap  Height above Distributor: cm (in)   = 51.44  (20.25)
Bed  Height above Distributor: cm (in)    = 27.31  (10.75)
Trap Height above bed surface: cm (in)    = 24.13  (9.5)
Static Bed Height: cm (in)                = 22.56  (8.88)
P1: cm Hg  (in Hg)                        = 7.3    (2.87)
dP: cm water  (in water)                  = 4.910  (1.933)
Temp:  C (F)                              = 16.5   (62.0)


            SAMP #       Weight of Sample
                           (grams)


               56              0.95
               57              0.61
               58              1.83
               59              0.84
               60              1.02
               61              0.76
               62              0.67
               63              1.06
               64              0.60    AVG    = 0.92  grams
               65              0.88    STN DV = 0.36  grams
```

```
Trap  Height above Distributor: cm (in)   = 51.44   (20.25)
Bed   Height above Distributor: cm (in)   = 26.67   (10.5)
Trap Height above bed surface: cm (in)    = 24.76   (9.75)
Static Bed Height: cm (in)                = 22.56   (8.88)
P1: cm Hg  (in Hg)                        = 6.5     (2.56)
dP: cm water  (in water)                  = 3.261   (1.284)
Temp:  C (F)                              = 16      (61.0)
```

	SAMP #	Weight of Sample (grams)			
	86	0.07			
	87	0.08			
	88	0.17			
	89	0.04			
	90	0.08			
	91	0.04			
	92	0.07			
	93	0.13			
	94	0.07	AVG	= 0.09	grams
	95	0.17	STN DV	= 0.05	grams

```
Trap  Height above Distributor: cm (in)   = 51.44   (20.25)
Bed   Height above Distributor: cm (in)   = 25.4    (10.0)
Trap Height above bed surface: cm (in)    = 26.03   (10.25)
Static Bed Height: cm (in)                = 22.56   (8.88)
P1: cm Hg  (in Hg)                        = 6.2     (2.44)
dP: cm water  (in water)                  = 2.581   (1.016)
Temp:  C (F)                              = 17      (63.0)
```

	SAMP #	Weight of Sample (grams)			
	66	0.05			
	67	0.15			
	68	0.14			
	69	0.07			
	70	0.11			
	71	0.10			
	72	0.18			
	73	0.08			
	74	0.11	AVG	= 0.12	grams
	75	0.16	STN DV	= 0.04	grams

189

TRAP HEIGHT = 16.12 in

Height of Pressure Tap above Distributor (inches)	Pressure for Samples 106-115 (cm H2O)	Pressure for Samples 126-135 (cm H2O)	Pressure for Samples 96-105 (cm H2O)	Pressure for Samples 116-125 (cm H2O)
1.6	52.6	54.4	55.6	58.5
2.6	48.7	49.9	51.3	52.9
3.6	40.3	41.8	43.3	44.4
4.6	34.6	35.9	37.9	39.6
5.6	27.9	29.2	31.3	33.9
6.6	20.6	22.8	25.2	27.1
7.6	13.8	15.5	18.9	20.6
8.6	7.8	9.4	12.3	14.6
9.6	1.8	3.2	5.3	7.6
10.6	0.0	0.3	0.9	2.5
11.6	0.0	0.0	0.0	0.3
12.6	0.0	0.0	0.0	0.0
13.6	0.0	0.0	0.0	0.0
14.6	0.0	0.0	0.0	0.0

TRAP HEIGHT = 18.25 in

Height of Pressure Tap above Distributor (inches)	Pressure for Samples 146-155 (cm H2O)	Pressure for Samples 136-145 (cm H2O)	Pressure for Samples 156-165 (cm H2O)	Pressure for Samples 166-175 (cm H2O)
1.6	52.7	54.3	55.8	57.9
2.6	49.0	49.9	51.5	52.6
3.6	41.0	41.6	43.3	44.9
4.6	34.6	36.1	38.1	39.9
5.6	28.0	29.3	31.6	33.5
6.6	21.5	22.5	24.9	26.6
7.6	14.9	15.8	18.8	20.7
8.6	8.5	9.9	12.2	14.5
9.6	2.4	3.4	5.0	7.8
10.6	0.0	0.1	0.9	2.5
11.6	0.0	0.0	0.0	0.3
12.6	0.0	0.0	0.0	0.0
13.6	0.0	0.0	0.0	0.0
14.6	0.0	0.0	0.0	0.0

```
Trap  Height above Distributor: cm (in)  = 40.95  (16.12)
Bed  Height above Distributor: cm (in)  = 28.58  (11.25)
Trap Height above bed surface: cm (in)  = 12.37  (4.88)
Static Bed Height: cm (in)              = 22.56  (8.88)
P1: cm Hg  (in Hg)                      = 8.0    (3.15)
dP: cm water  (in water)                = 6.858  (2.7)
Temp:  C (F)                            = 16     (61.0)


            SAMP #      Weight of Sample
                          (grams)


              116          4.18
              117          3.03
              118          2.32
              119          1.47
              120          2.34
              121          2.64
              122          1.73
              123          2.12
              124          1.96    AVG    = 2.41  grams
              125          2.38    STN DV = 0.76  grams




Trap  Height above Distributor: cm (in)  = 40.95  (16.12)
Bed  Height above Distributor: cm (in)  = 27.30  (10.75)
Trap Height above bed surface: cm (in)  = 13.65  (5.38)
Static Bed Height: cm (in)              = 22.56  (8.88)
P1: cm Hg  (in Hg)                      = 7.4    (2.91)
dP: cm water  (in water)                = 4.808  (1.893)
Temp:  C (F)                            = 16     (61.0)


            SAMP #      Weight of Sample
                          (grams)


               96          1.33
               97          0.81
               98          1.37
               99          1.56
              100          1.42
              101          1.48
              102          1.27
              103          2.05
              104          1.21    AVG    = 1.36  grams
              105          1.11    STN DV = 0.32  grams
```

```
Trap  Height above Distributor: cm (in)  = 40.95  (16.12)
Bed  Height above Distributor: cm (in)  = 26.67  (10.5)
Trap Height above bed surface: cm (in)  = 14.28  (5.62)
Static Bed Height: cm (in)              = 22.56  (8.88)
P1: cm Hg  (in Hg)                      = 6.6    (2.60)
dP: cm water  (in water)                = 3.259  (1.283)
Temp:  C (F)                            = 16     (61.0)


           SAMP #    Weight of Sample
                        (grams)

           126          0.36
           127          0.31
           128          0.21
           129          0.27
           130          0.18
           131          0.37
           132          0.34
           133          0.29
           134          0.34   AVG   = 0.28  grams
           135          0.16   STN DV = 0.08  grams



Trap  Height above Distributor: cm (in)  = 40 95  (16.12)
Bed  Height above Distributor: cm (in)  = 26.04  (10.25)
Trap Height above bed surface: cm (in)  = 14.91  (5.88)
Static Bed Height: cm (in)              = 22.56  (8.88)
P1: cm Hg  (in Hg)                      = 6.3    (2.48)
dP: cm water  (in water)                = 2.591  (1.020)
Temp:  C (F)                            = 16     (61.0)


           SAMP #    Weight of Sample
                        (grams)

           106          0.38
           107          0.12
           108          0.15
           109          0.17
           110          0.13
           111          0.18
           112          0.56
           113          0.05
           114          0.18   AVG   = 0.22  grams
           115          0.24   STN DV = 0.15  grams
```

192

```
Trap  Height above Distributor: cm (in)   = 46.36  (18.25)
Bed  Height above Distributor: cm (in)    = 28.58  (11.25)
Trap Height above bed surface: cm (in)    = 17.78  (7.00)
Static Bed Height: cm (in)                = 22.56  (8.88)
P1: cm Hg  (in Hg)                        = 8.1    (3.19)
dP: cm water  (in water)                  = 6.858  (2.7)
Temp:  C (F)                              = 16     (61.0)


            SAMP #       Weight of Sample
                            (grams)

              166           1.13
              167           1.18
              168           1.34
              169           0.93
              170           0.88
              171           1.01
              172           1.20
              173           1.15
              174           1.08    AVG    = 1.08  grams
              175           0.85    STN DV = 0.16  grams




Trap  Height above Distributor: cm (in)   = 46.36  (18.25)
Bed  Height above Distributor: cm (in)    = 27.30  (10.75)
Trap Height above bed surface: cm (in)    = 19.06  (7.5)
Static Bed Height: cm (in)                = 22.56  (8.88)
P1: cm Hg  (in Hg)                        = 7.3    (2.87)
dP: cm water  (in water)                  = 4.808  (1.893)
Temp:  C (F)                              = 16     (61.0)


            SAMP #       Weight of Sample
                            (grams)

              156           0.64
              157           0.48
              158           0.78
              159           0.58
              160           0.44
              161           0.58
              162           0.83
              163           0.57
              164           0.52    AVG    = 0.60  grams
              165           0.62    STN DV = 0.12  grams
```

```
Trap  Height above Distributor: cm (in)  = 46.36  (18.25)
Bed  Height above Distributor: cm (in)   = 26.67  (10.5)
Trap Height above bed surface: cm (in)   = 19.69  (7.75)
Static Bed Height: cm (in)               = 22.56  (8.88)
P1: cm Hg  (in Hg)                       = 6.6    (2.60)
dP: cm water  (in water)                 = 3.244  (1.277)
Temp:  C (F)                             = 16.5   (62.0)
```

	SAMP #	Weight of Sample (grams)
	136	0.03
	137	0.13
	138	0.06
	139	0.05
	140	0.07
	141	0.06
	142	0.05
	143	0.05
	144	0.11 AVG = 0.08 grams
	145	0.14 STN DV = 0.04 grams

```
Trap  Height above Distributor: cm (in)  = 46.36  (18.25)
Bed  Height above Distributor: cm (in)   = 26.04  (10.25)
Trap Height above bed surface: cm (in)   = 20.32  (8.00)
Static Bed Height: cm (in)               = 22.56  (8.88)
P1: cm Hg  (in Hg)                       = 6.3    (2.48)
dP: cm water  (in water)                 = 2.631  (1.036)
Temp:  C (F)                             = 16.5   (62.0)
```

	SAMP #	Weight of Sample (grams)
	146	0.01
	147	0.01
	148	0.02
	149	0.02
	150	0.03
	151	0.02
	152	0.01
	153	0.01
	154	0.02 AVG = 0.02 grams
	155	0.05 STN DV = 0.01 grams

194

```
Trap  Height above Distributor: cm (in) = 59.06  (23.25)
Bed  Height above Distributor: cm (in)  = 27.94  (11.00)
Trap Height above bed surface: cm (in)  = 31.12  (12.25)
Static Bed Height: cm (in)              = 22.56  (8.88)
P1: cm Hg  (in Hg)                      = 8.2    (3.23)
dP: cm water  (in water)                = 6.858  (2.7)
Temp:  C (F)                            = 16.5   (62.0)
```

```
            SAMP #      Weight of Sample
                            (grams)

              176            0.32
              177            0.22
              178            0.24
              179            0.52
              180            0.31
              181            0.42
              182            0.34
              183            0.31
              184            0.23   AVG    = 0.31  grams
              185            0.21   STN DV = 0.10  grams
```

```
Trap  Height above Distributor: cm (in) = 59.06  (23.25)
Bed  Height above Distributor: cm (in)  = 27.18  (10.70)
Trap Height above bed surface: cm (in)  = 31.76  (12.50)
Static Bed Height: cm (in)              = 22.56  (8.88)
P1: cm Hg  (in Hg)                      = 7.3    (2.87)
dP: cm water  (in water)                = 4.813  (1.895)
Temp:  C (F)                            = 16     (61.0)
```

```
            SAMP #      Weight of Sample
                            (grams)

             .186            0.25
              187            0.17
              188            0.14
              189            0.17
              190            0.12
              191            0.23
              192            0.16
              193            0.25
              194            0.18   AVG    = 0.18  grams
              195            0.17   STN DV = 0.04  grams
```

```
Trap  Height above Distributor: cm (in)  = 59.06  (23.25)
Bed  Height above Distributor: cm (in)  = 26.67  (10.50)
Trap Height above bed surface: cm (in)  = 32.39  (12.75)
Static Bed Height: cm (in)              = 22.56  (8.88)
P1: cm Hg  (in Hg)                      = 6.5    (2.56)
dP: cm water  (in water)                = 3.236  (1.274)
Temp:  C (F)                            = 16     (61.0)


              SAMP #     Weight of Sample
                            (grams)

                196        0.05
                197        0.07
                198        0.07
                199        0.04
                200        0.06
                201        0.09
                202        0.04
                203        0.07
                204        0.06    AVG    = 0.06   grams
                205        0.06    STN DV = 0.02   grams



Trap  Height above Distributor: cm (in)  = 59.06  (23.25)
Bed  Height above Distributor: cm (in)  = 26.04  (10.25)
Trap Height above bed surface: cm (in)  = 33.02  (13.00)
Static Bed Height: cm (in)              = 22.56  (8.88)
P1: cm Hg  (in Hg)                      = 6.3    (2.48)
dP: cm water  (in water)                = 2.619  (1.031)
Temp:  C (F)                            = 16     (61.0)


              SAMP #     Weight of Sample
                            (grams)

                206        0.01
                207        0.02
                208        0.01
                209        0.01
                210        0.01
                211        0.01
                212        0.01
                213        0.02
                214        0.01    AVG    = 0.01   grams
                215        0.01    STN DV = 0.004  grams
```

TRAP HEIGHT = 12.75 in

Height of Pressure Tap above Distributor (inches)	Pressure for Samples 256-265 (cm H2O)	Pressure for Samples 266-275 (cm H2O)	Pressure for Samples 276-285 (cm H2O)	Pressure for Samples 286-295 (cm H2O)
1.6	53.7	54.8	57.2	58.8
2.6	48.5	49.9	51.7	53.2
3.6	40.8	42.1	44.4	45.8
4.6	34.9	35.7	38.7	40.4
5.6	28.1	29.7	32.5	34.0
6.6	21.6	23.8	26.1	27.8
7.6	14.7	17.2	19.1	21.6
8.6	8.1	10.7	13.5	16.2
9.6	2.1	4.5	6.8	9.5
10.6	0.0	0.5	1.6	3.7
11.6	0.0	0.0	0.0	0.7
12.6	0.0	0.0	0.0	0.0
13.6	0.0	0.0	0.0	0.0
14.6	0.0	0.0	0.0	0.0

TRAP HEIGHT = 14.25 in

Height of Pressure Tap above Distributor (inches)	Pressure for Samples 216-225 (cm H2O)	Pressure for Samples 226-235 (cm H2O)	Pressure for Samples 236-245 (cm H2O)	Pressure for Samples 246-255 (cm H2O)
1.6	52.2	53.4	56.4	58.0
2.6	48.7	49.7	51.6	52.7
3.6	40.9	42.3	43.9	45.3
4.6	34.7	36.1	38.2	40.2
5.6	27.9	29.5	31.2	34.1
6.6	20.6	23.0	25.7	27.7
7.6	14.9	16.9	18.9	21.3
8.6	8.6	10.7	13.4	14.4
9.6	2.5	3.7	6.5	8.9
10.6	0.0	0.3	1.2	3.1
11.6	0.0	0.0	0.0	0.0
12.6	0.0	0.0	0.0	0.0
13.6	0.0	0.0	0.0	0.0
14.6	0.0	0.0	0.0	0.0

```
Trap  Height above Distributor: cm (in)   = 36.20  (14.25)
Bed  Height above Distributor: cm (in)   = 28.58  (11.25)
Trap Height above bed surface: cm (in)   = 7.62   (3.00)
Static Bed Height: cm (in)               = 22.56  (8.88)
P1: cm Hg  (in Hg)                       = 8.2    (3.23)
dP: cm water  (in water)                 = 6.98   (2.75)
Temp:  C (F)                             = 16.5   (62.0)


           SAMP #       Weight of Sample
                            (grams)


            246            3.34
            247            5.36
            248            4.64
            249            5.71
            250            4.17
            251            4.33
            252            4.55
            253            4.33
            254           *8.44    AVG    = 4.48  grams
            255            3.90    STN DV = 0.72  grams
                       * value not used in computing average.



Trap  Height above Distributor: cm (in)   = 36.20  (14.25)
Bed  Height above Distributor: cm (in)   = 27.30  (10.75)
Trap Height above bed surface: cm (in)   = 8.90   (3.50)
Static Bed Height: cm (in)               = 22.56  (8.88)
P1: cm Hg  (in Hg)                       = 7.3    (2.87)
dP: cm water  (in water)                 = 4.768  (1.877)
Temp:  C (F)                             = 16.5   (62.0)


           SAMP #       Weight of Sample
                            (grams)


            236            1.55
            237            1.88
            238            1.92
            239            1.80
            240            1.69
            241            2.05
            242            1.84
            243            1.80
            244            1.87    AVG    = 1.88  grams
            245            2.38    STN DV = 0.22  grams
```

```
Trap  Height above Distributor: cm (in)  = 36.20  (14.25)
Bed  Height above Distributor: cm (in)  = 26.67  (10.50)
Trap Height above bed surface: cm (in)  = 9.53   (3.75)
Static Bed Height: cm (in)              = 22.56  (8.88)
P1: cm Hg  (in Hg)                      = 6.6    (2.60)
dP: cm water  (in water)                = 3.218  (1.267)
Temp:  C (F)                            = 16.5   (62.0)


           SAMP #      Weight of Sample
                          (grams)

            226           0.93
            227           0.68
            228           0.61
            229           0.56
            230           0.81
            231           0.52
            232           0.38
            233           0.57
            234           0.75   AVG    = 0.62  grams
            235           0.44   STN DV = 0.17  grams




Trap  Height above Distributor: cm (in)  = 36.20  (14.25)
Bed  Height above Distributor: cm (in)  = 26.04  (10.25)
Trap Height above bed surface: cm (in)  = 10.16  (4.00)
Static Bed Height: cm (in)              = 22.56  (8.88)
P1: cm Hg  (in Hg)                      = 6.3    (2.48)
dP: cm water  (in water)                = 2.624  (1.033)
Temp:  C (F)                            = 16.5   (62.0)


           SAMP #      Weight of Sample
                          (grams)

            216           0.32
            217           0.35
            218           0.36
            219           0.30
            220           0.32
            221           0.35
            222           0.24
            223           0.30
            224           0.34   AVG    = 0.32  grams
            225           0.30   STN DV = 0.04  grams
```

199

```
Trap  Height above Distributor: cm (in)  = 32.39  (12.75)
Bed  Height above Distributor: cm (in)   = 28.58  (11.25)
Trap Height above bed surface: cm (in)   = 3.81   (1.50)
Static Bed Height: cm (in)               = 22.56  (8.88)
P1: cm Hg  (in Hg)                       = 8.1    (3.19)
dP: cm water  (in water)                 = 6.985  (2.75)
Temp:  C (F)                             = 17     (63.0)


          SAMP #       Weight of Sample
                          (grams)

            286            6.55
            287            7.51
            288            7.46
            289            8.05
            290            6.92
            291            7.38
            292            7.23
            293            7.65
            294            7.04      AVG    = 7.22  grams
            295            6.38      STN DV = 0.51  grams



Trap  Height above Distributor: cm (in)  = 32.39  (12.75)
Bed  Height above Distributor: cm (in)   = 27.30  (10.75)
Trap Height above bed surface: cm (in)   = 5.09   (2.00)
Static Bed Height: cm (in)               = 22.56  (8.88)
P1: cm Hg  (in Hg)                       = 7.3    (2.87)
dP: cm water  (in water)                 = 4.836  (1.904)
Temp:  C (F)                             = 17     (63.0)


          SAMP #       Weight of Sample
                          (grams)

            276            2.44
            277            3.77
            278            3.53
            279            4.04
            280            4.56
            281            3.81
            282            4.55
            283            5.60
            284            5.75      AVG    = 4.35  grams
            285            5.49      STN DV = 1.05  grams
```

```
Trap  Height above Distributor: cm (in)  = 32.39  (12.75)
Bed  Height above Distributor: cm (in)  = 26.67  (10.5)
Trap Height above bed surface: cm (in)  = 5.72   (2.25)
Static Bed Height: cm (in)              = 22.56  (8.88)
P1: cm Hg  (in Hg)                      = 6.6    (2.60)
dP: cm water  (in water)                = 3.269  (1.287)
Temp:  C (F)                            = 16.5   (62.0)


          SAMP #      Weight of Sample
                         (grams)

            266           0.74
            267           1.80
            268           1.17
            269           1.17
            270           1.87
            271           1.15
            272           1.58
            273           1.03
            274           1.00    AVG    = 1.31   grams
            275           1.56    STN DV = 0.37   grams




Trap  Height above Distributor: cm (in)  = 32.39  (12.75)
Bed  Height above Distributor: cm (in)  = 26.04  (10.25)
Trap Height above bed surface: cm (in)  = 6.35   (2.50)
Static Bed Height: cm (in)              = 22.56  (8.88)
P1: cm Hg  (in Hg)                      = 6.3    (2.48)
dP: cm water  (in water)                = 2.604  (1.025)
Temp:  C (F)                            = 16.5   (62.0)


          SAMP #      Weight of Sample
                         (grams)

            256           0.50
            257           0.76
            258           0.67
            259           0.51
            260           0.54
            261           0.58
            262           0.47
            263           0.65
            264           0.61    AVG    = 0.63   grams
            265           0.87    STN DV = 0.13   grams
```

APPENDIX J

This Appendix contains the output from the image analyzer. The output is arranged in the following order.

1.   Bed distribution

2.   4 cm freeboard height

3.   8 cm freeboard height

4.   12 cm freeboard height

5.   18 cm freeboard height

6.   22 cm freeboard height

7.   31 cm freeboard height

Each of the distributions at a given bed height applies only to the Uo/Umf = 3.81 condition. For each of the seven image analyzer outputs listed, the following three formats are used.

1.   Histogram of absolute particle frequency vs particle diameter.

2.   Cumulative percentage plot of particle size distribution.

3.   Table listing of the above data.

The dashed line on both the bar graphs and on the cumulative percentage plots represent the Gaussian distributions which fit the given set of data. This Gaussian distribution should be used only as a rough estimate of the data because the analysis included "particles" less than 70 microns. By viewing a blank slide with only the tape applied, these "particles" were confirmed to be bubbles and dirt entrapped in the adhesive on the tape used to hold the sample particles in place.

ABS.FREQUENCY

Image Analyzer Output
Bed Particle Distribution

COUNTS
IN RANGE
UND.FLOW
OVERFLOW
CLASSES... 40

INTERVAL 0.964651E-01
MINIMUM 0.489774E-01
MAXIMUM 3.90758
MEAN 0.983512
ST.DEV. 0.509569
MEDIAN 0.934644
MODE 1.23768

OCIRCLE

CUM.FREQUENCY %

COUNTS
IN RANGE
UND.FLOW
OVERFLOW
CLASSES 40

INTERVAL 0.964651E-01
MINIMUM 0.489774E-01
MAXIMUM 3.90758
MEAN 0.983512
ST.DEV. 0.509569
MEDIAN 0.934644
MODE 1.23768

OCIRCLE

CLASSIFICATION LIST FOR OCIRCLE   IN CHANNELS   1

UNDERFLOW   0   OVERFLOW   0

CLASS	FROM	TO	FREQUENCIES			
			ABS	REL	CUM. ABS	CUM. REL
1	.48977E-01	.14544	15.	4.89 %	15.	4.89 %
2	.14544	.24191	24.	7.82 %	39.	12.70 %
3	.24191	.33837	12.	3.91 %	51.	16.61 %
4	.33837	.43484	6.	1.95 %	57.	18.57 %
5	.43484	.53130	10.	3.26 %	67.	21.82 %
6	.53130	.62777	17.	5.54 %	84.	27.36 %
7	.62777	.72423	20.	6.51 %	104.	33.88 %
8	.72423	.82070	23.	7.49 %	127.	41.37 %
9	.82070	.91716	23.	7.49 %	150.	48.86 %
10	.91716	1.0136	20.	6.51 %	170.	55.37 %
11	1.0136	1.1101	14.	4.56 %	184.	59.93 %
12	1.1101	1.2066	23.	7.49 %	207.	67.43 %
13	1.2066	1.3030	27.	8.79 %	234.	76.22 %
14	1.3030	1.3995	12.	3.91 %	246.	80.13 %
15	1.3995	1.4960	17.	5.54 %	263.	85.67 %
16	1.4960	1.5924	7.	2.29 %	270.	87.95 %
17	1.5924	1.6889	7.	2.29 %	277.	90.23 %
18	1.6889	1.7853	11.	3.58 %	288.	93.81 %
19	1.7853	1.8818	4.	1.30 %	292.	95.11 %
20	1.8818	1.9783	1.	.33 %	293.	95.44 %
21	1.9783	2.0747	1.	.33 %	294.	95.77 %
22	2.0747	2.1712	5.	1.63 %	299.	97.39 %
23	2.1712	2.2677	1.	.33 %	300.	97.72 %
24	2.2677	2.3641	0.	0.00 %	300.	97.72 %
25	2.3641	2.4606	0.	0.00 %	300.	97.72 %
26	2.4606	2.5571	1.	.33 %	301.	98.05 %
27	2.5571	2.6535	1.	.33 %	302.	98.37 %
28	2.6535	2.7500	0.	0.00 %	302.	98.37 %
29	2.7500	2.8465	0.	0.00 %	302.	98.37 %
30	2.8465	2.9429	1.	.33 %	303.	98.70 %
31	2.9429	3.0394	0.	0.00 %	303.	98.70 %
32	3.0394	3.1359	1.	.33 %	304.	99.02 %
33	3.1359	3.2323	0.	0.00 %	304.	99.02 %
34	3.2323	3.3288	0.	0.00 %	304.	99.02 %
35	3.3288	3.4253	0.	0.00 %	304.	99.02 %
36	3.4253	3.5217	0.	0.00 %	304.	99.02 %
37	3.5217	3.6182	0.	0.00 %	304.	99.02 %
38	3.6182	3.7147	0.	0.00 %	304.	99.02 %
39	3.7147	3.8111	1.	.33 %	305.	99.35 %
40	3.8111	3.9076	2.	.65 %	307.	100.00 %

Image Analyzer Output
Height Distribution
4 cm Above Bed

Image Analyzer Output
Height Distribution
4 cm Above Bed

CLASSIFICATION LIST FOR OCIRCLE   IN CHANNELS   1

UNDERFLOW   0   OVERFLOW   0

CLASS	FROM	TO	ABS	FREQUENCIES REL	CUM. ABS	CUM. REL
1	.12769	.21427	9.	2.78 %	9.	2.79 %
2	.21427	.30086	11.	3.40 %	20.	6.17 %
3	.30086	.38745	3.	.93 %	23.	7.10 %
4	.38745	.47404	11.	3.40 %	34.	10.49 %
5	.47404	.56064	34.	10.49 %	68.	20.99 %
6	.56064	.64723	54.	16.67 %	122.	37.65 %
7	.64723	.73382	45.	13.89 %	167.	51.54 %
8	.73382	.82041	36.	11.11 %	203.	62.65 %
9	.82041	.90700	27.	8.33 %	230.	70.99 %
10	.90700	.99359	25.	7.72 %	255.	78.70 %
11	.99359	1.0802	18.	5.56 %	273.	84.26 %
12	1.0802	1.1668	15.	4.63 %	288.	88.89 %
13	1.1668	1.2534	9.	2.78 %	297.	91.67 %
14	1.2534	1.3400	6.	1.85 %	303.	93.52 %
15	1.3400	1.4265	5.	1.54 %	308.	95.06 %
16	1.4265	1.5131	7.	2.16 %	315.	97.22 %
17	1.5131	1.5997	1.	.31 %	316.	97.53 %
18	1.5997	1.6863	1.	.31 %	317.	97.84 %
19	1.6863	1.7729	2.	.62 %	319.	98.46 %
20	1.7729	1.8595	2.	.62 %	321.	99.07 %
21	1.8595	1.9461	1.	.31 %	322.	99.38 %
22	1.9461	2.0327	0.	0.00 %	322.	99.38 %
23	2.0327	2.1193	0.	0.00 %	322.	99.38 %
24	2.1193	2.2059	0.	0.00 %	322.	99.38 %
25	2.2059	2.2925	1.	.31 %	323.	99.69 %
26	2.2925	2.3790	0.	0.00 %	323.	99.69 %
27	2.3790	2.4656	0.	0.00 %	323.	99.69 %
28	2.4656	2.5522	0.	0.00 %	323.	99.69 %
29	2.5522	2.6388	0.	0.00 %	323.	99.69 %
30	2.6388	2.7254	0.	0.00 %	323.	99.69 %
31	2.7254	2.8120	0.	0.00 %	323.	99.69 %
32	2.8120	2.8986	0.	0.00 %	323.	99.69 %
33	2.8986	2.9852	0.	0.00 %	323.	99.69 %
34	2.9852	3.0718	0.	0.00 %	323.	99.69 %
35	3.0718	3.1584	0.	0.00 %	323.	99.69 %
36	3.1584	3.2449	0.	0.00 %	323.	99.69 %
37	3.2449	3.3315	0.	0.00 %	323.	99.69 %
38	3.3315	3.4181	0.	0.00 %	323.	99.69 %
39	3.4181	3.5047	0.	0.00 %	323.	99.69 %
40	3.5047	3.5913	1.	.31 %	324.	100.00 %

Image Analyzer Output
Height Distribution
8 cm Above Bed

RES. FREQUENCY
50.00
40.00
30.00
20.00
10.00
0.000

1.000   2.000   3.000   OCIRCLE

COUNTS   317
IN RANGE   317
UND.FLOW   0
OVERFLOW   0
CLASSES   46

INTERVAL
....0.555681E-01
MINIMUM
....0.148672
MAXIMUM
....2.29139
MEAN
....0.816219
ST.DEV.
....0.522185
MEDIAN
....0.761052
MODE
....0.553551

CUM.FREQUENCY %
100.0
80.00
60.00
40.00
20.00
0.000

1.000   2.000   3.000   OCIRCLE

COUNTS   317
IN RANGE   317
UND.FLOW   0
OVERFLOW   0
CLASSES   46

INTERVAL
....0.555681E-01
MINIMUM
....0.148672
MAXIMUM
....2.29139
MEAN
....0.816219
ST.DEV.
....0.522185
MEDIAN
....0.761052
MODE
....0.553551

Image Analyzer Output
Height Distribution
8 cm Above Bed

CLASSIFICATION LIST FOR DCIRCLE IN CHANNELS 1

UNDERFLOW 0 OVERFLOW 0

CLASS	FROM	TO	ABS	REL	CUM. ABS	CUM. REL
1	.14367	.20224	2.	.63 %	2.	.63 %
2	.20224	.25591	2.	.63 %	4.	1.26 %
3	.25591	.30938	3.	.95 %	7.	2.21 %
4	.30938	.36294	0.	0.00 %	7.	2.21 %
5	.36294	.41651	4.	1.26 %	11.	3.47 %
6	.41651	.47008	9.	2.84 %	20.	6.31 %
7	.47008	.52365	28.	8.83 %	48.	15.14 %
8	.52365	.57722	21.	6.62 %	69.	21.77 %
9	.57722	.63078	27.	8.52 %	96.	30.29 %
10	.63078	.68435	32.	10.09 %	128.	40.38 %
11	.68435	.73792	21.	6.62 %	149.	47.00 %
12	.73792	.79149	22.	6.94 %	171.	53.94 %
13	.79149	.84506	30.	9.46 %	201.	63.41 %
14	.84506	.89863	17.	5.36 %	218.	68.77 %
15	.89863	.95219	19.	5.99 %	237.	74.76 %
16	.95219	1.0058	11.	3.47 %	248.	78.23 %
17	1.0058	1.0593	11.	3.47 %	259.	81.70 %
18	1.0593	1.1129	9.	2.84 %	268.	84.54 %
19	1.1129	1.1665	8.	2.52 %	276.	87.07 %
20	1.1665	1.2200	10.	3.15 %	286.	90.22 %
21	1.2200	1.2736	2.	.63 %	288.	90.85 %
22	1.2736	1.3272	5.	1.58 %	293.	92.43 %
23	1.3272	1.3807	7.	2.21 %	300.	94.64 %
24	1.3807	1.4343	3.	.95 %	303.	95.58 %
25	1.4343	1.4879	1.	.32 %	304.	95.90 %
26	1.4879	1.5414	2.	.63 %	306.	96.53 %
27	1.5414	1.5950	1.	.32 %	307.	96.85 %
28	1.5950	1.6486	1.	.32 %	308.	97.16 %
29	1.6486	1.7021	1.	.32 %	309.	97.48 %
30	1.7021	1.7557	2.	.63 %	311.	98.11 %
31	1.7557	1.8093	0.	0.00 %	311.	98.11 %
32	1.8093	1.8629	2.	.63 %	313.	98.74 %
33	1.8629	1.9164	1.	.32 %	314.	99.05 %
34	1.9164	1.9700	1.	.32 %	315.	99.37 %
35	1.9700	2.0236	0.	0.00 %	315.	99.37 %
36	2.0236	2.0771	1.	.32 %	316.	99.68 %
37	2.0771	2.1307	0.	0.00 %	316.	99.68 %
38	2.1307	2.1843	0.	0.00 %	316.	99.68 %
39	2.1843	2.2378	0.	0.00 %	316.	99.68 %
40	2.2378	2.2914	1.	.32 %	317.	100.00 %

Image Analyzer Output
Height Distribution
12 cm Above Bed

ABS.FREQUENCY

110.0

55.00

0.000

2.000   4.000   6.000   OCIRCLE

COUNTS   329
IN RANGE   329
UND.FLOW
OVERFLOW
CLASSES   46

INTERVAL
....0.125249
MINIMUM
....0.621736E-01
MAXIMUM
....5.11212
MEAN
....0.719992
ST.DEV.
....0.446468
MEDIAN
....0.655370
MODE
....0.525272

CUM.FREQUENCY %

100.0

80.00

60.00

40.00

20.00

0.000

2.000   4.000   6.000   OCIRCLE

COUNTS   329
IN RANGE   329
UND.FLOW
OVERFLOW
CLASSES   46

INTERVAL
....0.125249
MINIMUM
....0.621736E-01
MAXIMUM
....5.11212
MEAN
....0.719992
ST.DEV.
....0.446468
MEDIAN
....0.655370
MODE
....0.525272

210

Image Analyzer Output
Height Distribution
12 cm Above Bed

CLASSIFICATION LIST FOR DCIRCLE   IN CHANNELS   1

UNDERFLOW   8   OVERFLOW   8

CLASS	FROM	TO	FREQUENCIES			
			ABS	REL	CUM. ABS	CUM. REL
1	.62174E-01	.18642	22.	6.87 %	22.	6.87 %
2	.18842	.31467	17.	5.31 %	39.	12.19 %
3	.31467	.44092	15.	4.69 %	54.	16.87 %
4	.44092	.56717	55.	17.19 %	109.	34.06 %
5	.56717	.69342	73.	22.81 %	182.	56.87 %
6	.69342	.81967	48.	15.00 %	230.	71.87 %
7	.81967	.94591	30.	9.37 %	260.	81.25 %
8	.94591	1.0722	18.	5.62 %	278.	86.87 %
9	1.0722	1.1984	14.	4.37 %	292.	91.25 %
10	1.1984	1.3247	6.	1.87 %	298.	93.12 %
11	1.3247	1.4509	9.	2.81 %	307.	95.94 %
12	1.4509	1.5772	3.	.94 %	310.	96.87 %
13	1.5772	1.7034	3.	.94 %	313.	97.81 %
14	1.7034	1.8297	3.	.94 %	316.	98.75 %
15	1.8297	1.9559	0.	0.00 %	316.	98.75 %
16	1.9559	2.0822	1.	.31 %	317.	99.06 %
17	2.0822	2.2084	1.	.31 %	318.	99.37 %
18	2.2084	2.3347	0.	0.00 %	318.	99.37 %
19	2.3347	2.4609	0.	0.00 %	319.	99.37 %
20	2.4609	2.5871	0.	0.00 %	319.	99.37 %
21	2.5871	2.7134	0.	0.00 %	319.	99.37 %
22	2.7134	2.8396	0.	0.00 %	319.	99.37 %
23	2.8396	2.9659	0.	0.00 %	319.	99.37 %
24	2.9659	3.0921	0.	0.00 %	319.	99.37 %
25	3.0921	3.2184	0.	0.00 %	319.	99.37 %
26	3.2184	3.3446	1.	.31 %	319.	99.69 %
27	3.3446	3.4709	0.	0.00 %	319.	99.69 %
28	3.4709	3.5971	0.	0.00 %	319.	99.69 %
29	3.5971	3.7234	0.	0.00 %	319.	99.69 %
30	3.7234	3.8496	0.	0.00 %	319.	99.69 %
31	3.8496	3.9759	0.	0.00 %	319.	99.69 %
32	3.9759	4.1021	0.	0.00 %	319.	99.69 %
33	4.1021	4.2284	0.	0.00 %	319.	99.69 %
34	4.2284	4.3546	0.	0.00 %	319.	99.69 %
35	4.3546	4.4809	0.	0.00 %	319.	99.69 %
36	4.4809	4.6071	0.	0.00 %	319.	99.69 %
37	4.6071	4.7334	0.	0.00 %	319.	99.69 %
38	4.7334	4.8596	0.	0.00 %	319.	99.69 %
39	4.8596	4.9859	0.	0.00 %	319.	99.69 %
40	4.9859	5.1121	1.	.31 %	320.	100.00 %

Image Analyzer Output
Height Distribution
18 cm Above Bed

COUNTS   329
IN RANGE   329
UND.FLOW   0
OVER.FLOW   0
CLASSES   40

INTERVAL
       0.5-1792E-01
MINIMUM
       0.110291
MAXIMUM
       2.67745
MEAN
       0.851930
ST.DEV.
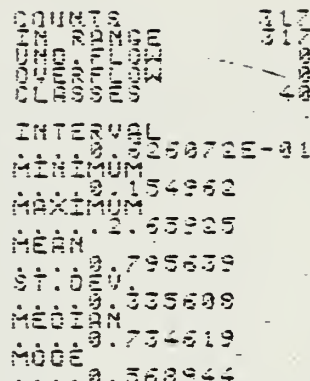   0.359393
MEDIAN
       0.786914
MODE
       0.776786
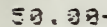
Image Analyzer Output
Height Distribution
18 cm Above Bed
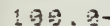
CLASSIFICATION LIST FOR DCIRCLE   IN CHANNELS   1

UNDERFLOW   0   OVERFLOW   0

CLASS	FROM	TO	FREQUENCIES			
			ABS	REL	CUM. ABS	CUM. REL
1	.11029	.17446	1.	.31 %	1.	.31 %
2	.17446	.23864	9.	2.50 %	9.	2.81 %
3	.23864	.30282	1.	.31 %	10.	3.12 %
4	.30282	.36700	5.	1.56 %	15.	4.69 %
5	.36700	.43118	4.	1.25 %	19.	5.94 %
6	.43118	.49536	17.	5.31 %	36.	11.25 %
7	.49536	.55954	16.	5.00 %	52.	16.25 %
8	.55954	.62372	26.	8.12 %	78.	24.37 %
9	.62372	.68789	32.	10.00 %	110.	34.37 %
10	.68789	.75207	31.	9.69 %	141.	44.06 %
11	.75207	.81625	35.	10.94 %	176.	55.00 %
12	.81625	.88043	21.	6.56 %	197.	61.56 %
13	.88043	.94461	26.	8.12 %	223.	69.69 %
14	.94461	1.0088	20.	6.25 %	243.	75.94 %
15	1.0088	1.0730	13.	4.06 %	256.	80.00 %
16	1.0730	1.1371	13.	4.06 %	269.	84.06 %
17	1.1371	1.2013	7.	2.19 %	276.	86.25 %
18	1.2013	1.2655	6.	1.87 %	282.	88.12 %
19	1.2655	1.3297	7.	2.19 %	289.	90.31 %
20	1.3297	1.3939	2.	.63 %	291.	90.94 %
21	1.3939	1.4580	4.	1.25 %	295.	92.19 %
22	1.4580	1.5222	7.	2.19 %	302.	94.37 %
23	1.5222	1.5864	4.	1.25 %	306.	95.62 %
24	1.5864	1.6506	4.	1.25 %	310.	96.87 %
25	1.6506	1.7148	1.	.31 %	311.	97.19 %
26	1.7148	1.7789	4.	1.25 %	315.	98.44 %
27	1.7789	1.8431	2.	.63 %	317.	99.06 %
28	1.8431	1.9073	0.	0.00 %	317.	99.06 %
29	1.9073	1.9715	0.	0.00 %	317.	99.06 %
30	1.9715	2.0357	0.	0.00 %	317.	99.06 %
31	2.0357	2.0999	0.	0.00 %	317.	99.06 %
32	2.0999	2.1640	1.	.31 %	318.	99.37 %
33	2.1640	2.2282	0.	0.00 %	318.	99.37 %
34	2.2282	2.2924	0.	0.00 %	318.	99.37 %
35	2.2924	2.3566	0.	0.00 %	318.	99.37 %
36	2.3566	2.4207	0.	0.00 %	318.	99.37 %
37	2.4207	2.4849	0.	0.00 %	318.	99.37 %
38	2.4849	2.5491	1.	.31 %	319.	99.69 %
39	2.5491	2.6133	0.	0.00 %	319.	99.69 %
40	2.6133	2.6774	1.	.31 %	320.	100.00 %

213

Image Analyzer Output
Height Distribution
22 cm Above Bed

Image Analyzer Output
Height Distribution
ZZ cm Above Bed

CLASSIFICATION LIST FOR DCIRCLE IN CHANNELS 1

UNDERFLOW   0   OVERFLOW   0

CLASS	FROM	TO	FREQUENCIES			
			ABS	REL	CUM. ABS	CUM. REL
1	.12008	.20410	14.	4.47 %	14.	4.47 %
2	.20410	.28812	6.	1.92 %	20.	6.39 %
3	.28812	.37214	5.	1.60 %	25.	7.99 %
4	.37214	.45616	7.	2.24 %	32.	10.22 %
5	.45616	.54018	14.	4.47 %	46.	14.70 %
6	.54018	.62420	31.	9.90 %	77.	24.60 %
7	.62420	.70823	23.	7.35 %	100.	31.95 %
8	.70823	.79225	37.	11.82 %	137.	43.77 %
9	.79225	.87627	25.	7.99 %	162.	51.76 %
10	.87627	.96029	25.	7.99 %	187.	59.74 %
11	.96029	1.0443	32.	10.22 %	219.	69.97 %
12	1.0443	1.1283	24.	7.67 %	243.	77.64 %
13	1.1283	1.2124	25.	7.99 %	268.	85.62 %
14	1.2124	1.2964	17.	5.43 %	285.	91.05 %
15	1.2964	1.3804	6.	1.92 %	291.	92.97 %
16	1.3804	1.4644	6.	1.92 %	297.	94.89 %
17	1.4644	1.5484	7.	2.24 %	304.	97.12 %
18	1.5484	1.6325	1.	.32 %	305.	97.44 %
19	1.6325	1.7165	5.	1.60 %	310.	99.04 %
20	1.7165	1.8005	1.	.32 %	311.	99.36 %
21	1.8005	1.8845	0.	0.00 %	311.	99.36 %
22	1.8845	1.9685	0.	0.00 %	311.	99.36 %
23	1.9685	2.0525	0.	0.00 %	311.	99.36 %
24	2.0525	2.1366	0.	0.00 %	311.	99.36 %
25	2.1366	2.2206	0.	0.00 %	311.	99.36 %
26	2.2206	2.3046	0.	0.00 %	311.	99.36 %
27	2.3046	2.3887	0.	0.00 %	311.	99.36 %
28	2.3887	2.4727	0.	0.00 %	311.	99.36 %
29	2.4727	2.5567	0.	0.00 %	311.	99.36 %
30	2.5567	2.6407	0.	0.00 %	311.	99.36 %
31	2.6407	2.7247	0.	0.00 %	311.	99.36 %
32	2.7247	2.8089	0.	0.00 %	311.	99.36 %
33	2.8089	2.8929	0.	0.00 %	311.	99.36 %
34	2.8929	2.9768	0.	0.00 %	311.	99.36 %
35	2.9768	3.0608	0.	0.00 %	311.	99.36 %
36	3.0608	3.1448	0.	0.00 %	311.	99.36 %
37	3.1448	3.2289	0.	0.00 %	311.	99.36 %
38	3.2289	3.3129	0.	0.00 %	311.	99.36 %
39	3.3129	3.3969	1.	.32 %	312.	99.68 %
40	3.3969	3.4809	1.	.32 %	313.	100.00 %

Image Analyzer Output
Height Distribution
31 cm Above Bed

ABS.FREQUENCY

COUNTS   317
IN RANGE   317
UND.FLOW   0
OVERFLOW   0
CLASSES   48

INTERVAL
...0.526072E-01
MINIMUM
...0.154962
MAXIMUM
...2.65925
MEAN
...0.795639
ST.DEV.
...0.335608
MEDIAN
...0.734619
MODE
...0.568944

OCIRCLE

CUM.FREQUENCY %

COUNTS   317
IN RANGE   317
UND.FLOW   0
OVERFLOW   0
CLASSES   48

INTERVAL
...0.526072E-01
MINIMUM
...0.154962
MAXIMUM
...2.65925
MEAN
...0.795639
ST.DEV.
...0.335608
MEDIAN
...0.734619
MODE
...0.568944

OCIRCLE

Image Analyzer Output
Height Distribution
31 cm Above Bed

CLASSIFICATION LIST FOR OCIRCLE   IN CHANNELS   1

UNDERFLOW   0   OVERFLOW   0

| CLASS	FROM	TO	FREQUENCIES			
			ABS	REL	CUM. ABS	CUM. REL
1	.15496	.21757	11.	3.47 %	11.	3.47 %
2	.21757	.28018	0.	0.00 %	11.	3.47 %
3	.28018	.34278	2.	.63 %	13.	4.10 %
4	.34278	.40539	9.	2.84 %	22.	6.94 %
5	.40539	.46800	9.	2.84 %	31.	9.78 %
6	.46800	.53061	20.	6.31 %	51.	16.09 %
7	.53061	.59321	39.	12.30 %	90.	28.39 %
8	.59321	.65582	30.	9.46 %	120.	37.85 %
9	.65582	.71843	31.	9.78 %	151.	47.63 %
10	.71843	.78103	29.	9.15 %	180.	56.78 %
11	.78103	.84364	25.	7.89 %	205.	64.67 %
12	.84364	.90625	17.	5.36 %	222.	70.03 %
13	.90625	.96886	18.	5.68 %	240.	75.71 %
14	.96886	1.0315	21.	6.62 %	261.	82.33 %
15	1.0315	1.0941	11.	3.47 %	272.	85.80 %
16	1.0941	1.1567	7.	2.21 %	279.	88.01 %
17	1.1567	1.2193	5.	1.58 %	284.	89.59 %
18	1.2193	1.2819	10.	3.15 %	294.	92.74 %
19	1.2819	1.3445	3.	.95 %	297.	93.69 %
20	1.3445	1.4071	1.	.32 %	298.	94.01 %
21	1.4071	1.4697	3.	.95 %	301.	94.96 %
22	1.4697	1.5323	4.	1.26 %	305.	96.21 %
23	1.5323	1.5949	4.	1.26 %	309.	97.48 %
24	1.5949	1.6575	1.	.32 %	310.	97.79 %
25	1.6575	1.7201	3.	.95 %	313.	98.74 %
26	1.7201	1.7829	1.	.32 %	314.	99.05 %
27	1.7829	1.8454	0.	0.00 %	314.	99.05 %
28	1.8454	1.9080	0.	0.00 %	314.	99.05 %
29	1.9080	1.9706	0.	0.00 %	314.	99.05 %
30	1.9706	2.0332	0.	0.00 %	314.	99.05 %
31	2.0332	2.0958	1.	.32 %	315.	99.37 %
32	2.0958	2.1584	1.	.32 %	316.	99.68 %
33	2.1584	2.2210	0.	0.00 %	316.	99.68 %
34	2.2210	2.2836	0.	0.00 %	316.	99.68 %
35	2.2836	2.3462	0.	0.00 %	316.	99.68 %
36	2.3462	2.4088	0.	0.00 %	316.	99.68 %
37	2.4088	2.4714	0.	0.00 %	316.	99.68 %
38	2.4714	2.5340	0.	0.00 %	316.	99.68 %
39	2.5340	2.5966	0.	0.00 %	316.	99.68 %
40	2.5966	2.6593	1.	.32 %	317.	100.00 %

APPENDIX K

This Appendix contains the photographs of the oscilloscope traces obtained while sampling. Each of the pictures is labeled with the sample number for which it represents.
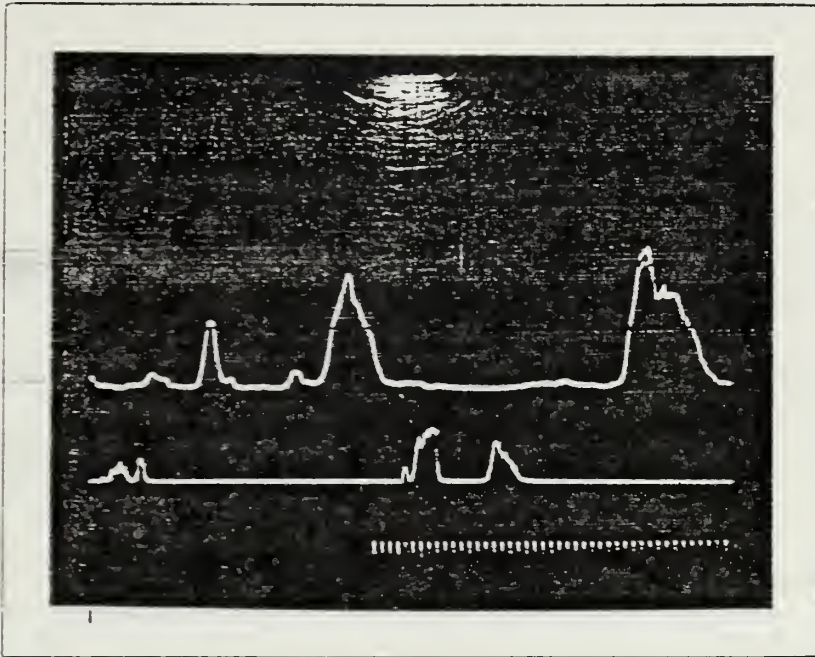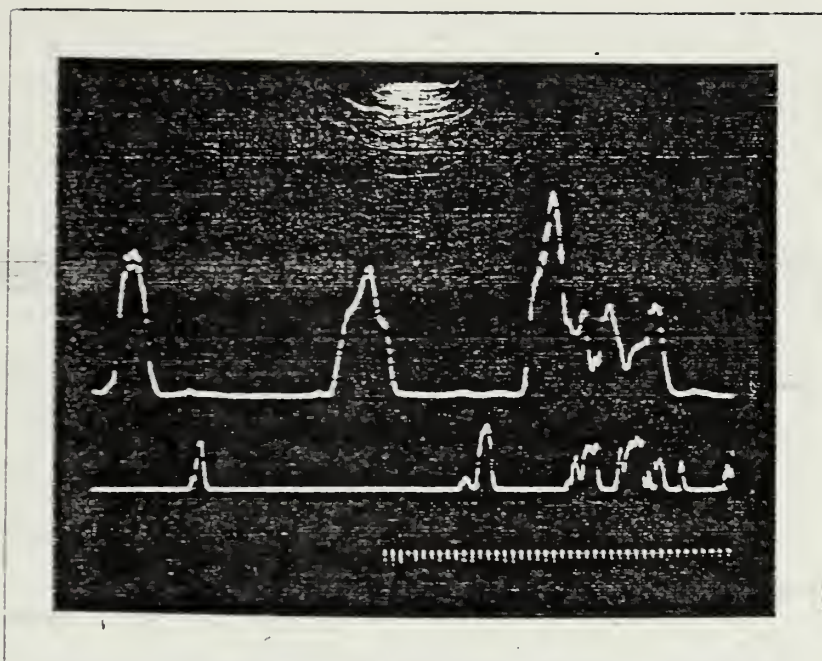
Oscilloscope Trace for Sample Number 56
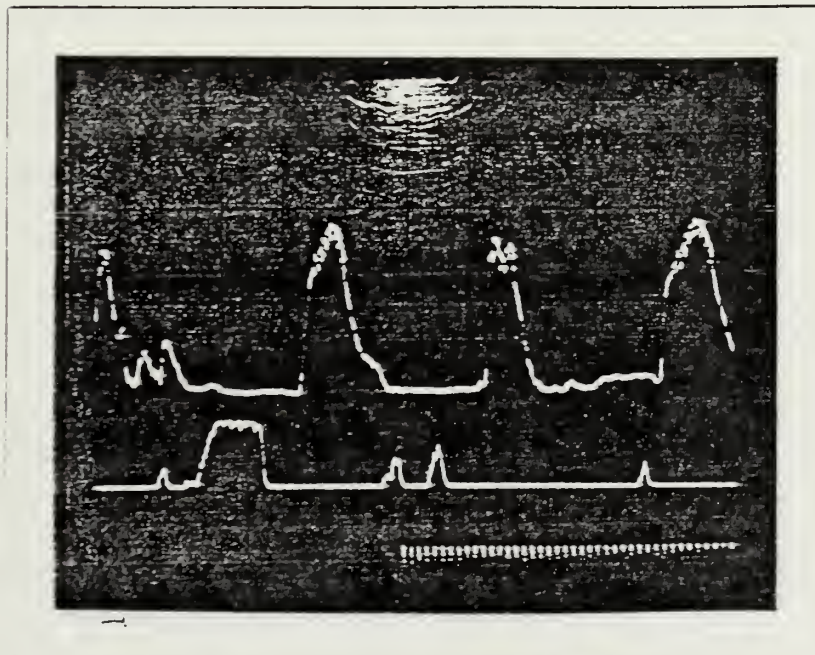
Oscilloscope Trace for Sample Number 57

Oscilloscope Trace for Sample Number 58

Oscilloscope Trace for Sample Number 59

220

Oscilloscope Trace for Sample Number 60

Oscilloscope Trace for Sample Number 62

221

Oscilloscope Trace for Sample Number 63

Oscilloscope Trace for Sample Number 64

Oscilloscope Trace for Sample Number 66

Oscilloscope Trace for Sample Number 67
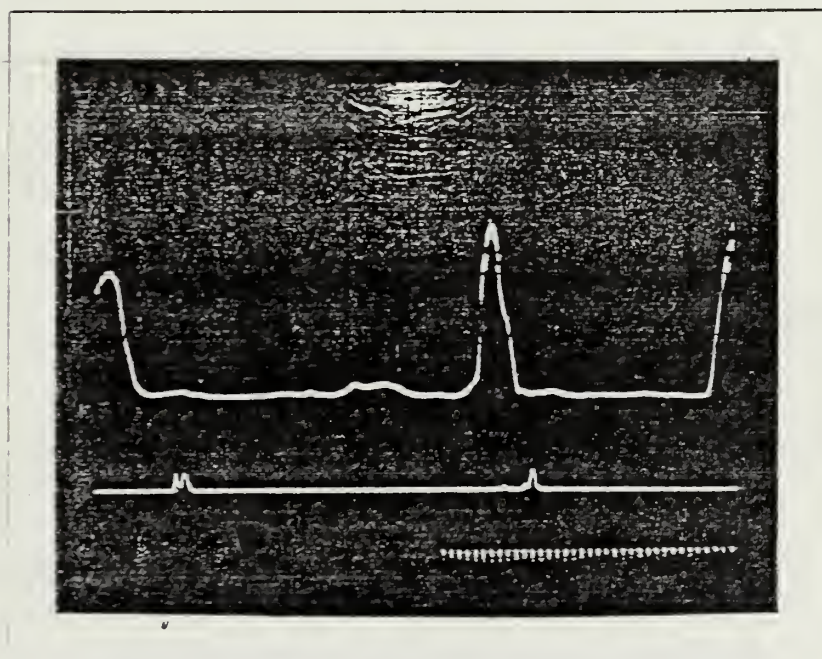
223

Oscilloscope Trace for Sample Number 69

Oscilloscope Trace for Sample Number 70

Oscilloscope Trace for Sample Number 77

Oscilloscope Trace for Sample Number 79

225

Oscilloscope Trace for Sample Number 83

Oscilloscope Trace for Sample Number 84
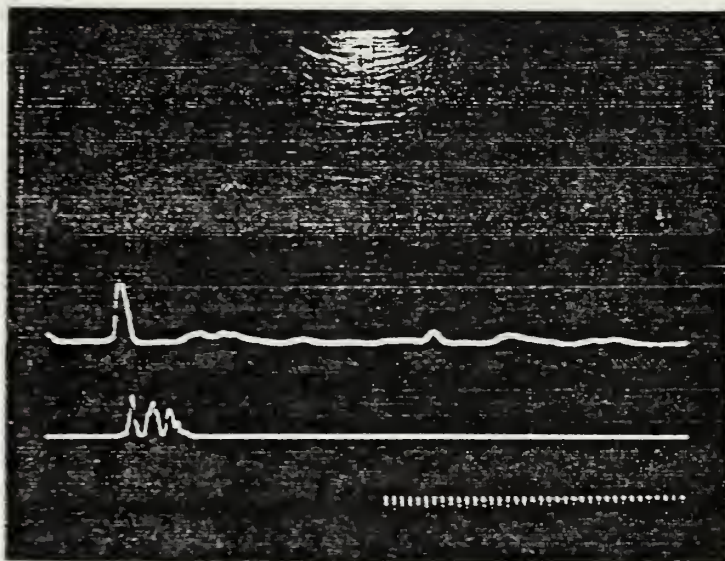
226

Oscilloscope Trace for Sample Number 86

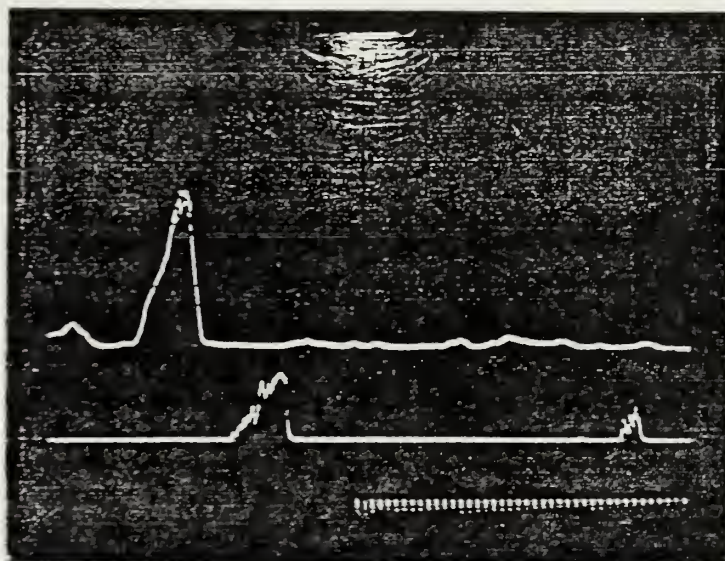Oscilloscope Trace for Sample Number 88

227

Oscilloscope Trace for Sample Number 89

Oscilloscope Trace for Sample Number 90

228
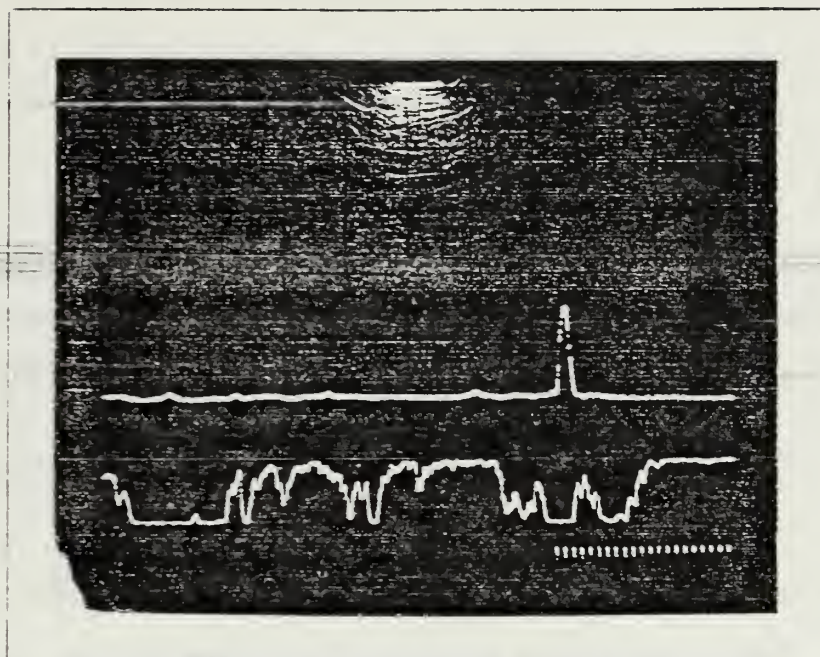
Oscilloscope Trace for Sample Number 92
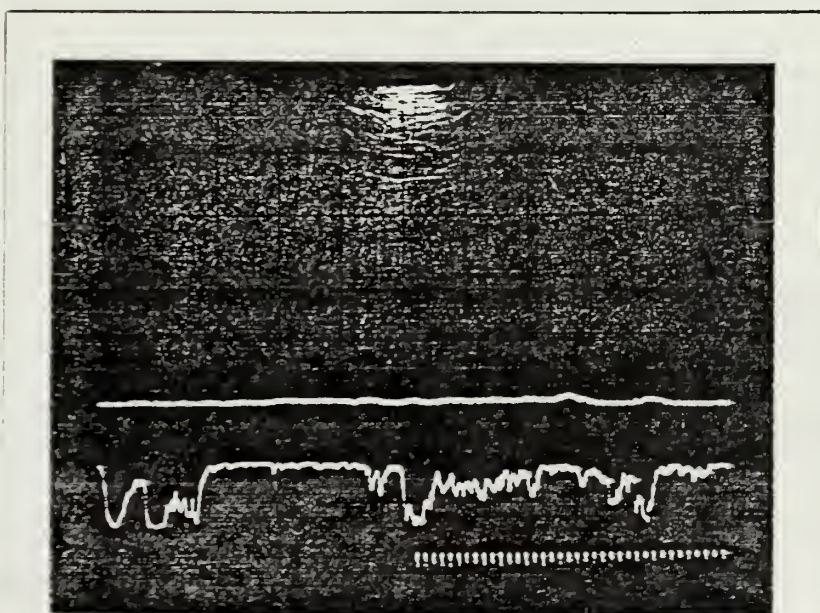
Oscilloscope Trace for Sample Number 93
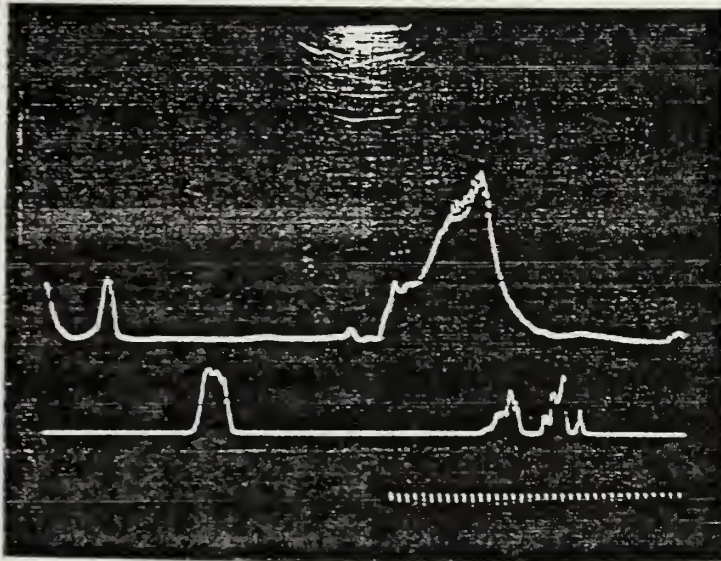
229
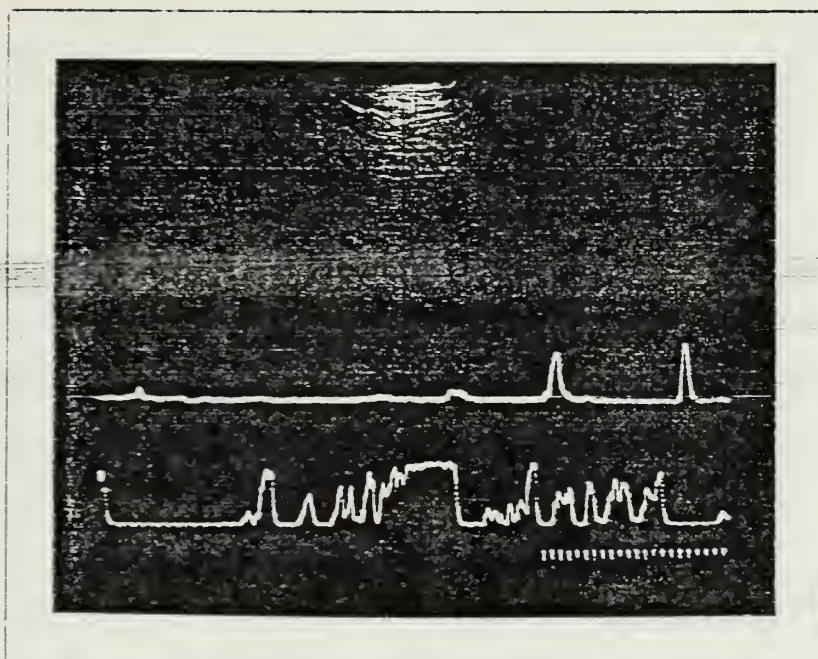
Oscilloscope Trace for Sample Number 94
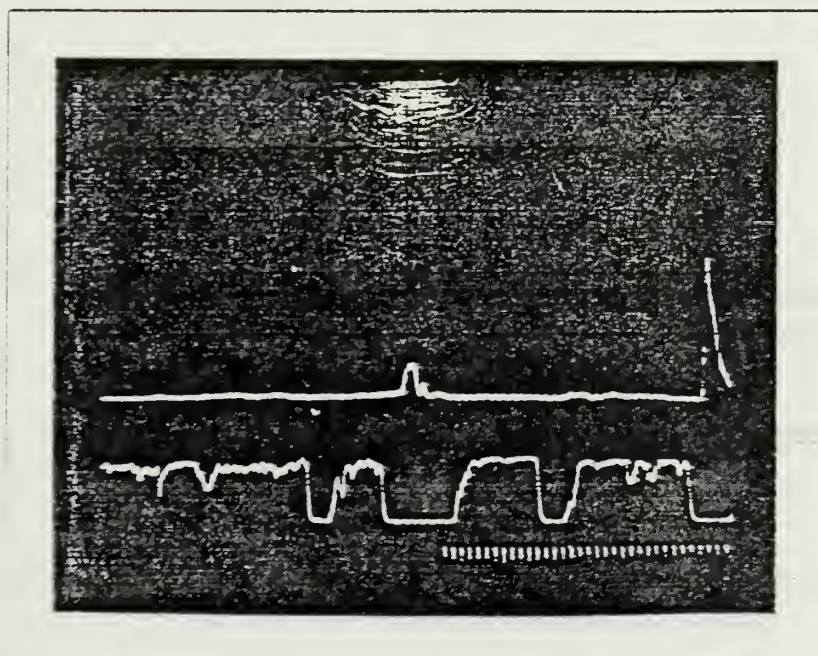
Oscilloscope Trace for Sample Number 95
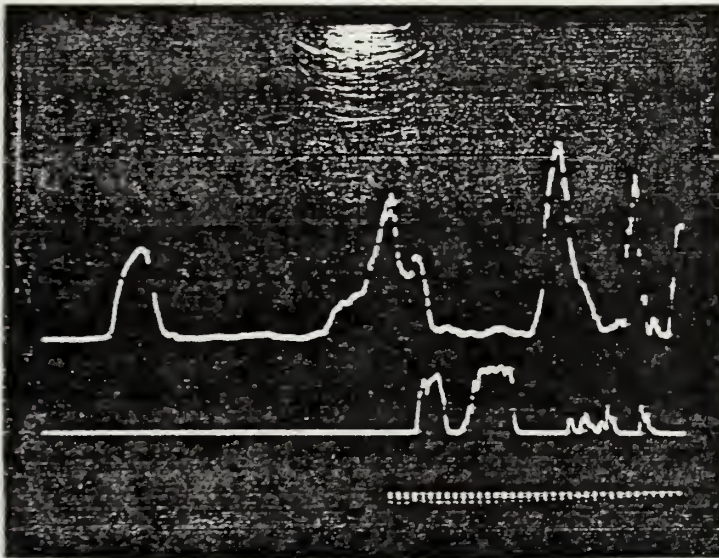
230
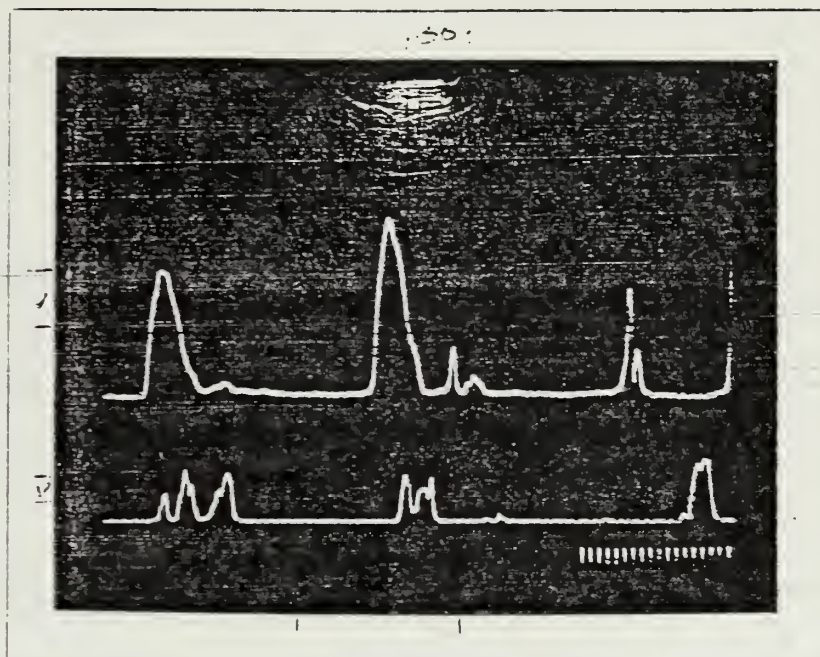
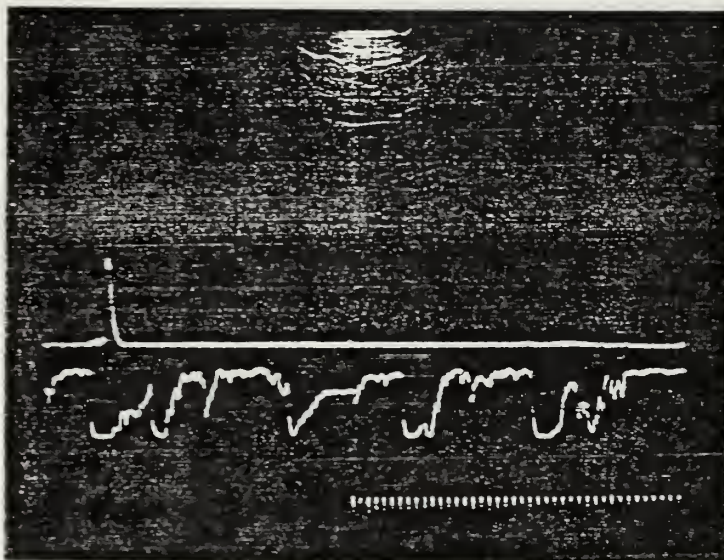Oscilloscope Trace for Sample Number 96
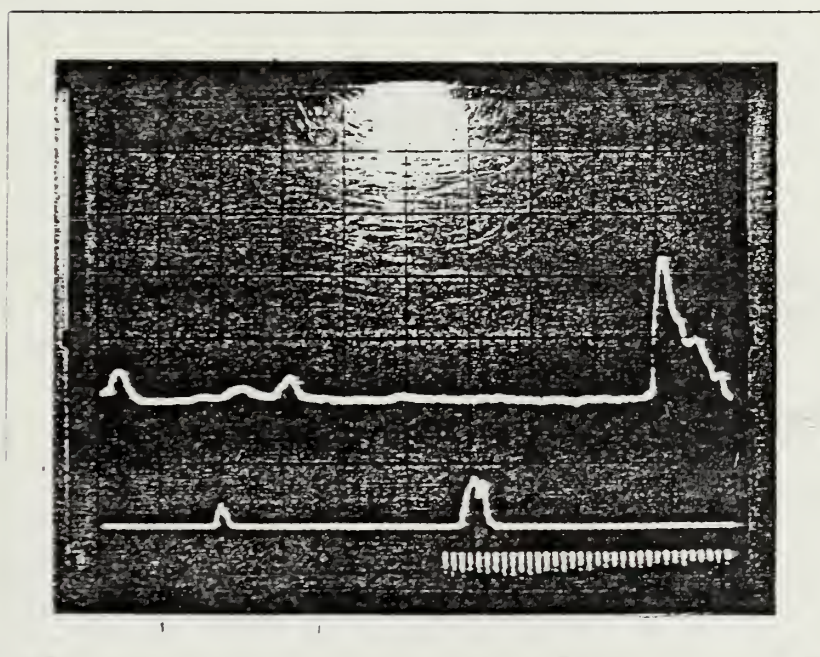
Oscilloscope Trace for Sample Number 97

231
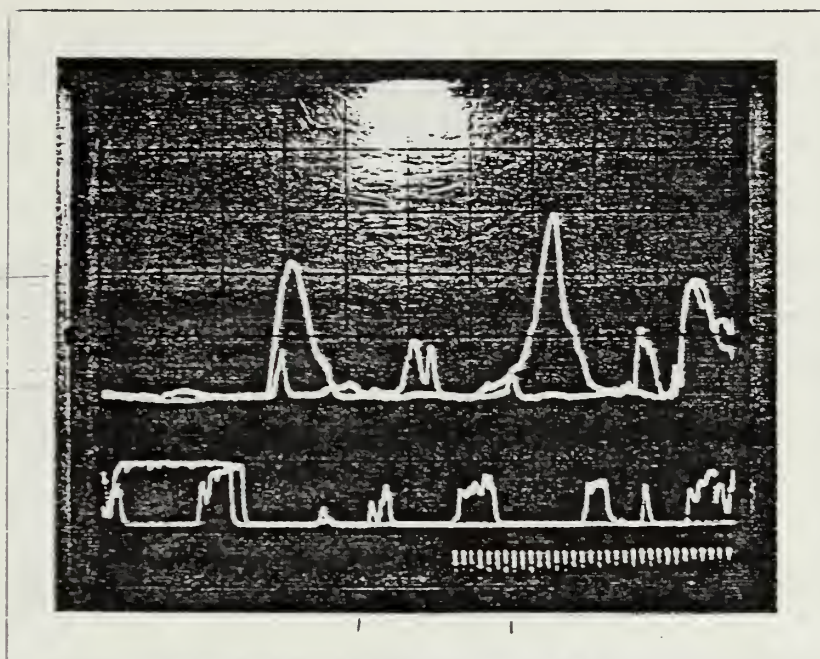
Oscilloscope Trace for Sample Number 98
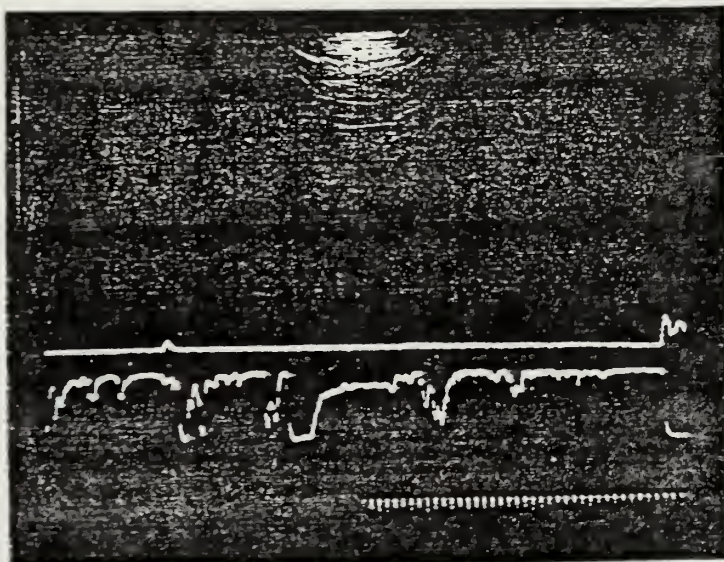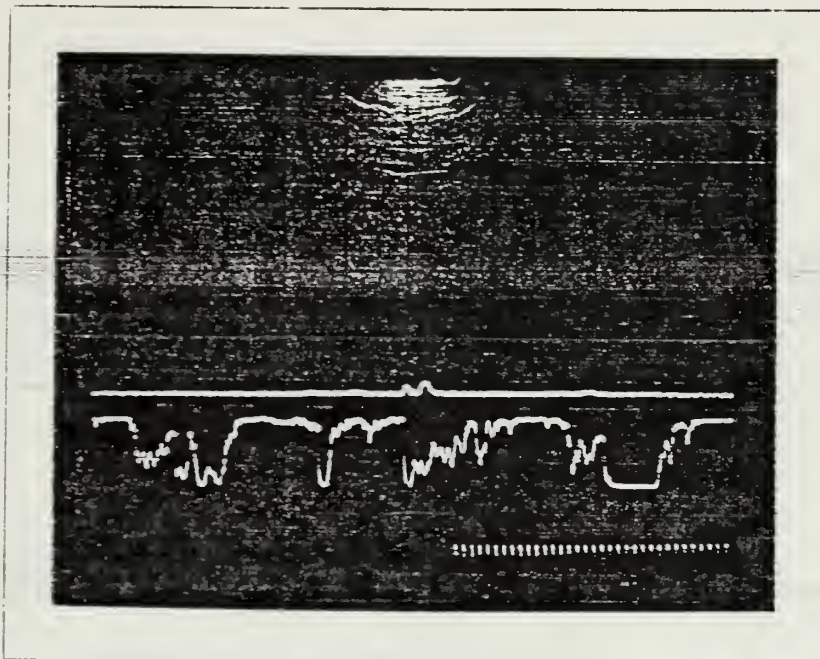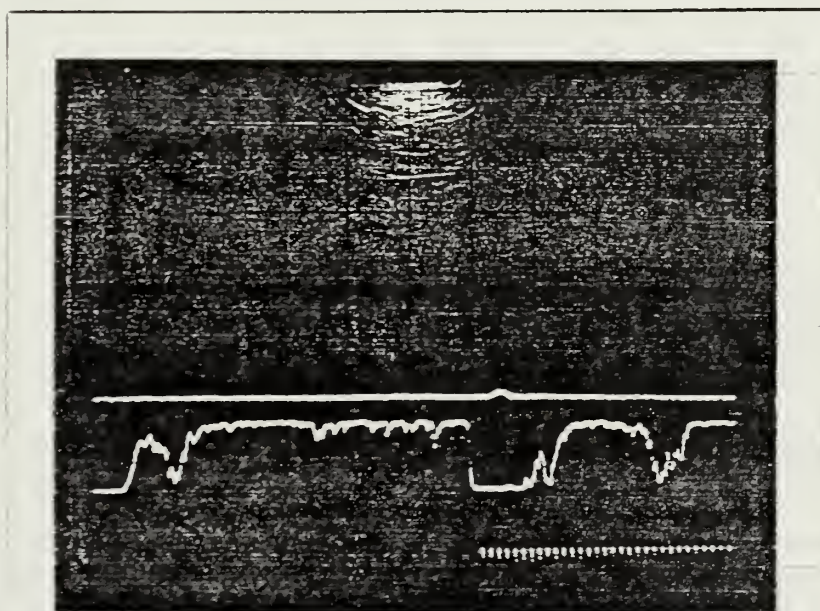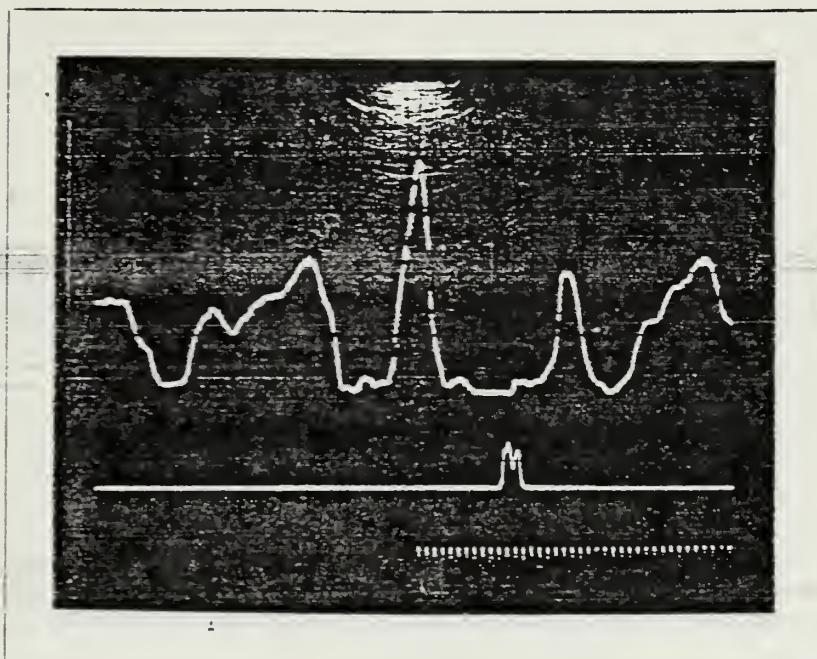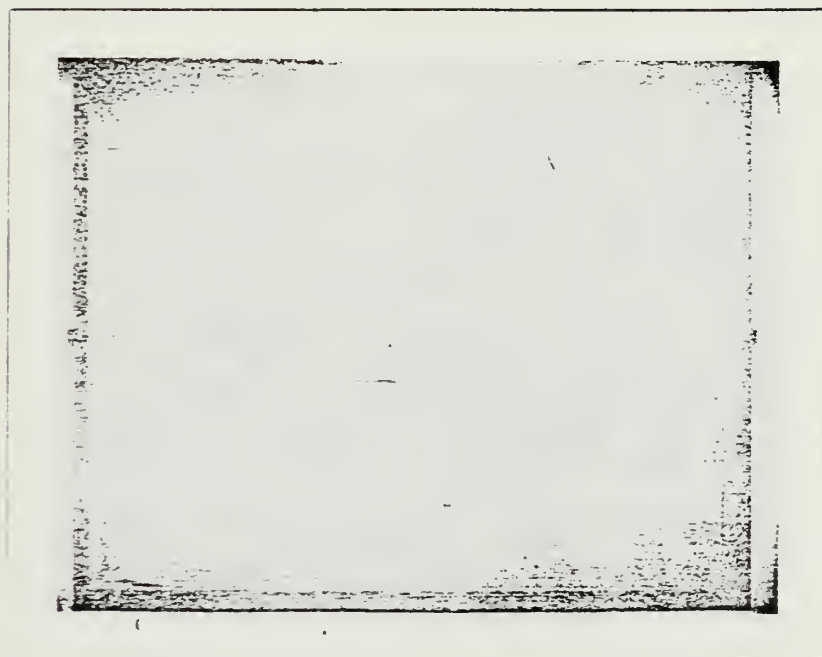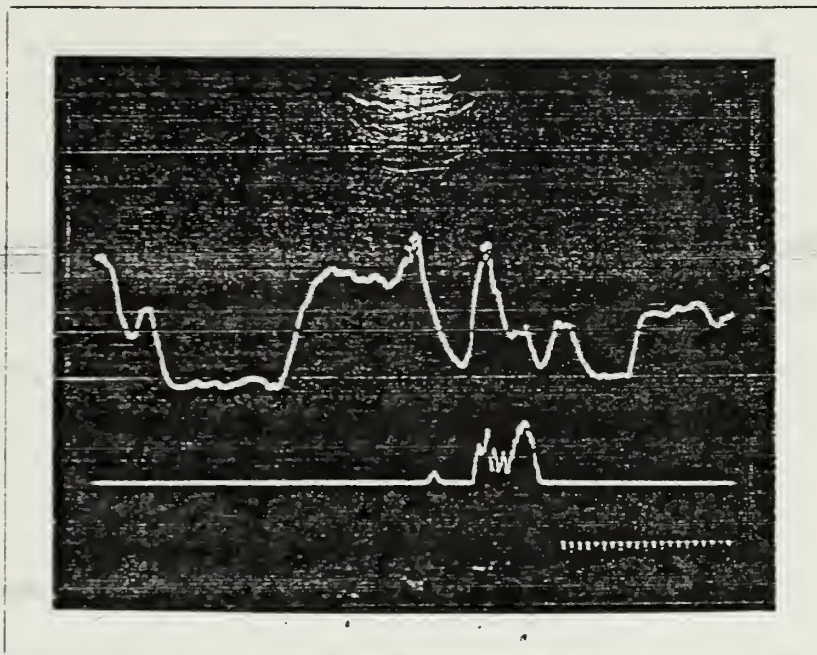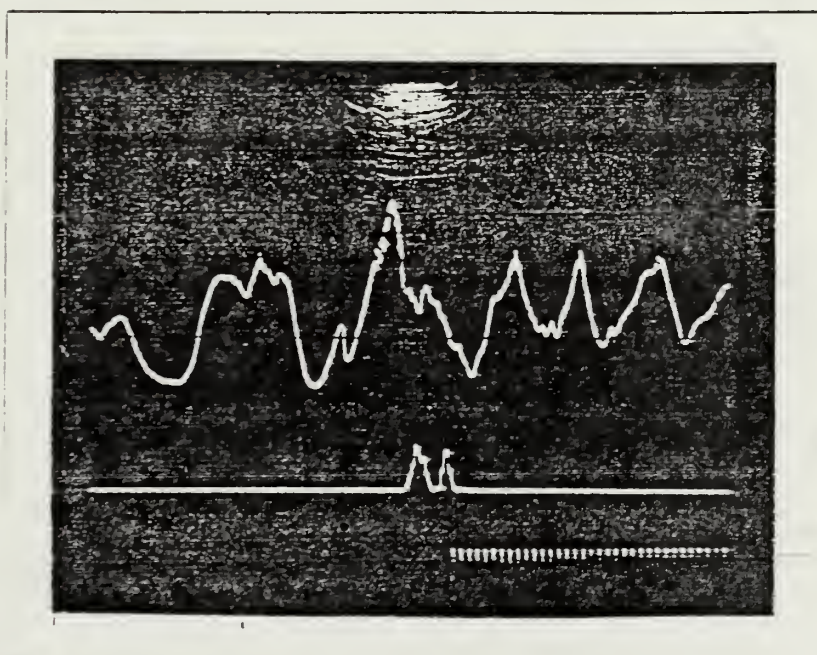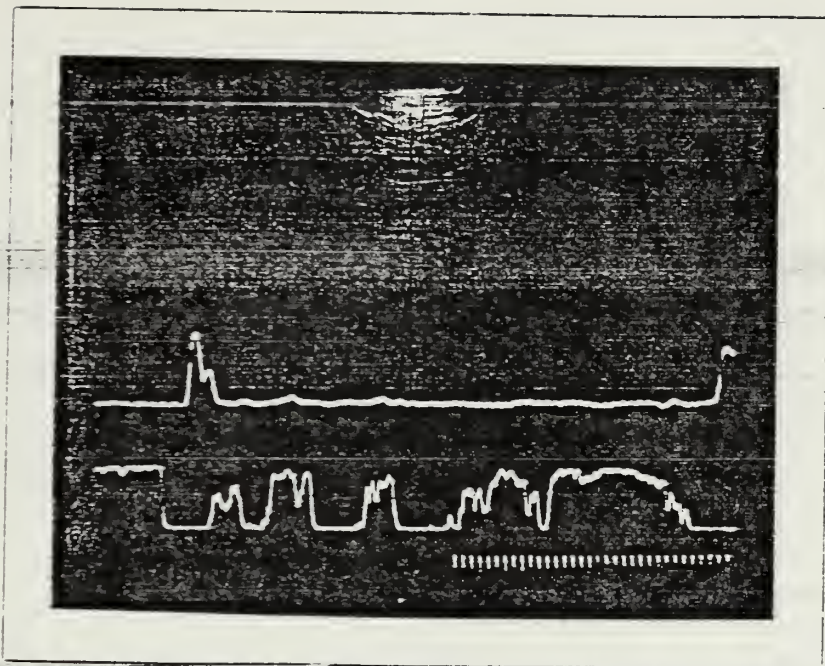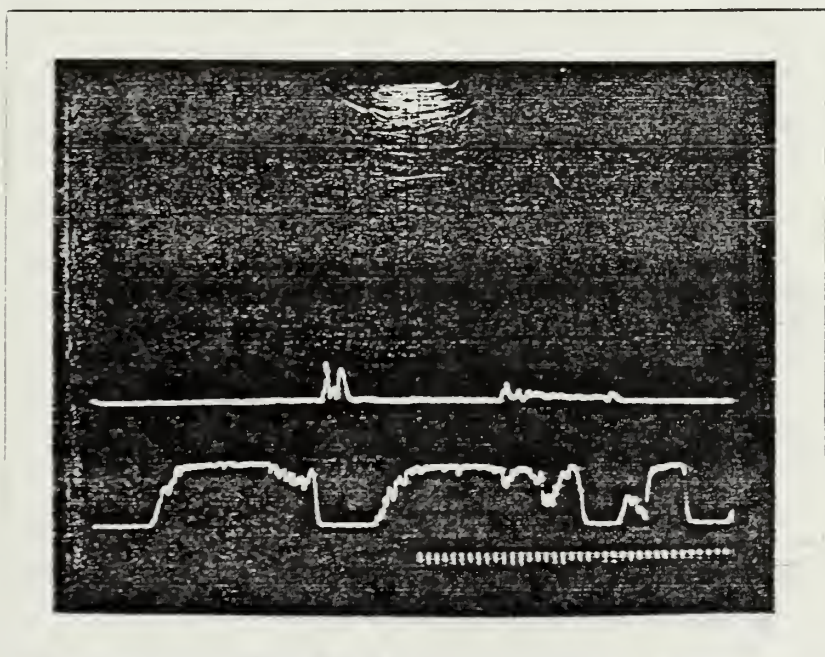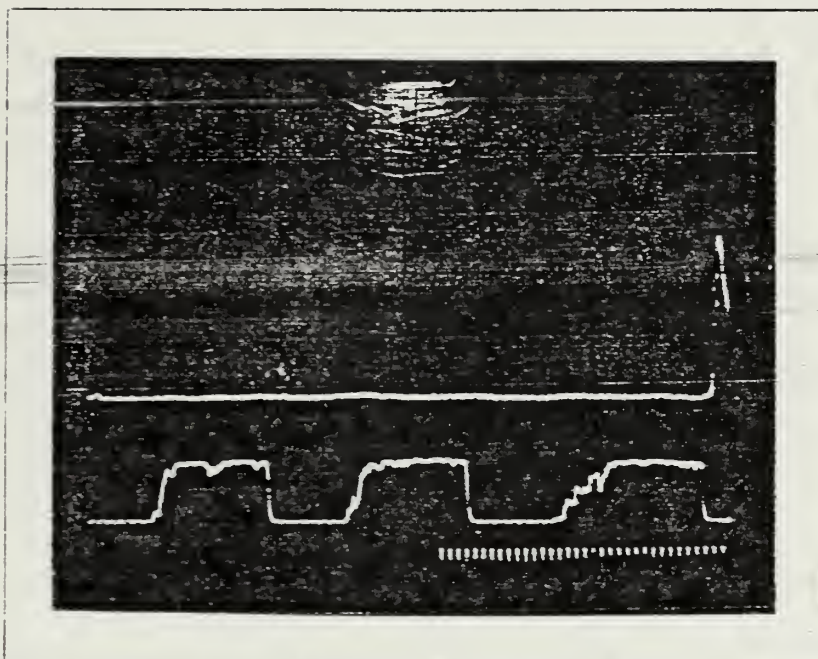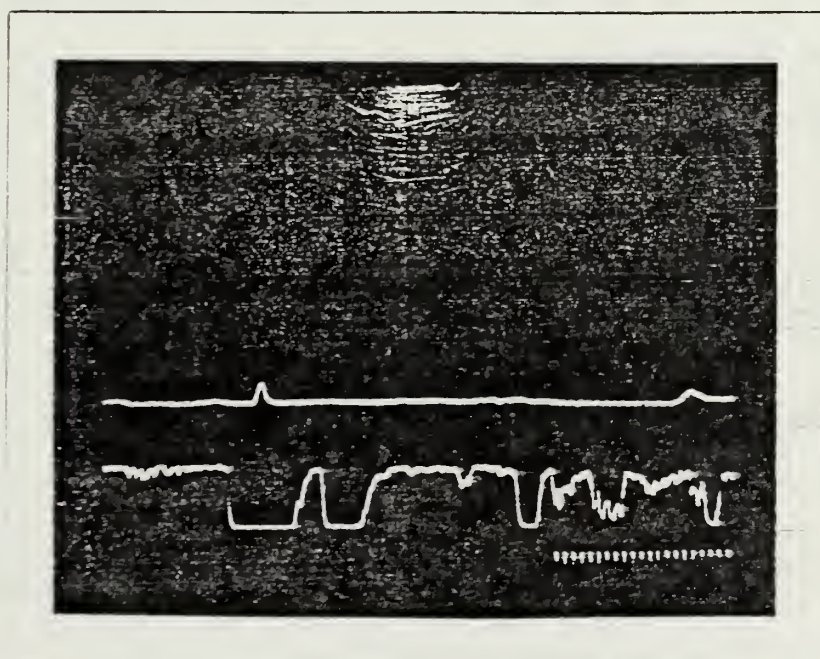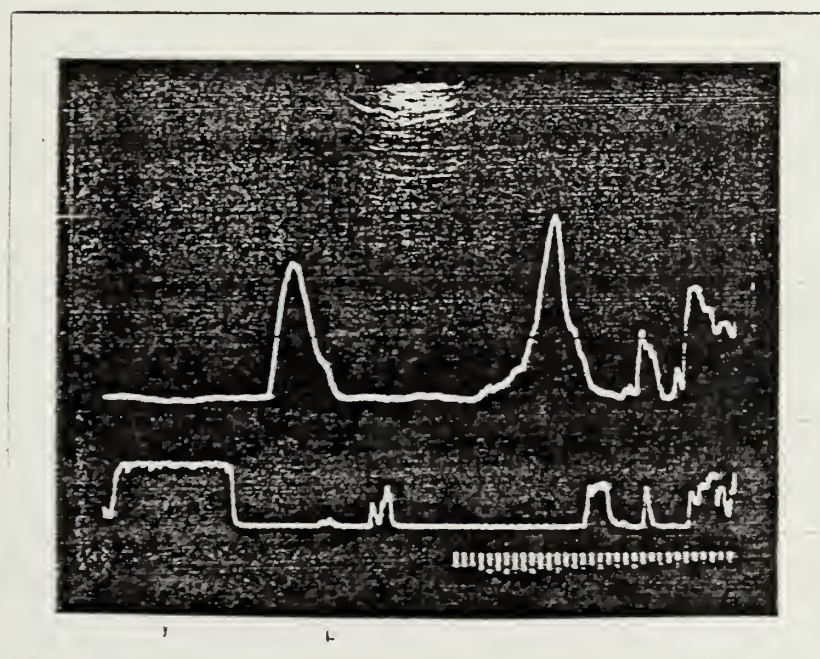

Oscilloscope Trace for Sample Number 99

232
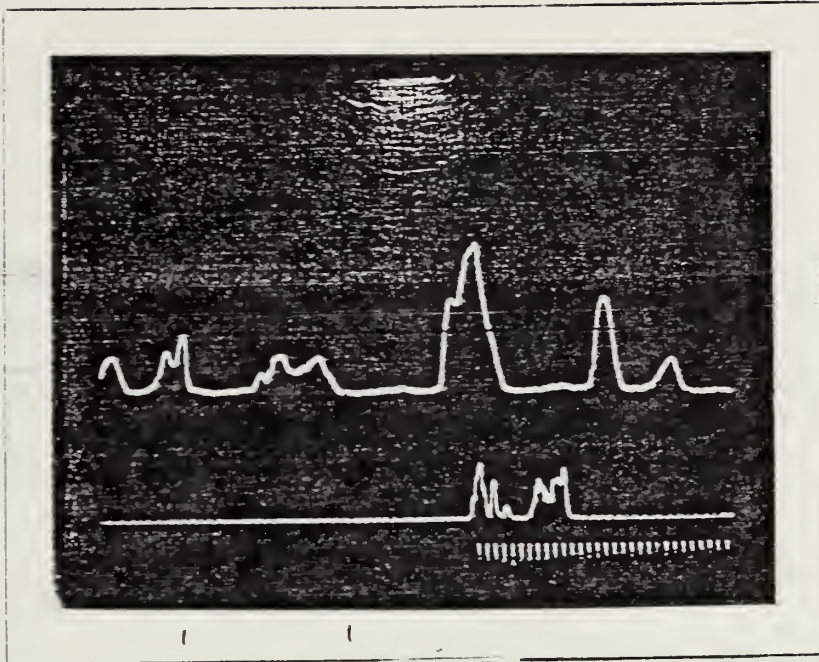
Oscilloscope Trace for Sample Number 100
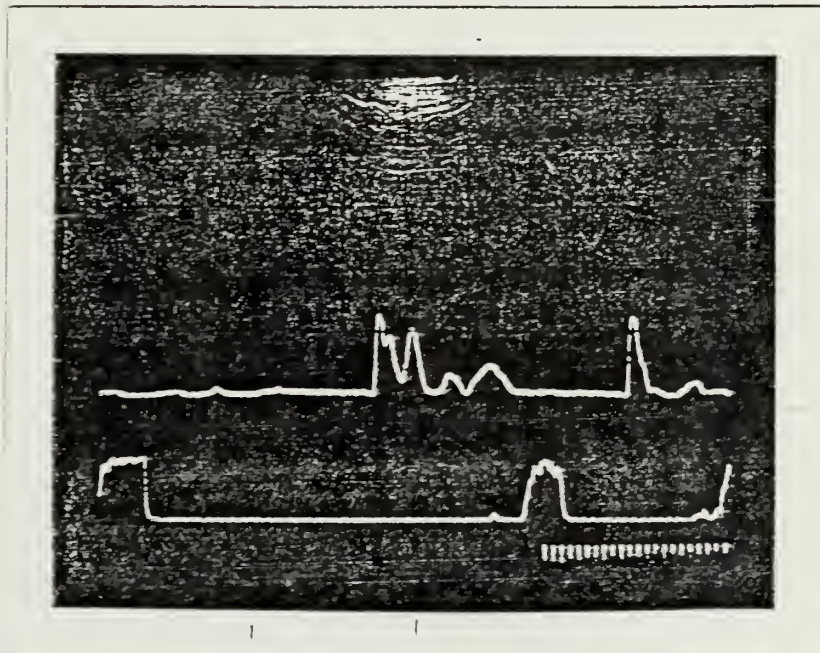
Oscilloscope Trace for Sample Number 101

233
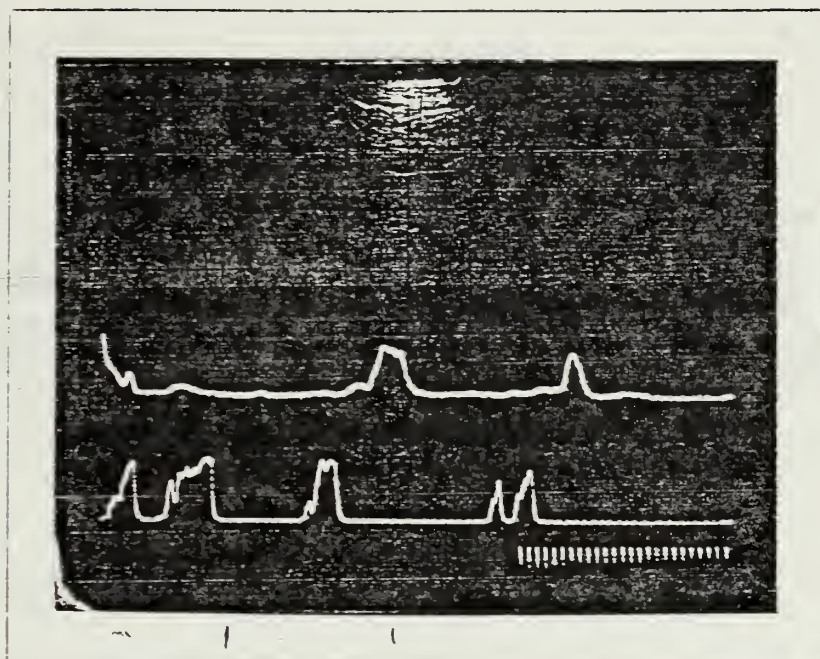
Oscilloscope Trace for Sample Number 102

234

APPENDIX L

This Appendix contains a complete listing of the particle
trajectory computer model used in this research. In addition, an
in depth program description and flow diagram is included.

Model Computer Program

This section describes the computer program listed in

Appendix K. To assist in understanding the program logic, the

program itself contains numerous comment statements. The program

consists of a main program and seven (7) subroutines. The main

program controls the input of parameters, trajectory calculations,

and output selections. The subroutines control the actual data

output in either table form or graphics. The following is an in-

depth description of the program:

Lines   Description

50-150   This section is used to explicitly define
                the major variables used within the program.
                The large arrays are defined in common block
                form to save memory. Constants used in the
                program are also defined.

190-610   This section is used to input variable data
                to the program. Three options exist for the
                bed particle distribution input:

                1) The default condition sets the quantity
                of each particle to unity. This option is
                generally used when a height determination
                is required or being sought after.

                2) The particle number option allows the
                entry of bed distribution by the number of
                particles present in each diameter range.
                This is used when data from the image
                analyzer was being used.

                3) The last option is used when the particle
                size distribution is determined from a sieve
                analysis and the data is measured in grams
                mass. The program will then determine the

236

particle number density based on the
                        assumption that the particls are spherical.

650-690   These lines convert the velocity input
                values from Ft/s to m/s.

700-710   Determine the slope of the triangular jet
                using the input amplitude and duration.

720-800   Initialize the data arrays to zero (0).

810-1660   This section calculates the trajectory for
                each diameter particle. This WHILE condition
                contains the following 8 subsections.

   820-840   Initialize the height of the particle to
                pass the first WHILE statement. Calculate
                the particle diameter to be used.

   850-1340   Calculate the particles trajectory
                parameters while the particle is above the
                bed surface. This DO loop contains the
                following 6 subsections.

   860-940   If the elapsed time since the particle left
                the bed is less than the jet duration time,
                the add the jet velocity to Uo.

   950-990   Calculates the relative velocity of the air
                with respect to the particle. Determine the
                sign of the drag force.

   1010-1060   Calculate Reynold's number.

   1100-1170   Calculate the drag on the particle and then
                determine the particles new velocity and
                position.

   1180-1220   If the particles velocity is positive,
                record the new max height and elapsed time.

   1230-1320.   Add 1 count to the probability array in the
                storage position representing the particles
                height/2. By using the DIV statement, a
                height window (dH) of 2 cm is created.

1350-1370   Change all heights from Ft/s to m/s

1380-1430   Multiply probability distribution by bed
                distribution weighting factor.

1440-1500   Determine the maximum value and normalize

                                237

the data such that the maximum is 100.

1510-1560	Calculate the particle entrainment by summing the total volume of each particle distribution at a given height.
1570-1660	Normalize the entrainment data to 100 and calculate the ln value if not equal to zero.
1700-1820	Display output menu.
1830-2210	Controls the selected output.
2220	End of MAIN program
2260-2520	Sub Display_Data is used to list input parameters used and the maximum height attained by each diameter particle.
2560-3930	Sub Display_graphics controls the processing and output of graphic information. This subprogram contains the following 4 sections.
2640-3120	Performs scaling for determining graphic dimensions and limits.
3130-3240	Creates graphic display and labels the X and Y axis.
3250-3830	Controls the plotting of selected graphic output.
3840-3920	Prints hard copy.
3980-4130	Function routine for determining scaling factor for graphic display.
4180-4280	Finds the limit of data within an INTEGER array to limit the X axis on a plot to the range in which the Y values are non-zero.
4330-4460	Determines the maximum value stored in an INTEGER array.
4510-4640	Same as 4330-4460 except for REAL array.
4690-4770	Same as 4180-4280 except for REAL array.

END of PROGRAM

```
10     !........MAIN Program.......
20     !
30     !
40     !
50     OPTION BASE 1
60     INTEGER Answer,Specify,Point,View,Bed_min,I
70     REAL Uo,Uoo,Uj,Del_t,Part_height,Slope,Jet_t,Jt
80     COM INTEGER Distribution(50,80),Distrib_density(50,80),REAL Height(2,50),B
ed_particle(50),Entrainment(2,80)
90     DIM Homes[2],Clears[2]
100    Clears=CHRS(255)&CHRS(75)                        ! CLEAR SCR key
110    Homes=CHRS(255)&CHRS(84)                         ! HOME key
120    Viscosity_kin=1.486E-5                          ! air, m*m/s
130    Density_air=1.201                               ! kg/m*m*m
140    Density_part=7.36E+3                            ! kg/m*m*m
150    Gravity=9.30665                                 ! m/s*s
160    !
170    ! Input variables
180    !
190    PRINTER IS 1                                    ! Output to CRT
200    INPUT "Enter mean air velocity Uo (Ft/s): ",Uo
210    INPUT "Enter amplitude of jet velocity (Ft/s): ",Uj
220    INPUT "Enter initial particle velocity Uoo (Ft/s): ",Uoo1
230    INPUT "Enter duration of jet (s): ",Jet_t
240    INPUT "Enter time increment for iteration (s): ",Del_t
250    INPUT "Do you desire to input the bed particle distribution (1 yes,0 no):"
,Answer
260    IF Answer=0 THEN            ! Bed dist not wanted    ! Bed dist not wanted
270      FOR I=1 TO 50                                 ! Set bed dist to 1
280        Bed_particle(I)=1.
290      NEXT I
300    ELSE
310      IF Answer=1 THEN                              ! Bed dist wanted
320        INPUT "Input will be: weight in grams (1) or number (2): ",Specify
330        IF Specify=1 OR Specify=2 THEN
340          PRINT "Enter data for each diameter"      ! Enter gram or #
350          Min_bed=1
360          FOR I=1 TO 50                             ! Each diameter
370            PRINT "D= ";I*10+70;" um"
380            INPUT Bed_particle(I)
390            IF Bed_particle(I)<Bed_particle(Min_bed) THEN Min_bed=I
400          NEXT I
410          IF Specify=1 THEN                         ! If weight entry
420            FOR I=1 TO 50                           ! Calculate #
430              Bed_particle(I)=6*Bed_particle(I)/(PI*(I*10+70)^3*Density_part)
440              IF Bed_particle(I)<Bed_particle(Min_bed) THEN Min_bed=I
450            NEXT I
460          END IF
470        ELSE
480          GOTO 320
490        END IF
500      ELSE
510        GOTO 250
520      END IF
530    END IF
540    Max_bed=1
550    FOR I=1 TO 50                                   ! Find largest #
560      IF Bed_particle(I)>Bed_particle(Max_bed) THEN Max_bed=I
```

239

```
570    NEXT I
580    Max_value=100/Bed_particle(Max_bed)                    ! determine scaler
590    FOR I=1 TO 50                                          ! Scale data max=100
600      Bed_particle(I)=Bed_particle(I)*Max_value
610    NEXT I
620    !
630    ! Compute data
640    !
650    U1=Uo
660    Uo1=Uoo1
670    Uo=Uo*.3048                                            ! Change to m/s
680    Uoo1=Uoo1*.3048
690    Uj1=Uj*.3048
700    IF Jet_t=0 THEN Jet_t=1
710    Slope=2.*Uj1/Jet_t                                     ! Triangle jet pulse
720    FOR I=1 TO 50
730      Height(1,I)=0.                                       ! Zero height array
740      Height(2,I)=0.                                       ! Zero number array
750      FOR J=1 TO 30
760        Distribution(I,J)=0                                ! Zero dist array
770        Entrainment(1,J)=0.                                ! Zero entrain array
780        Entrainment(2,J)=0.
790      NEXT J
800    NEXT I
810    FOR I=1 TO 50                                          ! For each particle
820      Part_height=.000001                                  ! Set for WHILE state.
830      Uoo=Uoo1                                             ! Initial V constant
840      Diameter_part=(I-7)*1.0E-5                           ! Particle Dia um
850      WHILE Part_height>0
860        Jt=Jet_t/2.
870        Time_now=Height(2,I)*Del_t                         ! Time of part flight
880        IF Time_now<Jet_t THEN                             ! part in jet?
890          IF Height(2,I)*Del_t<Jt THEN                     ! 1st half of jet
900            Uo=Uo+Slope*Height(2,I)*Del_t
910          ELSE
920            Uo=Uo+Uj1-Slope*Height(2,I)*Del_t              ! 2nd half of jet
930          END IF
940        END IF
950        Relative_vel=Uo-Uoo                                ! Rel V seen by part
960        Sign=1                                             ! Set sign positive
970        IF Relative_vel<0 THEN                             ! Is V negative?
980          Sign=-1                                          ! Set sign negative
990        END IF
1000       !                                                  Calculate Re
1010       Reynolds_no=Relative_vel*Diameter_part/Viscosity_kin
1020       Reynolds_no=ABS(Reynolds_no)
1030       IF Reynolds_no=0. THEN
1040         Acceleration=-Gravity
1050         GOTO 1150
1060       END IF
1070       !                                                  Calculate drag
1080       ! Uses data correlation for drag coefficient good for Re<1E5
1090       !
1100       Drag_coeff=24/Reynolds_no+6/(1+SQR(Reynolds_no))+.4
1110       Drag=Sign*Drag_coeff*Density_air*Relative_vel*Relative_vel*PI*Diameter
_part*Diameter_part/8
1120       !                                                  Calculate acceleration
1130       Acceleration=Drag/(Density_part*PI*Diameter_part^3/6)-Gravity
1140       !                                                  Calculate del velocity
1150       Velocity=Uoo+Acceleration*Del_t
```

240

```
1160      !                                                  Calculate new position
1170      Part_height=Part_height+(Velocity+Upo)*Del_t/2
1180      IF Upo>0 THEN                                    ! Part still rising?
1190        Height(1,I)=Part_height                       ! Save position
1200        Height(2,I)=Height(2,I)+1                     ! Inc t for max rise
1210      END IF
1220      Upo=Velocity                                    ! Set new V for next inc
1230      Point=(100*Part_height) DIV 2                   ! 2 cm wide storage bins
1240      IF Point>79 THEN                                ! Set default for fatal
1250        Point=79
1260      END IF
1270      IF Point<=0 THEN                                ! Set default for fatal
1280        Point=0
1290      END IF
1300      PRINT I,Point                                   ! Indicate como working
1310      !                                         Save # times part in height bin
1320      Distribution(I,Point+1)=Distribution(I,Point+1)+1
1330    END WHILE
1340  NEXT I
1350  FOR I=1 TO 50
1360    Height(1,I)=Height(1,I)*100                       ! Change to cm
1370  NEXT I
1380  FOR I=1 TO 50
1390    Value=Bed_particle(I)              ! Part size weight factor from bed dist
1400    FOR J=1 TO 80
1410      Distrib_density(I,J)=Distribution(I,J)*Value    ! Weight dist values
1420    NEXT J
1430  NEXT I
1440  Max_dist=FNMax_int(Distrib_density(*),50,80)        ! Find max value
1450  Factor=100./Max_dist                               !' Scale for 100 max
1460  FOR I=1 TO 50
1470    FOR J=1 TO 80
1480      Distrib_density(I,J)=Distrib_density(I,J)*Factor ! Scale values
1490    NEXT J
1500  NEXT I
1510  FOR I=1 TO 50     ! Mass density/unit area   at height above bed
1520    Volume=PI*((I+7)/1000)^3/6                       ! Volume Cu cm
1530    FOR J=1 TO 80
1540      Entrainment(1,J)=Entrainment(1,J)+Volume*Distrib_density(I,J)
1550    NEXT J
1560  NEXT I
1570  Max_entrain=1
1580  FOR I=1 TO 80                                      ! Find maximum
1590    IF Entrainment(1,I)>Entrainment(1,Max_entrain) THEN Max_entrain=I
1600  NEXT I
1610  Factor=100/Entrainment(1,Max_entrain)              ! Normalize to 100
1620  FOR I=1 TO 80
1630    Entrainment(1,I)=Entrainment(1,I)*Factor
1640    IF Entrainment(1,I)<=0. THEN 1660
1650    Entrainment(2,I)=LOG(Entrainment(1,I))
1660  NEXT I
1670  !
1680  ! Output Control Section
1690  !
1700  PRINTER IS 1                                       ! Output to CRT
1710  PRINT USING "9,3/"
1720  PRINT "1)     Display height vs diameter data"
1730  PRINT "2)     Display height vs diameter graph"
1740  PRINT "3)     Display density vs height as function of dia graph"
1750  PRINT "4)     Display density vs diameter as a function of height graph"
```

```
1760  PRINT "5)       Display same as 3 but with bed density"
1770  PRINT "6)       Display same as 4 but with bed density"
1780  PRINT "7)       Display density vs diameter of bed mass"
1790  PRINT "8)       Display entrainment density above bed"
1800  PRINT "9)       Display Ln entrainment density above bed"
1810  PRINT "10)      EXIT PROGRAM"
1820  INPUT "Enter number of desired display: ",Answer
1830  SELECT Answer
1840    CASE =1
1850      CALL Display_data(U1,Up1,Uj,Jet_t,Del_t,Homes,Clears)
1860    CASE =2
1870      CALL Display_graph(Clears,Homes,Answer,View)
1880    CASE =3
1890      INPUT "Enter particle size to be viewed (80-570 um)(0 for all): ",View
1900      IF View=0 THEN 1920
1910      IF View<80 OR View>570 THEN 1890
1920      View=(View DIV 10)-7
1930      CALL Display_graph(Clears,Homes,Answer,View)
1940    CASE =4
1950      INPUT "Enter desired height above bed surface (0-158 cm): ",View
1960      IF View<0 OR View>158 THEN 1950
1970      View=(View DIV 2)+1
1980      CALL Display_graph(Clears,Homes,Answer,View)
1990    CASE =5
2000      INPUT "Enter particle size to be viewed (80-570 um)(0 for all): ",View
2010      IF View=0 THEN 2030
2020      IF View<80 OR View>570 THEN 2000
2030      View=(View DIV 10)-7
2040      CALL Display_graph(Clears,Homes,Answer,View)
2050    CASE =6
2060      INPUT "Enter desired height above bed surface (0-158 cm): ",View
2070      IF View<0 OR View>158 THEN 2060
2080      View=(View DIV 2)+1
2090      CALL Display_graph(Clears,Homes,Answer,View)
2100    CASE =7
2110      CALL Display_graph(Clears,Homes,Answer,View)
2120    CASE =8
2130      CALL Display_graph(Clears,Homes,Answer,View)
2140    CASE =9
2150      CALL Display_graph(Clears,Homes,Answer,View)
2160    CASE =10
2170      STOP
2180    CASE ELSE
2190      GOTO 1820
2200  END SELECT
2210  GOTO 1700
2220  END
2230  !
2240  !
2250  !
2260  ! Sub used to list input parameters and max height at time t per diameter
2270  SUB Display_data(U1,Up1,Uj,Jet_t,Del_t,Homes,Clears)
2280  COM INTEGER Distribution(*),Distrib_density(*),REAL Height(*),Bed_particle
(*),Entrainment(*)
2290  OUTPUT 2;Homes;                                   ! Home and Clear screen
2300  OUTPUT 2;Clears;
2310  !                                                  Print output
2320  PRINT "                           cm/s"
2330  PRINT "Mean Bed Velocity=        ";U1*30.48
2340  PRINT "Initial Particle Velocity= ";Up1*30.48
```

242
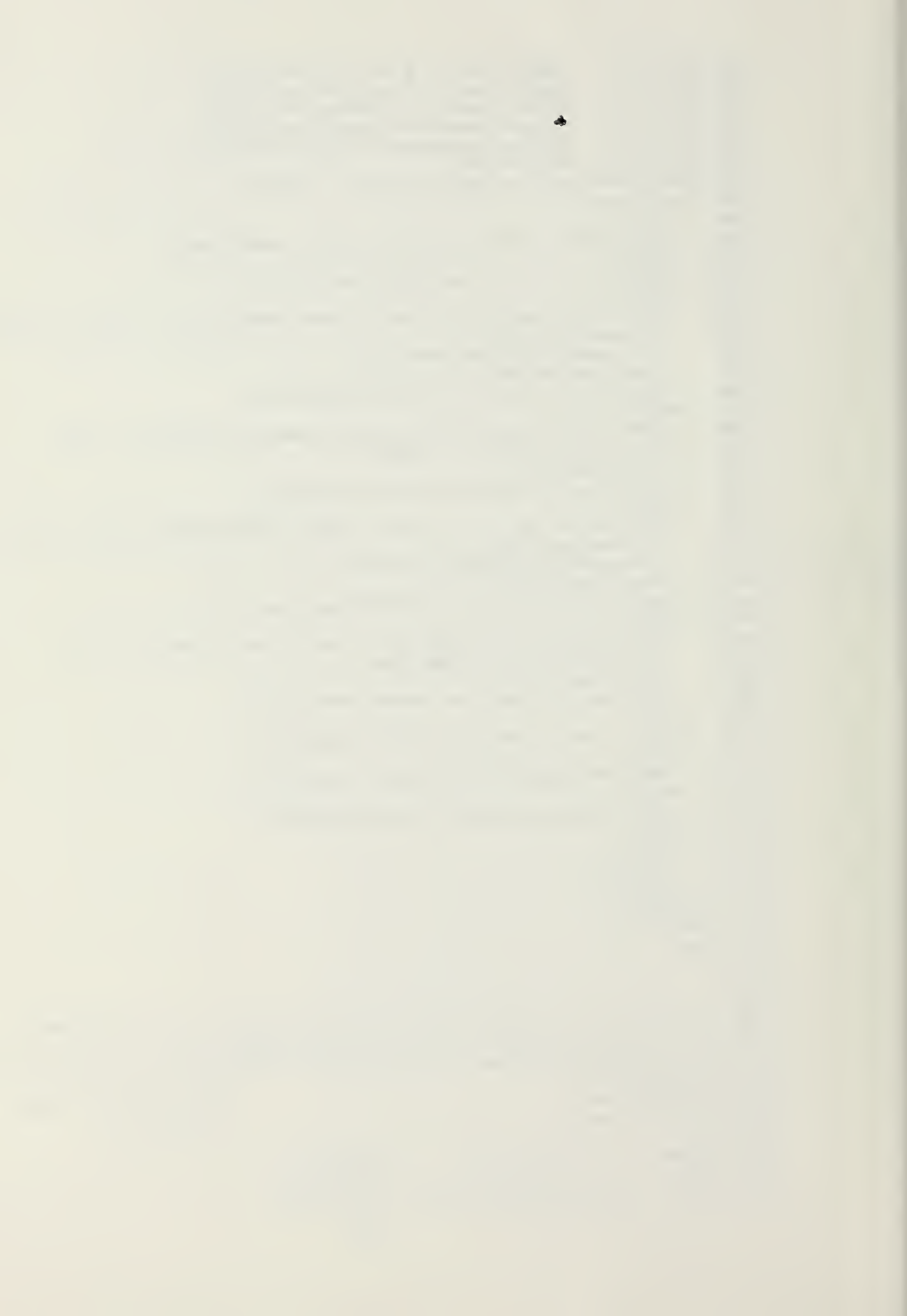
```
2350    PRINT "Peak Jet Velocity=              ";Uj*30.48
2360    PRINT "Gas Jet Duration=              ";Jet_t
2370    PRINT
2380    PRINT "  Diameter"," Height","  Time","   Diameter";" Height";"
Time"
2390    PRINT "     um","   cm "," seconds","      um","     cm","   seconds
"
2400    PRINT
2410    FOR I=1 TO 50 STEP 2
2420      PRINT USING "2(5X,3D,5X,3D.D,5X,D.DDD,5X)";(I+7)*10,Height(1,I),Height(2
,I)*Del_t,(I+8)*10,Height(1,I+1),Height(2,I+1)*Del_t;
2430    NEXT I
2440    PRINTER IS 1
2450    INPUT "Print hard copy? (1)= yes, (0)= no: ",Answer
2460    IF Answer=1 THEN
2470      PRINTER IS 701
2480      GOTO 2320
2490    ELSE
2500      IF Answer<>0 THEN 2450
2510    END IF
2520    SUBEND
2530    !
2540    !
2550    !
2560    ! Sub used to control graphics output of data
2570    SUB Display_graph(Clear$,Home$,INTEGER Data_set,View)
2580    COM INTEGER Distribution(*),Distrib_density(*),REAL Height(*),Bed_particle
(*),Entrainment(*)
2590    REAL Xmax,Ymax,Xtick,Ytick,Xmin,Ymin
2600    OUTPUT 2;Home$;
2610    OUTPUT 2;Clear$;
2620    GINIT                                           ! Initialize graphics
2630    GRAPHICS ON
2640    SELECT Data_set                                 ! Scale plot routines
2650      CASE =2
2660        Xmax=600.
2670        Ymax=FNMax_real(Height(*),1,50)
2680        Xtick=50.
2690        Ytick=FNScale(Ymax)
2700      CASE =3
2710        Ymax=FNMax_int(Distribution(*),50,80)
2720        Xmax=FNData_limit(Distribution(*),50,80)
2730        Xtick=FNScale(Xmax)
2740        Ytick=FNScale(Ymax)
2750      CASE =4
2760        Xmax=600.
2770        Ymax=FNMax_int(Distribution(*),50,80)
2780        Xtick=50.
2790        Ytick=FNScale(Ymax)
2800      CASE =5
2810        Xmax=FNData_limit(Distrib_density(*),50,80)
2820        Ymax=100.
2830        Xtick=FNScale(Xmax)
2840        Ytick=FNScale(Ymax)
2850      CASE =6
2860        Xmax=600.
2870        Ymax=FNMax_int(Distrib_density(*),50,80)
2880        Xtick=50.
2890        Ytick=FNScale(Ymax)
2900      CASE =7
```

```
2910        Xmax=500.
2920        Ymax=100.
2930        Xtick=50.
2940        Ytick=10
2950     CASE =8
2960        Xmax=FNData_limitr(Entrainment(*),1,30)
2970        Ymax=100.
2980        Xtick=FNScale(Xmax)
2990        Ytick=10.
3000     CASE =9
3010        Xmax=FNData_limitr(Entrainment(*),1,90)
3020        Ymax=5.
3030        Ymin=-3.
3040        Xtick=FNScale(Xmax)
3050        Ytick=.5
3060        Y_axis=-2.5
3070        GOTO 3110
3080  END SELECT
3090  Y_axis=0.
3100  Ymin=-Ytick
3110  Xmin=-2.*Xtick
3120  X_axis=0.
3130  WINDOW Xmin,1.1*Xmax,Ymin,1.1*Ymax              ! Set graphics scale
3140  AXES Xtick,Ytick,X_axis,Y_axis                  ! Set graph axis
3150  LORG 5                                          ! Label X-axis
3160  FOR I=X_axis TO Xmax STEP Xtick*2
3170    MOVE I,Y_axis
3180    LABEL I
3190  NEXT I
3200  LORG 8                                          ! Label Y-axis
3210  FOR I=Y_axis TO Ymax STEP Ytick
3220    MOVE X_axis,I
3230    LABEL I
3240  NEXT I
3250  SELECT Data_set                                 ! Plot data
3260    CASE =2
3270      MOVE 80,Height(1,1)
3280      FOR I=2 TO 50
3290        DRAW (I+7)*10,Height(1,I)
3300      NEXT I
3310    CASE =3
3320      Begin=View
3330      Finish=View
3340      IF View<0 THEN                              ! Plot all if<0
3350        Begin=1
3360        Finish=50
3370      END IF
3380      FOR I=Begin TO Finish
3390        MOVE 0,Distribution(I,1)
3400        FOR J=1 TO Xmax/2
3410          DRAW 2*J,Distribution(I,J)
3420        NEXT J
3430      NEXT I
3440    CASE =4
3450      MOVE 80,Distribution(1,View)
3460      FOR I=2 TO 50
3470        DRAW (I+7)*10,Distribution(I,View)
3480      NEXT I
3490    CASE =5
3500      Begin=View
```

244

```
3510       Finish=View
3520       IF View<0 THEN                                      ! Plot all if <0
3530         Begin=1
3540         Finish=50
3550       END IF
3560       FOR I=Begin TO Finish
3570         MOVE 0,Distrib_density(I,1)
3580         FOR J=1 TO Xmax/2
3590           DRAW 2*J,Distrib_density(I,J)
3600         NEXT J
3610       NEXT I
3620     CASE =6
3630       MOVE 30,Distrib_density(1,View)
3640       FOR I=2 TO 50
3650         DRAW (I+7)*10,Distrib_density(I,View)
3660       NEXT I
3670     CASE =7
3680       MOVE 30,Bed_particle(1)
3690       FOR I=2 TO 50
3700         DRAW (I+7)*10,Bed_particle(I)
3710       NEXT I
3720     CASE =8
3730       MOVE 0,Entrainment(1,1)
3740       FOR I=2 TO 30
3750         DRAW I*2,Entrainment(1,I)
3760       NEXT I
3770     CASE =9
3780       MOVE 0,Entrainment(2,1)
3790       FOR I=2 TO 30
3800         IF Entrainment(2,I)=0. THEN 3840
3810         DRAW I*2,Entrainment(2,I)
3820       NEXT I
3830   END SELECT
3840   INPUT "Print graph (1) yes, (0) no: ",Answer
3850   IF Answer=1 THEN
3860     DUMP DEVICE IS 701                                   ! Dump to printer
3870     DUMP GRAPHICS
3880     GCLEAR
3890   ELSE
3900     IF Answer<>0 THEN 3840
3910   END IF
3920   GCLEAR
3930   SUBEND
3940   !
3950   !
3960   !
3970   ! Function determines graphics axis scaleing
3980   DEF FNScale(Ymax)
3990   IF Ymax>100 THEN
4000     Tick=20.
4010   ELSE
4020     IF Ymax<=100 AND Ymax>20 THEN
4030       Tick=10.
4040     ELSE
4050       IF Ymax<=20 AND Ymax>4 THEN
4060         Tick=2.
4070       ELSE
4080         Tick=.5
4090       END IF
4100     END IF
```

245

```
4110  END IF
4120  RETURN Tick
4130  FNEND
4140  !
4150  !
4160  !
4170  ! Function determines max extent of data for X-axis limit
4180  DEF FNData_limit(INTEGER Data_1(*),Row_max,Col_max)
4190  Col=1
4200  REPEAT
4210    Sum=0.
4220    FOR I=1 TO Row_max
4230      Sum=Sum+Data_1(I,Col)
4240    NEXT I
4250    Col=Col+1
4260  UNTIL Sum=0 OR Col=Col_max-1
4270  RETURN Col+2
4280  FNEND
4290  !
4300  !
4310  !
4320  ! Function determines max value in integer array
4330  DEF FNMax_int(INTEGER Data_1(*),Row_max,Col_max)
4340  R_max=1
4350  C_max=1
4360  FOR I=1 TO Row_max
4370    FOR J=1 TO Col_max
4380      IF Data_1(I,J)>Data_1(R_max,C_max) THEN
4390        R_max=I
4400        C_max=J
4410      END IF
4420    NEXT J
4430  NEXT I
4440  Max=Data_1(R_max,C_max)
4450  RETURN Max
4460  FNEND
4470  !
4480  !
4490  !
4500  ! Function determines maximum value in real array
4510  DEF FNMax_real(Data_1(*),INTEGER Row_max,Col_max)
4520  R_max=1
4530  C_max=1
4540  FOR I=1 TO Row_max
4550    FOR J=1 TO Col_max
4560      IF Data_1(I,J)>Data_1(R_max,C_max) THEN
4570        R_max=I
4580        C_max=J
4590      END IF
4600    NEXT J
4610  NEXT I
4620  Max=Data_1(R_max,C_max)
4630  RETURN Max
4640  FNEND
4650  !
4660  !
4670  !
4680  ! Function determines max extent of data for X-axis limit
4690  DEF FNData_limitr(Data_1(*),Row,Col_max)
4700  Col=1
```

```
4710    IF Data_1(Row,Col)<=0 OR Col=Col_max THEN
4720      Limit=Col+2
4730      RETURN Limit
4740    END IF
4750    Col=Col+1
4760    GOTO 4710
4770    FNEND
```

APPENDIX M

This Appendix contains the calibration data for the
anemometer probe. The calibration was conducted in a small wind
tunnel using a pitot tube connected to a micromanometer capable of
measuring pressures to within 0.001 ins. of water.
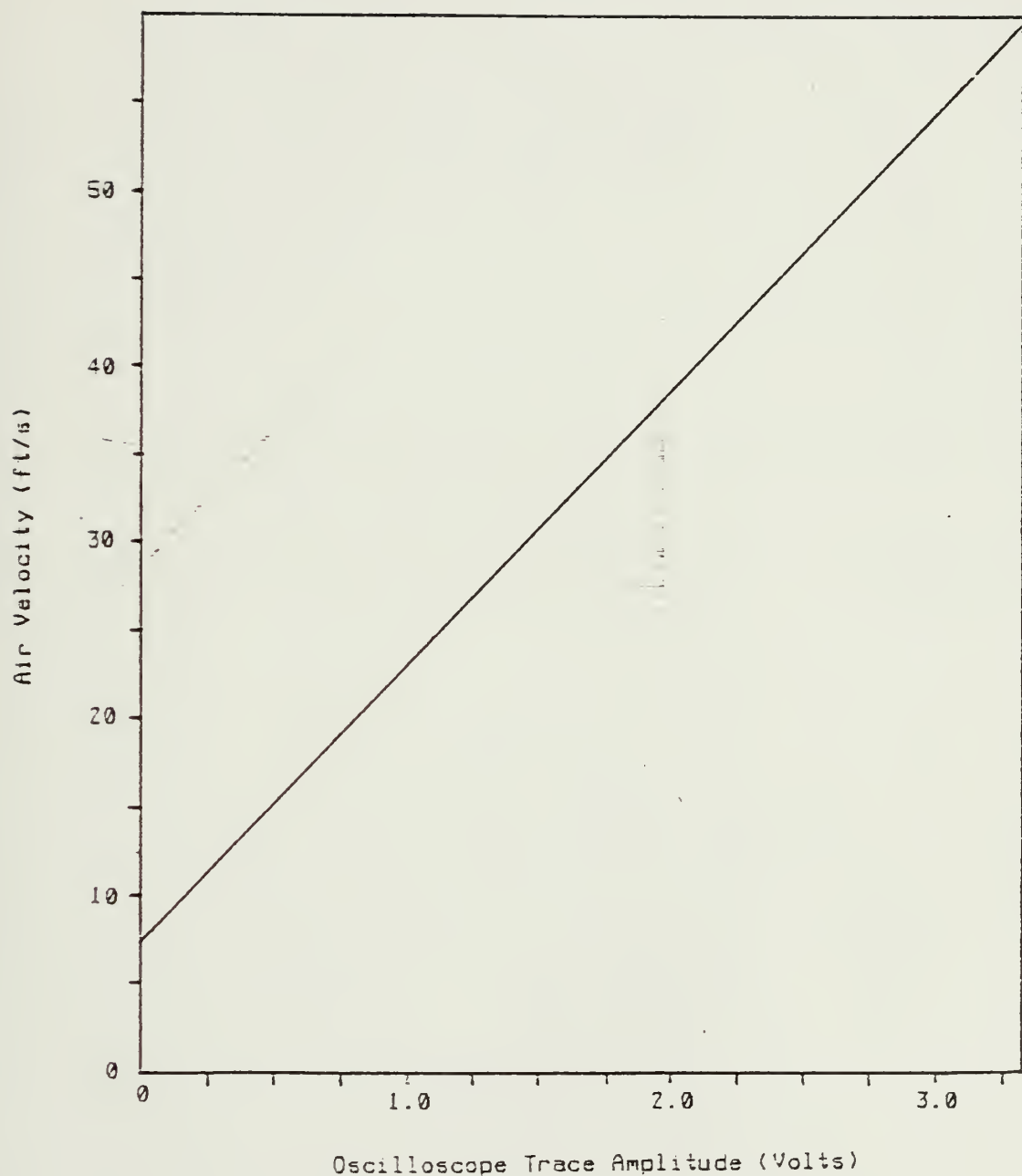
Fig. M-1   Calibration of Anemometer Probe.
Oscilloscope Voltage vs Air Velocity.

214773

Thesis
P5453   Piper
c.1   A determination of
           particle density dis-
           tributions above
           fluidized beds.